The 2014 Cessna Aircraft Company/Raytheon Missile Systems/AIAA Design/Build/Fly Competition Flyoff was held at Cessna East Field in Wichita, KS on the weekend of April 11-13, 2014. This was the 18th year the competition was held. Of the 100 entries this year, a total of 80 teams submitted written reports to be judged. And 71 teams attended the flyoff (19 international). All the teams that attended completed the technical inspection. Approximately 700 students, faculty, and guests were present.

The theme for this year was a "Back Country Rough Field Bush Plane":

- Taxi Mission simulated rough field operations using corrugated roofing panels
- Flight mission 1 was a ferry flight scored on the number of laps which could be flown in 4 minutes
- Flight mission 2 was a maximum load mission with team-chosen number of cargo blocks for three laps
- Flight mission 3 was an emergency medical mission carrying two simulated patients and attendants on a timed three-lap flight.

The Mission Score was the sum of the three Flight Scores, and factored by the Taxi Score (1 if completed, 0.2 if not). As usual, the Final Score is the product of the Mission Score and written Report Score, divided by airplane RAC (empty weight). More details can be found at the competition website: http://www.aiaadbf.org

Despite strong winds for most of the weekend and a 1-hour suspension on Sunday for a passing thunderstorm, the flyoff set new records. There were 209 flight attempts, of which 105 resulted in a valid flight score. 49 teams had successful flight scores and 61 completed the taxi mission. 20 teams completed all three flight missions. The quality of the teams, readiness to compete, and execution of the flights was outstanding.

First place went to University of Southern California with a score of 407.24, second place to University of California Irvine at 352.86 and third to San Jose State University at 326.37. A full listing of the results is shown below. The best paper award, sponsored by the Design Engineering TC for the highest report score, went to Cal Poly San Luis Obispo with a score of 98.70.

We owe our thanks for the success of the DBF competition to the efforts of many volunteers from Cessna Aircraft, the Raytheon Missile Systems, and the AIAA sponsoring technical committees (Applied Aerodynamics, Aircraft Design, Flight Test, and Design Engineering). These volunteers collectively set the rules for the contest, publicize the event, gather entries, judge the written reports, and organize the flyoff. Thanks also go to the Corporate Sponsors: Cessna Aircraft, Raytheon Missile Systems, and the AIAA Foundation for their financial support. Special thanks to Cessna Aircraft for hosting the flyoff this year.

Finally, this event would not be nearly as successful without the hard work and enthusiasm from all the students and advisors. If it weren't for you, we wouldn't keep doing it.

David Levy
For the DBF Governing Committee

CAL POLY

California Polytechnic State University, San Luis Obispo

2013-2014 AIAA Design/Build/Fly Report

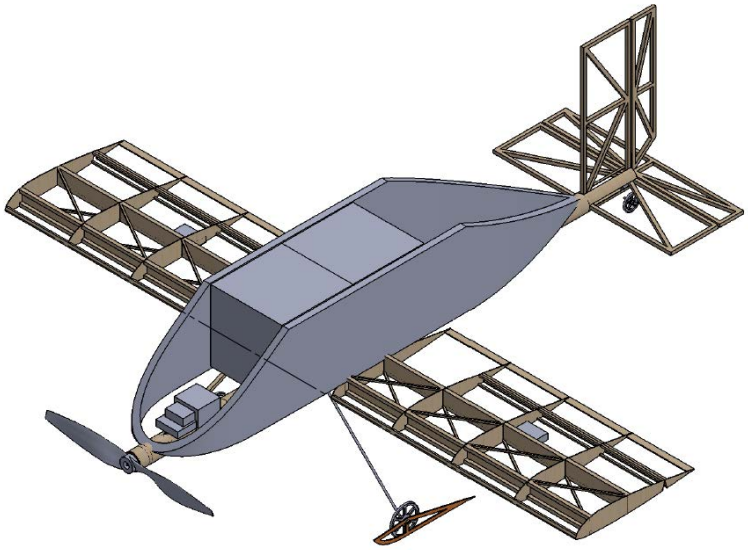

Contents

1 Executive Summary

This report details the design process used by California Polytechnic State University, San Luis Obispo to compete in the 2013/2014 AIAA Design/Build/Fly competition. The goal of the competition was to design an aircraft that best meets the mission requirements and maximizes the scoring equations. This year's competition required a light, fast aircraft capable of carrying six inch cubes and two 9x4x2 inch blocks accompanied by two 4x2x6 inch blocks simulating a medical evacuation. The final design was created through extensive analysis, testing, and hard work by a completely volunteer student team at Cal Poly.

1.1 Design Summary

The goal of the design process was to create the highest possible scoring aircraft while satisfying all of the requirements. Due to many different performance parameters greatly affecting each other, the most important factors needed to be identified. To isolate the most important parameters, a sensitivities analysis was performed on the total score equation. This analysis revealed that empty takeoff weight and speed were the two most important factors, weight being about twice as important as speed. As a result, most design decisions were driven by weight minimization, and a weight increase for speed was only acceptable if the percent speed gain was twice the percent weight gain.

1.2 Mission Requirements

There are a total of four missions that must be completed in the competition. While empty weight was the most important scoring factor in the competition, the aircraft must not sacrifice its ability to complete each of the missions with a competitive score. It was very important to determine how each mission will impact the overall design of the aircraft and the final score that can be achieved.

Mission 1 is a speed mission that tests how many laps the aircraft can complete in a four minute time limit. This mission is entirely about airspeed; however, the sensitivities analysis revealed that weight should be sacrificed for speed only if the payoff is significant.

The second mission tests the ability of the aircraft to carry large, heavy cargo. The aircraft must complete three laps with an internal payload. The large payload size in this mission was one of the driving factors for the fuselage size. In this mission, each team is given a choice of how much cargo to carry. The payload weight requirement of Mission 3 was a large factor in determining how much cargo the aircraft would carry for this mission.

The third mission is a timed mission with an internal payload. The aircraft must carry a specified payload for three laps as quickly as possible. This mission's requirements along with the short takeoff constraint drove many of the design choices for the aircraft. The weight of the aircraft on this mission and the speed scoring criteria were the main factors for the propulsion system design. The payload size was a large determinant for the size and shape of the fuselage as well.

Finally, the aircraft will go through a taxi test to assess its handling ability on rough ground surfaces. The taxi mission has a five minute time limit and the same internal payload as Mission 3. Due to the scoring criteria for this mission, the aircraft does not need to complete this mission particularly fast or well, it only needs to complete it. Consequently, all design choices for this mission were chosen to have the smallest

possible impact on the score of other missions. This mission primarily affected the design of the landing gear.

1.3 System Performance

The final design was a 2.3 pound low-wing, conventional aircraft capable of carrying two six inch cargo blocks. It has a maximum velocity of 60 feet per second, a takeoff distance of 39 feet fully loaded, and it can complete four full laps in four minutes. Carrying the Mission 3 payload, the plane is expected to finish three laps in three minutes. The team believes that the aircraft's balance between lightweight construction and speed will be highly competitive in this year's competition.

2 Management Summary

At the beginning of the 2013/2014 school year, the club gained quite a few new members, freshmen in particular. The new members complemented the return of a healthy number of experienced members. Throughout the year, close to 20 people played a role in the team, with about 10 of those being first time club members. The club benefited from the enthusiasm and wealth of fresh ideas from the new members to supplement the many years of experience from the older members. Though the focus was always on competing in the competition, the second priority was always helping newer members gain experience to continue the club's success into the future.

2.1 Team Organization

To fulfill the goal of giving newer members as much experience as possible, the team structure was somewhat fluid for the younger members. Generally, older members split up and lead the design effort in different disciplines, while the rest of the team was allowed to pick which discipline they were interested in, or switch between groups as they saw fit. This allowed everyone to be exposed to each aspect of the design process. During both the conceptual and detail design phases, the club was divided into sub-groups with the following foci: aerodynamics, structures/CAD, propulsion, controls, manufacturing, and report writing. In the earlier stages, the manufacturing team was also responsible for testing and design validation. A senior member led each sub-group and reported to one of the two co-leads.

2.2 Hierarchical Chart

The team tried very hard to keep the club experience casual. However, structure was needed for accountability and communication. The team used a simple hierarchical structure to establish organization and leadership among the team. This structure can be seen in Figure 2.1. Many members contributed to multiple groups and occasionally two groups worked together on certain design aspects. Figure 2.1 also shows members under the groups in which they made the largest contributions.

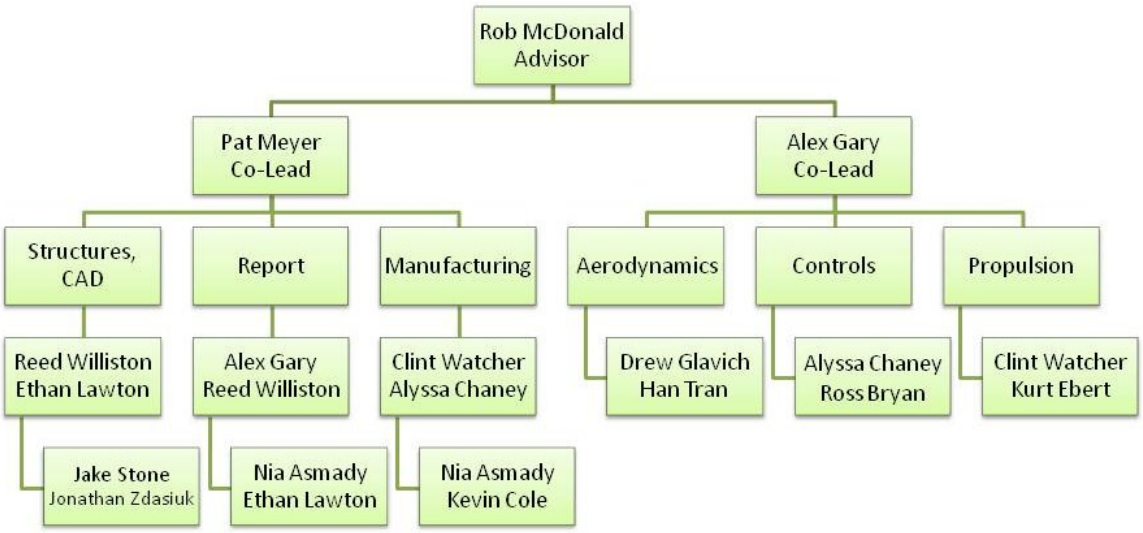

Figure 2.1 Team Organization

2.3 Milestone/Gantt Chart

Due to the hard deadlines for the report and competition, it was extremely important to stay on a reasonable schedule throughout the course of the year. To reduce the amount of last minute work, an aggressive schedule was set at the beginning of the year. A Gantt chart detailing both major and specific goals and deadlines was created to be followed as can be seen in Figure 2.2. Though the deadlines set internally by the club are fluid, they were expected to be met with quality, finished work. The division of labor and influx of members allowed the team to stay on track throughout the majority of the year.

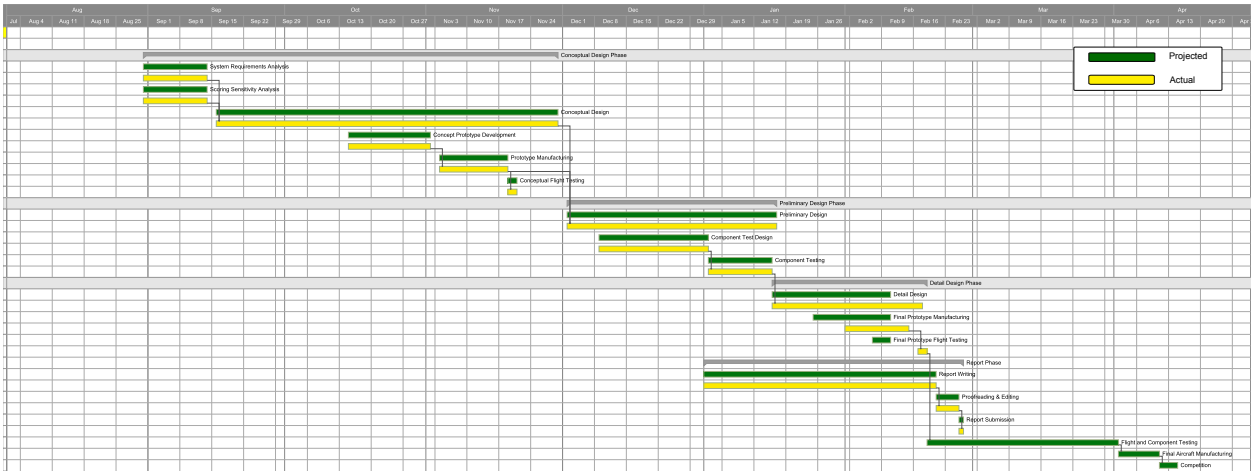

Figure 2.2 Gantt Chart including projected and actual timelines.

3 Conceptual Design

The conceptual design phase was used to fully understand the rules and to select a single design configuration that would maximize the total scoring equation. A sensitivities analysis was performed on the scoring equations, which showed that empty weight was the most important factor of the design, followed by speed. Using the results of the sensitives analysis to weigh various performance characteristics, a qualitative and quantitative survey of general configurations was performed and a general configuration was selected. To ensure the resulting design was feasible, a proof of concept prototype was built and flight tested.

3.1 Mission Requirements

The 2013/2014 Design/Build/Fly competition consists of three flight missions and one ground mission. Each of the mission scores are determined by different parameters and contribute to the overall competition score.

3.1.1 Mission and Scoring Summary

The total competition score is shown in Equation 1 where WRS is the written report score, TS is the taxi score, M_i is the score from the i^{th} mission, and RAC is the heaviest empty weight of the plane after each mission.

$$Total\ Score = WRS * \frac{TS(M_1 + M_2 + M_2)}{RAC} \tag{1}$$

Flight Lap

All three flight missions require either flying a certain number of laps or flying as many laps as possible in a given amount of time. The standard flight lap is shown in Figure 3.1 with a safe operating altitude of 100 feet.

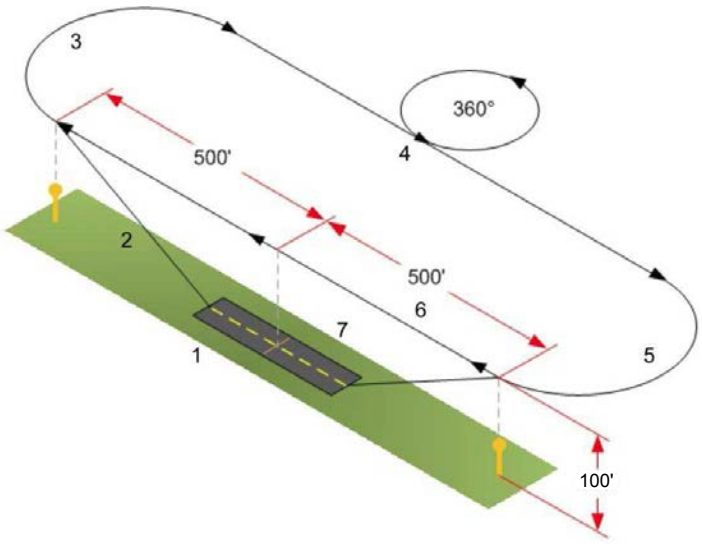

Figure 3.1 Standard Flight Lap

Each lap requires the following in order to be considered successful:

1. Rolling takeoff in less than 40 feet
2. Climb to safe altitude
3. U-turn 500 feet upwind of start
4. 1000 foot downwind leg with a 360 degree turn away from the runway
5. 180 degree turn from downwind to upwind
6. 500 foot upwind leg past the start line
7. Successful Landing after completion of all laps or time limit

Whether or not the landing is successful will be determined by the competition judges based on the amount of significant damage incurred upon landing.

Ferry Flight

Mission 1 is a ferry flight mission without a payload. It consists of a four minute timed flight where the time is started as soon as the throttle is advanced. A lap is counted as the aircraft passes over the start/finish line. A lap that is unfinished when the time limit is reached will not be counted. After the time limit is reached, the aircraft must land successfully to receive a score for the mission. The scoring criteria for Mission 1 is given in Equation 2.

$$M1 = 2 * \frac{N_{Laps}}{N_{Laps,max}} \tag{2}$$

Maximum Load Mission

Mission 2 is a cargo flight mission with no time limit. It consists of a three lap flight with cargo stored internally. The cargo consists of six inch wooden cubes provided by the competition officials. Each cube will weigh one pound and will have its center of gravity near the centroid. The team is left to decide the number of cubes carried as cargo. Upon completion of all three laps, the plane must complete a successful landing to receive a score. The scoring criteria for Mission 2 is given in Equation 3.

$$M2 = 4 * \frac{N_{Cargo}}{N_{Cargo,max}} \tag{3}$$

Emergency Medical Mission

Mission 3 is a timed cargo flight mission with a specified cargo. It consists of a three lap flight with cargo stored internally. The cargo consists of four wooden blocks provided by the competition officials. The blocks will each weigh 0.5 pounds and have their center of gravity near the geometric center. The cargo is represented by two patient blocks that are 9x4x2 inches and two attendant blocks that are 6x2x4 inches. The patient blocks must lay horizontally and the attendant blocks must stand vertically. The attendants will stand along the sides of the patients during flight and must be separated from each other by two inches. Additionally, the patients must be separated by two inches side to side and each patient must have two inches of empty space immediately above it. The aircraft will complete three laps as fast as possible. A lap

will be recorded as the aircraft crosses the start/finish line. The time will begin as soon as the throttle is advanced for takeoff and stop when the aircraft crosses the start/finish line on the last lap. The aircraft must complete a successful landing to receive a score. The scoring criteria for Mission 3 is given in Equation 4.

$$M3 = 6 * \frac{T_{fastest}}{T_{team}} \tag{4}$$

Rough Field Taxi

This mission is a timed taxi test with a specified cargo. It consists of taxiing the aircraft across a 40x8 foot course within a time limit of five minutes. The aircraft must carry the same payload as outlined in Mission 3. The course will be across corrugated fiberglass roofing panels oriented perpendicular to the 40 foot course direction. The panels are corrugated with a spacing of 0.625 inches high by 3 inches wide. Additionally, two obstacles will be placed at one-third and two-thirds of the distance along the course. They will span half of the course distance alternating sides from the centerline to the edge and will stand 3.5 inches tall by 1.5 inches wide. The mission will be deemed successful if the aircraft travels from one side of the course to the other within the allotted time limit without damaging the aircraft. If the aircraft departs the course or becomes airborne, the attempt will be deemed unsuccessful. A successful attempt will receive a score of $TS = 1$ and an unsuccessful attempt will receive a score of $TS = 0.2$.

3.1.2 Scoring Sensitivities Analysis

An ideal aircraft would maximize the total mission score (TMS) by outperforming all other airplanes in each of the three missions. However, the missions require the aircraft to perform well in several different areas. The first and third missions emphasize speed whereas the second mission emphasizes payload capacity. Additionally, the sum of the mission scores is divided by empty weight. Since it is not possible to improve the performance of one metric without negatively affecting another, it is necessary to determine the most important metric.

In order to determine the most important metric, a sensitivities analysis was performed on a simplified version of the TMS. The TMS was simplified by making the assumption that the aircraft would successfully complete the taxi mission and receive a taxi score of one. The simplified TMS becomes Equation 5.

$$TMS = \frac{2(\frac{N_{Laps}}{N_{Laps,max}}) + 4(\frac{N_{Cargo}}{N_{Cargo,max}}) + 6(\frac{T_{fastest}}{T_{team}})}{EW} \tag{5}$$

This equation is a function of four variables:

1. The ratio of laps flown by Cal Poly in Mission 1 to the maximum flown by any team, $\frac{N_{Laps}}{N_{Laps,max}}$
2. The ratio of cargo pieces carried by Cal Poly in Mission 2 to the maximum carried by any team, $\frac{N_{Cargo}}{N_{Cargo,max}}$
3. The ratio of fastest Mission 3 time to Cal Poly's Mission 3 time, $\frac{T_{fastest}}{T_{team}}$
4. The aircraft empty weight, EW

The sensitivities analysis was performed by computing the percent change in the TMS for a percent change

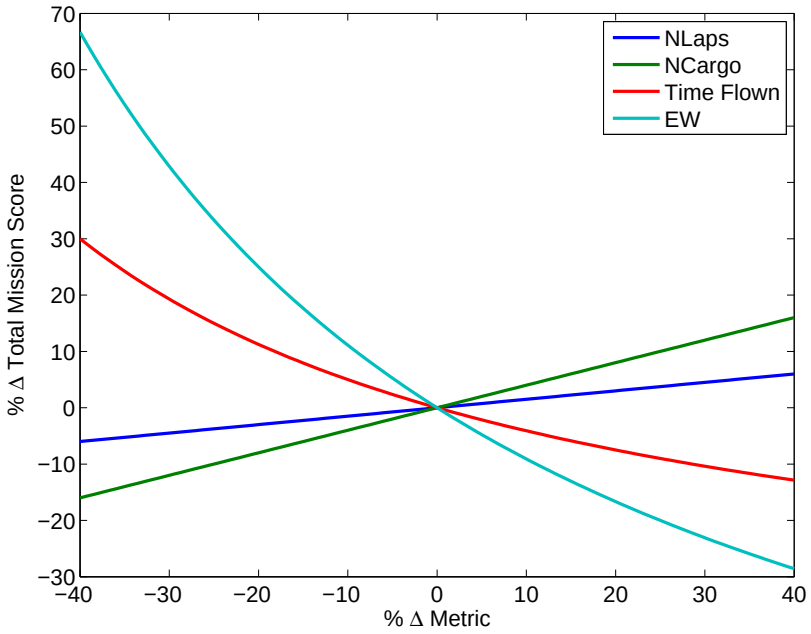

Figure 3.2 Percent Change in Total Flight Score for a Percent Change in Scoring Variable

in each of the four variables. In order to perform this analysis, a set of baseline parameters had to be assumed. Based on previous competition experience and initial sizing estimates, the following values were used: $\frac{N_{Laps}}{N_{Laps,max}}$ of 2, $\frac{N_{Cargo}}{N_{Cargo,max}}$ of $\frac{1}{6}$, $\frac{T_{fastest}}{T_{team}}$ of 1/2, and an EW of 2 pounds. The visualization of this analysis is shown in Figure 3.2.

Figure 3.2 shows that weight has the largest affect on the TMS, but it is closely followed by the time flown in Mission 3. In order to quantify the difference, the slopes of each line were inspected. Based on the slopes, empty weight is 2.22 times as important as time flown on Mission 3. Therefore, throughout the design process, this difference was used to justify decisions between reducing weight or adding speed.

3.1.3 Design Constraints

There are a few design constraints that apply to the aircraft in general that have a large impact in the overall design of the aircraft. For all three missions, the aircraft is limited to a 40 foot takeoff distance. There is also a current draw limit of 15 Amps from the battery pack with a 1.5 pound battery weight limit. The combination of these three requirements have huge consequences on the design of the propulsion system. With the battery weight limiting voltage and the current limited as well, there is effectively a cap on the power that can be produced from the propulsion system. For the heavy payload missions, this becomes an issue during the short takeoff where the aircraft will need as much power as it can get. Consequently the aircraft needs to generate relatively high lift to takeoff quickly. To simulate a bush plane design, the aircraft will be required to have a certain clearance distance underneath the wing. Since the aircraft has a low wing design, this constraint required the landing gear to be somewhat taller than otherwise necessary. Lastly, the differing shapes of the internal cargo for the second and third missions creates a nontrivial volume requirement for the interior structure of the aircraft.

3.2 Mission to Design Requirements

Applying the sensitivities analysis, general scoring parameters, and design constraints to the aircraft allowed the team to derive qualitative design requirements. The 40 foot takeoff distance coupled with the battery weight and current limit requirements create the design requirement of a relatively high $C_{L,MAX}$. These coupled requirements also favor the lightest possible airplane because a lighter airplane will need less power to meet the takeoff distance requirement. The sensitivities analysis also suggests that the lightest possible airplane will have the highest total mission score. In order to create the lightest airplane possible, the smallest payload possible should be flown. The minimum payload capacity in the mission requirements is two pounds based on Mission 3. In order for this to remain the maximum payload of the aircraft, no more than two pieces of cargo can be carried during Mission 2.

Another major mission requirement is the taxi test and minimum ground clearance. These mission requirements result in the need for longer landing gear with a wheel base no larger than half of the wingspan. The Mission 2 and Mission 3 payload configurations place many constraints on the shape of the fuselage that need to be considered during the fuselage design process. Finally, the sensitivities indicate that speed is the second most important factor of the design. This creates the design requirement of a low drag airplane with high wing loading.

3.3 Solutions Considered, Selection Process, and Results

After transforming the mission requirements into design requirements, many different configurations could complete the mission. In order to reduce the design space, several different designs were qualitatively and quantitatively compared and the best designs were investigated further.

3.3.1 Initial Concepts

In order to reduce the number of configurations to investigate, seven different configurations were qualitatively compared in terms of five key characteristics: empty weight, speed, takeoff distance, payload integration, and handling. These characteristics were then ranked from best to worst in each category. Based on the sensitives analysis, each of these characteristics were assigned a different weight of importance. The results of this comparison are shown in Table 3.1 where the highest score is best.

From this analysis, the conventional, flying wing, and twin fuselage configurations scored the best. The team decided to focus future design efforts only on the conventional configuration for several different reasons. First, the conventional configuration scored 54.3% higher than the next closest design, the flying wing, which means it is significantly better suited for the missions than the rest of the configurations explored. Second, the runner up designs both have major drawbacks that would likely result in a heavier airplane than the conventional and weight is the most important criteria. Flying wings can be fast, lightweight planes, but they have extremely poor takeoff performance based on previous competition experience. To meet the 40 foot takeoff requirement, a larger propulsion system and wing area would be required compared to a conventional aircraft. Twin fuselage designs generally work well for building extremely light, long wings, but they significantly limit payload configuration options. Since the payload in both Missions 2 and 3 is large and consists of only a few pieces, the combined volume of both fuselages is likely to be larger than the volume of a single fuselage on a conventional plane. This will result in a twin fuselage plane that has more drag,

Table 3.1 Initial Qualitative Comparison of General Configurations

	Weight	Conventional	Flying Wing	Tandem	Delta	BWB	Biplane	Twin Fuse
Empty Weight	0.8	6	7	2	3	4	1	5
Speed	0.5	5	7	3	4	6	2	1
Takeoff Dist	0.8	7	1	5	3	2	6	4
Payload	0.2	7	1	5	4	3	6	2
Handling	0.2	7	2	1	4	3	6	5
Total Score		**15.7**	10.5	8.3	8.4	9	9	9.1

and thus is slower than a conventional design. For those reasons, the team moved forward focusing only on a conventional design. After the conventional design was selected, the team still needed to consider different conventional configurations.

3.3.2 High Wing Conventional

The first conventional design considered was a high wing airplane. A high wing design is generally a very stable aircraft which is one of the reasons it was considered. It is also easier to keep the airflow in front of the vertical and horizontal stabilizers clean as the majority of the fuselage would be below the tail. However, there are several drawbacks to the high wing design. With a high wing, it is difficult to transfer landing loads from the landing gear into the wing box. Either the fuselage must have major structural components or the gear must be long enough to reach the wing directly. Another issue with the high wing is that the fuselage will require major structure to create a floor for the cargo to be placed on, which means the fuselage may become unnecessarily heavy.

3.3.3 Low Wing Conventional

The second conventional design considered was a low wing airplane. A low wing airplane has the advantage of a lighter fuselage design for several reasons. First, no landing loads will be transfered through the fuselage which will greatly reduce the required structure. Second, much of the required structure for the floor can be shared with the wing spars and tail boom. Being able to share major structure between the wing and fuselage should allow for a much lighter airplane than the high wing design. However, since the center of gravity in a low wing plane is above the wing, this design could potentially be roll unstable.

3.3.4 Landing Gear Configurations

Since the rough field taxi test presents a unique design requirement, both tricycle and tail dragger landing gear configurations were considered. Tricycle gear can be easier to control on paved ground, but during the taxi test it could result in the nose dipping and prop striking if the main gear were on a peak and the nose gear was in a valley. Also, when the nose gear enters a valley the motor will point down which will vector thrust down and make it more difficult to roll over the next peak. A tail dragger configuration can be

more difficult to control while taxiing and during takeoff, but it can make tighter turns than tricycle gear. A tail dragger configuration also has the benefit of vectoring thrust up since the motor will face up when all three wheels are on the ground. This should make it easier to roll over the corrugated roofing. A tail dragger configuration also has the potential to be lighter than tricycle gear since the tail wheel and rudder can share a single servo. In addition, the nose gear of a tricycle will weigh more than the tail gear of a tail dragger.

In order to reduce the amount of thrust required to overcome the corrugated roofing, different types of wheels and skis were considered. Using bigger wheels makes it easier to roll over obstacles, but it increases drag in flight. Skis could potentially make it much easier to go over obstacles without adding as much drag as large wheels in flight. However, if only skis were used, the friction during takeoff would be much larger than wheels and require a larger propulsion system. Therefore, the team decided to consider a combination of wheels and skis. The wheels would provide reduced friction during takeoff, and the skis would stop the wheels from sinking into the valleys during the rough field taxi test reducing the force required to traverse the course.

3.3.5 Tail Configurations

In order to stabilize the airplane, the team considered several different tail configurations: a conventional tail, T-tail, H-tail, and V-tail. Figure 3.3 shows each of these configurations.

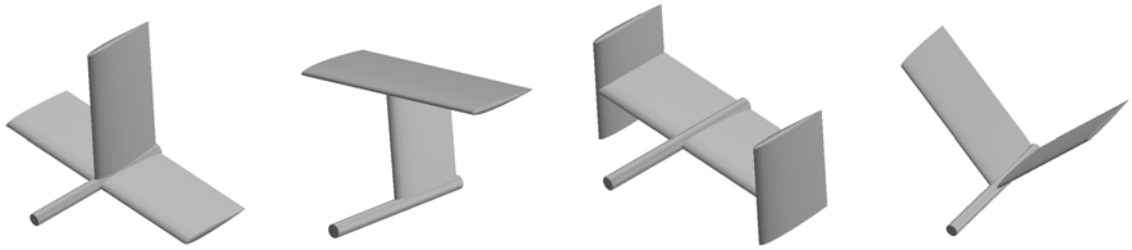

(a) Conventional Tail **(b) T-tail** **(c) H-tail** **(d) V-tail**

Figure 3.3 Tail Configurations Considered

A conventional tail configuration consists of a single vertical stabilizer placed on top of a horizontal stabilizer. The horizontal stabilizer and control surface counteract the negative pitching moment of the wing during steady level flight. The vertical stabilizer provides stability and control about the yaw axis of the aircraft. A conventional tail is easy to design and build as it is extremely common. Furthermore, conventional tail configurations can be very light.

A common variation of the conventional tail is the T-tail. The T-tail configuration places the horizontal tail at the top of the vertical stabilizer. The main benefit of a T-tail is being able to move the horizontal tail out of the wing wake and propwash. This makes the horizontal stabilizer more efficient and can be smaller than on a conventional tail. Placing the horizontal on top of the vertical tail also increases the efficiency of the vertical stabilizer because the horizontal acts as a wing plate. Therefore, the vertical tail size can be reduced. However, placing the horizontal on top of the vertical stabilizer requires an increase in the structure supporting the vertical stabilizer because higher loads are being placed at the tip of the vertical. This increased structure usually makes a T-tail configuration heavier than a conventional tail.

An H-tail was considered because it is an efficient tail due to the vertical stabilizers capping the horizontal

stabilizer which effectively increases the horizontal stabilizer aspect ratio. Placing the vertical stabilizers such that they are vertically centered about the horizontal stabilizer would reduce the torsional loads. Another benefit of an H-tail is the possibility of increased rudder control by moving the vertical stabilizers away from the centerline and fuselage. However, the H-tail would require longer landing gear in order to obtain the necessary rotation on takeoff. This and the increased structure to mount two vertical stabilizers would increase the overall weight compared to a conventional tail configuration.

Finally, a V-tail was considered because it produces less drag than a conventional tail. The drag benefits of a V-tail come from two sources. For given required horizontal and vertical areas, a V-tail will have less wetted area than a conventional tail. The angle the V-tail is offset from horizontal is the inverse tangent of the ratio of vertical tail area to horizontal tail area. The length of the V-tail stabilizers is the hypotenuse of a triangle with the horizontal and vertical tail spans as the two legs. However, a NACA paper[1] shows that the area of the V-tail needs to be increased beyond this to provide the proper control authority. The second reduction in drag for a V-tail comes from less interference drag than a conventional tail. The control system on a V-tail is much more complex because the rudder and elevator are coupled into an ruddevator.

The tail configuration selected was the conventional tail. The conventional tail was selected because it is the lightest, easiest to control, and easiest to build. The T-tail and H-tail were not selected mainly because of the extra weight that is required to support a stabilizer not placed near the main structure of the aircraft. However, if the team found that either stabilizer was being blanked out by the fuselage, the T-tail and H-tail would be reconsidered. Finally, the V-tail was eliminated because the NACA paper shows the wetted area will still be roughly the same and the increased complexity of the control system was undesirable.

3.3.6 Payload Configurations

In order to design the outer mold line of the fuselage, the payload configuration for both Mission 2 and Mission 3 needed to be determined. Figure 3.4 shows the three different payload configurations that the team considered.

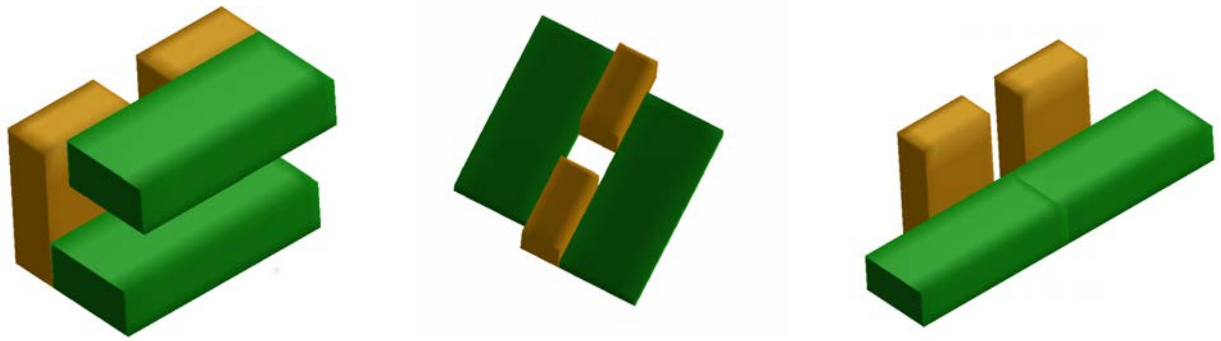

(a) Bunk Bed **(b) Side-by-side** **(c) Lengthwise**

Figure 3.4 Payload Configurations Considered

The first solution considered was the bunk bed configuration shown in Figure 3.4a. In this configuration the two patients are placed above one another and the attendants are placed on one side. This configuration

[1] Purser, Paul E., and John P. Campbell. "Experimental verification of a simplified vee-tail theory and analysis of available data on complete models with vee tails." (1945).

allows for a fuselage that is short in the streamwise direction. A shorter fuselage could result in a shorter aircraft which means a lighter aircraft. However, this solution requires a tall fuselage, eight inches, resulting in a large amount of frontal area (48 square inches) which means a large amount of drag. Another issue with this fuselage is that a bunk for the top patient must be created. This extra structure that must support the top patient would add a significant amount of weight to the aircraft.

The second solution considered was the side-by-side configuration shown in Figure 3.4b. In this configuration the two attendants are placed along the centerline of the airplane and the patients are located on either side. The idea behind this configuration was to integrate the patients into the wing and to only have a short fuselage cover the patients and minimize the portion of the fuselage that needed to be six inches tall. Also in this configuration only a single cube would be carried for Mission 2 as the portion of the fuselage that was both six inches tall and wide would only be six inches long. This solution would have the least amount of volume possible, but would have a low Mission 2 score carrying only a single cube. Furthermore, the rule requiring a two inch space above the patients results the largest frontal area of any of the solutions considered (52 square inches).

The third solution considered was the lengthwise configuration shown in Figure 3.4c. In this configuration the two patients are placed end to end and the attendants are then placed on one side. In this arrangement the frontal area is minimized to that of the cubes in Mission 2 (36 square inches). This arrangement also allows for two cubes to be carried which doubles the Mission 2 score. However, with this design the fuselage is much longer than the other two designs which means a longer tail boom will be required and therefore more weight.

The final payload configuration selected was the lengthwise arrangement. This design had the least frontal area compared to the other two concepts and did not require any additional structure such as a second floor that would increase weight. The long tail will increase the aircraft's weight, but the reduced frontal area will increase both Mission 1 and Mission 3 scores. Also, this configuration is the only one that allows for two cubes to be carried which will double the Mission 2 score.

3.3.7 Selection Validation

To ensure that the selected low wing aircraft with a conventional tail was a feasible design that could meet this year's requirements, the team built a foam prototype. The goal of this prototype was to test several key design decisions before moving forward into the preliminary design phase. First, the team wanted to ensure that building a stable low wing aircraft with decent handling qualities was possible. The team was concerned that with a low wing aircraft the center of gravity would be above the wing and that the airplane would respond like an inverse pendulum. In terms of stability, the team was also concerned about the very long fuselage design and its effect on both roll and dutch roll stability. All of the analysis performed indicated that the design was possible and the successful flight of the initial prototype confirmed that the selected design was reasonable.

Another concern the team had about the design was meeting the short takeoff distance requirement of 40 feet while not exceeding the current limit of 15 Amps, because last year's competition aircraft suffered a devastating crash after blowing a fuse on takeoff. In order to create the worse case scenario for the short takeoff requirement, the prototype was weighed down to four pounds, the predicted heaviest mission weight. Figure 3.5 shows the prototype meeting the takeoff distance and the on board data logger confirmed

Figure 3.5 First Prototype Meeting Takeoff Requirement

a maximum current draw of less than 15 Amps.

The final concerns with the conceptual design that needed validation was the unique landing gear configuration. The team was concerned that while the landing gear skis would keep the aircraft from sinking into the corrugated roofing, they also might create too much friction and prevent the aircraft from being able to traverse the rough surface. Another concern with the skis was the ability to steer the aircraft while on the roofing. Therefore, a taxi test mission was performed with the ski landing gear, and the aircraft was able to successfully complete the mission. Furthermore, the ski landing gear outperformed the landing gear with exceptionally large wheels.

After validating the initial design with several test flights and a taxi test, the team as a whole felt confident in the aircraft conceived during the conceptual design phase. Therefore, the team moved forward into the preliminary design phase with a conventional low wing tail dragger.

4 Preliminary Design

The preliminary design phase was used to make key design decisions and perform trade studies in order to finalize the design created in the conceptual design phase. Preliminary models were created to estimate performance values that could be improved upon in the detailed design phase. In this section the design methodology, aircraft sizing, mission model, aircraft characteristics, and expected mission performance were document. The conceptual design prototype was modified and a new prototype was made with adjustments from research, analysis, and testing.

4.1 Design Methodology

An iterative design process was implemented to maximize the total flight score by repeatedly improving the aircraft design. This process was aided by the ability to rapidly create, analyze, and test prototype airframes.

4.1.1 Iterative Design Process

The conceptual design was formulated through a trade study which was validated by the flight test of a foam prototype. Further analysis was performed on all systems of this initial design, and improvements were made. Prototype aircraft were created for flight testing purposes, with all aspects being documented in order to make required improvements. This cyclical process converged to a final airframe design.

4.1.2 Rapid Prototyping

The iterative design process was dependent on the team's ability to rapidly build prototypes. This effort was aided by the use of Cal Poly's CNC hot wire foam cutter as well as the CNC laser cutter. With rapid machining of the main components, frequent updates on a working solid model, and a group of members dedicated to manufacturing, prototypes could be built in as little as one to two weeks. This allowed for a multitude of flight and component testing that provided invaluable data and pilot feedback to be used in the next design iteration.

4.2 Sizing and Trade Studies

In aircraft design, performance characteristics are heavily dependent on each other. Unfortunately it is nearly impossible to increase performance in one area without negatively affecting performance in another. Therefore, throughout the design process many trade studies were performed when sizing various aspects of the aircraft. Since weight was the most important factor based on the sensitivities analysis, it was the most important factor in nearly all of the trade studies performed. While tail sizing is the only trade study and sizing presented in this section, trades and sizing were performed in nearly every aspect of the design process from propulsion system design to servo selection.

4.2.1 Tail Sizing

In order to size the aircraft tail, tail volume coefficients were used. Equation 6 shows the formula used to compute the horizontal tail volume coefficient where L_h is the horizontal tail's distance from the aircraft's center of gravity, S_h is the trapezoidal area of the horizontal tail, S_w is wing area, and MAC is the mean aerodynamic chord.

$$V_h = \frac{L_h * S_h}{S_w * MAC} \tag{6}$$

Equation 7 shows the formula used to compute the vertical tail volume coefficient where L_v is the vertical tail's distance from the aircraft's center of gravity, S_v is the trapezoidal area of the vertical tail, S_w is wing area, and b is wingspan.

$$V_v = \frac{L_v * S_v}{S_w * b} \tag{7}$$

Based on previous Design/Build/Fly experience and remote controlled aircraft data, the tail volume coefficients used were 0.45 for the horizontal tail and 0.07 for the vertical tail. Since the tail volume coefficients can be achieved by varying the distance of the tail from the wing or by increasing the size of the tail for a given wing planform, a trade study was performed with the goal of minimizing weight. In this trade study weight per unit length of tail boom and weight per area of tail surface were estimated. With this information, the weight of the tail boom and tail surfaces was plotted versus boom length and the minimum weight boom length was selected.

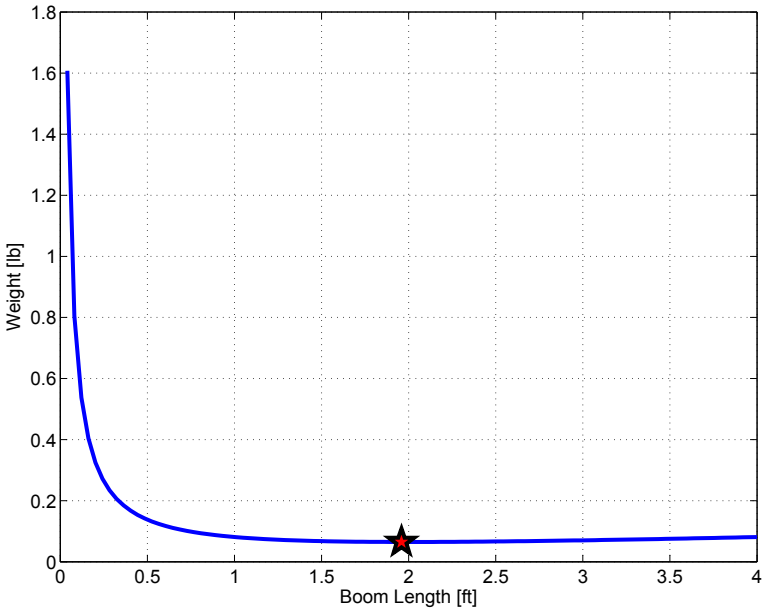

Figure 4.1 Tail and Boom Weight as a Function of Boom Length

Figure 4.1 shows the weight trade-off between tail boom length. The red star in Figure 4.1 is the minimum weight point on the plot and was chosen as our tail boom length. The tail areas were then determined from the tail volume coefficients. The span and chord of the tail surfaces were set such that they would stall before the wing. The final tail dimensions are show in Table 4.1.

Table 4.1 Final Tail Dimensions

Dimension	Length [inch]
Boom Length	22.75
Vertical Height	11
Horizontal Span	15
Tail Chords	6

4.3 Mission Model

A mission model was created to predict performance capabilities and uncertainties. It was also used as a tool for designing the aircraft's propulsion system. The mission model used an energy analysis method to compute the milliamp-hours required for each of the missions. Therefore, this created a minimum battery cell size for the propulsion system design.

4.3.1 Model Analysis

The mission model was created using the drag polar obtained from the parasite drag build-up combined with the induced drag obtained from AVL and is shown in section 4.4.2. In order to account for the sources of drag that cannot be accurately modeled in a drag build-up, such as control rods, control horns, and control surface gaps, the parasite drag value was tripled. This approximation matches experimental data from previous years.

Since the aircraft experiences different values of drag during different portions of the flight lap, the lap was broken into different parts. The first part consisted of straight portions, and the second part consisted of the turning portions of the lap. In order to reduce the complexity of the mission model several assumptions were made. A steady-level flight assumption was made during the straight portions of the course, and constant load factor turns were assumed during the rest of the course. For Mission 1 a six G turn was assumed, while three G turns were assumed for the heavy aircraft in Missions 2 and 3.

In order to compute the energy required for each mission lap, the drag force for each leg of the lap was multiplied by the distance of that leg and summed together. In order to find the milliamp hours required for each lap, the energy required was divided by the estimated battery pack voltage. The results of the mission analysis are shown in Table 4.2.

Table 4.2 Mission Model Results

Mission	Engery/Lap (Joules)	Power/Lap (milliamp hours)	Laps	Power/Mission (milliamp hours)
Ferry	2219	202	5	1008
Maximum Load	2306	210	3	629
Medical	2659	242	3	725

4.3.2 System Uncertainties

The largest source of uncertainty comes from the overall propulsion system since different motors, batteries, and electronic speed controllers have varying efficiencies that depend on one another. Therefore, this makes it difficult to model the overall efficiency of the propulsion system and how that effects the true energy required during the missions. For these reasons as well as not having made final component selections, the efficiency of the system was assumed to be 60 percent.

Another significant source of uncertainty in the system is atmospheric wind. This was assumed to be zero in the mission model. However, there will likely be wind which will affect the total drag on the aircraft as well as the efficiency of the propeller at a different advance ratio. Additionally, the steady-level flight assumption introduces uncertainty into the model since R/C aircraft almost never fly in a steady-level trimmed condition

due to wind gusts and frequent turns.

4.4 Aircraft Characteristics

Improving the characteristics of the initial prototype created in the conceptual design phase was the main focus of the preliminary design phase. The design improvements and decisions are included in this section and the new aircraft characteristics were closely compared to the initial prototype to ensure design changes were having the desired effects.

4.4.1 Airfoil Selection

In order to get the best performance and characteristics out of the aircraft the airfoil needed to be carefully selected. Airfoil selection affects the aircraft's drag (induced, parasite, and trim), takeoff distance, and stability. Therefore, a careful process was performed to ensure the best airfoil was selected.

Design Requirements

Before an airfoil could be selected, the overall design requirements derived in section 3.2 needed to be applied the airfoil. The short takeoff distance meant an airfoil with a high maximum lift coefficient was desirable. To increase the aircraft's speed and reduce power requirements, an airfoil with low drag characteristics during cruise was desirable. The airfoil also needed to have good structural characteristics which meant it needed to be thick enough to contain the wing spars as well as provide sufficient torsional rigidity to maintain the desired wing shape. Finally, the ideal airfoil would have a small pitching moment to minimize trim drag.

Selection Method

In order to explore a large set of possible airfoils, the entire University of Illinois at Urbana-Champaign airfoil database was downloaded.[1] To efficiently analyze over 1500 airfoils in the database, the team wrote a MATLAB script to automate the execution of XFOIL[2], a subsonic viscous two dimensional aerodynamics code. Using this tool, all of the airfoils were analyzed over a wide range of angle of attacks in order to determine the performance of each airfoil for all of the predicted flight conditions.

To narrow the selection of airfoils, constraints were placed on the maximum lift coefficient and the maximum thickness in order to meet the takeoff requirements and maintain structural viability. Therefore, any airfoil that did not have a maximum lift coefficient of at least 1.5 and a maximum thickness of at least 12 percent was eliminated from the list of airfoils. After this down selection process, 169 airfoils remained. In order to select between the remaining foils, they were sorted based on the drag coefficient at the estimated cruise condition and the ratio of drag coefficient to the pitching moment coefficient at the estimated cruise condition. Only two airfoils remained in the top twenty of both sorted lists. Figure 4.2 shows the two competing airfoils.

To make the final decision between the atr72sm and oaf128, the overall performance of the airfoils needed to be examined instead of just cruise point performance because in the preliminary design phase the cruise

[1] http://aerospace.illinois.edu/m-selig/ads/coord_database.html
[2] http://web.mit.edu/drela/Public/web/xfoil/

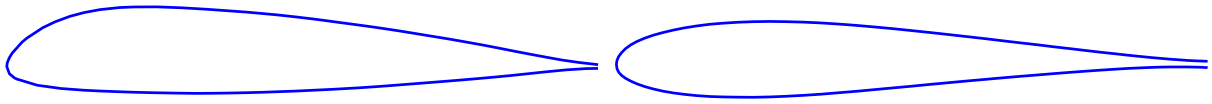

Figure 4.2 Top Two Airfoil Candidates: atr72sm gapped (Left), oaf128 (Right)

lift coefficient, C_L, is an estimate and the aircraft may operate at a slightly different point. Also, the cruise C_L changes during each of the missions, so having low drag and low pitching moment over all of the missions was important. Figures 4.3-4.5 show comparisons of the C_L versus angle of attack, α, curves, moment coefficient, C_M, versus α, and drag polars at a Reynold's number of 450,000. In addition to the atr72sm and oaf128 airfoils, an atr72sm airfoil with a trailing edge gap was analyzed because it is not possible to manufacture an airfoil with a perfectly sharp trailing edge. This was not necessary for the oaf128 since it already had a gapped trailing edge.

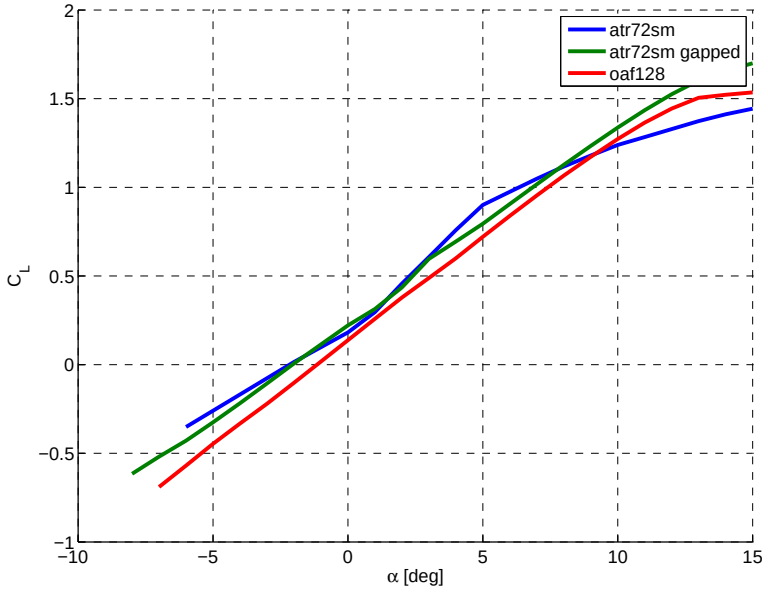

Figure 4.3 Comparison of C_L versus α curves

Based on Figure 4.3, both the gapped atr72sm and oaf128 have extremely similar C_L versus α curves. However, the gapped atr72sm does have a slightly higher $C_{L,max}$ which should improve takeoff performance.

Figure 4.5 shows the two dimensional drag polars for each of the different airfoils. All of the drag polars are fairly similar; however, the drag bucket on the oaf128 is over a wider range of C_L values. The other main difference between the polars is that both the normal and gapped version of the atr72sm have a lower minimum drag value. Table 4.3 summarizes the key performance characteristics of the airfoils being considered.

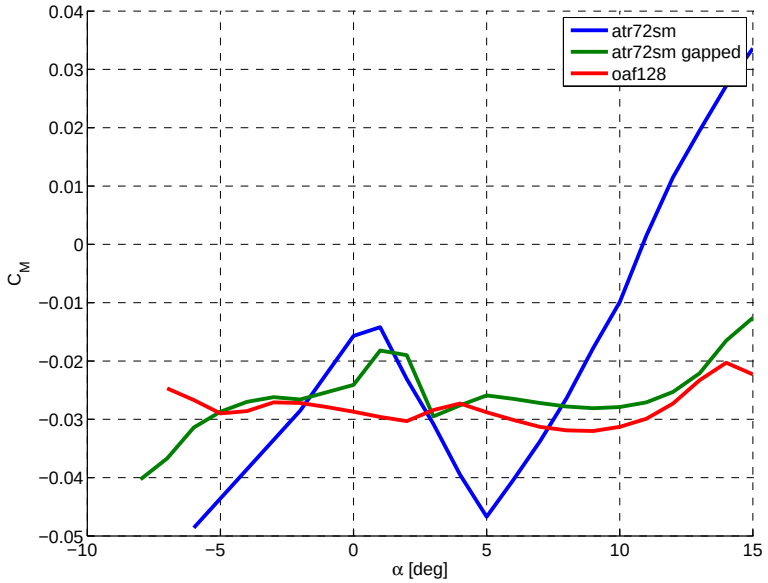

Figure 4.4 Comparison of C_M versus α curves

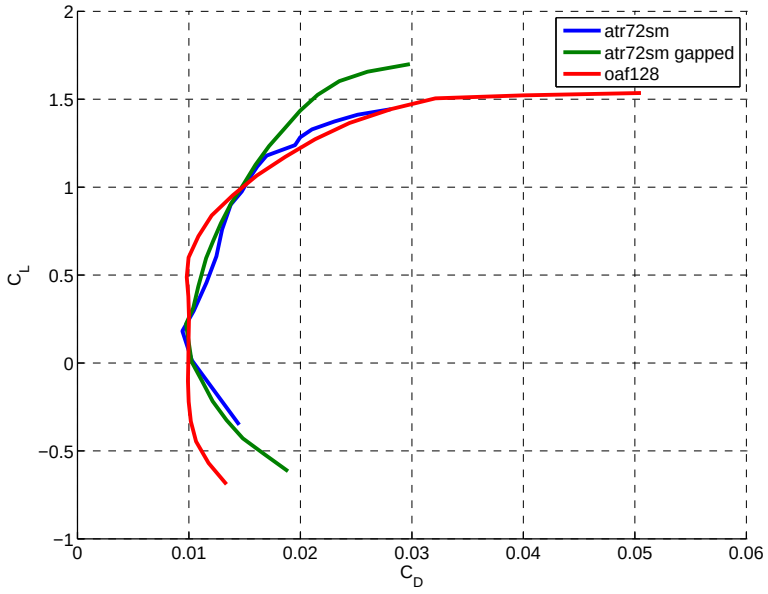

Figure 4.5 Comparison of 2-D Drag Polars

Table 4.3 Candidate Airfoil Performance

Airfoil	$C_{L,max}$	C_D @ Cruise	$\frac{C_L}{C_D}$ @ Cruise
atr72sm	1.5207	0.0095	20.2989
atr72sm gapped	1.6925	0.0098	19.7088
oaf128	1.5351	0.0100	19.3197

The final airfoil selected for the design was the atr72sm. It was selected over the oaf128 because it had a higher $C_{L,max}$, lower cruise drag, and a reasonably small pitching moment at the cruise condition that

meant the trim drag should not be large. In order to confirm this assumption about the trim drag, an AVL model was created and trimmed using both airfoils. The trim drag difference was insignificant. While the oaf128 did have a larger drag bucket, the overall performance of the atr72sm was superior. Furthermore, the atr72sm would be easier to manufacture than the oaf128 because it had almost no concave portions which are difficult to cover with Microlite.

4.4.2 Drag Build Up

Proper modeling of drag is necessary to accurately predict the performance of the vehicle. The accuracy of the drag estimation correlates with the number of corrective elements that are considered in the model. Table 4.4 displays a matrix of possible drag sources in a standard estimation scheme for both parasite and induced drag as defined in Raymer's *Aircraft Design*.

Table 4.4 Drag Matrix from Raymer's *Aircraft Design*

	Shear Forces	Pressure Forces		
		Separation	Shock	Circulation
Parasite Drag	Skin Friction Scrubbing Drag Interference Drag Profile Drag	Viscous Separation Shock-Induced Separation "Drag Rise" Interference Drag Profile Drag Camber Drag	Wave Drag Shock-Induced Separation "Drag Rise"	–
Induced Drag	Supervelocity Effect on Skin Friction	Camber Drag Supervelocity Effect on Profile Drag	Wave Drag Due to Lift	Drag Due to Lift Trim Drag Wave Drag Due to Lift

The matrix shown in Table 4.4 was reduced to a two-variable drag equation, shown in Equation 8.

$$C_D = C_{D,p} + C_{D,i} \tag{8}$$

In order to estimate the total aircraft drag, a combination of empirical and numerical methods were used. The method for obtaining the parasite drag coefficient, $C_{D,p}$, and induced drag coefficient $C_{D,i}$, are explained in detail in the following sections.

Parasite Drag Model

The parasite drag estimation follows the outline as presented in Table 4.4. Since the flow is within the low Reynolds number range, however, a few factors were considered negligible. Such terms include the shock-induced, wave drag, and scrubbing drag.

This method estimates the subsonic parasite drag of each component of the aircraft using a flat-plate

skin-friction drag analysis and a component "form factor" that estimates the pressure drag due to viscous separation. Interference effects of the component on the drag are estimated as a factor, where the total parasite drag is determined as the product of these terms and the wetted area. This can be expressed as Equation 9, where C_f is the component skin friction coefficient, FF is the component form factor, Q is the component interference drag factor, S_{wet} is the component wetted area, and S_{ref} is the reference area, taken as the wings planform area.

$$C_{D,p} = \sum \frac{C_f * FF * Q * S_{wet}}{S_{ref}} \tag{9}$$

This estimation technique implements the flat-plate skin friction analysis, where the skin friction coefficient C_f depends on the local Reynolds number, *Re* . The Reynolds number for each component was calculated to be between 158,000 and 928,000. Figure 4.6, taken from the white paper titled *Estimating R/C Model Aerodynamics and Performance* by Dr. Leland Nicolai, shows that the flow could be either turbulent or laminar in this region.

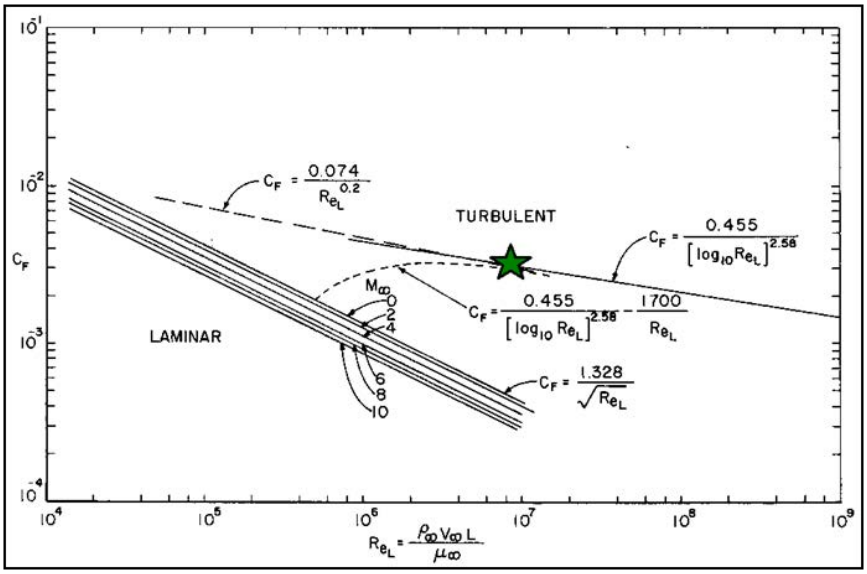

Figure 4.6 Skin Friction Coefficient as a Function of Reynold's Number

However, this parasite drag build-up considered the flow to be fully turbulent. This was believed to be a valid assumption considering the imperfect nature of manufacturing techniques and the effect of protuberances, such as linkages, control horns, and control surface gaps. Therefore, the skin friction was modeled using the von Karman-Schoener turbulent model, shown in Equation 10, where the Reynolds number was calculated based on an average speed of 60 feet per second and flying conditions at Wichita, Kansas. The fuselage form factor was found using Equation 11, as defined in Raymer's *(*Aircraft Design). Similarly, the wing's form factor was calculated using Equation 12,where $\frac{x}{c}$ is the location of maximum thickness and $\frac{t}{c}$ is the magnitude of maximum thickness of the wing as a percentage of the mean aerodynamic chord.

$$C_f = \frac{0.455}{(\log_{10} Re)^{2.58}} \tag{10}$$

$$FF = (1 + \frac{60}{f^3} + \frac{f}{400}) \tag{11}$$

$$FF = 1 + \frac{0.6}{\frac{x}{c}}(\frac{t}{c}) + 100(\frac{t}{c})^4 \tag{12}$$

Following the form factor, parasite drag is increased due to the mutual interference between components. This is described by the inference factor term, Q. Recommended values were used as given in Raymers *Aircraft Design*. For a conventional tail, the interference factor of four to five percent was suggested as a valid assumption. The latter value was selected to account for the extra drag from the gap between the tail surface and its control surfaces.

Table 4.5 Component Parasite Drag Build-Up

Component	L (inches)	Re x 10^5	Cf	FF	Q	S_{Wet} (inches^2)	Cd,p
Fuselage	35	9.28	0.0045	2.3	1	904	0.0197
Horizontal Tail	6.13	1.58	0.0065	1.1	1.05	184	0.0028
Vertical Tail	6.13	1.58	0.0065	1.1	1.05	135	0.0021
Wing	10	4.47	0.0035	1.39	1.05	960	0.0102
Landing Gear	-	-	-	-	-	6	0.0061
Total						2189	0.0409

Induced Drag Model

In order to accurately model the induced drag of the aircraft, Mark Drela's Athena Vortex Lattice (AVL) program was used. It is a standard vortex lattice code that uses horseshoe vortices to model the inviscid flow of the wing and tail surfaces. It can also model bodies, but in the documentation it states that they should normally be left out of the analysis. Instead, the fuselage was modeled as a vertical airfoil. Figure 4.7 shows the AVL model used for the induced drag analysis.

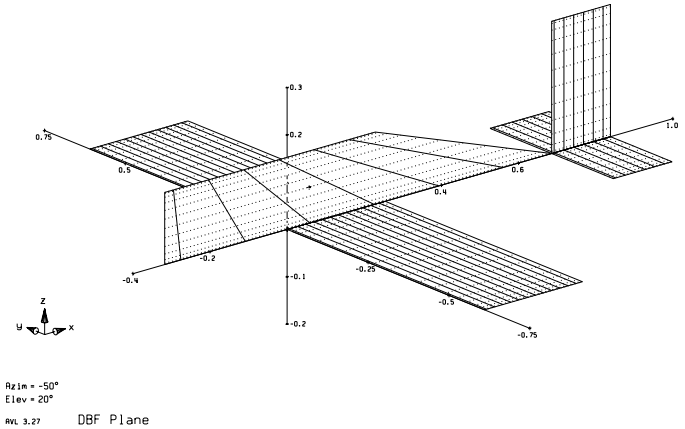

Figure 4.7 AVL Induced Drag Model

In order to obtain induced drag values, $C_{D,i}$, over a range of lift coefficients that could be combined with the parasite drag build-up, an angle of attack sweep was performed. Because a range of C_L's were analyzed,

a constant span efficiency did not have to be assumed. This creates a more accurate model of the aircraft's induced drag. The mass properties from the SolidWorks model were also included in the AVL model, so that a trim condition could be imposed. By applying a trim condition, the drag added by the control surfaces to maintain the desired zero pitching, rolling, and yaw moments was included in the drag model. One of the limitations of AVL is that it is an inviscid solver which means that it will not detect when the aircraft stalls. To ensure a valid model, no C_L values greater than the $C_{L,max}$ value obtained from XFoil were used. Since AVL does not provide a routine to perform an α sweep, the team developed a MATLAB interface to perform this task in an automated and repeatable way to ensure no error was introduced from manually recording C_L and $C_{D,i}$ values.

Drag Polar

To obtain the drag polar for the entire aircraft, the viscous drag terms from the parasite drag build-up were combined with the induced drag values from AVL. The resulting overall drag polar is shown in Figure 4.8. This information was given to other groups in the team in order to estimate key performance characteristics.

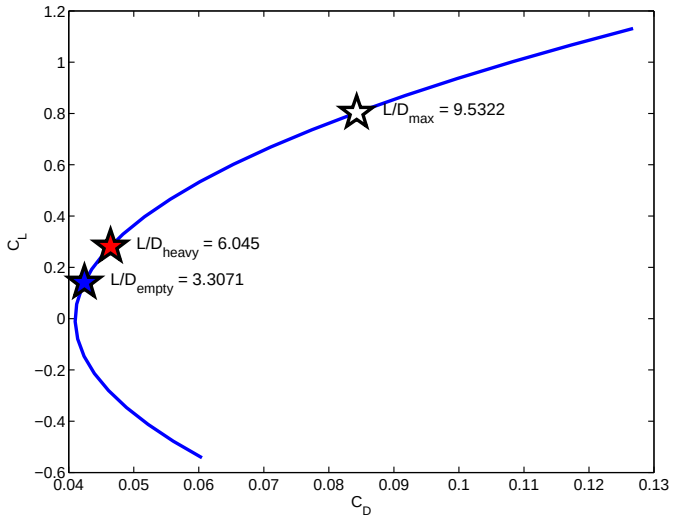

Figure 4.8 Total Drag Polar

4.4.3 Stability and Control

In order to fly an airplane without an advanced control system, the airplane needs to be both statically and dynamically stable. The static stability of an aircraft is a measure of the aircraft's response to a perturbation in pitch. If it is statically stable, the aerodynamic moments and forces should tend to force the plane back to its trimmed condition. The dynamic stability is similar to that of static stability in the sense that a dynamically stable aircraft should return to a trimmed condition if perturbed. However, examining the dynamic stability of an aircraft provides insight into the time required to return to the trimmed condition in more than just longitudinal modes.

Static Stability

It is difficult, if not impossible, to fly a statically unstable R/C aircraft. To ensure this did not happen with this design, the static stability of the aircraft was analyzed. Static margin is the simplest and most common way to describe an aircraft's static stability. It is defined as the distance between the center of gravity and the neutral point of the aircraft. If the center of gravity is located in front of the neutral point on the aircraft, it is said to have a positive static margin and any perturbation in the pitch of the aircraft will create an aerodynamic moment that returns the plane back to steady-level flight. An airplane is said to have negative static margin if the center of gravity is located downstream of the neutral point. In this case, any perturbation in the pitch of the aircraft will be compounded by an aerodynamic moment that will continue increasing angle of attack until the airplane stalls. If the center of gravity and the neutral point are at the same point on the aircraft, it is said to be neutrally stable.

For a conventional aircraft, an extended tail and a horizontal stabilizer are used to help move the aerodynamic neutral point aft and ensure the plane is statically stable. For any type of aircraft, the static margin, K_{sm}, is calculated using Equation 13.

$$K_{sm} = -\frac{C_{M_\alpha}}{C_{L_\alpha}} = \frac{x_{np} - x_{cg}}{MAC} \tag{13}$$

Positive static margin is required for a statically stable aircraft, and, in general, a five to ten percent static margin is acceptable. Having more than a ten percent static margin makes the airplane harder to maneuver. Having less than a five percent static margin may make the airplane overly responsive to elevator inputs and difficult for the pilot to control without the help of complicated flight computers. Negative static margin causes the airplane to be unstable, making it impossible for a pilot to control.

A positive static margin correlates to a statically stable aircraft. Because the static margin is positive, Table 4.6 shows that the plane is longitudinally stable for all three missions. Additionally all of the static margins are relatively small, which means there are small forces on the tail. This is desirable because the smaller the forces are on the tail, the more efficient the plane will be in flight and the more responsive the controls will be. For each mission, the static margin will be slightly higher than ideal, but will not significantly degrade the performance of the aircraft.

Table 4.6 Static Stability

Mission	$\mathbf{C_{M\alpha}}$	$\mathbf{C_{L\alpha}}$	$\mathbf{K_{sm}}$
Ferry	-0.43708	4.207255	10.4%
Maximum Payload	-0.36815	4.207255	8.8%
Medical Evacuation	-0.38100	4.207255	9.1%

Dynamic Stability

The root locus in Figure 4.9 shows that the fully loaded airplane only has one unstable pole. The root locus for the empty mission was very similar and omitted from the plot for clarity. The spiral pole has a slightly positive real component which indicates that the aircraft is unstable in this mode. If the airplane were to be pushed laterally by a large crosswind, then it would slowly begin to roll and eventually diverge if the pilot did not make any correction. However, because the divergence occurs slowly, the pilot can still maintain

control. The rest of the poles are dynamically stable and will return to steady-level flight conditions after any perturbation in pitch or side-slip angle without any corrective input from the pilot. Therefore, the plane is dynamically stable in roll, dutch roll, and longitudinal motion.

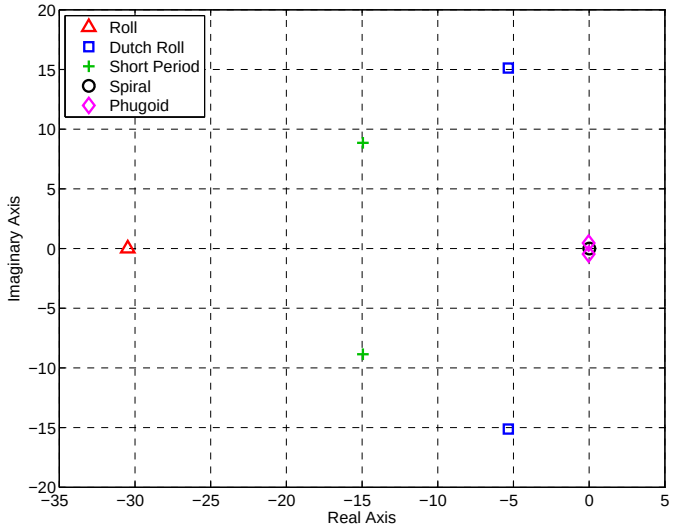

Figure 4.9 Pole-Zero Map from AVL Model

Control Surface Sizing

To provide the pilot with adequate control over the aircraft, a conventional control system that consisted of a rudder, elevator, and ailerons was used. Once this control system was selected, analysis needed to be performed in order to properly size each surface. In order to reduce manufacturing complexity, the rudder and elevator surfaces were designed to span the entire vertical and horizontal stabilizers respectively. Therefore, only the chord of these control surfaces needed to be determined. A maximum load case of flaring on a fast landing (35 mph) was used to determine the elevator chord. Several AVL models with different sized elevators were analyzed, and the smallest one that could maintain control authority without exceeding a 25 degree deflection angle was selected. A maximum deflection angle of 25 degrees was choosen to avoid stalling the control surface. From this the elevator was selected to be 33 percent of the horizontal chord. In order to maintain a simple interface between the rudder and elevator, the rudder chord was designed to be the same chord as the elevator.

In order to size the ailerons, the percent span and percent chord of the ailerons were varied in AVL and the hinge moments and deflections were calculated for entering and maintaining a six G turn. Once again any sizes which required deflections of more than 25 degrees were considered unacceptable to avoid control surface stall. The larger control surfaces provided more control authority, but decrease the overall lift generated by the wing. Therefore, the smallest control surface that could maintain the required control authority was selected. The resulting alieron size was 63 percent of the half span and 25 percent of the chord. All of these control surface sizes were validated with flight tests to ensure that the airplane had acceptable handling qualities.

4.4.4 Structural Design

As weight is the largest scoring factor in the competition this year, every effort was made to limit the weight of the aircraft. This was done even at the expense of other characteristics such as drag or structural strength where possible. To achieve this, the aircraft was designed with only two main structural components to carry the majority of the loads.

Wing Structure

The first main structural component was the wing. The wing was designed using longitudinally oriented wing ribs to provide shape for the wing surface. The ribs are located with an approximately five inch spacing from the fuselage to wingtips. They are connected by four spars in a box pattern running the entire span of the wing. The spars are spaced approximately 3.25 inches lengthwise and one inch vertically. A shear web is placed in front of the forward set of ribs and behind the rear set of ribs to handle torsion loads. Constructing the spars and shear web in this manner creates an I-beam type structure that has a much higher moment of inertia than the spars alone. Additionally, there are balsa sticks running diagonally from each spar-rib junction to the one across from it. This type of structure provides a large resistance to the bending load produced by wing lift, while minimizing weight.

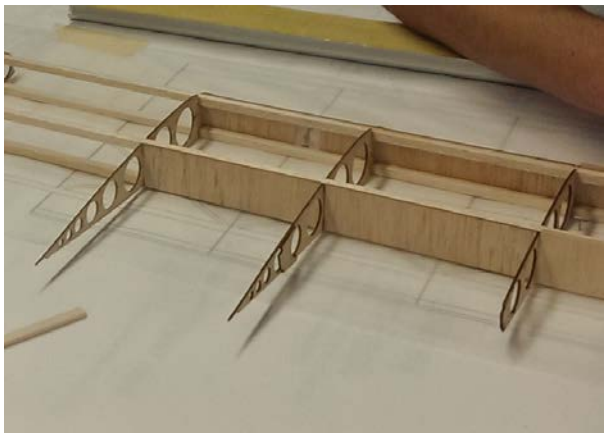

Figure 4.10 An example of wing structure design.

Two other wing structures which have proved successful for the club in the past were built and tested. One of these used carbon tubes as spars. This design did not incorporate a shear web or diagonal sticks. Instead, the very strong and stiff carbon rods were required to absorb the applied loads. This design was quickly ruled out as it was significantly heavier than the selected wing structure. It was decided that regardless of the potential gains in strength that carbon provides, this wing design was simply too heavy to produce an aircraft that would score competitively. The third structure that was built used balsa spars and a shear web in the same configuration as the selected design. Instead of using the cross beams, it used a D-box on the leading edge to absorb the torsion in the wing. This design involved wrapping a thin sheet of balsa around the wing ribs to enclose the area in front of the forward wing spars. This design proved to be slightly lighter than the selected wing, however, it failed under a smaller torsion load than the selected design when tested. It was decided that in this case, the weight savings was not enough to justify the loss in strength.

Backbone Structure

The second main structural component was the backbone of the aircraft. The idea behind the backbone was to have a single, strong structural member running the length of the aircraft that integrated each component in a way that was structurally sound. Based on past experience, it was decided that this backbone concept would provide a weight savings over a structural fuselage of equal strength. The backbone is a tube made

from a thin, rolled sheet of balsa wood. Throughout the length of the backbone, thin, circular balsa ”coins” are placed at approximately three inch spacing inside the tube to resist buckling. As it is a circle, this structure has relatively high torsion strength for its weight. Figure 4.11 shows an example of this type of construction. Ideally, the backbone would run the entire length of the airplane unbroken. Due to the small vertical spacing between the wing spars, and the team's choice to support the payload directly above the wing, the backbone had to either be broken at the wing spars, or pass beneath them. Each of these cases presented challenges in transferring both bending and torsion loads between the wing spars and the backbone. Passing the backbone underneath the spars presents the difficulty of securely attaching a circular piece to a flat piece tangent to it. Making this connection strong against normal and shear forces in every direction seemed both difficult and heavy. Instead, it was decided to pass the backbone through the wing spars. This requires essentially sandwiching the forward and rear spar pairs between two sections of backbone. Between the wing spars, a carbon fiber tube was used to transfer loads between the two ends of the backbone. This carbon tube is held into the balsa tube by thicker coins filling the space between the two components. At the interface between the backbone and the wing spars, the backbone was capped off using a balsa coin and glued to the shear web on the wing spars.

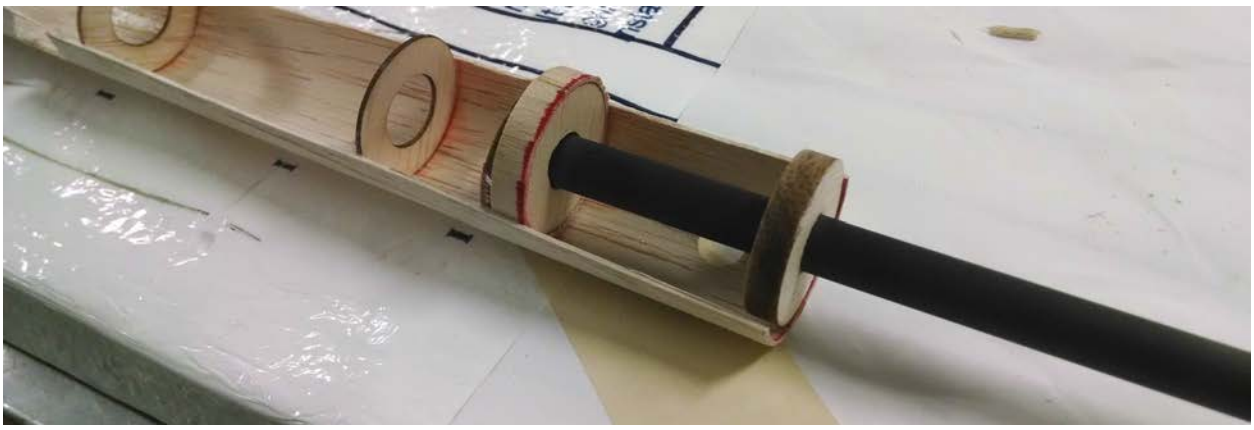

Figure 4.11 A Cutaway of the Backbone Structure, Showing Balsa Wrap, coins, and Carbon Backbone.

The tail assembly is simply built directly into the backbone. The tail sits in slots cut into the backbone and the backbone is capped on the end to minimize the loss of strength associated with cutting the backbone. This allows all the torsion and bending experienced by the tail to be directly transferred into the main structure of the aircraft.

The main landing gear is supported at the junction between the backbone, carbon tube, and wing spars. A piece that wraps around the carbon tube and sits between the wing spars was integrated into the structure. The landing gear struts slide directly into this piece. The loads experienced by the main landing gear are transferred into the junction between the wing spars and carbon tube. The rear landing gear is integrated into the connection between the backbone and tail assembly. The tail wheel is controlled and supported by a wire that runs vertically along the front of the rudder. To minimize the amount of force transferred from the tail wheel into the rudder, the wire runs through a support that fills in the connection between the backbone and tail assembly. Most of the forces and moments experienced by the tail wheel will be transferred into the backbone-tail interface rather than the rudder.

The motor is also integrated directly into the balsa wood backbone. It is screwed into the back of the plywood coin that caps the front of the backbone. Additionally, it is supported internally by balsa coins that fill the space between the motor and backbone.

Fuselage Structure

Lastly, the payload, the most significant source of internal load on the aircraft, must be securely and safely integrated into the airplane. The team made every attempt to use the existing structure to support the payload so as to not add extra weight specifically for the payload. The selection of a low wing configuration made this easier as the payload could be placed on top of the main wing and backbone structure. The wing spars and backbone were designed such that they made a level, uninterrupted floor for the large payload to sit on. Small stops were put in place on the floor to constrain the payload longitudinally. A foam fuselage housing was designed to contain the payload in the spanwise direction as well as keep the aircraft as aerodynamic as possible. There are a few points integrated into both the floor and the foam housing that screws are set into. These screws are used as a tie-down locations for kevlar string that secures the payload from moving vertically. Since the floor of the airplane is made of the strongest structural members on the aircraft, very little reinforcement was needed to accommodate the payload.

4.4.5 Propulsion Design

In order to design the propulsion system, a propulsion model that could estimate key performance characteristics was required so that trades between performance of different systems could be made. The model consisted of a simplified electric motor model, UIUC propeller data, and a battery model. The entire propulsion model was created in MATLAB and combined all of these models to compute thrust, current, and RPM for a given motor, propeller, and voltage.

The electric motor model was based on simplified steady-state DC motor equations. Equation 14 can be used to compute the RPM of a DC motor where K_V is the voltage constant and V_i is the ideal voltage supplied to the motor.

$$RPM = K_V V_i \tag{14}$$

However, the model needs to include the voltage drop due to propeller loading. With this additional consideration RPM can be computed using Equation 15 where R_A is constant and V is the input voltage and function of the throttle input.

$$RPM = K_V(V - IR_A) \tag{15}$$

The current, I, is a function of the RPM, propeller power coefficient, C_p, and motor no load current, I_0. Therefore, Equation 15 becomes Equation 16, the final equation for RPM used in the motor model.

$$RPM = K_V[V - I(RPM, C_p, I_0)R_A] \tag{16}$$

Since the equation for RPM is itself a function of RPM an iterative approach has to be used to solve for the

actual motor RPM.

Once the RPM is computed for a given motor, propeller, voltage, and velocity combination, current and thrust can be easily found. Current can be found using Equation 17.

$$I = \frac{V - \frac{RPM}{K_V}}{R_A} \tag{17}$$

The thrust can be found using Equation 18 where C_T is the thrust coefficient of the propeller, ρ is density, v is velocity, and d_{nd} is the non dimensional propeller diameter.

$$T = C_T(RPM, v, d_{nd})\rho\left(\frac{RPM}{60}\right)^2 d_{nd}^4 \tag{18}$$

Once the propulsion model was developed, different motor propeller combinations were explored that would provide enough thrust to meet the 40 foot takeoff requirement. In order to estimate the ground roll distance an approach from a white paper by Leland M. Nicolai was used.[3] Equation 19 shows the equation used to compute the takeoff ground roll distance where V_{TO} is the takeoff velocity and a_{mean} is the acceleration at 70 percent of the takeoff velocity.

$$S_G = \frac{V_{TO}^2}{2a_{mean}} \tag{19}$$

The takeoff velocity is defined in Equation 20 where W is weight, S is wing area, and C_{Lmax} is the two dimensional C_{Lmax} of the wing.

$$V_{TO} = \left[2\frac{W}{S\rho 0.8 C_{Lmax}}\right]^{\frac{1}{2}} \tag{20}$$

Equation 21 can be used to find the mean acceleration where T is thrust, D is drag, F_C is the rolling friction coefficient, and L is lift. Lift and drag can be computed using the aerodynamic models from the previous sections.

$$a = \left(\frac{g}{W}\right)[(T - D) - F_C(W - L)] \tag{21}$$

Therefore, for a desired takeoff distance the required thrust can be found. Figure 4.12 shows the relationship between thrust to weight and wing loading for the required 40 takeoff distance. Since the wing area and airfoil were already selected, the thrust required could be determined for the predicted heavy weight of four pounds. From this curve the thrust required at the takeoff velocity was 1.95 pounds. The star on Figure 4.12 shows the design point for the aircraft. The design point lies on the curve even though anywhere above the line could be selected because adding more thrust will increase the aircraft's weight and according to the scoring sensitivities the lightest aircraft will score the best.

Once a thrust was selected, several different motors with several different propeller combinations were run through the propulsion model. Using the propulsion model it was determined that a Neu 1105 motor with

[3]Nicolai, Leland M."Estimating R/C Model Aerodynamics and Performance"

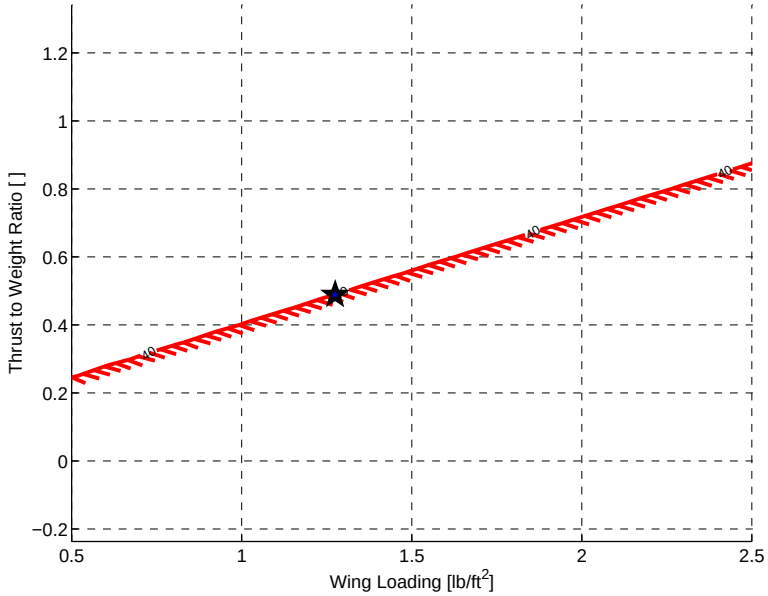

Figure 4.12 Thrust to Weight Ratio versus Wing Loading

a 6.7 gear box would be used with a 13x10 propeller for Mission 2 and Mission 3. For Mission 1 a 13x4 propeller would be used since it will operate more efficiently during cruise, but provide less static thrust.

In order to determine the number of cells needed to provide the required voltage, a battery model was used. Since, the battery voltage drops considerably from its nominal voltage when current is applied this must be taken account for when selecting the number of battery cells. Based on test data from previous years, the relationship between current and voltage for NiMh battery cells can be determined using Equation 22 where n_{cells} is the number of cells.

$$V = (1.35 - 0.022I) * n_{cells} \tag{22}$$

Based on this, eleven cells were needed to provide the necessary voltage to power the motor at 15 Amps.

4.5 Preliminary Mission Performance

Using values computed during the preliminary analysis, the vehicle's performance was found for each mission. These values were then used to obtain the parameters required for the scoring equations.

The first mission depended on the number of laps flown, and Figure 4.13 shows the relationship for the number of laps as a function of cruise velocity. The second mission scoring parameter was simply the number of cubes the aircraft was designed to hold. For the third mission the total time to fly three laps was computed using the total distance for each lap divided by the cruise velocity.

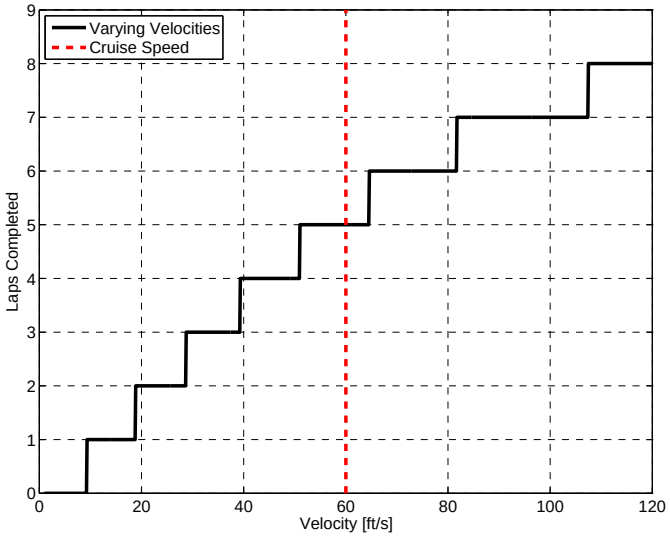

Figure 4.13 Speed vs. Laps Completed with 5G Turns

Table 4.7 summarizes the key performance parameters of the aircraft for each flight mission and the associated mission score. In order to compute the mission scores the same assumptions from the sensitivities analysis were used for performance of other teams. None of the mission scores are likely to be the highest at the competition. However, the rated aircraft cost-adjusted score should be quite competitive because of the importance of empty weight.

Table 4.7 Mission Performance and Scores

	Vehicle Parameter	Scoring Parameter	Score
Mission 1	Airspeed 60 ft/s	Number of Laps 5 laps	1.25
Mission 2	Heavy Weight 4 lbs	Number of Cargo 2	2
Mission 3	Heavy Weight 4 lbs	Flight Time 150 sec	3.60
		Total Flight Score RAC Adjusted	6.85 3.43

5 Detail Design

Detail design of the aircraft began as the latter stages of the preliminary design wrapped up. The detail design process tends to be shorter than preliminary design, but is equally important. To achieve the highest possible score, the entire detail design process was completed with weight in mind. While ease of manufacturing and similar considerations must factor in, weight was given the highest priority. The overall dimensions of the aircraft, structural features, and the subsystems were all designed to their final configurations in this phase.

5.1 Dimensions and Parameters

Table 5.1 shows the major dimensional parameters of the aircraft. These parameters were primarily a result of preliminary design choices and were driven largely by the wing and tail sizing requirements. Table 5.2 contains the parameters that describe all of the aerodynamic surfaces of the aircraft. These two tables provide a starting point for the detail design process.

Table 5.1 Aircraft Dimensional Parameters

	Length [inch]	**Width** [inch]	**Height** [inch]
Aircraft	44.5	48	20.25
Fuselage	36.75	7	7.25

Table 5.2 Aerodynamic Surface Dimensional Parameters

	Airfoil	**Span** [inch]	**Chord** [inch]	**Area** [inch^2]	**Max Thickness**	**Aspect Ratio**
Wing	atr72sm gapped	48	10	480	14.5%	4.8
Vertical Stabilizer	Flat Plate	11.25	6	67.5	.25 in	1.875
Horizontal Stabilizer	Flat Plate	15	6	90	.25 in	2.5

5.2 Structural Characteristics

During the aircraft design process, each piece of the aircraft was modeled SolidWorks. Initially, these models were put through stress and bending analyses, using the built-in finite element analysis (FEA) tools in SolidWorks to test for feasibility. As the design progressed, many of these models could be stress tested using realistic loads that would be experienced in flight which enabled their design to be refined to achieve acceptable strength without excess weight. Although, the ability to quickly simulate a stress test using computer software is a very powerful tool, it has many significant limitations. FEA tools assume that the material is a continuum and displays uniform behavior. In reality, these structures are built using discrete pieces which are cut and glued together. Depending on the quality of the cut and glue joint, the real life performance may closely match the FEA prediction, or may display highly degraded performance. Also, some of the aircraft components have a thin plastic covering. This type of coating was not included in the FEA simulations due to the lack of information on its structural qualities and since the plastic is sufficiently thin it is not considered a solid member. However, the coating should provide a small increase in strength. Regardless, these FEA models are very useful as predictions for the relative performance between designs.

When fully loaded, the aircraft weighs a little more than four pounds. The wing is required to support the entire weight of the plane through the turns. A single wing was simulated using a two pound distributed load, which should be approximate steady level flight conditions. The FEA simulation predicted a minimum factor of safety of approximately 6.5 at the wing centerline with a maximum deflection of approximately 0.24 inches at the wing tip. This corresponds to a three G turn with a 2.167 factor of safety. Given the slight

increase in strength provided by the covering and the decrease in strength from the glue joints, this factor of safety is considered acceptable for construction. Because this aircraft is designed for cargo transport it will not be performing any high-G turns during flight. Based on this analysis, this wing design meets the needs of the aircraft with an acceptable factor of safety.

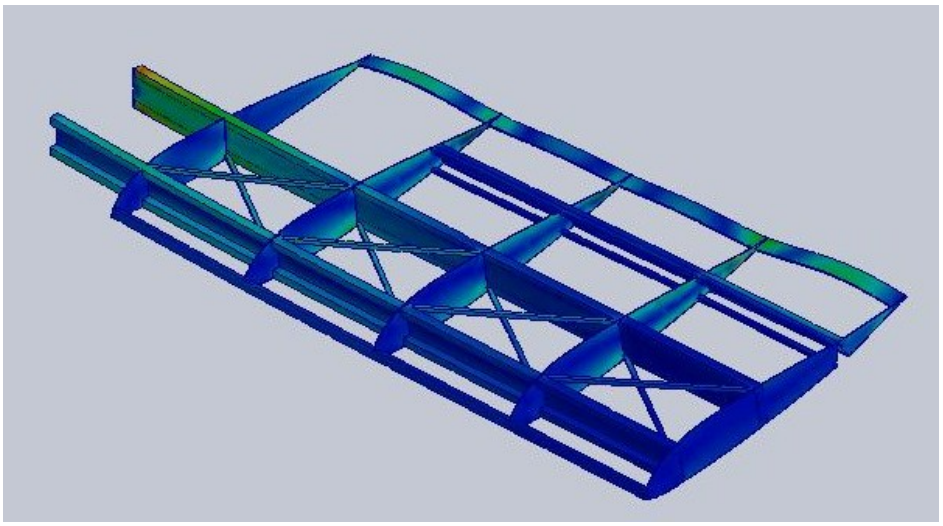

Figure 5.1 Wing Stress Under a Distributed Load.

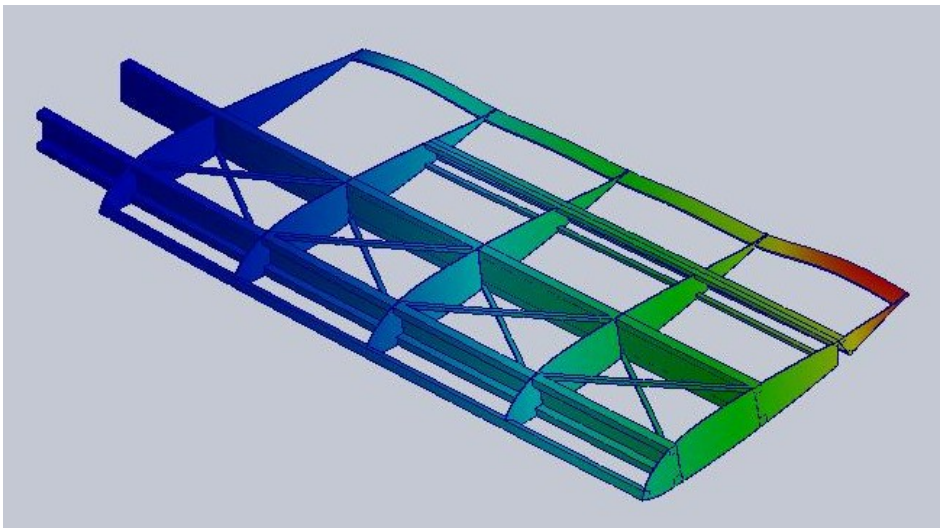

Figure 5.2 Wing Deflection Under a Distributed Load.

The other main structural component in the aircraft is the balsa backbone. It is broken into two pieces on either side of the wing box. Due to the limited capabilities of the student version of SolidWorks, the backbone with carbon connection rod cannot be simulated using FEA. Since the carbon fiber is incredibly strong, it is assumed to be sufficiently reliable to carry any load experienced by the plane. Each half of the backbone will be analyzed separately to gain an understanding of the strength of the whole piece. The tail section must carry any torsion and bending forces induced by lift from the tail and the loads induced by the landing gear on the runway. It is expected that a typical load for either of these is approximately one

pound. The simulation will be run for a one pound load distributed across the entire tail vertical stabilizer. The FEA simulation predicts a minimum factor of safety of approximately 5.2 at the connection to the wing spars and a maximum deflection of 0.24 inches at the end of the tail. Based on this analysis, this section of the backbone should meet the needs of the aircraft with an acceptable safety margin. The front part of the backbone is constructed in the same manner and will not experience larger forces than the rear. Both pieces should be suitable for use on the aircraft.

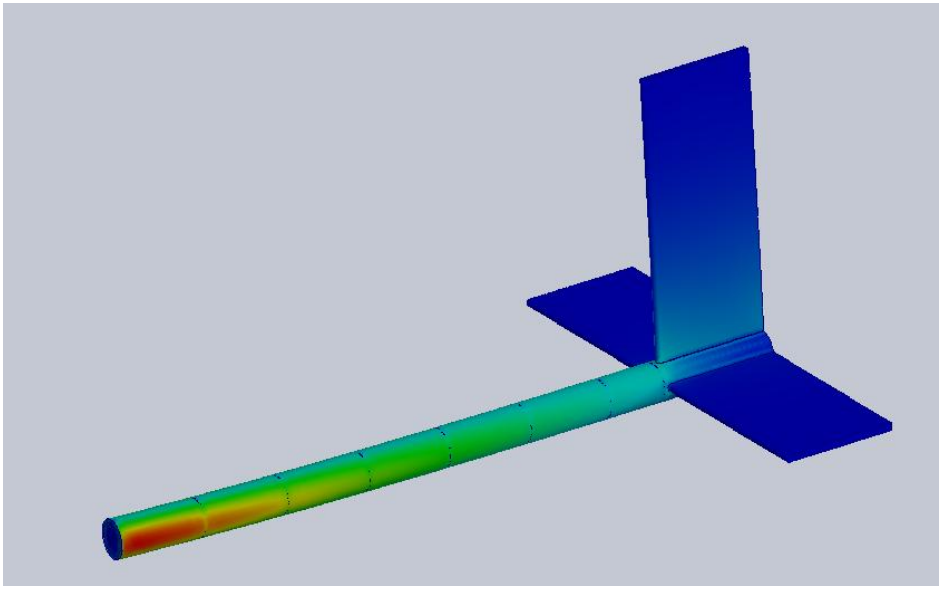

Figure 5.3 Backbone Stress Under a Distributed Tail Load

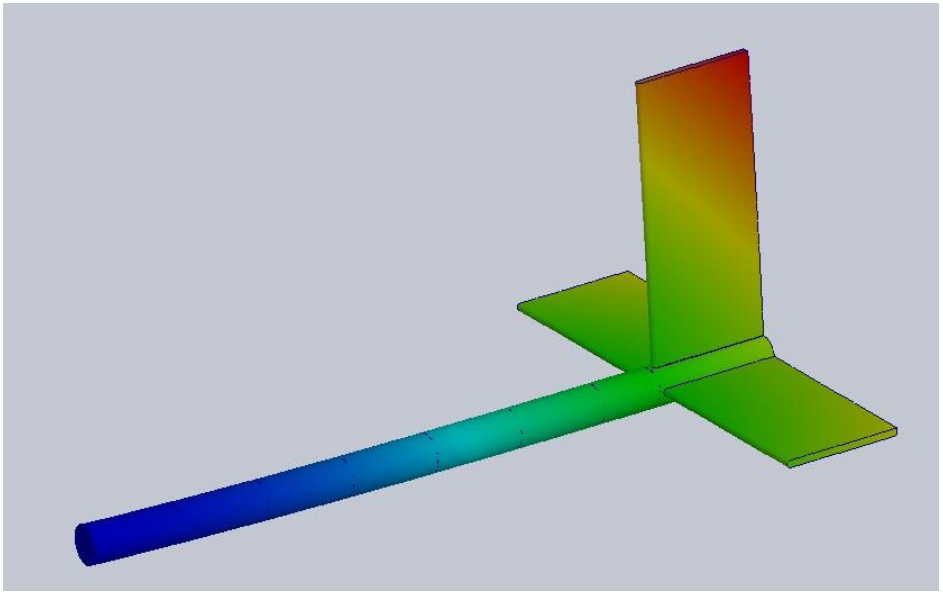

Figure 5.4 Backbone Deflection Under a Distributed Tail Load.

5.3 Subsystems Design

The subsystem design primarily involves choosing electronic components for the aircraft. These choices have a dramatic effect on aircraft flight performance as the capability and weight of the components vary. From the preliminary design section, the minimum requirements for each component were known at this stage. Each considered component was first found to be capable of performing the required task. From there, the choice was made based on weight, quality, and size.

5.3.1 Servo Selection

The aircraft is controlled using a familiar layout of wing ailerons, a vertical tail rudder, and a horizontal tail elevator. These control surfaces are actuated using servos stored in either the wing or the fuselage. In order to obtain hinge moment coefficients, a model of the aircraft was analyzed in AVL. The hinge moment coefficient is defined in Equation 23, where HM is the aerodynamic moment at the pivot point of the control surface, q is the dynamic pressure, S in the planform area, and c is the mean aerodynamic chord. The hinge moments were calculated at maximum velocity with control surface deflections of 25 degrees. This is considered to be the worst case scenario for the control surfaces. As long as the selected servo can handle this hinge moment, it will be able to perform under all normal flight conditions experienced by the aircraft. The simulation in AVL produced hinge moment coefficients as seen in Table 5.3. The hinge moments calculated using Equation 23 are shown in Table 5.3.

$$C_{HM} = \frac{HM}{qSc} \tag{23}$$

Since the aileron servos will be placed inside of the wing structure, there is an additional size limitation of those servos. Using all of these design constraints, servos that would suit our needs were compared using a database of specification. The selected servos were the MKS DS450 for the ailerons, the Protech B1044 for the elevator and the Bluebird BMS-303JST for the rudder. These servos and the ones they were compared against can be seen in Table 5.4.

Table 5.3 Hinge Moments

Surface	C_{HM}	HM [inch-ounces]
Elevator	6.03E-03	13.2
Aileron	1.37E-02	29.9
Rudder	4.50E-03	9.8

Table 5.4 Servo Selection

Brand	Model	Modulation	Control [in-oz]	Weight [oz]	Length [in]	Width [in]	Height [in]
Blue Bird	BMS-303	Analog	11	0.15	0.75	0.29	0.61
Blue Bird	BMS-303DD	Digital	11	0.13	0.75	0.29	0.61
Blue Bird	BMS-303JST	Analog	11	0.12	0.75	0.29	0.61
MKS	DS 460	Digital	37.8	0.34	0.89	0.39	0.93
MKS	DS 450	Digital	43.1	0.34	0.89	0.39	0.93
Hyperion	DS11-SCB	Digital	47.2	0.35	0.93	0.45	0.83
Dymond	D47	Digital	20	0.17	0.89	0.32	0.79
Protech	B1049	Analog	20.8	0.17	0.79	0.31	0.64
Protech	B1044	Analog	18.1	0.16	0.75	0.3	0.63

5.3.2 Electronic Speed Controller Selection

Once the propulsion model was finalized, an electronic speed controller (ESC) could be selected. Due to the current limit of 15 Amps, a speed controller with a maximum range of at least 15-20 Amps would be required for a sufficient safety margin. Additionally, the ESC would need a maximum voltage of at least 14 volts. A list of acceptable ESCs was compiled from a database using these requirements. The selected ESC, the Castle Creations Talon 15, and those that it was compared against can be seen in Table 5.5. The primary considerations for this choice were the weight of the ESC and its features. This will meet the needs of the propulsion system with an acceptable margin of safety.

Table 5.5 ESC Selection

Manufacturer	Model	Weight [oz]	Max Current [A]	Max Voltage [V]	Length [in]	Width [in]	Height [in]
Castle Creations	Talon 25	0.63	25	22.2	1.72	0.72	0.32
Castle Creations	Talon 15	0.25	15	14.8	1.1	0.58	0.32
Castle Creations	Thunderbird 18	0.6	18	15	1.32	0.9	0.34
ElectriFly	GPMM1820	0.92	25	14.8	1.58	1.02	0.31
FlightPower	FPWFTC18A4SB	0.64	18	14.8	1.85	1.02	0.28

5.3.3 Receiver Selection

Several different factors played into the selection of the receiver. The fail safe restrictions in the competition require a programmable receiver which cuts the list of available choices down considerably as many receivers are not capable of meeting this requirement. Additionally, a minimum of five channels are needed to control the various components on the aircraft. Receivers that utilize a 2.4 GHz frequency were favorable due to decreased interference. Lastly, receivers with greater maximum output voltage were advantageous due to the ability to draw more power from the lightest possible servos. Table 5.6 contains a list of receivers that meet the design needs. Ultimately, the Hitec Minima 6L was chosen because of its reduced weight and features.

Table 5.6 Receiver Selection

Brand	**Model**	**Weight** [oz]	**# Channels**	**Min** [V]	**Max** [V]	**Length** [in]	**Width** [in]	**Height** [in]
HITEC	Minima 6T	0.23	6	4.8	8.4	1.22	0.82	0.28
HITEC	Minima 6L	0.14	6	4.8	8.4	1.25	0.82	0.43
HITEC	Maxima 6	0.23	6	3.7	9	1.3	0.82	0.42
HITEC	Optima 6 Lite	0.35	6	4.8	7.4	1.77	0.73	0.37
Spektrum	AR610	0.3	6	3.5	9.6	1.19	1.03	0.48

5.4 Weight and Balance

Creating a weight and balance table for the aircraft during and after the design process is very important for a few reasons. First, to verify the sources of weight across the whole aircraft and identify places that weight could be reduced. Second, to account for each component's contribution to the center of gravity of the aircraft. To do this, a datum was established at the nose of the aircraft where the +X axis is upstream of the nose, the +Y axis is out the right wing, and the +Z axis is down. The following three tables are a complete account of each piece of the aircraft, listing their respective weights and center of gravity locations.

Table 5.7 accounts for only the empty aircraft components. Since the first mission is unloaded, this table contains the weights and balance for Mission 1. Table 5.8 and Table 5.9 contain the weights and balance of the payloads for their respective missions and the empty aircraft.

Table 5.7 Empty Aircraft Weight and Balance Table

Component	**Mass** [ounces]	**X** [inches]	**Y** [inches]	**Z** [inches]
Right Wing Servo	0.70	-19.30	14.40	0.40
Left Wing Servo	0.70	-19.30	-14.40	0.40
Rudder Servo	0.70	-29.90	0.00	-0.90
Elevator Servo	0.70	-28.20	0.00	-0.90
Battery Pack	9.18	-23.80	0.10	-0.20
Receiver Pack	1.95	-4.18	0.00	-0.90
Receiver	0.50	-4.50	0.00	-1.50
ESC	0.80	-5.90	0.00	-1.30
Motor	6.80	-2.10	0.00	0.00
Wires	1.00	-18.00	0.00	0.00
Backbone	1.60	-19.00	0.00	0.00
Wing Structure	4.96	-17.30	0.00	0.00
Tail Horizontal	1.28	-41.80	0.00	0.00
Tail Vertical	0.96	-41.70	0.00	-5.94
Tail Wheel	0.05	-42.40	-0.10	1.90
Tail Gear Strut	0.20	-42.40	-0.10	0.70
Tail Gear Mount	0.16	-42.01	0.00	0.40
Front Wheels	0.32	-15.40	0.00	7.70
Front Gear Strut	0.16	-15.40	0.00	4.50
Front Gear Mount	0.32	-15.30	0.00	0.20
Foam Fuse	1.76	-16.30	0.00	-3.30
Floor Spars	0.48	-16.10	0.00	-0.54
Propeller	1.76	-0.16	0.00	0.00
Totals:	**37.04**	**-16.46**	**0.02**	**-0.39**

As seen in Table 5.7 the empty aircraft weighs 37.04 ounces. The center of gravity is located slightly behind the quarter chord of the wing, but still far enough in front of the aerodynamic center to remain stable. Table 5.8 shows the total weight and center of gravity for the payload in Mission 2. The weight for this mission is 69.04 ounces and the center of gravity has moved slightly forward. This will cause the aircraft to be more stable, but less responsive. Table 5.9 shows the total weight and center of gravity for the payload in Mission 3. The values, and consequently, performance should be nearly identical to Mission 2.

Table 5.8 Mission 2 Weight And Balance Table

Component	**Mass** [ounces]	**X** [inches]	**Y** [inches]	**Z** [inches]
Empty Airplane	37.04	-16.46	0.02	-0.39
Payload Cube #1	16	-12.63	0	-3.65
Payload Cube #2	16	-18.625	0	-3.65
Totals:	**69.04**	**-16.07**	**0.01**	**-1.90**

Table 5.9 Mission 3 Weight And Balance Table

Component	**Mass** [ounces]	**X** [inches]	**Y** [inches]	**Z** [inches]
Empty Airplane	37.04	-16.07	0.01	-1.90
Patient #1	8	-20.125	1	-1.65
Patient #2	8	-11.125	1	-1.65
Attendant #1	8	-12.75	-2	-3.65
Attendant #2	8	-19.75	-2	-3.65
Totals:	**69.04**	**-16.01**	**-0.22**	**-2.25**

5.5 Performance Parameters

During the detail design process, realistic flight performance parameters can be estimated. From this, along with the data collected from the various prototype flights, a realistic prediction of the performance of the aircraft can be made. This process was also useful to compare the predicted performance from the preliminary design to the demonstrated performance so adjustments could be made.

5.5.1 Flight Performance

Using demonstrated performance from the prototype aircraft flown, a flight performance analysis was conducted. The results of this analysis can be seen in Table 5.10.

Table 5.10 Flight Performance Metrics

	Mission 1	Mission 2	Mission 3
Cruise Speed [$\frac{ft}{s}$]	60	54	54
Stall Speed [$\frac{ft}{s}$]	20.5	29	29
Maximum Instantaneous Turn [g's]	6.0	3.0	3.0
Static Margin [% of MAC]	10.4%	8.8%	9.1%
Wing Loading [$\frac{lb}{ft^2}$]	0.695	1.295	1.295

5.5.2 Mission Performance

The results of the performance analysis and data from prototype aircraft flights were used to estimate the final mission performance and scoring. This can be seen in Table 5.11.

Table 5.11 Predicted Mission Performance

Mission	Empty Weight [oz]	Takeoff Weight [oz]	Mission Variable	Score
Mission 1	37.04	37.04	5 laps	1.25
Mission 2	37.04	69.04	2 cubes	2.0
Mission 3	37.04	69.04	150 seconds	3.6
Taxi Test	37.04	69.04	Pass	1.0
Total Score				**6.85**

5.6 Drawing Package

During the design process, a complete model of the aircraft was constructed in the 3D solid modeling software SolidWorks. The following drawings are from that model. This drawing package includes a three view drawing showing the major dimensions of the aircraft, a structural arrangement drawing, a systems layout drawing, and two drawings showing the location and configuration of the two payloads. Some components have been hidden for clarity. For example, a significant part of the plane was covered with MicroLite which is not shown in the drawings.

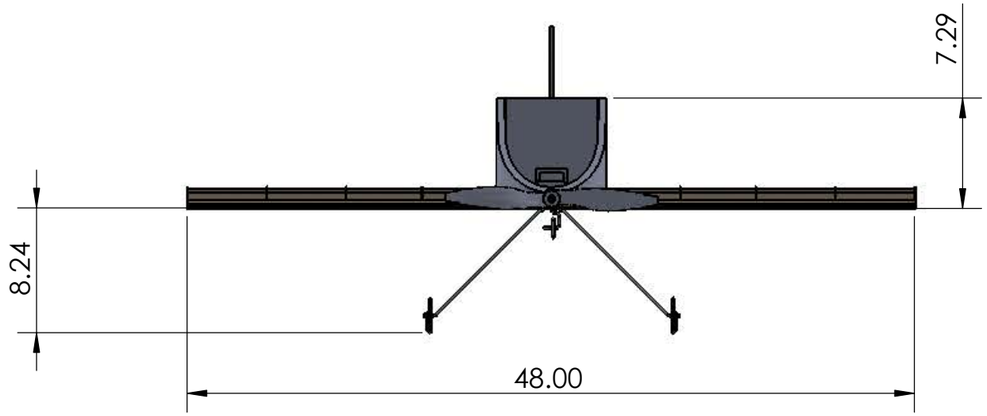

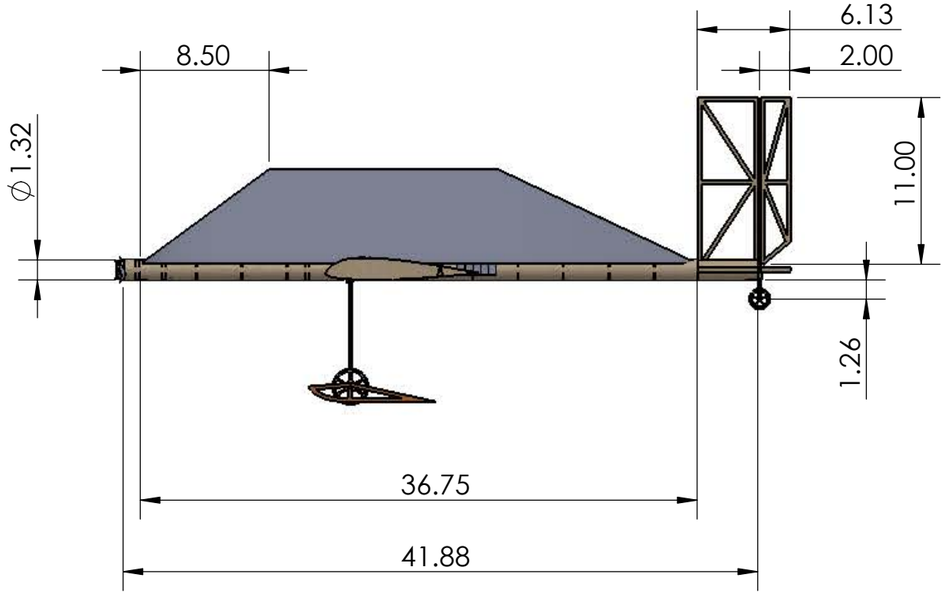

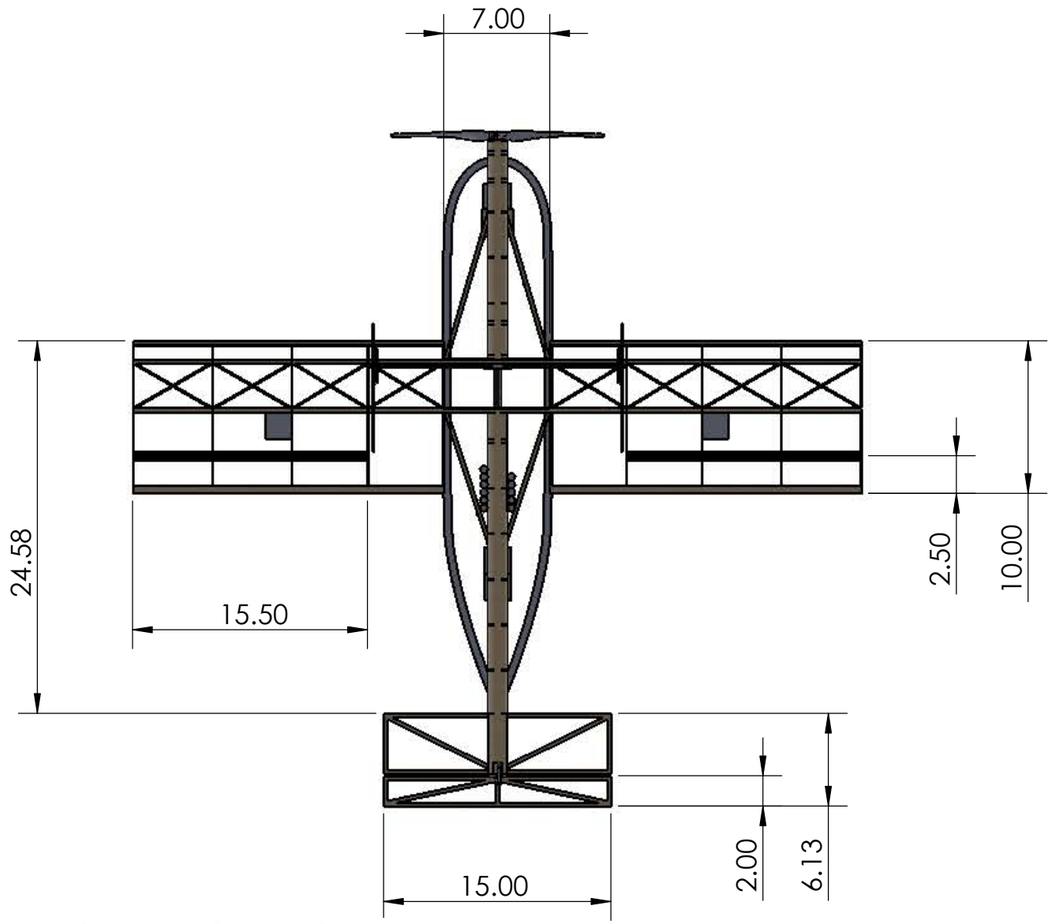

CALIFORNIA POLYTECHNIC STATE UNIVERSITY SAN LUIS OBISPO
DESIGN/BUILD/FLY 2013/2014

DOCUMENT TITLE:

AIRCRAFT 3-VIEW

SIZE	APPROVAL DATE:	DRAWING NUMBER
B	02/20/2014	2014-01

UNLESS OTHERWISE SPECIFIED ALL DIMENSIONS ARE GIVEN IN INCHES	APPROVED BY: Reed Williston

SCALE 1:10	REPORT PAGE 42	SHEET 1 of 5

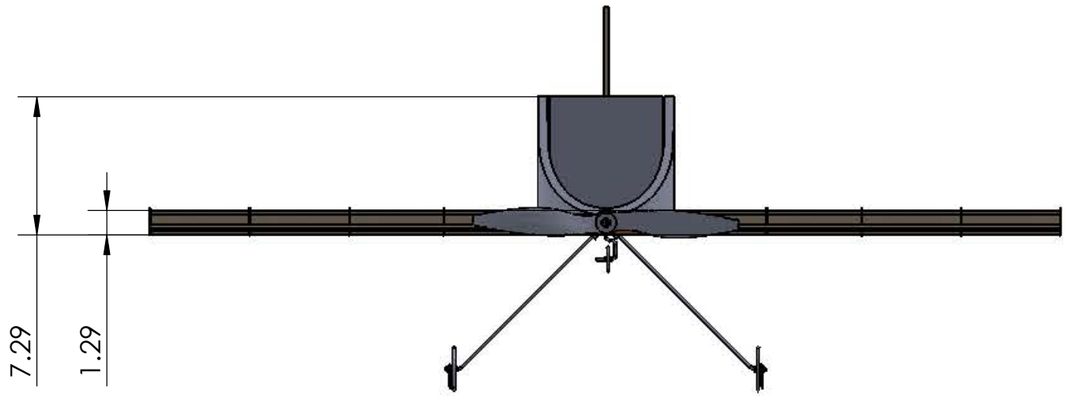

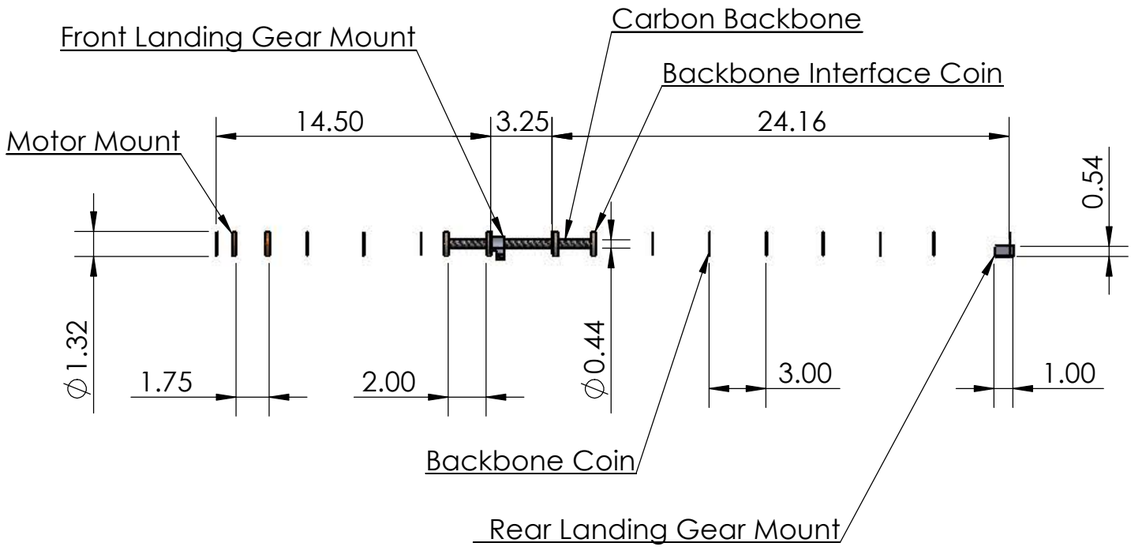

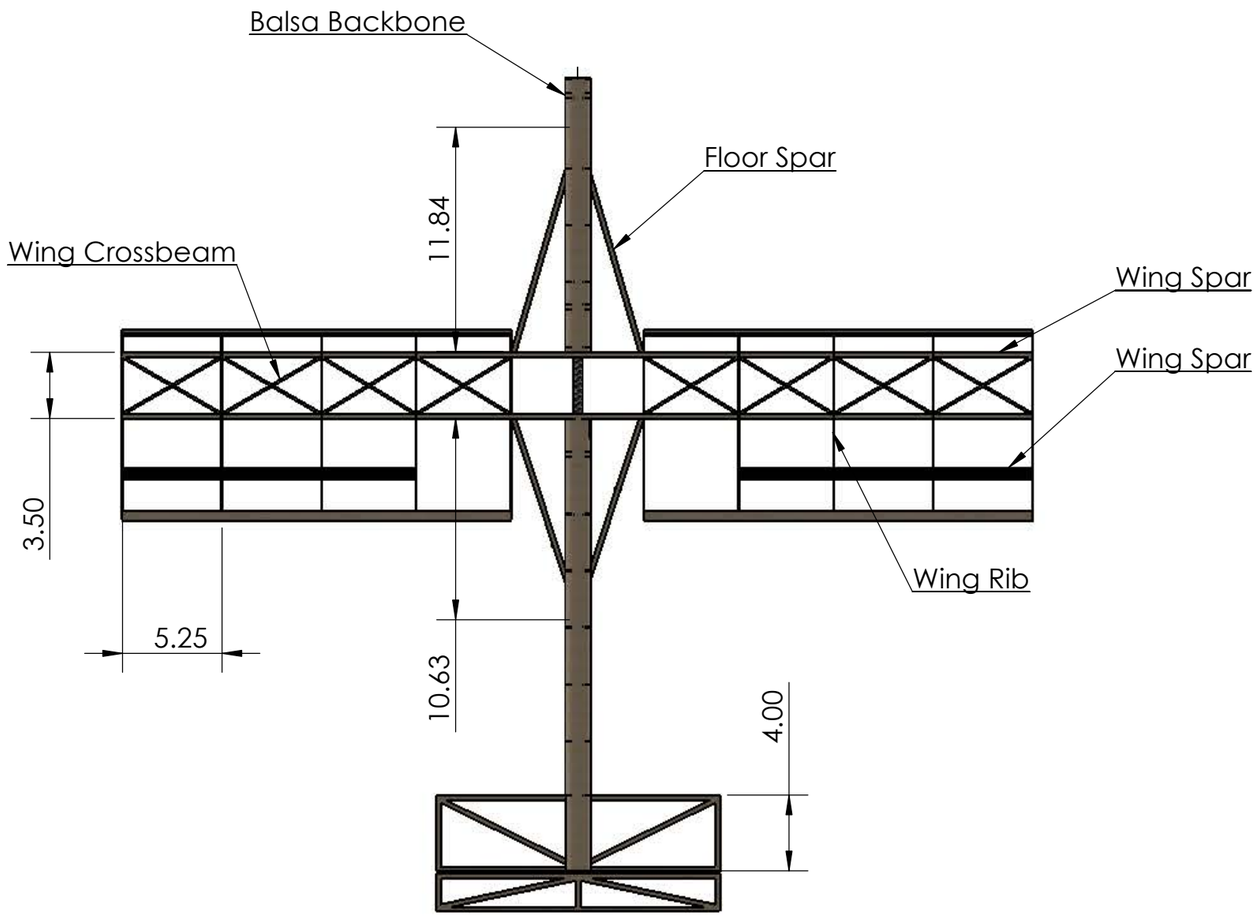

SolidWorks Student License
Academic Use Only

CALIFORNIA POLYTECHNIC STATE UNIVERSITY SAN LUIS OBISPO
DESIGN/BUILD/FLY 2013/2014

DOCUMENT TITLE:

Structural Design

SIZE	APPROVAL DATE:	DRAWING NUMBER
B	02/20/2014	2014-02

UNLESS OTHERWISE SPECIFIED ALL DIMENSIONS ARE GIVEN IN INCHES	APPROVED BY: Reed Williston

SCALE 1:8	REPORT PAGE 43	SHEET 2 of 5

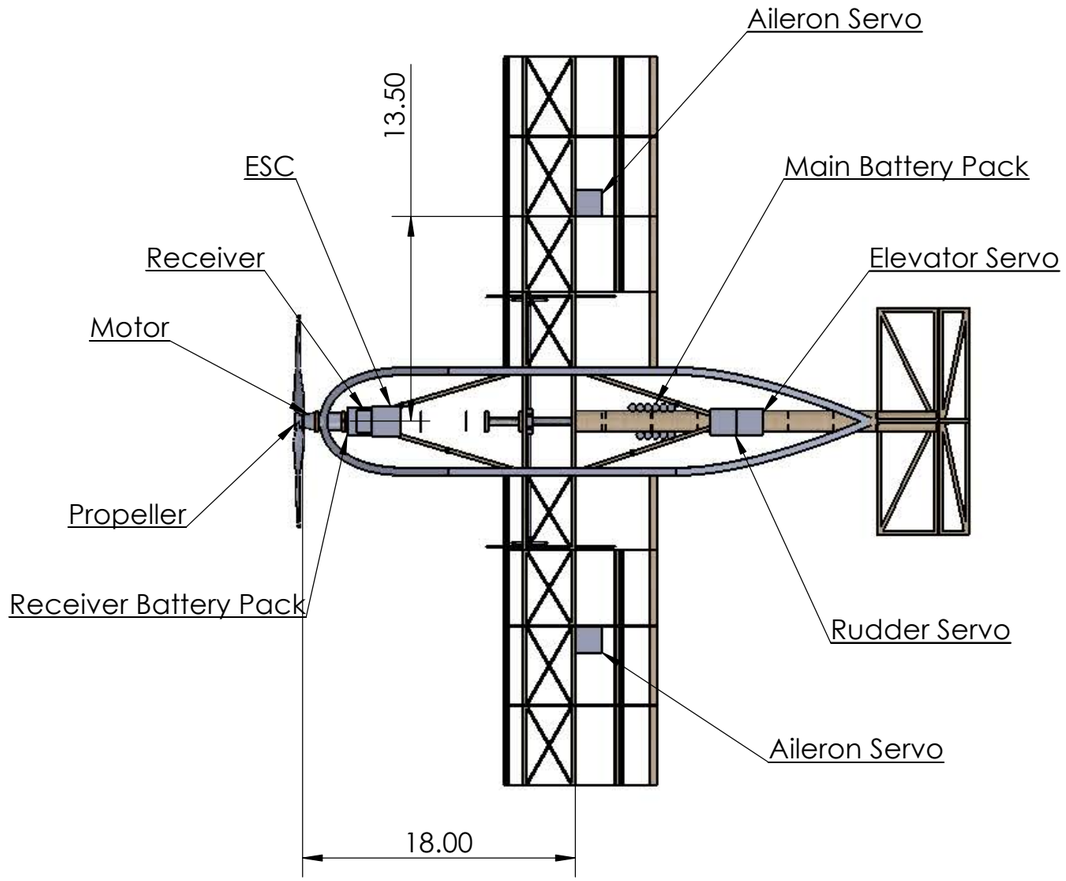

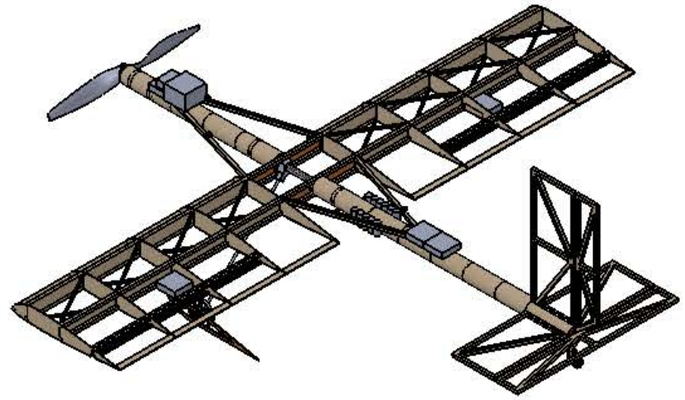

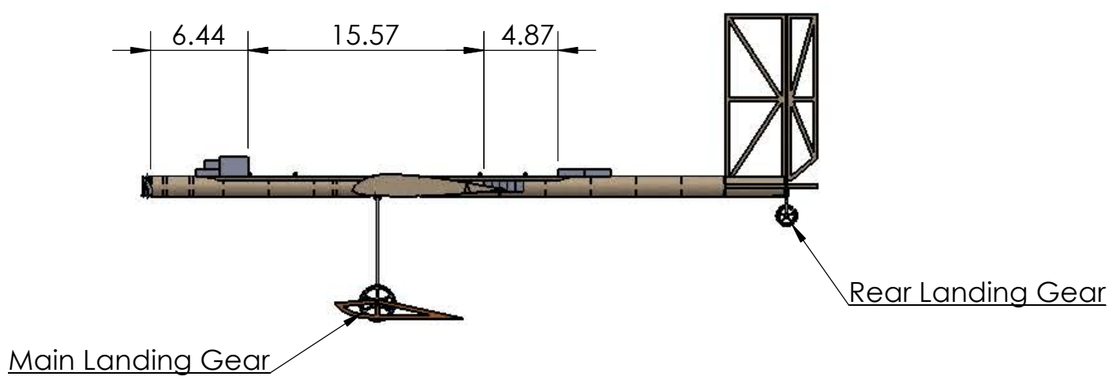

CALIFORNIA POLYTECHNIC STATE UNIVERSITY SAN LUIS OBISPO
DESIGN/BUILD/FLY 2013/2014

DOCUMENT TITLE:

Systems Layout

SIZE	APPROVAL DATE:	DRAWING NUMBER
B	02/21/2014	2014-03

UNLESS OTHERWISE SPECIFIED ALL DIMENSIONS ARE GIVEN IN INCHES	APPROVED BY: Reed Williston

SCALE 1:10	REPORT PAGE 44	SHEET 3 of 5

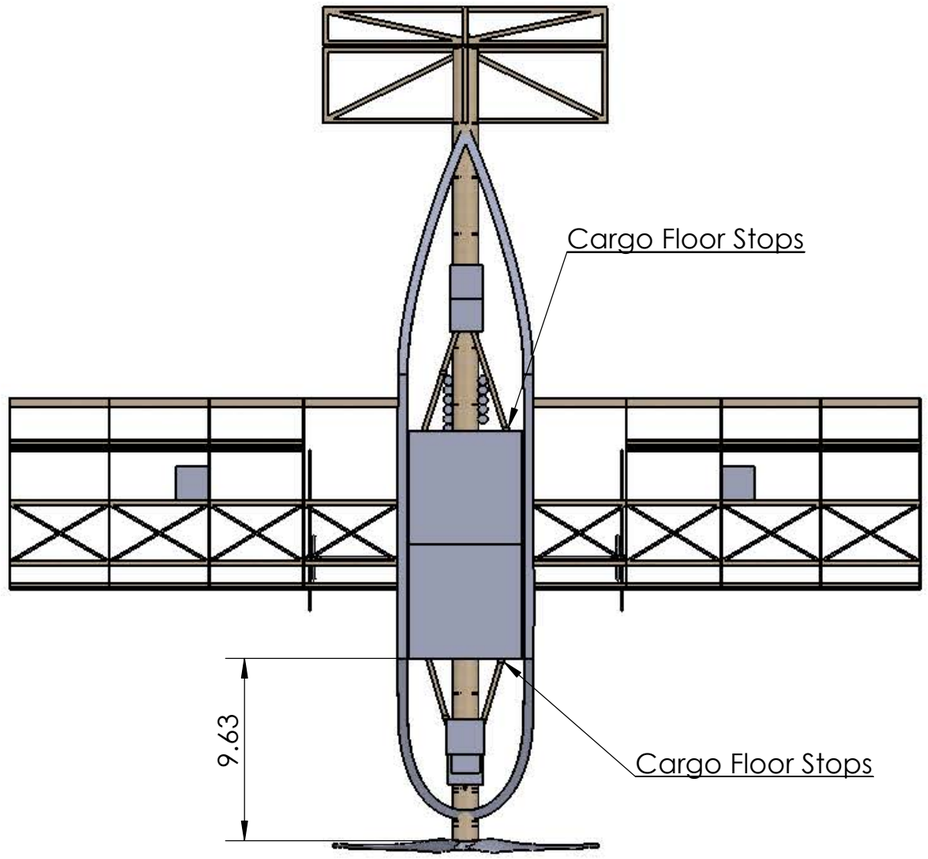

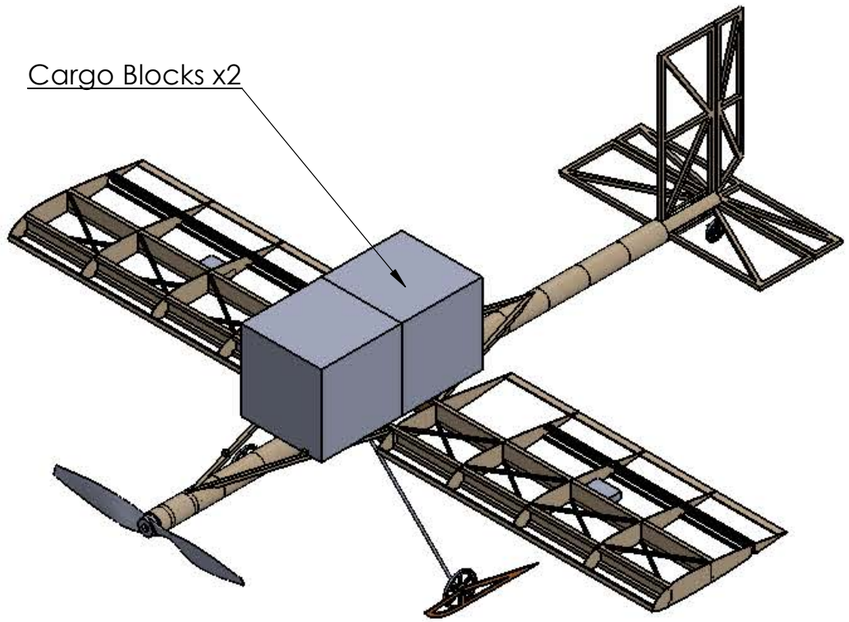

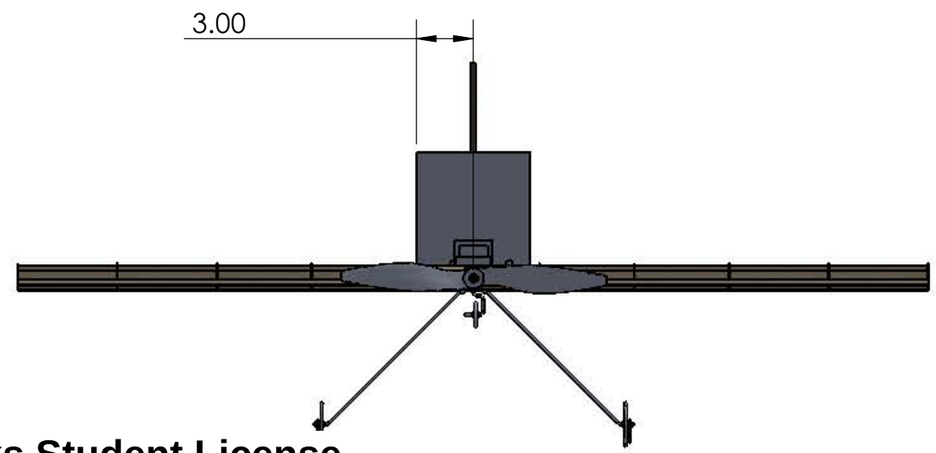

CALIFORNIA POLYTECHNIC STATE UNIVERSITY SAN LUIS OBISPO
DESIGN/BUILD/FLY 2013/2014

DOCUMENT TITLE:

Payload Layout 1

SIZE	APPROVAL DATE:	DRAWING NUMBER
B	02/20/2014	2014-04

UNLESS OTHERWISE SPECIFIED ALL DIMENSIONS ARE GIVEN IN INCHES	APPROVED BY: Reed Williston

SCALE 1:8	REPORT PAGE 45	SHEET 4 of 5

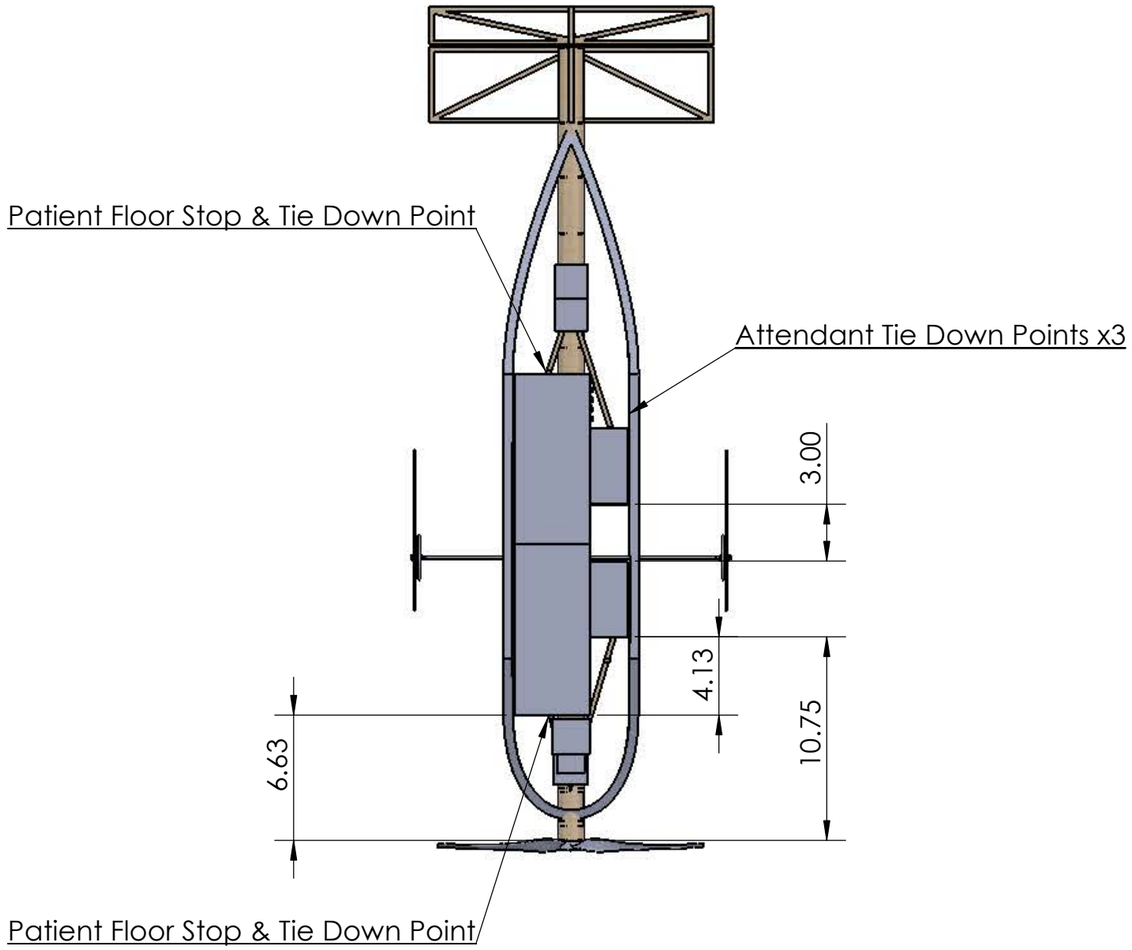

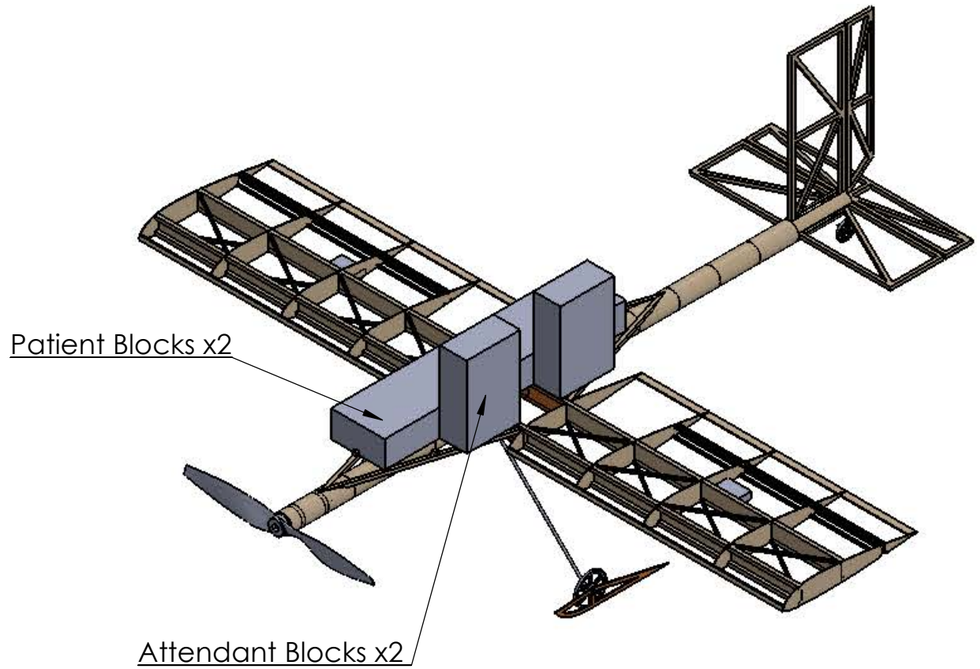

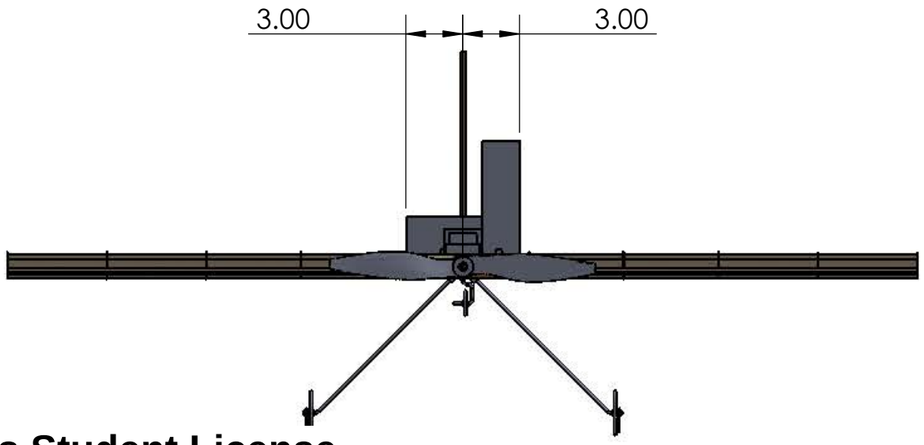

CALIFORNIA POLYTECHNIC STATE UNIVERSITY SAN LUIS OBISPO
DESIGN/BUILD/FLY 2013/2014

DOCUMENT TITLE:

Payload Layout 2

SIZE	APPROVAL DATE:	DRAWING NUMBER
B	02/20/2014	2014-05

UNLESS OTHERWISE SPECIFIED ALL DIMENSIONS ARE GIVEN IN INCHES

APPROVED BY: Reed Williston

SCALE 1:8	REPORT PAGE 46	SHEET 5 of 5

6 Manufacturing Plan and Processes

Throughout the year, manufacturing techniques and challenges were considered in all design choices. As was discussed earlier, the goal of the design was to produce a very light aircraft that could still meet the load requirements for flight and landing mission segments. By incorporating manufacturing choices into the design approach, an optimally light aircraft could be produced in a timely manner to allow for quick iteration on design choices.

6.1 Manufacturing Process and Techniques

The manufacturing process selection can be a significant contributor to overall aircraft weight savings and flight score. The team's manufacturing choices were somewhat limited by available equipment and expertise. The techniques considered for this competition year were balsa build-ups, composites, and foam construction. Manufacturing techniques were chosen for each main component as was necessary for the expected loads.

6.1.1 Balsa Build-Up

Balsa build up techniques rely on balsa's low density to achieve very light structures. Although balsa does not necessarily have as good of a strength to weight ratio as some composite structures, its much lower density allows for lighter structures that can still handle the loads seen at this scale of aircraft. The team also has a significant amount of experience with balsa structures, meaning more complex build-ups can be completed quickly and proficiently.

6.1.2 Composites

Composite structures are attractive due to their very high strength to weight ratios. Carbon fiber and kevlar based composites have been the most common in use. However, composite structures are generally stronger than is necessary except for the most limiting cases. Composite structures are also more difficult to construct complex pieces due to a lack of available equipment.

6.1.3 Foam

Foam structures are useful for their ability to be made quickly and easily with a CNC hot wire foam cutter. Foam structures are generally heavier than balsa build-ups, but they can also be made extremely light when used in non-loaded cases. Care must be taken with foam to use proper adhesives to avoid degradation.

6.2 Wing Construction

The wing was built using a balsa build-up that was then covered with Microlite. Balsa ribs and shear webs for the wing were cut using a CNC laser cutter. These ribs and shear webs were attached to the balsa spars using a foam jig to ensure a proper alignment at every joint. This jig was used over a structural drawing of the wing to ensure proper placement of all interior components. Torsional stiffness was added to the wing box by placing balsa crossbeams such that aerodynamic twist of the wing loaded them in compression. Leading and trailing edge non-structural spars were added to ensure airfoil shaping was held in the span-

wise direction at the critical points. All joints were joined using CA glue for it's light weight and strength. Microlite was then tacked along the ribs of the wing with a hot iron and shrunk to ensure a tight, smooth, and strong skin for the wing.

6.3 Backbone Construction

The backbone was constructed using CNC laser cut rib disks and balsa sheet for the exterior shell. Slots for the tail integration in the rear portion of the backbone and a hole for the engine wires in the front section were also cut using the CNC laser cutter. The balsa sheeting for the shell was wetted and formed around a tube of slightly larger diameter than the final diameter of the backbone to allow for rib placement after drying. Ribs were aligned using markings along the shell of the backbone along with a square to ensure all ribs were placed as perpendicular to the axis of the backbone as possible.

Once both the front and back sections of backbone were assembled, a carbon tube was run through the center wing box to integrate the two main structural elements of the aircraft. Thicker ribs were used in the backbone at the interface with the carbon tube to allow for a larger surface to transfer the bending moment and torsional stresses. The shear web of this center section of the wing box was replaced with plywood to ensure a strong enough joint to take the bending and torsional stresses being transferred to the wing by the backbone. A 3-D printed part was used to integrate the landing gear with this carbon section of the backbone and connect this load with the wing box as well.

6.4 Fuselage Construction

The main factor determining fuselage construction was minimizing weight. Because the fuselage was non-structural, a foam shell was chosen as the lightest method. The foam was cut on a CNC hot wire to achieve a minimum thickness while maintaining enough strength for potential aerodynamic loads in sideslip. Connections to the wing and backbone structure were done with foam safe CA and epoxy to minimize degradation of the foam structure. The top bay door was made from a minimal balsa structure that was then covered with Microlite. The fairings of the fuselage were also covered in Microlite to minimize weight.

6.5 Milestone Chart

A key to this year's competition was holding to a strict manufacturing schedule. This schedule is shown in Figure 6.1, and allowed for tests to be completed on time for key design choices.

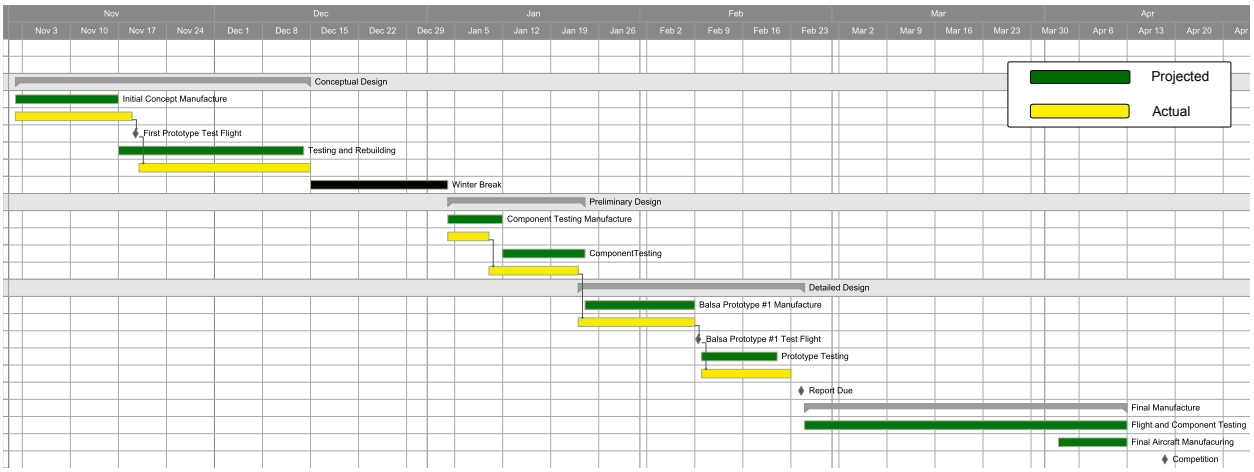

Figure 6.1 Manufacturing Milestone Chart

7 Testing Plan

Testing was performed throughout the design phase as a vital tool to efficiently improve the aircraft score by focusing on optimizing the targeted system with minimal total error.

7.1 Testing Schedule

Many design choices throughout the year require testing data to make informed decisions. To ensure this data is available, the team will adhere to a testing schedule as closely as possible. This schedule is presented in Figure 7.1.

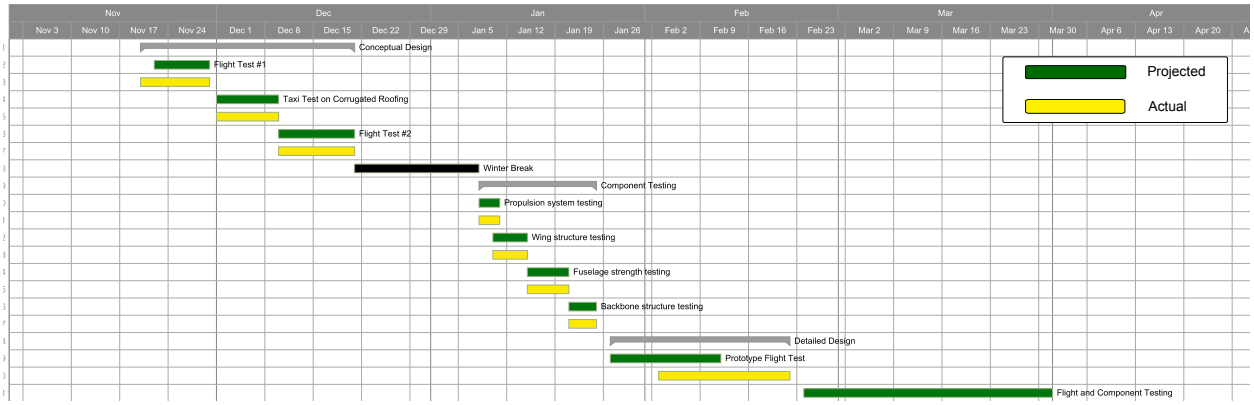

Figure 7.1 Testing Schedule

7.2 Flight Testing

Based on the conceptual design, a prototype foam model was built. This prototype was used primarily for proof of concept testing. For each flight test performed, the team used a flight test card to collect and record data. A sample of this test card can be seen in Figure 7.3. The test card ensured consistent flight data

and allowed for easy comparisons between test flights. The first prototype was flown at the design weight of 4 lbs using a rough configuration that came out of the conceptual design phase. Initially, the aircraft was tail heavy, underpowered and had a difficult time navigating the taxi-test. One of the main concerns of the prototype was meeting the required takeoff distance with enough margin for varying weather conditions at the actual competition. Over the next week, modifications were made to the propulsion system, landing gear and center of gravity location to remedy these issues. On the second flight test, the airplane flew very well, meeting the takeoff constraint. The airplane flew level and fast while handling the taxi test fairly well. The takeoff from the second test flight can be seen in Figure 7.2 showing the successful takeoff before the 40 foot mark. This was enough validation to enter the preliminary design phase based on this aircraft design.

Figure 7.2 Foam Prototype Meeting Takeoff Distance Fully Loaded

During the preliminary design phase, the foam prototype was repeatedly modified and flown as design choices were made. This allowed the team to iteratively design various parts of the airplane with real flight test data.

As the detail design phase came to a close, a balsa prototype meant to simulate the actual competition airplane was built and flown. The team was unable to build the aircraft as light as initially planned, partially due to the heavier electronic components available at the time. This aircraft did not meet the takeoff constraint, however the next aircraft will take advantage of lighter electronic components specifically chosen for its design. With these changes, it is expected that the aircraft will meet the takeoff constraint. Regardless of this, the flight tests yielded valuable data on the performance of the aircraft and its ability to complete the missions required for competition. The airplane was flown empty to ensure static and dynamic stability. These initial tests were also flown to ensure that the pilot had an acceptable amount of control of the aircraft. Tests with the payload installed were performed to ensure that the airplane performed as expected with a much larger wing loading. Further designs and flight testing between now and the competition will allow the team to fine tune the design and manufacturing of the airplane.

Cal Poly Design/Build/Fly Flight Log

Please make sure to attach the vehicle information to all of the flight logs for the corresponding vehicle

Flight #: _____ Take-Off Time: _____:_____ AM PM

Flight Data: _____/_____/_____ Flight Duration: _____ Min _____ Sec

Weather/Wind: _____ Battery Used: _____

CG Location: _____ Total Takeoff Weight: _____

Pre-Flight Safety Checklist:

Payload Secure	Full Surface Control Deflection
C.G. Forward of ¼ Chord	Radio Range Check
Radio Connection	
Full Motor Speed Control	

Mission/Goal:

_____
_____
_____

Payload:

_____
_____

Notes and Pilot Comments:

_____
_____
_____
_____
_____

Figure 7.3 Flight Test Card

7.3 Taxi Testing

Taxi testing had to be considered a higher priority for this year's competition compared to previous years due to the actual taxi mission. Testing was used to find the best way to complete the taxi mission without adding an extreme amount of weight to the aircraft as analytical methods of optimization were inadequate. The team determined the most efficient way to achieve this was to create skis to slide over the surface while allowing for enough clearance between the wheel and flat ground for normal taxiing during takeoff and landing. The configuration of the first prototype skis can be seen in Figure 7.4. The first taxi test went well and the airplane taxied across the corrugated roofing with a small amount of difficulty. With more tests, it was found that by lowering the skis as much as possible while still allowing clearance on flat ground gave

the best control and easiest taxiing over the roofing. One thing to note was that the rear tail wheel was not modified in order to maintain control of the airplane over the corrugated roofing. The team found that adding a ski to the rear wheel would only add extra weight and reduce ground controllability of the airplane. The material and exact shape of the skis will be tested more in the future in order to ensure the skis are strong enough to complete the taxi mission while keeping the weight as low as possible.

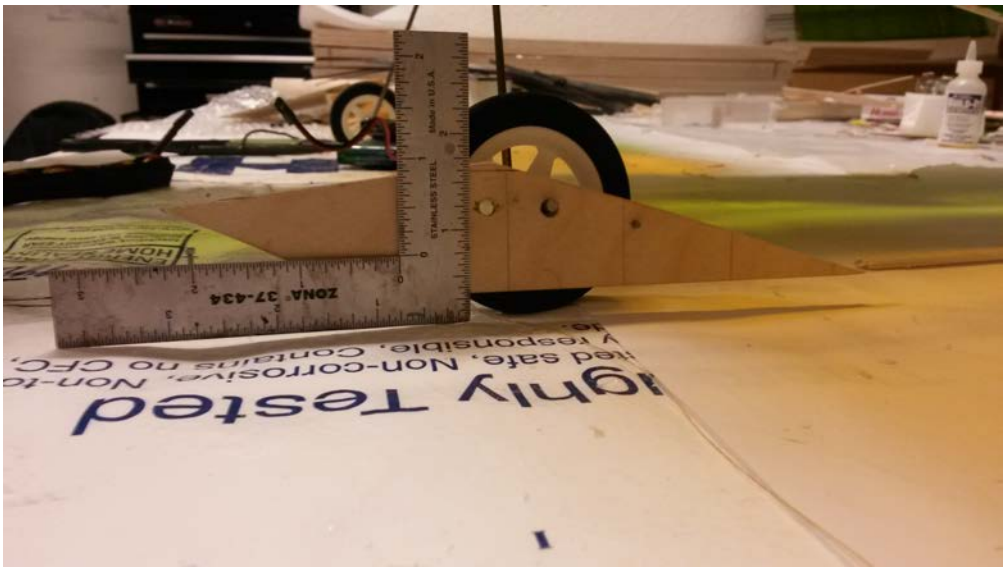

Figure 7.4 Ski Configuration for the Landing Gear.

7.4 Tests Performed

Throughout the entire design process, testing was performed to validate the choices being made. Most aspects of the aircraft were tested in some form to ensure that the design studies were yielding realistic results.

7.4.1 Wing Structural Testing

During the preliminary design phase, a few different wing designs that have proven to be successful in the past were tested against each other for torsional strength. The primary consideration was the trade off between strength and weight. The three wing designs tested included: carbon spars and balsa ribs, balsa spars and ribs with a balsa D-box, and balsa spars and ribs with balsa cross beams. A testing bed was constructed to constrain the wing sections to experience a load that was primarily torsion. One of the wings sections during the test can be seen in Figure 7.5.

Figure 7.5 Failed Wing Section During Torsional Testing

The results of the wing testing are shown in Table 7.1. As can be seen, the balsa cross beam structure held over 1 foot-pound before experiencing any type of failure. Although the carbon supported wing structure held the most weight, it also had almost twice the amount of deflection compared to the balsa cross beam at the same load. One more reason the balsa cross beam beat the carbon supported structure was due to overall weight of the carbon structure being almost twice the total weight of the balsa based structures. In the end, the wing design with cross beams was chosen because although it was slightly heavier than the D-box it resisted the most torsional loading while experiencing the least amount of deflection. Further testing on the same structural design is planned to optimize the weight of the wing while maintaining the necessary load carrying capability.

Table 7.1 Wing Structure Testing

Wing Type	Load (ft-lbs)	Leading Edge Deflection (in)	Failure
Cross-Beam	1.21	0.24	Glue Joint
	1.51	0.25	Structural
D-Box	0.959	0.37	Glue Joint
	1.558	0.68	Structural
Carbon Support	1.767	0.42	Structural

7.4.2 Backbone Structural Testing

During the manufacturing phase for the second prototype, there was concern from some of the club members that the motor mount would not be sufficient to hold the motor during takeoff where thrust is maximum. A quick test proved that the design provided an adequate safety margin. A string was tied around the prop collar and connected to a fish scale where the load could be easily read. The design was tested to a factor of safety of three without any signs of failure. The test was not continued until failure as this was considered a sufficient safety margin. A picture of this test can be seen in Figure 7.7. Bending and torsion strength

of the backbone was also tested to ensure they could withstand loads seen during heavily loaded flight. The other highest risk portions of the backbone construction were the slot attachments for the tail and the connection to carbon rod through the wing box. These areas were tested with the tail mounted and found to be sufficiently strong enough to withstand any loads it would see during flight and landing.

Figure 7.6 Propulsion Testing

Figure 7.7 Motor Mount Testing.

7.4.3 Propulsion Testing

At last year's competition, the team suffered a devastating crash during the third mission takeoff. The propulsion system did not perform as expected and exceeded the current limit. This blew the fuse between the battery and the electronic speed control, or ESC, resulting in complete power loss to the motor. To guarantee that this mistake was not made again, the propulsion system was throughly tested to ensure that the 15 Amp current limit would not be violated. A static thrust test using the ESC and batteries that are to be used in the competition airplane was performed at full throttle for approximately six minutes. During this test, data was recorded to prove that the system was performing as expected. The testing setup can be seen in Figure 7.6. No surprises came up during the test and it was considered a success. The test showed that the current never crossed the competition limit of 15 amps and the voltage stayed well below the acceptable limit for the electronics used in the aircraft. Further testing of the propulsion system's power and current draw was completed during every flight test. This data was taken with a Phoenix Ice 40-Amp ESC and analyzed to ensure the limits were not exceeded.

7.4.4 Other Component Testing

The landing gear mount was made from ABS plastic using a 3-D printer. There was some uncertainty over the strength of this plastic and its ability to resist a bending load from the landing gear. The first test proved very useful. The landing gear mount broke under a much smaller load than anticipated and was promptly redesigned to be much stronger. The second iteration of the piece provided a sufficient safety margin. An image of the testing setup is shown in Figure 7.8. Although the second iteration of the part was much stronger, it weighed three times the original part. This piece will be optimized in order to reduce the weight while still maintaining the necessary strength. Due to the part being created by a 3-D printer, the percent of infill can be changed to find the correct ratio of strength to weight.

Figure 7.8 Landing Gear Mount Testing.

8 Performance Results

This section of the report discusses the performance results of the tests covered in the previous section. The performance results discussed here were used to validate previous theoretical work and ensure their accuracy while analyzing design choices and changes. This validation was focused on critical subsystems and overall flight performance.

8.1 Subsystem Performance

Subsystem performance testing was done to ensure component models were accurate to their physical correspondents. This validation of subsystem performance was completed for the propulsion system, main structures, and aerodynamics.

8.1.1 Propulsion System

Propulsion system testing was done on a fully built prototype to compare between expected thrust values and realistic values with actual installation losses. The results of this testing are summarized in Table 8.1.

As can be seen from the test data, the propulsion model gave values roughly 20% higher than the actual thrust provided.

Using these tests, it was decided to fair the fuselage front as the airfoil shape was still providing too much blockage for the propulsion system. However, these thrust values were still high enough to meet the takeoff requirement, so a propulsion system redesign is unlikely.

Table 8.1 Installed Propulsion System Testing

	Average Thrust	Maximum Thrust	Maximum Voltage	Maximum Current
Full Fuselage	1.51	1.57	12.8	12.3
Faired Fuselage	1.65	1.73	12.8	12.3

The other major areas of concern for the propulsion system were current draw and heat generation. Heat generation was a concern as the motor was operating near its continuous power limit in an enclosed structure. After running the motor at full throttle for 6 minutes, the motor reached a maximum temperature of 112 °F, which is within the operating limits. The current draw was then measured during test flights to ensure the current limit was not broken. Figure 8.1 shows an example of these results. As can be seen, the current peaks at roughly 12.5 Amps, safely below the given current limits. The maximum current drawn across all test flights was 13.9 Amps, leaving enough safety margin to give the team confidence the fuse will not be blown during competition.

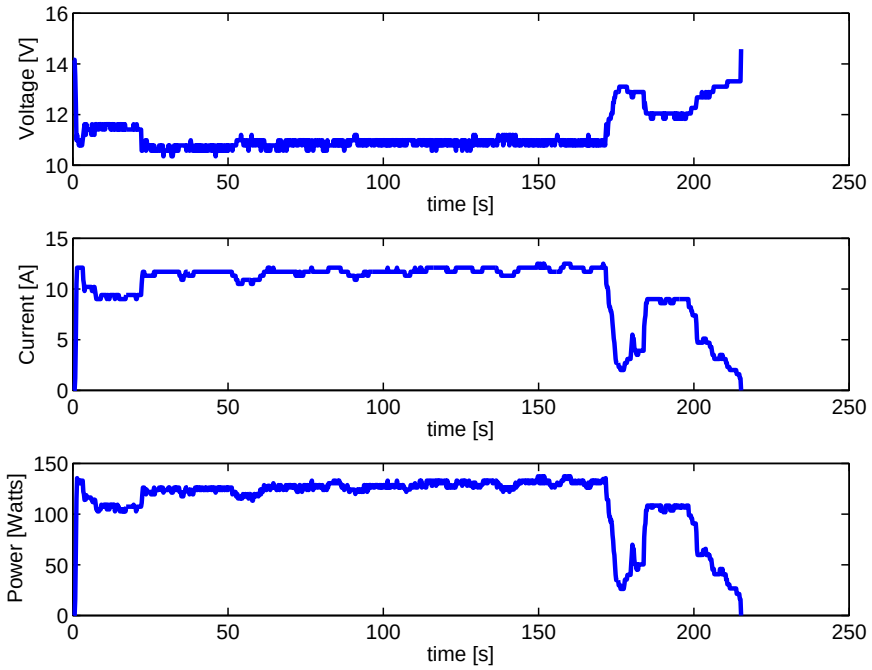

Figure 8.1 Propulsion Data from Flight Testing.

8.1.2 Structures

The main structural components of the aircraft were tested to ensure the stress simulations completed with the Solidworks stress analysis tool accurately modeled the system. The key components of our aircraft to

be tested were the wing and the backbone.

Wing Structure

The wing structure was tested both for bending moment and torsional stresses. Torsional stress testing was done to determine the internal structural layout of the wing. As was discussed in the testing section of this report, a balsa cross-beam design was used to mitigate torsional loads. Testing showed no unexpected results in torsion, and the team is confident that any in flight loads can be handled.

Further testing was completed to ensure the wing structure would be able to handle other loads seen in the air. This mainly focused on the bending moment loads produced by lift acting on the wing. A semi-elliptical lift distribution was applied to the wing equivalent to that experienced during fully loaded steady level flight to compare actual deflections to the Solidworks model. As expected, the deflections of this test were slightly higher than the theoretical model. This is likely due to non-homogeneous behavior in the balsa construction and imperfect glue joints, but the end result was within reasonable limits. Continuing until failure, the wing sustained a load roughly equivalent to a 4.5 G turn. This is much lower than the expected failure at a 6.5 G load from the Solidworks model, but still higher than any expected loads throughout a fully loaded mission flight and landing.

Backbone

The backbone structure was tested for support of bending moment loads. A representative backbone was created to test the loads at the wing box joint. Testing showed that the backbone deflection at the tail was mostly consistent with the Solidworks model of the backbone. Testing showed the backbone would be able to support all expected aerodynamic loads on the tail, and failed in shear between ribs as expected, not at the joint with the carbon fiber rod. This increased confidence that this design choice would be sufficient to pass the bending loads through the wing box.

8.1.3 Aerodynamics

Aerodynamic performance was done through a simple glide test. This test was completed with a representative foam prototype for ease of manufacture and ruggedness. Throwing this foam prototype from the highest available building allowed a lift to drag ratio, L/D_{max}, to be determined. This test resulted in an experimental L/D_{max} of 5.7. Compared with the predicted value of 9.53, the aircraft operated at roughly half of the maximum performance expected. This large gap caused some concern among the team. However, it is unlikely that the pilot was holding the correct attitude for L/D_{max}, and the performance of the actual aerodynamics was expected to be significantly lower than the theoretical values. This is because of unaccounted for drag factors, such as manufacturing imperfections, scrub drag from the motor, and other non-modeled phenomena. This error was not considered significant enough to make large scale aerodynamics changes, but the drag model was revised accordingly.

8.2 Aircraft Flight Performance

With both the foam and balsa prototype aircraft, multiple mission test flights were run. The goal of these flights was to verify the aircraft's estimated performance from detail design as well as estimate the competition mission performance. Before each flight the aircraft was weighed, the center of gravity was labeled

and every battery was fully charged. Each flight provided validation that the aircraft would meet the takeoff requirement and provided valuable performance data. The results of these tests indicate that a maximum of approximately 1100 mAh of power are required to complete a mission. Although it would be possible to lower the capacity of the current batteries to save some weight, these gains would be small at best. The lower current draw from a smaller capacity pack would reduce the power available to meet the takeoff constraint. Also, a change to a lower capacity rating would significantly decrease the power margin maintained to account for possible adverse wind conditions at the competition site. In addition, these flight tests confirmed the predicted lap times and other key mission parameters from detail design. A summary of these results is shown in Table 8.2.

Table 8.2 Comparison of Predicted and Demonstrated Flight Performance

	Scoring Parameter	Prediction	Demonstrated
Mission 1	Number of Laps	5	**5**
Mission 2	Number of Cargo	2	**2**
Mission 3	Flight Time	150	**165**

Given the results of the completed tests, Cal Poly Design/Build/Fly club is confident we have produced a highly competitive design for the 2013/2014 competition year. The year has been filled with long nights and hard hours, but the process has been fun and fulfilling . The Cal Poly team is excited to once again be competing in this international event.

Figure 8.2 Balsa Prototype Takes Flight

USC University of Southern California

AIAA/Cessna/Raytheon Design/Build/Fly 2013-2014

MISCHIEF

Table of Contents

Acronyms, Abbreviations, and Symbols

AIAA	American Institute of Aeronautics and Astronautics
DBF	Design/Build/Fly
USC	University of Southern California
NACA	National Advisory Committee on Aeronautics
AR	Aspect Ratio
Re	Reynolds number
b	Span
c	Chord
s	Wing area
t/c	Thickness-to-chord ratio
MAC	Mean Aerodynamic Chord
α	Angle of attack
C_{d0}	Airfoil minimum coefficient of drag
C_{Di}	Aircraft induced drag coefficient (vortex drag)
C_{D0}	Aircraft parasite drag coefficient
C_D	Aircraft drag coefficient
$C_{l,\max}$	Airfoil minimum lift coefficient
C_L	Aircraft lift coefficient
$C_{L,\max}$	Aircraft maximum lift coefficient
C_{l_β}	Lateral stability coefficient
C_{n_β}	Directional stability coefficient
e	Oswald efficiency factor
W/S	Wing loading
L/D	Lift/drag, aerodynamic efficiency
ω_n	Natural frequency
ζ	Damping coefficient
τ	Time constant
NiCad	Nickel cadmium
NiMH	Nickel-metal hydride
I_0	Idle current
KV	Speed constant
J_{design}	Propeller pitch/diameter ratio
mAh	Milli-amp hours
MDO	Multi-disciplinary optimization
Rx	Receiver
Tx	Transmitter
ESC	Electronic Speed Control
FoM	Figure of Merit
N_{laps}	Number of complete laps
N_{payloads}	Number of payloads carried
M_1	Mission 1 score
M_2	Mission 2 score
M_3	Mission 3 score
TOFL	Takeoff field length
RAC	Rated Aircraft Cost
EW	Empty weight
SF	Size factor
TFS	Total flight score
V_{cruise}	Cruise velocity
V_{stall}	Stall velocity
R/C	Rate of climb
r	Turning radius
δ_a	Aileron deflection angle
δ_e	Elevator deflection angle
δ_r	Rudder deflection angle

1 Executive Summary

The objective for the 2013-2014 AIAA Design/Build/Fly contest is to develop a backcountry rough field bush plane that will fly four contest missions in beautiful Wichita, KS. After analyzing the scoring equations, it was clear that empty weight has the greatest influence, followed by speed, and then landing gear capability. In addition, the 40 ft takeoff field length is one of the shortest in contest history. A conventional monoplane configuration was found to be optimum since it requires relatively less landing gear complexity, provides high-lift capability, and reduces weight of fabrication. To minimize weight, the fuselage was constructed from a Kevlar, carbon fiber and foam truss structure. The wing and tail loads were carried by single spars constructed of balsa shear webbing and carbon spar caps. Landing gear was made from carbon fiber, balsa and foam. The fuselage is a load-bearing monocoque structure constructed from Kevlar, with an inlaid foam and carbon tow truss structure to transfer flight and landing loads. To meet the 40 ft takeoff field length, the team designed an airfoil with minimal cruise drag and incorporated flaps to be used on takeoff.

The first contest mission is a non-flight taxi mission, in which the aircraft must taxi across a rough field in under five minutes. This taxi mission field consists of fiberglass roofing panels and two obstacles that the aircraft must maneuver. The requirement for ground-handling drove the design for steerable landing gear by means of a differential braking system.

The first flight mission, a ferry flight, scores the number of complete laps flown in four minutes. The requirement for speed drove the Mission 1 design for a high pitch of propeller.

The second flight mission, an internal payload flight, consists of flying three laps around the competition course while carrying as many internal (1 lb., 6 in. x 6 in. x 6in.) cargos as possible. The team's score analyses showed that speed was more important than payload quantity; therefore, only three cargos are carried internally. The internal payload mounts for securing the cargos consist of fishing line (nylon), hooks, and balsa corner pieces.

The third flight mission, a payload and speed mission, requires the aircraft to carry a configuration of internal payloads (two patients on gurneys, each with their own medical attendant). The aircraft would then have to complete three competition course laps as fast as possible. These internal payloads were also secured with the fishing line and foam pieces, chosen to minimize weight and assembly time.

The University of Southern California's aircraft, *Mischief*, is capable of completing 6 laps in Mission 1, with a cruise speed of 76 ft/s (23.2 m/s). The aircraft can complete the three required laps while carrying 3 internal cargos during Mission 2, with a total flight weight of 5.24 lb (2.38 kg). The aircraft can complete the three required laps while carrying the required Mission 3 payloads, with a total flight weight of 4.18 lb (1.89 kg) and a cruise speed of 78 ft/s (23.8 m/s). The aircraft is predicted to complete Mission 3 with the internal and external payloads in 135 seconds. The aircraft has an EW (empty weight) of 2.24 lb (1.02 kg), yielding an RAC (rated aircraft cost) of 2.24. Missions 2 and 3 payloads can be loaded in two and three minutes, respectively, meeting the five minute loading time limit. Further improvements to the design will be made in order to minimize EW and maximize the speed of the aircraft, while maintaining mission completion and system reliability. Figure 1 shows the final design of the competition aircraft.

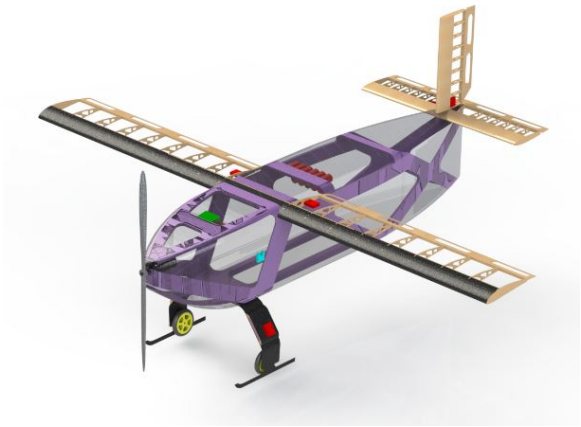

Figure 1: The USC 2013-2014 DBF entry, *Mischief*.

2 Management Summary

The 2013-2014 USC AeroDesign Team consisted of approximately 30 students, from freshmen to graduate students, who contributed to the team's efforts on an extracurricular basis. Industry advisers and USC faculty members also assisted the team through guidance and suggestions at weekly meetings and design reviews. The design reviews were conducted in a professional setting where the team presented the Preliminary Design (October 2013) and the Critical Design (January 2014).

2.1 Team Organization

The USC AeroDesign Team employed a hierarchical team structure led by the Program Manager and Chief Engineer to establish responsibilities and promote collaboration. The Program Manager ensured the timely adherence to the master schedule, headed team meetings, organized design reviews, and collaborated with the Operations Manager to obtain funding and manage team logistics. The team further consisted of ten technical subteams, each headed by a student leader to guide general members. The Chief Engineer directly supervised these subteams to ensure effective communication throughout the design, fabrication, and testing processes. The organizational structure and class standing of each captain are shown in Figure 2.

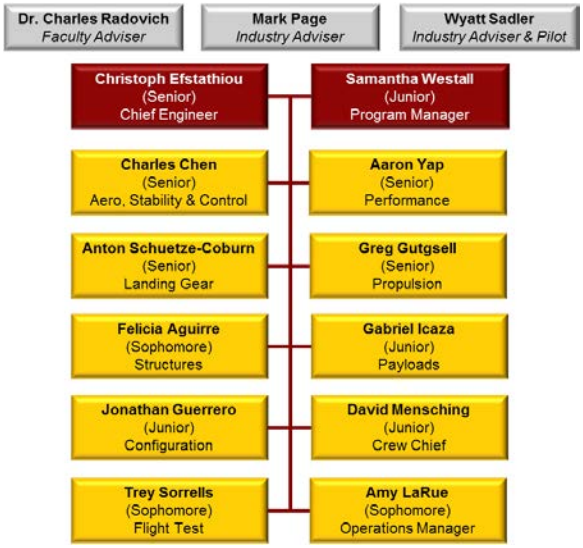

Figure 2: The AeroDesign Team's structure.

2.2 Project Schedule

The Program Manager created and maintained a Gantt chart as well as the broad overview chart with planned and actual schedules, shown in Figure 3, to track the phases of design, manufacturing, testing, and important milestones.

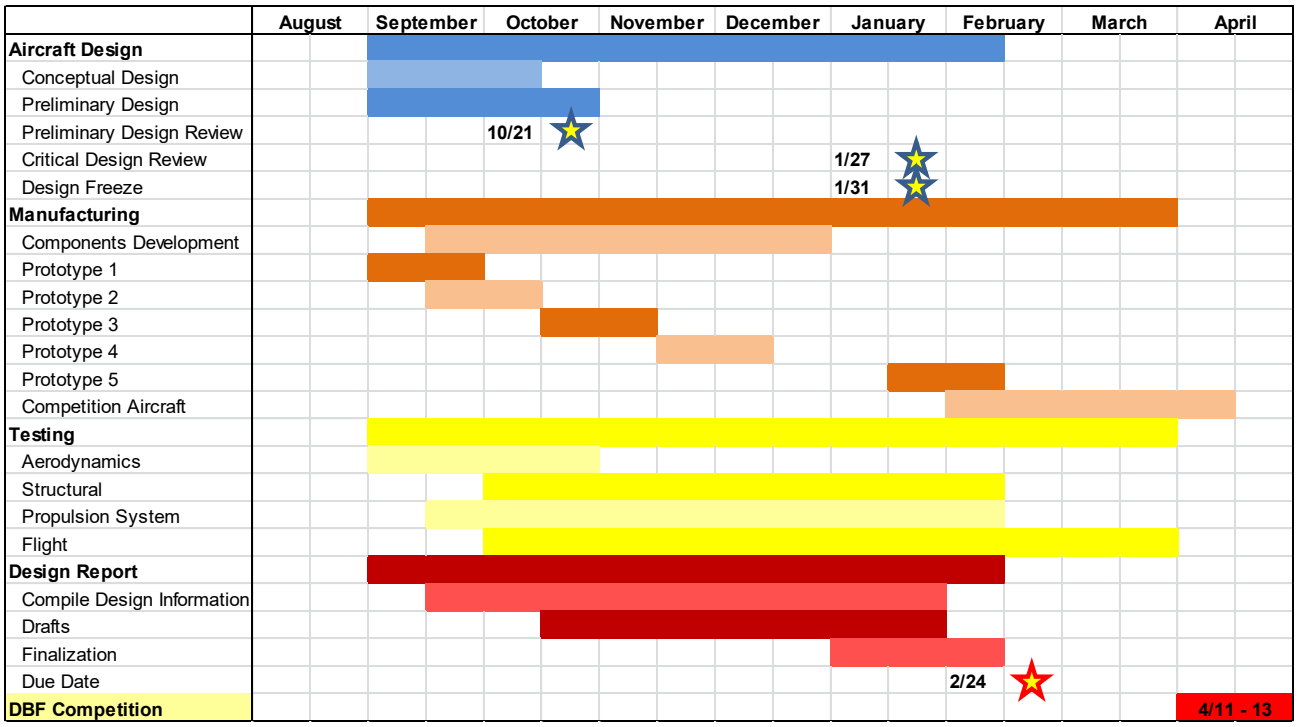

Figure 3: Master schedule for 2013-2014 showing the team's actual event timing. Stars indicate major milestones.

3 Conceptual Design

In the conceptual design phase, the competition requirements were analyzed with sensitivity studies of the scoring equations n order to identify the trade factors that has the strongest influence on maximizing the team's total score. A mix of configuration options was then evaluated against these trade factors to determine the preferred aircraft configuration. The result of this analysis guided the team to determine the overall aircraft configuration and prioritize component design to obtain the highest-scoring aircraft possible.

3.1 Mission Requirements and Constraints

The 2014 American Institute of Aeronautics and Astronautics (AIAA) Design/Build/Fly (DBF) Competition comprises four aircraft missions: one taxi mission, one speed mission, and two payload-carrying missions. These missions required that the final aircraft meet various other requirements, including:

- Take off within a 40 ft (12.2m) runway on all flight missions
- Carry and secure payloads within an internal volume
- Use either NiCad or NiMH batteries with maximum pack weight of 1.5 lb (0.7 kg)
- Limit power system current draw with a 15 Amp fuse
- Pass a structural safety test where the fully-loaded aircraft is lifted at the wingtips

The aircraft must fly at least one competition lap for all three missions. One lap consists of two 1000 ft (300 m) straightaways, two 180°turns, and one 360°turn. The 2-D schematic of this flight course is shown in Figure 4.

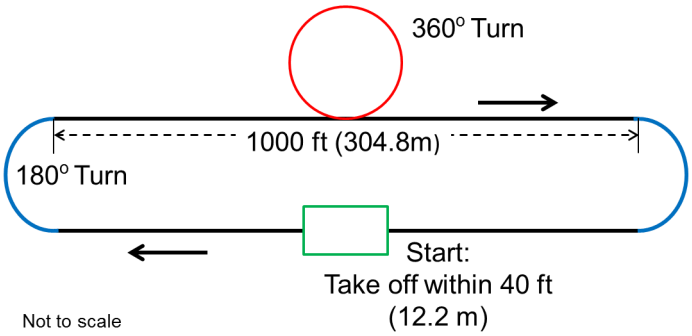

Figure 4: AIAA Design/Build/Fly competition flight course layout showing the start, turns, and flight direction.

3.1.1 Scoring Summary

The overall score for the 2014 AIAA DBF Competition is given by Equation 1.

$$\text{Score} = \frac{\text{Written Report Score} \times \text{Total Mission Score}}{\text{RAC}} \tag{1}$$

where the $\text{Written Report Score}$ is based on the quality of the design report, and the $\text{Total Mission Score}$ is given by the product of the Taxi Score, TS, and Flight Score, FS (Equation 2):

$$\text{Total Mission Score} = \text{TS} \times \text{FS} \tag{2}$$

The Taxi Score is a binary multiplier with a value of 1.0 if the taxi mission is completed, or 0.2 if the aircraft fails to complete the objective. The Flight Score, FS, is given by the sum of the individual mission flight scores (Equation 3):

$$\text{FS} = \text{M1} + \text{M2} + \text{M3} \tag{3}$$

where M1, M2, and M3 describe the scores for Missions 1, 2, and 3, respectively. These Mission Scores are further developed in Section 3.1.2. The Rated Aircraft Cost, RAC, is given by Equation 4, and is composed solely of the aircraft Empty Weight, EW.

$$\text{RAC} = \text{EW} \tag{4}$$

The Empty Weight will be measured after each successful scoring flight, and the final value for EW will be determined according to Equation 5, and taken as the maximum over all three flight missions.

$$\text{EW} = \text{Max}(\text{EW1}, \text{EW2}, \text{EW3}) \tag{5}$$

where the Empty Weight value is taken as the maximum over all three flight missions.

3.1.2 Mission Scoring

Ground Taxi Mission: Rough Field Taxi

The objective of the Rough Field Taxi Mission is to taxi across a 40 ft x 8 ft (12.2 m x 2.4 m) course comprising fiberglass roofing panels. The aircraft must demonstrate ground-handling ability over this course within five minutes, and carry the same payload as required by Mission 3 (detailed under Mission 3). The score for this mission, TS, is given by Equation 6:

$$\text{TS} = \begin{cases} 1.0 & \text{upon successful completion} \\ 0.2 & \text{upon failure to complete} \end{cases} \tag{6}$$

where a successful completion requires no damage to the airplane. The attempt is disqualified if the airplane becomes airborne or if it departs the side of the course. The Taxi Mission course layout is depicted in Figure 5, where the obstacles are ”standard 2x4’s (actual dimension 1.5 in. x 3.5 in. on edge) placed on edge (3.5 in. vertical)”.

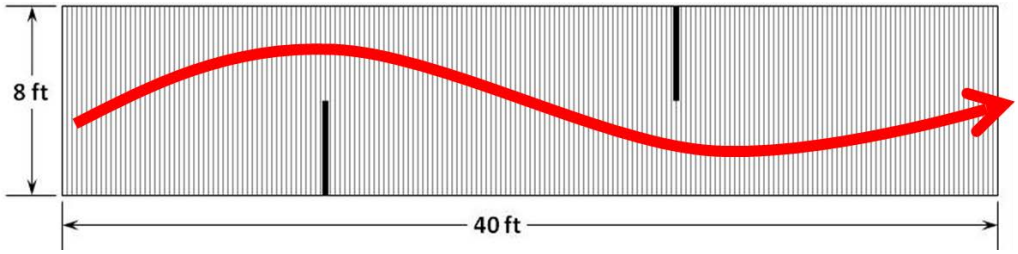

Figure 5: Taxi mission course layout showing obstacles and a taxi path.

Flight Mission 1: Ferry Flight

The objective of the Ferry Flight mission is to fly as many complete laps as possible within four minutes after taking off within the 40 ft (12.2 m) field length. Timing begins when the aircraft is throttled up for takeoff. No payload is installed during this mission. The score for this mission, M1, is given by Equation 7:

$$\mathrm{M1} = 2 \times \frac{N_{\mathrm{Laps_{USC}}}}{N_{\mathrm{Laps_{Max}}}} \tag{7}$$

where $N_{\mathrm{Laps_{USC}}}$ is USC's number of complete laps and $N_{\mathrm{Laps_{Max}}}$ is the maximum number of laps flown by any team at the competition.

Flight Mission 2: Maximum Load

The objective of the Maximum Load mission is to fly with a high internal payload ratio. The aircraft must carry a team-chosen number of 6 in. x 6 in. x 6 in. (15.2 cm x 15.2 cm x 15.2 cm) wooden blocks, ballasted to 1 lb (0.45 kg) each, and complete three competition laps after taking off within the 40 ft (12.2 m) field length. The score for this mission, $\mathrm{M2}$, is given by Equation 8:

$$\mathrm{M2} = 4 \times \frac{N_{\mathrm{Cargo_{USC}}}}{N_{\mathrm{Cargo_{Max}}}} \tag{8}$$

where $N_{\mathrm{Cargo_{USC}}}$ is the number of cargo carried by USC and $N_{\mathrm{Cargo_{Max}}}$ is the maximum number of cargo carried by any team. For an image of the payload required for this mission and for the medical mission, see Figure 7 in Section 3.4.3.

Flight Mission 3: Emergency Medical Mission

The objective of the Emergency Medical mission is to quickly fly three laps while carrying payloads representing medical passengers. The passenger load consists of two patients and two attendants. The patients are on gurneys simulated by wooden blocks 9 in. (22.9 cm) long x 4 in. (10.2 cm) wide x 2 in. (5.1 cm) high, ballasted to 0.5 lb (2.3 kg) each. The attendants are positioned beside each patient and are simulated by wooden blocks 6 in. (15.2 cm) tall x 2 in. (5.1 cm) wide x 4 in. (10.2 cm) long, ballasted to 0.5 lb (2.3 kg) each. Thus, each patient and attendant pair weighs 1 lb (4.6 kg). Timing begins when the aircraft is throttled up for takeoff. The score for this mission, $\mathrm{M3}$, is given by Equation 9:

$$\mathrm{M3} = 6 \times \frac{t_{\mathrm{Fastest}}}{t_{\mathrm{USC}}} \tag{9}$$

where t_{Fastest} is the fastest successful time flown of any team and t_{USC} is the time flown by USC.

3.2 DesignObjectives

3.2 Design Requirements

The AIAA DBF competition will be scored according to the Score Equation, given previously by (Equation 1). The design constraints and mission parameters that contributed to the score were translated into a set of design objectives, which are summarized in Table 1.

Table 1: Design parameters.

Score Parameter	Design Objective
Taxi Mission	Ability to taxi over roofing panels
TOFL Requirement	Sufficient power (thrust), wing area
Mission 1: Number of laps	High L/D at cruise
Mission 2: Number of Cargo	Maximize takeoff capability and internal cargo volume
Mission 3: Time	Maximize flight speed
Empty Weight	Minimize system weight

3.2 ScoreAssumptions

Since the design criteria of the missions conflict, the total score equation (Equation 1) was analyzed to determine the relative importance of each score parameter, and thus design objective. The Flight Score (Equation 3) is dependent on the highest performer in each mission, so the team analyzed the performance of similar aircraft from previous competitions, shown in Table 2. A baseline aircraft, representative of what the team is capable of building to complete all missions, is also outlined. The research leading to these assumptions is detailed in the subsequent paragraph.

Table 2: Score analysis assumptions.

Score Parameter	Top Performance Assumption	USC's Baseline Assumption
$N_{Laps_{Max}}$	8	5
$N_{Cargo_{Max}}$	4	2
$t_{Fastest}$	80 s	120 s
EW	-	2 lb

Compared to the 2012-2013 AIAA DBF competition rules, there is a reduction of the fuse limit on current from 20 A to 15 A, and a reduction in required payload from 3 lb to 2 lb, so the team expects this year's plane to be lighter and slower than the team's 2012-2013 DBF entry. Based on the TOFL restriction, the 15 A current limit, and the 1.5 lb battery pack limit, the team expects to see a maximum number of 8 laps for M1 from any team, consistent with the upper limit in previous years, requiring a flight velocity of 95 ft/s (29 m/s). For Mission 2, the payloads require a volumetric density of 216 in^3/lbm (7801 cm^3/kg), and the team expects the maximum number of cargo carried to be 4.

Additionally, based on historical competition results, the flight speeds on Mission 1 and Mission 3 have been comparable because of the increased flight weight (and thus drag due to lift) and reduced duration due to a lower number of laps being flown than in Mission 1. Therefore the fastest time was estimated to be 80 s based on the maximum expected flight speed of 95 ft/s (29 m/s).

The team also considered the headwind in Wichita, KS, which has a historically non-zero wind. The weather patterns around the competition weekend in April for the past 20 years were analyzed to estimate a reasonable average headwind. Weather data obtained from !!! is presented in Table 3, showing average wing speeds for morning, mid-day and late afternoon time periods at the contest site.

Table 3: Historical wind speeds in Wichita, Kansas, for three time periods of interest.

Morning (7AM – 12PM)	13.8 ft/s (4.2 m/s)
Afternoon (12PM – 3PM)	15.7 ft/s (4.8 m/s)
Late Afternoon (3PM – 6PM)	13.6 ft/s (4.1 m/s)

Successful completion of the Taxi Mission was also considered a high priority. A major concern of taxiing over the roofing panels and being able to turn is that it would require a stronger landing gear with larger wheels and more robust steering mechanism, which would have increased weight. However, since the term including the taxi score can be factored to TS/EW, completing the Taxi Mission is crucial (Taxi Score = 1.0), unless it increases the empty weight by a factor of 5, at which point not completing the Taxi Mission (Taxi Score = 0.2) would score higher.

With these assumptions, limitations and expected maxima, the team investigated the sensitivity of the score equation with respect to the major score variables. For this, the team found a baseline airplane that could complete all three missions, carrying 2 payloads (equivalent to Mission 3 payload weight) for Mission 2, with a payload-to-empty weight fraction of 0.5. This resulted in a baseline airplane that could fly 5 laps for Mission 1, carry 2 cargos for Mission 2, and complete Mission 3 in 120 s, as given by Table 2.

Figure 6 shows the percentage change in total flight score as a function of a percentage change in a single score variable on the x-axis. The origin (0,0) represents the baseline aircraft, and any variation is a percentage change in its scoring parameters.

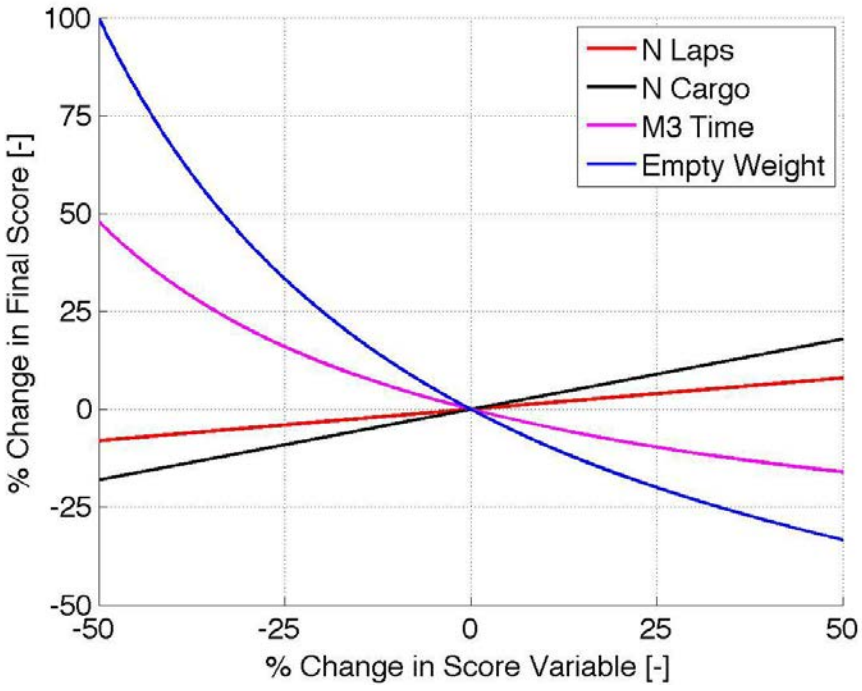

Figure 6: Sensitivity of the final score to a change in score variables.

The score sensitivity analysis shows that the score coefficients for the missions (the factor preceding the performance term, *i.e.* 2 in M1 and 4 in M2) are important in determining the relative importance of each mission. Figure 6 shows that the final score is most sensitive to a reduction in empty weight, since the RAC (given by the empty weight) divides the

sum of the three flight mission scores, and is thus more important than any of the individual scores. Next, the speed of the aircraft will be important as it affects both the number of laps the aircraft is capable of flying (M1 score) as well as how fast it can fly 3 laps with 2lb of payload (M3 Score). Finally, the score is least sensitive to increasing the payload weight for M2, because adding a third cargo (50% increase in capability) would only increase the final score by 22%, but this would also require a higher empty weight.

3.3 Design Requirements Objectives

Considering this score sensitivity analysis, the team concluded that the required plane must be light, fast, and capable of completing the Taxi Mission. To begin working towards these goals, the team formulated the mission and aircraft design requirements, shown in Table 4 in order of importance, with 5 being the most important.

Table 4: Mission and Aircraft design requirements.

Relative Importance	Mission Requirement	Aircraft Requirement	Figures of Merit
5	Pass Taxi Mission	Steerable, rough-field-capable landing gear	Landing Gear Complexity
4	40 ft TOFL with maximum payload	High lift capability, thrust/weight	$C_{L_{Max}}$, S, Weight
3	Minimize EW		# Joints, Weight, Spar Design, Landing Gear Complexity, Internal Volume
2	Maximize N_{Laps}, Minimize t_{USC}	Low drag, efficient propulsion	$C_{D,0}$, S, Weight
1	Carry M2 & M3 payloads	Sufficient payload volume	S, Internal Volume

From these priorities, it was determined that the team must design an aircraft by considering landing gear capability, aerodynamic and performance characteristics, and structural integration of each component, while focusing on minimizing the total empty weight.

3.3.1 Configurations

3.3 Configuration Selection

Once the design requirements and figures of merit were determined, the team evaluated several aircraft configurations to determine which one would score highest. A preliminary study narrowed the options to three: a conventional monoplane, a blended wing body, and a tailless wing-body, shown in Table 5.

Table 5: Considered aircraft configurations.

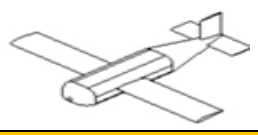		
Monoplane	**Tailless Wing/Body**	**BWB**

3.3.1 Aircraft Configuration

Since the team could not fully optimize each configuration for a comprehensive comparison, a more immediate comparison method was used to choose a configuration. This method used a series of estimates and assumptions that quantitatively compared how different configurations performed across a range of design parameters. The top five design parameters were chosen based on the score analysis described in Section 3.2 and were ranked from 1 to 5, with 5 being the most important parameter. From this, figures of merit (FoM)were determined, as shown in Table 4.

Each FoM was weighted against one another by assigning each a value of 1 and then multiplying that value by the rank of the design parameter under which the FoM was categorized. The values for all FoMs were summed and a FoM Score Factor was calculated by dividing an individual FoMs value by the sum of all values. For instance, because Internal Volume appears under both (3) Minimize EW and (1) Carry M2 & M3 payloads, Internal Volume has 4 out of the total 42 distributed points. Therefore, Internal Volume has a FoM weight of $4/42 = 0.095$.

Next, the three configurations listed in Table 4 were ranked against one another with respect to each FoM from 1 to 3, with 3 being the best performer. Different configurations could share a rank for FoMs so two or more configurations could receive high marks for a single FoM. The FoM rank was then multiplied by its respective score factor yielding weighted FoM ranks for each configuration. Weighted FoM ranks were summed and the configuration with the largest sum was the most competitive aircraft for the competition.

Table 6 shows the completed downselect along with FoM Weight and the total score of each configuration. Note that because TOFL and RAC are functions of weight and were taken as top priorities, the FoM of weight received the heaviest score factor.

Table 6: Aircraft configuration downselect.

Figure of Merit	FoM Value	FoM Score Factor	Monoplane	Tailless Aircraft	Blended Wing Body
Weight	9	0.214	1	3	3
Landing Gear Complexity	8	0.190	3	1	1
S	7	0.167	2	2	3
$C_{L_{Max}}$	6	0.142	3	2	1
Internal Volume	4	0.095	3	2	1
# Joints	3	0.071	2	1	3
Spar Design	3	0.071	3	2	1
C_{D_0}	2	0.048	1	2	3
Total	**42**	**1.00**	**2.23**	**1.95**	**2.00**

AircraftConfigurationDownselect

Due to the 40 ft TOFL requirement, the importance of the Taxi Mission and empty weight, the team used this downselect process to select the monoplane configuration.

3.3.2 Empennage

Based on the chosen monoplane configuration, an empennage was chosen to provide necessary stability and control characteristics, while minimizing drag and minimizing RAC. The following designs were compared, and a configuration downselect is shown in Table 7.

- **Conventional –** This design is easiest to integrate into the fuselage structure, which results in the lightest configuration choice. Pitch and yaw control are not coupled, allowing these to be sized separately.
- **T-tail –** In this configuration, the horizontal is mounted on top of the vertical stabilizer, which allows it to be mounted clear of the wing wake. However, considerably more structural weight must be added to mount and support the horizontal stabilizer.
- **V-tail –** The stabilizers form a V-shape, which provide both pitch and yaw control. This design is easier to integrate than a T-tail, but is still heavier than a conventional tail. The coupling of pitch and yaw control also results in coupling between longitudinal stability and lateral-directional stability.

A V-tail was built for two early iterations. It was found that in order to obtain sufficient directional stability to account for crosswind flight and crosswind landings in Wichita, the V-tail needed to be unnecessarily large, which resulted in excess longitudinal stability. It was found that a conventional tail that could obtain the desired stability and control characteristics, as listed in Section 4.4.2, was smaller in total surface area than a V-tail, and lighter to integrate. These factors drove the decision to select a conventional configuration.

3.3.2 EmpennageDownselect

Table 7: Empennage downselect.

Figure of Merit	FoM Value	Conventional	T-tail	V-tail
Weight	0.55	1.00	-1.00	-1.00
Drag	0.20	0.00	0.00	1.00
Stability and Control	0.25	0.00	1.00	-1.00
Total	**1.00**	**0.55**	**-0.30**	**-0.60**

3.4 Aircraft Components Selection, Processes, and Results

Following the aircraft configuration process and selection, similar studies were performed for individual propulsion, landing gear, and payloads components. Each configuration choice was quantified using similar downselects as detailed in Sections 3.4.1 to 3.4.3. The highest-scoring components were then selected for the preliminary design.

3.4.1 Propulsion

The DBF contest rules stated that electric motors must be used, and placed limits on battery chemistry, battery weight and current within the system. The batteries must be NiMH or NiCad. The overall battery weight must not exceed 1.5 lb (680 g) and the system is current-limited with a 15 A fuse.

Motor Selection

The propulsion subteam was responsible for choosing a lightweight, efficient, and powerful motor configuration. The four motor configurations that were considered are described below and are shown as part of the downselect in Table 8.

- **Pusher –** Single motor aft of the fuselage.
- **Tractor –** Single motor located on the foremost point on the aircraft.
- **Wing-mounted –** Twin motors mounted on the endplates joining the wings.
- **Pull/push –** Twin motors mounted in-line, fore and aft of the fuselage.

Table 8: Motor configuration downselect.

Figure of Merit	Score Factor	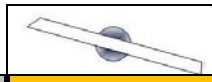 Pusher	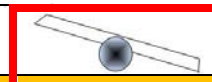 Tractor	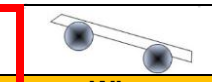 Wing-mounted	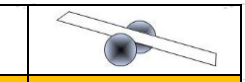 Pull/push
Weight	0.4	1	1	-1	-1
Landing Gear Interference	0.3	-1	0	0	-1
Efficiency	0.3	-1	0	-1	-1
Total	1.0	-0.2	0.7	-0.7	-1

The 2013-2014 DBF contest rules enforce a ground clearance requirement by passing a standard 2x4 on edge, under each wing no further than half of its semi-span. The pusher configuration did not afford this necessary ground clearance for the landing gear, so that option was discarded. The potential aerodynamic benefits (from counter-rotating propellers [7]) of the wing-mounted configuration were shown to be minor compared to the increased weight of two motors, from past team experience [8]. Also, the pull-push configuration increased the weight and complexity of the aircraft for no gain in efficiency. Thus, the tractor configuration yielded the largest benefit. This configuration provided the best weight-to-power ratio, ground clearance for landing gear, and presented no unnecessary complications in fabrication processes.

3.4.2 Landing Gear

3.4.2 LandingGearDownselect

The landing gear team was responsible for designing a gear to meet takeoff, landing and Taxi Mission requirements while simultaneously minimizing weight and drag. Four configurations were selected for initial comparison and are shown in Table 9. The tricycle configuration was set as the neutral-zero baseline with regards to the figures of merit.

Table 9: Landing gear downselect.

Figure of Merit	FoM Value	 Tricycle	 Wing-Tip Tricycle	 Bicycle	 Tail-Dragger
Ground Handling	0.35	0	1	-1	1
Durability	0.25	0	0	0	1
Stability	0.15	0	1	-1	0
Weight	0.10	0	0	1	1
Drag	0.15	0	-1	1	0
Total	1.00	0.00	0.35	-0.25	0.70

The landing gear FoMs emphasized the configurations' effects on ground handling, which was necessary for meeting the TOFL and Taxi Mission requirements. Durability was of second importance because of the vibrations caused during

the Taxi Mission. Weight and drag were also emphasized, as a reduction in both would yield a greater overall score. After evaluating the configurations given above, a conventional gear with a tail-dragger was chosen, which two main wheels forward of the center of gravity and either a tail wheel or skid. The tail dragger was chosen for its strong ground handling and stability characteristics as well as the ability to set the aircraft close to its stall angle in order to achieve $C_{L,\text{max}}$ within the TOFL limitation. The team had success in the past with this configuration and chose it this year as it was the lightest and most reliable.

3.4.3 Payloads

3.4.3 PayloadsBlocks

As stated in Section 3.1.2, the contest payloads are wooden blocks, ballasted to 1 lb (4.5 kg) each for Mission 2 and 0.5 lb (2.3 kg) each for Taxi Mission and Mission 3. At the 2013-2014 DBF competition the contest officials supply the cargos, whose dimensions are shown in Figure 7.

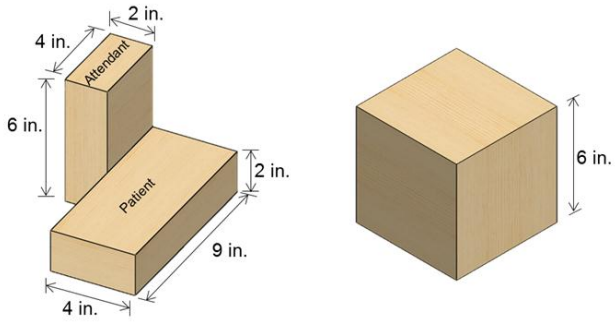

Figure 7: Payloads for Mission 3 (left) and Mission 2 (right).

Mission 2: Maximum Load

The Mission 2 payload configuration selection was governed by three primary constraints: fitting a minimum of one block into the fuselage as per DBF rules, minimizing fuselage volume to reduce RAC, and minimizing frontal area of the fuselage for better aerodynamic performance (less drag). To determine the optimal number of cargos to fly in Mission 2, the team conducted a trade study, which is detailed in Section 4.3.1. From this study it was determined that the highest score would be earned by carrying 3 blocks. From these requirements, three possible configurations for 3 paylaods were considered as shown in Figure 8.

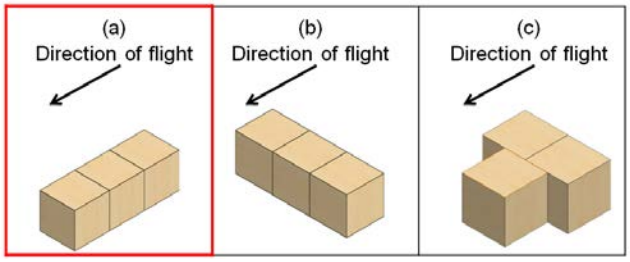

Figure 8: Possible internal payload arrangements for Mission 2 with respect to the line of flight.

Based on the need for a reduced frontal area and fuselage volume, the team determined that the Mission 2 payloads must be lined up inside the fuselage one behind the other along the line of flight, shown in Figure 8(a). This configuration

was then used to help determine the Mission 3 payload configuration.

Mission 3: Emergency Medical Mission and Taxi Mission

As stated by the contest rules, The Mission 3 and Taxi Mission payload configuration was subject to the following constraints:

- The attendant must be oriented vertically and the patient horizontal and flat.
- The attendant must be immediately adjacent to the side of the patient.
- The patients must be separated by a minimum of 2 in. side to side or above/below. No 2 in. spacing is required at the ends.
- At least 2 in. space above the patient will be an ”air space” with no structure or systems present.
- The attendants must be separated by at least 2 in. from each other.

From these initial constraints, two configurations were proposed as shown in Figure 9

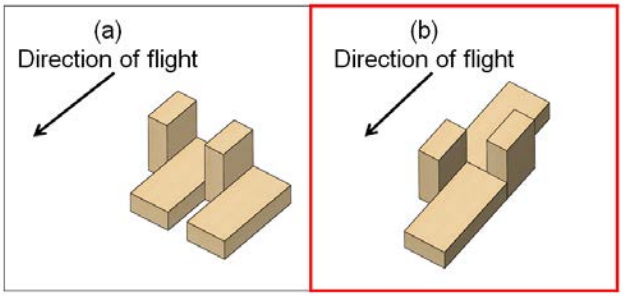

Figure 9: Possible configurations for the Emergency Medical Mission, with respect to the direction of flight.

As is discussed in Section 4.3.1, the length of three Mission 2 payloads is equivalent to the length of the Mission 3 payloads if the medical passengers are oriented inside the fuselage as depicted in Figure 9(b). For this reason, and because of the need to reduce fuselage volume and frontal area, configuration (b) was chosen for Mission 3.

Payload Restraints

In the preliminary design of the payload mounting system, the team had four main focus points: weight, volume, security and installment time. The chosen mechanism must be lightweight and small because they are part of the empty weight used to determine the RAC, as stated by DBF contest rules. The system must also adequately secure the cargo from shifting in flight, and be assembled in a maximum of five minutes. Based on these requirements, four different mechanisms were considered in a downselect process: Velcro, magnets, nylon nuts and bolts, and fishing line and foam wedges. Each mechanism was given a score of -1, 0 or 1 for each Figure of Merit, and the scores were then added with respect to each FoM value. As shown in Table 10, system weight had the largest importance, followed by volume, security and installment time.

Table 10: Payload mechanism downselect.

Figure of Merit	FoM Value	Velcro	Magnets	Nylon Nuts and Bolts	Fishing Line Straps
Weight	0.40	0	-1	-1	1
Volume	0.25	1	0	-1	1
Security	0.25	0	0	1	1
Installment Time	0.10	1	1	-1	0
Total	**1.00**	**0.35**	**-0.30**	**-0.50**	**0.90**

Velcro and magnets were considered because they would be simple to assemble and require relatively small internal volumes. Nylon nuts and bolts were tested because they would provide the best security if used to pin down the cargos. However, these options were dropped from consideration after DBF rule clarifications indicated that the payloads would be supplied by the contest officials and could not be drilled into or bonded. This rule did not preclude the fishing line and foam wedge mechanism, which was tested in the team's lab and verified at flight tests. Figure 10 and Figure 11 show these tests with Mission 2 and Mission 3 payloads inside carbon fiber and Kevlar fuselages fabricated by the team.

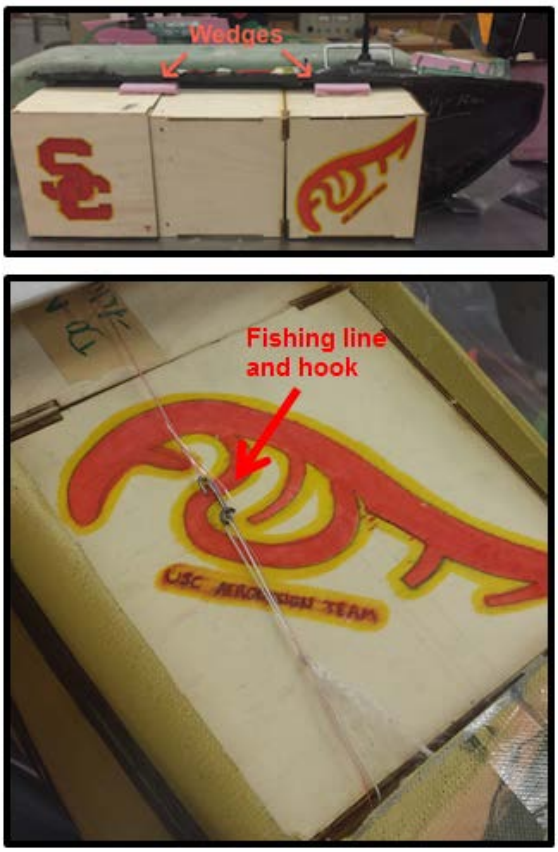

Figure 10: Foam wedges (top) and fishing line and hook mechanism (bottom) tested for Mission 2 payloads.

For the above tests, one end of each fishing line strap was bonded to the inside of the fuselage with Cyanoacrylates adhesive (CA), and they were connected at the opposite ends with a hook and loop. Foam wedges were placed between

the payload and the fuselage wall to prevent cargo movement.

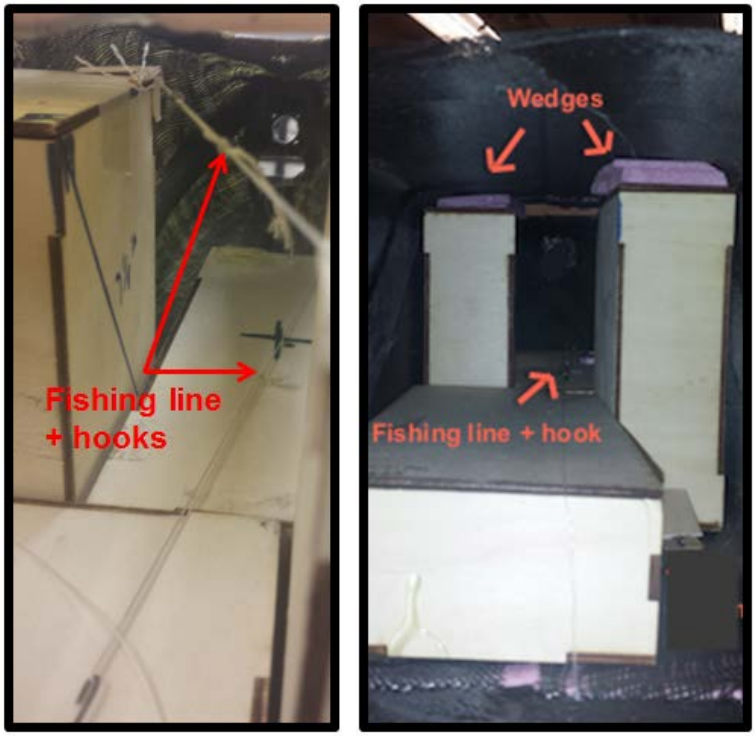

Figure 11: Fishing line, hooks and foam wedges tested for Mission 3 payloads. The left image shows payloads secured with only fishing line and hooks.

While foam wedges were successful at securing the cargos, it was found that the fishing line alone was sufficient. The team therefore decided to use fishing line and hooks as the payload securing system.

4 Preliminary Design

After selecting a general configuration, the aerodynamics, propulsion, landing gear, and structures subteams sized their respective aircraft components to meet design requirements and maximize design goals. The methodology involved performing trade studies using software simulation to obtain initial sizing and predict theoretical results to be tested.

4.1 Design and Analysis Methodology

The preliminary design phase constituted the team's iterative process that determined the specifications of the major aircraft components: the wings, the structure, and the power system.

Wings

- **Wing area –** Wing area is the most important parameter as it is the main source of lift, while also serving as an opportunity to advance the team's lightweight build efforts. The critical sizing constraint was the 40 ft (12.2 m) takeoff field length while carrying the maximum payload weight for Mission 2.

- **Aspect ratio –** Aspect ratio is also an important characteristic when considering a lightweight aircraft with a short takeoff field length requirement, as higher aspect ratios offer better takeoff and turning performance than low aspect ratio wings. Therefore, the team designed a wing with high aspect ratio to meet the TOFL requirement and to help reduce weight.
- **Airfoil –** The team designed a custom airfoil to meet the required takeoff C_l and achieve optimum L/D in cruise to improve performance.

Structures

- **Wing spars –** The wing spars were designed to be lightweight while supporting the largest in-flight and landing loads expected for the wings and empennage.
- **Fuselage –** The fuselage connects all aircraft components, thus requiring efficient load paths from the internal components to the ground. The fuselage must also have minimal weight and drag contributions so as to decrease weight, increase speed, and ultimately increase total score.

Propulsion

- **Motor, propeller, and battery pack –** These components were selected in order to maximize thrust and performance for the aircraft, while minimizing total package weight and staying within the 15 A fuse power constraint. Motor gearing can be altered to widen the effective speed constant range, along with propeller size to maximize mission performance.

4.2 Mission Model

The performance team optimized all important aircraft parameters using multidisciplinary design optimization (MDO) methods to determine the highest scoring design. MDO was implemented via PlaneTools, a package of simulation modules, classes, and objects written by the team in MATLAB. The primary module in PlaneTools simulated a full mission of the input aircraft according to the competition rules (independent of Taxi Mission score and report score) by modeling four maneuvers of the competition course, shown in Figure 12. Each maneuver had limitations in its governing equation in the mission model as summarized below.

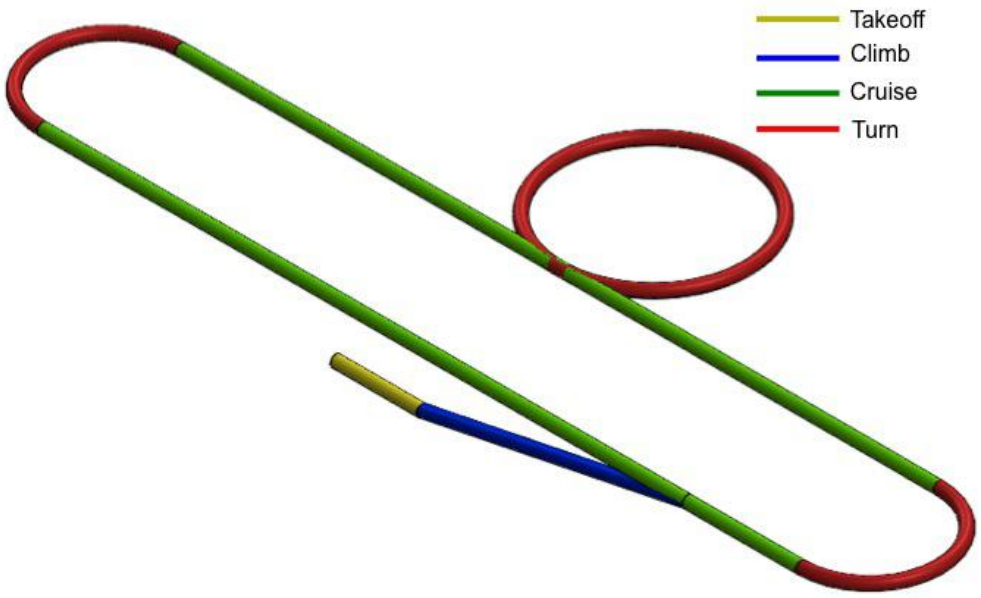

Figure 12: Competition flight course used in the mission model of PlaneTools.

1. **Takeoff –** This maneuver was assumed to be performed at maximum throttle. Flaps were deployed during takeoff for all missions to increase $C_{L,\max}$.
2. **Climb –** The aircraft was assumed to climb to 75 ft (22.9 m) above the 1,378 ft (420 m) altitude of Wichita, Kansas. The rate of climb (R/C) was calculated via the difference in thrust and drag on takeoff and multiplied by the proportion of the takeoff speed to the plane's weight.
3. **Cruise –** This phase of flight was assumed to be level, unaccelerated flight with equal thrust and drag. An optimum cruise throttle setting was selected so that the aircraft did not exceed battery capacity and not more than half of the capacity remained at the end of the mission.
4. **Turn –** A sustained turn with constant speed was assumed for both types of turning maneuvers (two 180°turns and one 360°turn). The load factor on the aircraft structure was assumed based on known properties of the wing structure.

Fundamental aircraft and aerodynamic equations were used to calculate important output parameters such as TOFL, R/C, V_{cruise}, and r [9]. The mission model also included the following uncertainties and assumptions:

- **Winds –** A headwind of 15 ft/s (4.6 m/s) was assumed for takeoff and cruise equations based on the historical weather patterns of Wichita, Kansas [5].
- **Battery performance –** Battery specifications (resistance and capacity) used in the mission model were based on laboratory testing and flight tests rather than on manufacturer specifications (which tended to overestimate performance). Battery voltage was assumed to be constant throughout flight.
- **Propeller performance –** The coefficients of thrust (C_T) and power (C_p) of different propellers were based on the APC propeller performance data and verified via static testing[6].

The mission model also neglected ground rolling friction, interference drag, and compressibility effects. Since most inputs were estimates in the model, the outputs were estimates as well. In order to account for these uncertainties, extensive testing was performed in the laboratory and at flight tests to ensure that outputs from the mission model were as close to the actual aircraft performance as possible.

Since PlaneTools is an object-oriented program, the mission model is programmed as a class with several operations to simulate missions on any user-defined plane. The role of the mission model in PlaneTools is represented by Figure 13. First, the aircraft Components were defined. These Components then defined a Plane, which was the input of the overall Mission Model. The team used the model to run mission simulations with different defined Planes. This object-oriented approach allowed the team to isolate each component of the aircraft and perform trade studies more effectively.

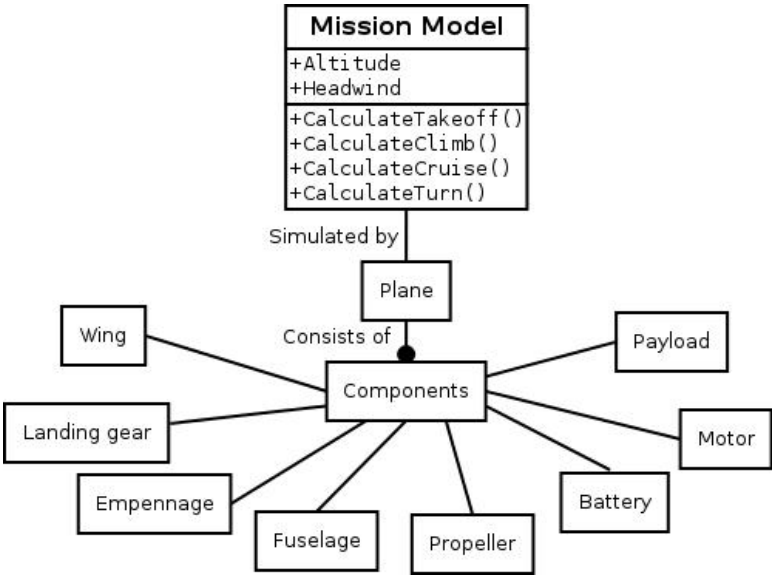

Figure 13: PlaneTools object model.

4.3 Design and Sizing Trades

Design and sizing trade studies were performed iteratively to develop the highest-scoring aircraft that satisfied all requirements based on the competition rules. These trade studies began with initial estimates and were updated progressively after each design iteration.

4.3.1 Number of Cargos

The quantity of cargos to be carried in Mission 2 was the first parameter identified since all other parts of the aircraft were designed to satisfy the mission's other requirements. The minimum number of cargos considered was 2, because that payload weight of 2 lb (9.2 kg) was equivalent to the payload weight for Mission 3. It was estimated that the aircraft empty weight would increase by 0.6 lb (272 g) and that the fuselage length would increase by 8 in. (0.2 m) for every additional cargo added. However, because the payload configuration for Mission 3 was equivalent to the length of 3 cargos for Mission 2 in terms of volume, any number of cargos below 4 had the same fuselage length. Furthermore, the performance of the aircraft would also increase with each additional cargo added because more power would be required to make TOFL. Based on estimations and appropriate inputs in the mission model discussed in Section 4.2, a

trade study was performed on payload quantity. The results are shown in Figure 14, where 3 cargos scored higher than 2 cargos, and where carrying 4 cargos failed to meet the TOFL requirement. The trade study led to the conclusion that carrying 3 cargos for Mission 2 would be optimal.

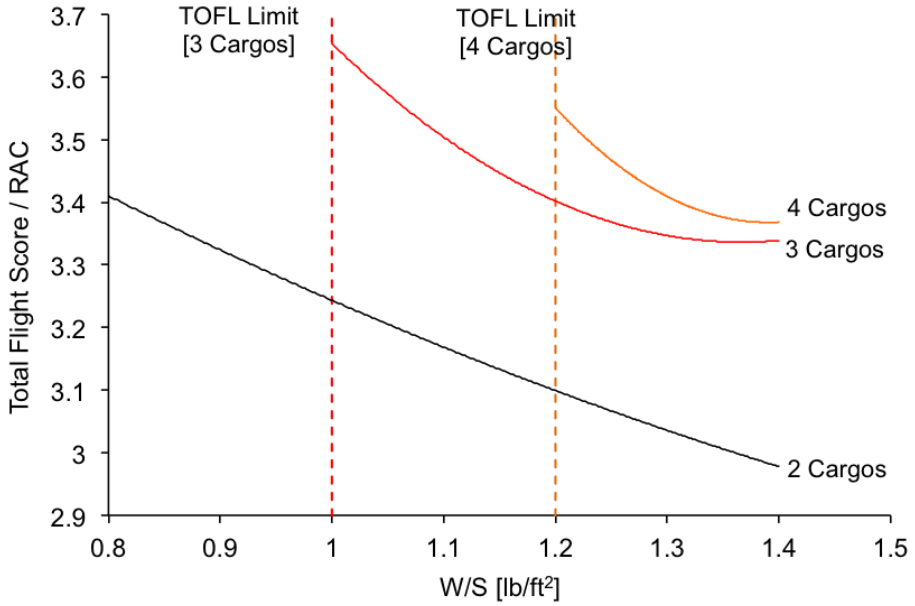

Figure 14: Trade study between number of cargos and TFS/RAC.

4.3.2 Wing Geometry

Trade studies were conducted to determine the maximum-scoring aircraft with the optimum wing geometry. This was completed by determining the effect of variations in AR and s on the score, as shown in Figure 15.

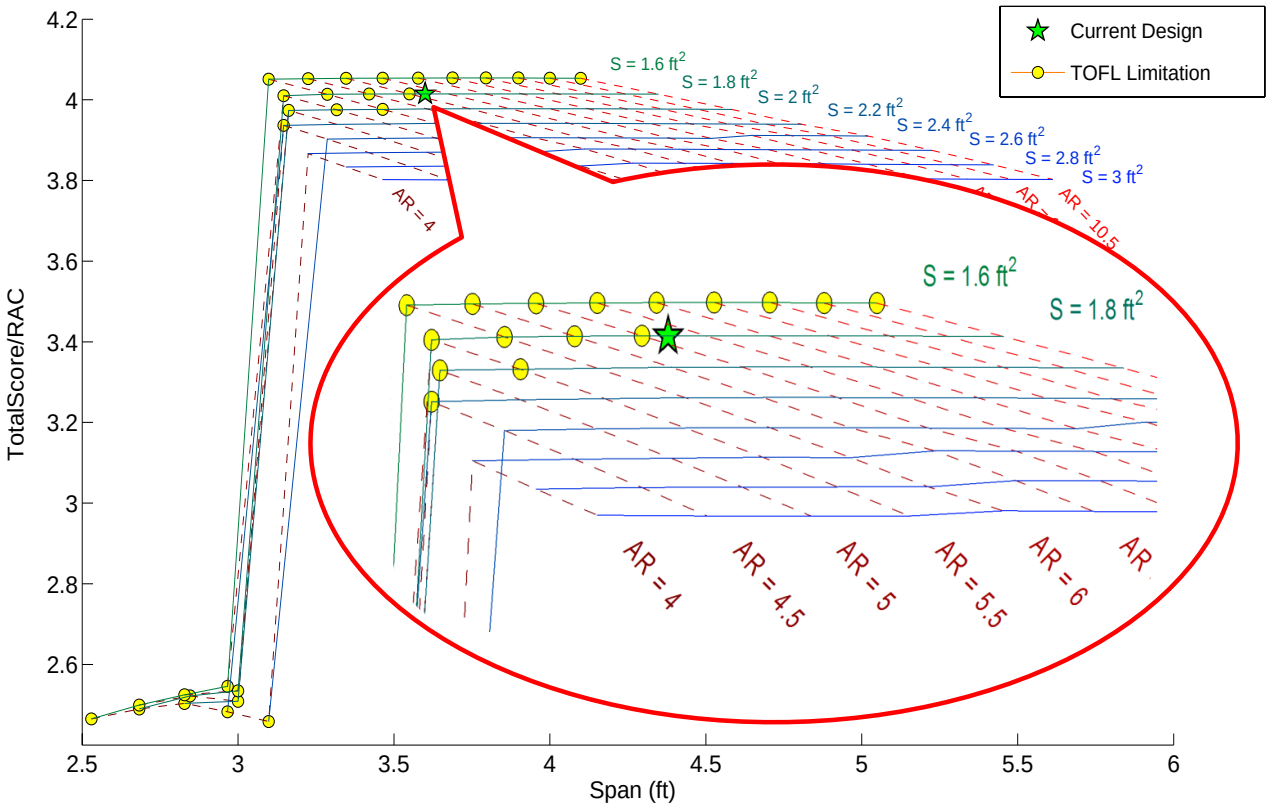

Figure 15: Carpet plot of varying wing area as a function of TFS/RAC. The green star indicates the chosen design.

The sharp drop on the left hand side of the plot represents failure to fly 3 laps in Mission 2 with the input propulsion package. The plot also shows that a high-scoring aircraft will need to have small wing area as it increases cruise speed and decreases empty weight. However, aircraft with small wing area require a longer TOFL. In order to meet the TOFL requirement, a higher aspect ratio wing is required to improve wing efficiency and decrease induced drag, thus reducing TOFL. The highest-scoring aircraft that met all these requirements was found and represented by the green star on the plot. The preliminary wing geometry had a wing area of 1.8 ft^2 (0.17 m^2), aspect ratio of 7.2, and total flight score over rated aircraft cost of 4.0.

4.3.3 Aerodynamics

Airfoil Selection

The short TOFL and 15 A fuse requirements dictated the need for a high $C_{l,\max}$ wing airfoil. Additionally, since Missions 1 and 3 are speed critical, low drag coefficients at cruise C_l were required.

Many airfoils were analyzed using XFOIL at the estimated mission Reynolds number (Re_c) of 250,000, a regime in which this flow analysis tool provided valid results [4]. The use of 12°flaps was considered for all analysis. Figure 16 shows the polars for the three final airfoils: the BA527ls, CC46-415, and CC48-513, which are all team-designed airfoils. The BA527ls has a lower C_d than the other airfoils at the Mission 1 and Mission 3 cruise C_l of 0.13 and 0.25, respectively, but with its low $C_{l,\max}$ of 1.71 with flaps deployed, the wing would need to be unnecessarily large to make TOFL. The CC46-415, with a $C_{l,\max}$ of 1.87 with flaps, was used on the team's competition plane in 2013, which had a similar

short TOFL requirement. The chosen airfoil was the CC48-513, which has a $C_{l,\max}$ of 2.00, yet has a lower C_d than the CC46-415 at all cruise C_l.

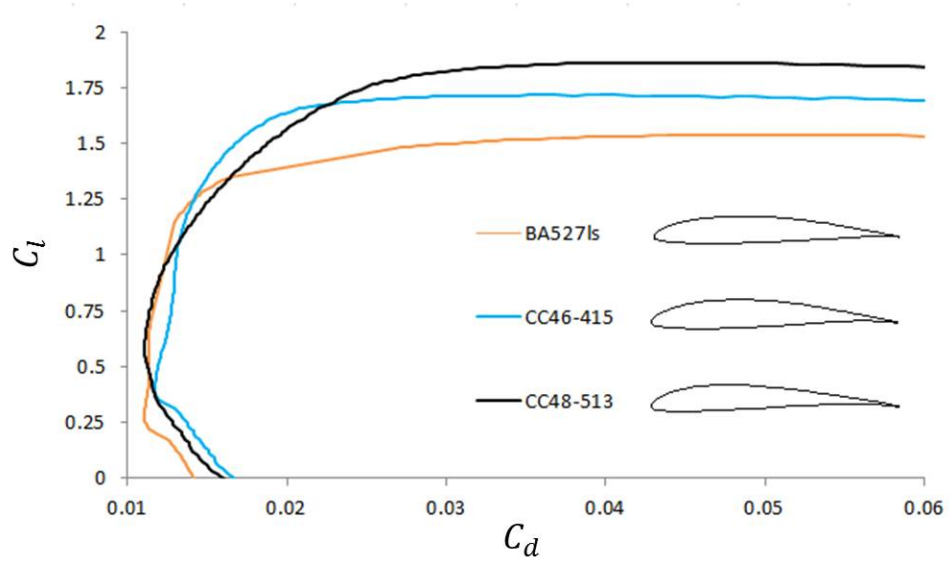

Figure 16: Polars for the BA527ls, CC46-415, and CC48-513, the three final airfoil candidates, analyzed in XFLR5 at $Re_c = 250000$.

Computational Flow Analysis

Athena Vortex Lattice (AVL), an open source inviscid flow solver, was used to analyze the flow over the aircraft. The AVL geometry and relevant dimensions are shown in Figure 17.

Wing	
Airfoil	CC48-513
Span, b	3.60 ft (1.10 m)
MAC, c	0.50 ft (0.15 m)
Planform Area, S	1.80 ft^2 (0.15 m^2)
Aspect Ratio, AR	7.2
Incidence Angle	-2°
Horizontal Tail	
Airfoil	NACA0012
Span, b	1.38 ft (0.42 m)
MAC, c	0.38 ft (0.12 m)
Planform Area, S	0.52 ft^2 (0.048 m^2)
Incidence Angle	-2°
Tail Arm	1.91 ft (0.58 m)

Vertical Tail	
Airfoil	NACA0012
Span, b	0.70 ft (0.21 m)
MAC, c	0.38 ft (0.12 m)
Planform Area, S	0.27 ft^2 (0.025 m^2)
Tail Arm	1.91 ft (0.58 m)

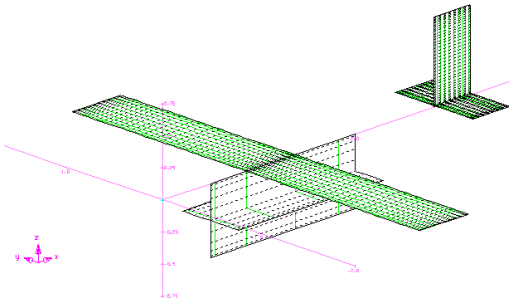

Figure 17: AVL model and dimensions for primary aerodynamic surfaces.

4.3.3 Trim Deflections

The AVL solutions were then used to perform Trefftz plane analysis to determine the aircraft angle of attack and the trim elevator deflections. Acceptable bounds of $\pm 5^\circ$ for α and $\pm 3^\circ$ for tail deflection were set for low trim drag, to optimize for the speed-sensitive Missions 1 and 3. From Table 11, it can be seen that these characteristics are within acceptable bounds.

Table 11: Trim deflections for cruise conditions.

	M1 Cruise	M2 Cruise	M3 Cruise
e	0.21	0.64	0.52
α [º]	-2.6	-0.3	-1.1
Elevator [º]	-0.9	-2.4	-1.9
C_L	0.13	0.31	0.25
C_D	0.0295	0.0327	0.0313
C_{D_i}	0.0035	0.0067	0.0053
C_{D_p}	0.026	0.026	0.026
SM [%]	15	16	15
x_{CG}	1.0 ft (0.3 m)	1.0 ft (0.3 m)	1.0 ft (0.3 m)

Figure 18 shows the Trefftz plot for Mission 2, in which the plane is most heavily loaded. The pink curve denotes the lift coefficient normalized with respect to the wing chord. It can be seen that the lift distribution is positive along the entire span. The Trefftz plot also shows that the inner third of the wing will stall before the outer two-thirds of the wing, which protects the wing against tip stall.

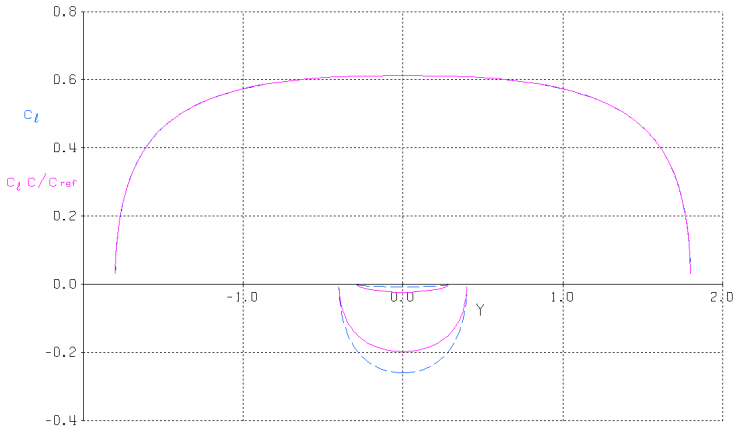

Figure 18: Trefftz plot for Mission 2 cruise conditions. Spanwise units given in feet.

4.3.4 Propulsion

The initial propulsion system was designed with initial constraints: a 15 A fuse, a 40 ft (12.2 m) TOFL requirement and a maximum battery pack weight of 1.5 lb (0.7 kg). With a high emphasis on weight, the propulsion team attempted to design and implement the lightest propulsion package possible.

NiMH cells were chosen due to their higher energy compared to NiCad cells. The 11-cell battery pack, comprised of Elite

1500 2/3 A cells, has a nominal resting voltage of 13.2 V. The power drawn from the batteries is given by Equation 10.

$$\text{Power} = \text{Voltage} * \text{Current} \tag{10}$$

This shows that the same power can be achieved when the system is operating at high voltage and low current as when it is operating at low voltage and high current. This fact allows the propulsion package to have a reduced voltage (and thereby reduced weight) while generating the same power output.

A trade study between wing area and number of battery cells conducted by the performance subteam showed that the highest projected score was with an 11-cell pack of Elite 1500s for all missions. The voltage drop at takeoff was found to be as low as 60% of the rated voltage of the pack; therefore, at takeoff the available power is:

$$\text{Power} = 0.60 \times \text{Voltage} \times \text{Current} \tag{11}$$

A power of 220 watts is therefore required for takeoff:

$$\text{Power} = 0.60 \times \text{Voltage} \times \text{Current}_{\text{takeOff}} = 0.60 \times 13.2\ \text{V} \times 28\ \text{A} = 220\ \text{W} \tag{12}$$

The takeoff current estimation of 28 A was based on data taken during flight testing. The gross takeoff weight of Mission 3 dictated the power loading (in W/lb) from which the maximum current of the system can also be found:

$$\text{M3 gross weight} \times \text{power loading} = \text{maximum current required} \tag{13}$$

$$\frac{220\ \text{W}}{4\ \text{lb}} = 55\ \text{W/lb} \tag{14}$$

$$\text{Current} = \frac{\text{Power}}{\text{Voltage}} = \frac{220\ \text{W}}{13.2\ \text{V}} = 17\ \text{A} \tag{15}$$

The required current of 17 amps exceeds the 15 A rating of the fuse. Therefore, fuse testing was conducted by the team in order to determine the feasibility of maintaining this current loading on the slow-blow fuse (see Section 7.1 for more details) as well as the elevated current of 28 A at takeoff.

4.3.5 Structures

The main objective of the structures subteam was to develop the most weight-efficient structure for the airplane due to the direct correlation between RAC and total score. Design efforts were focused on wing and fuselage structure.

The wing's structural design was constrained by the wing geometry (Section 4.3.2) and maximum aerodynamic loads. The score analysis of Section 3.2 drove the decision for a balsa built-up wing. The primary wing structure was a full-span spar designed to transfer loads into the fuselage. Trade studies were performed on different materials and sizes of the spar cap and shear web using an Excel-based analytical tool, SparSizer, developed by one of the team advisers. Preliminary analysis was done using the wing dimensions in Figure 17. The spar was designed as an I-beam with carbon fiber caps and balsa wood shear web. The maximum gross weight of the preliminary airplane was estimated to be 5.0 lb (2.3 kg). Analysis in SparSizer was done on a half-span wing providing half the required lift. Cap and shear web thickness were then varied to achieve a factor of safety of 1.5 throughout the wing spar. Figure 19 shows

the performance of the chosen spar design. The figure trend shows that the spar's mid-section shear web was thicker relative to the wing tip.

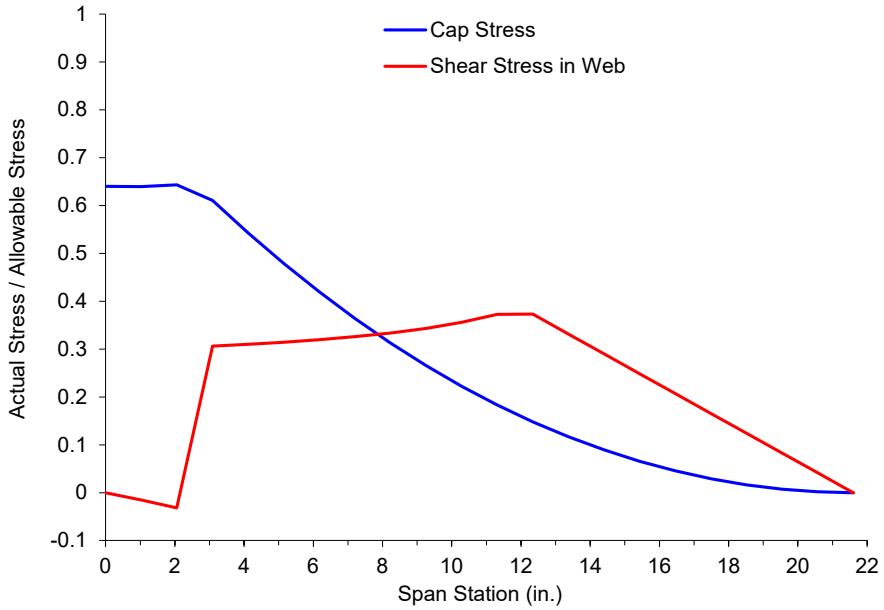

Figure 19: Stress in the spar as a function of span station.

4.3.6 Landing Gear

4.3.6 WheelDiameter

Because of this year's Taxi Mission, an initial downselect process was utilized for Taxi Mission completion. Having chosen a traditional tail dragger as the landing gear, the landing gear team performed tests to determine the relationship between wheel diameter and force required to cross the roofing panels. Multiple wheel diameters were laser cut out of plywood and attached to one of the team's prototype aircraft. A fish scale was used to pull the plane and determine the force required to get over the first hump of the roofing panels. These results are seen in Table 12.

Table 12: Front wheel diameter testing.

Front Wheel Diameter	Force required to taxi over roofing panel [N]
3.0 in. (7.6 cm)	15.6
5.0 in. (12.7 cm)	11.6
7.0 in. (17.7 cm)	9.8
9.0 in. (22.9 cm)	8.9
11.0 in. (27.9 cm)	7.2

Initial testing results show that a 9.0 in. (22.9 cm) wheel attached to a fully weighted tail-dragger plane was required to overcome the first roofing panel ridge without any additional mechanisms. A stiff diameter wheel of that size had the potential to weigh more than desired. A similar test was used to determine the dragger wheel sensitivity; results showed no relation between rear wheel size and force required.

Other methods for taxiing the roofing panels included using small wheels along with the belly of the aircraft, or vertical or horizontal skids. Horizontal skids were quickly fabricated for testing and with a 3.0 in. (7.6 cm) wheel. When the skid was integrated with the 3.0 in. (7.6 cm) wheel, it was found to be equivalent to a 9.8 in. (25 cm) wheel diameter without

a skid. Since the horizontal skids showed promise, a Taxi Mission mechanism downselect was used to determine the Taxi Mission landing gear configuration. A similar FoM system was used as in Section 3.4.2 with a large-wheel aircraft as the neutral-zero baseline. All values were tabulated and are shown in Table 13.

Table 13: Landing gear downselect.

Figure of Merit	Weight	Large Wheels	Belly	Horizontal Skids	Vertical Skids
Rough Field Capability	0.40	0	0	1	1
Stability	0.15	0	1	1	1
Weight	0.10	0	1	1	1
Drag	0.15	0	1	-1	0
Durability	0.20	0	-1	0	0
Total	1.00	0.00	0.20	0.50	0.65

The Taxi Mission mechanism downselect results showed that a vertical skid with a small protruding wheel was the winning option.

With a mechanism to slide across the roofing panels, steering was the next area of concern. Initial testing for a steerable tail dragger was not fruitful. With little weight on the rear of the aircraft the tail wheel tended to bounce across the plastic. Two clear solutions were realized. First, the weight could be shifted back in the fuselage for the Taxi Mission. Another option was that steering could come from the main gear. With weight being a concern, the team developed differential braking for the front two wheels. The differential braking required a torsional spring for each wheel that clamps down onto the wheel hub. When only one brake was clamped on, the propeller pivoted the aircraft around that wheel. Assuming that the tire material created sufficient friction with the PVC plastic, a plane with skids on the main gear was able to steer during the Taxi Mission every time the protruding wheel hit the roofing panels.

4.4 Aerodynamics, Stability, and Control Characteristics

Stability and control analysis was performed in AVL to ensure the aircraft was optimized for performance, and to verify static and dynamic stability in the five modes of motion.

4.4.1 Aerodynamics Characteristics

Lift Estimates

AVL was used to estimate the drag of the aircraft over a range of C_L. Figure 20 plots the L/D versus C_L and shows the cruise and turn lift coefficients for Missions 1 and 3, since these are the time-sensitive missions. While the plane operates below $(L/D)_{\max}$ for cruise, it operates close to $(L/D)_{\max}$ for both Mission 1 and 3 turn conditions, which accounts for roughly 65% of the energy in each lap due to high-*g* loadings.

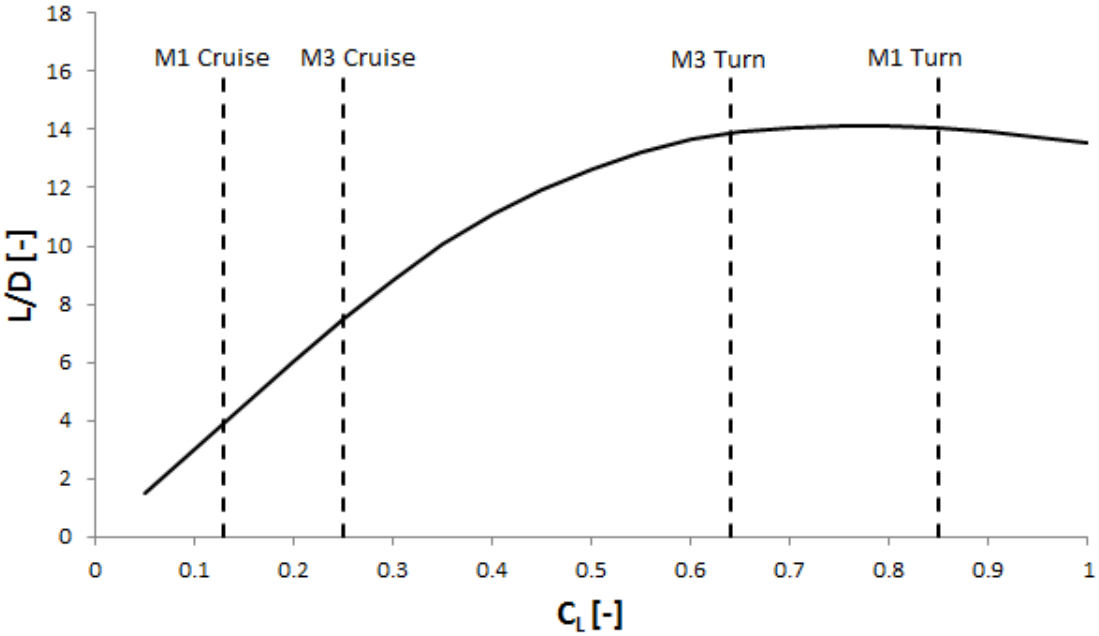

Figure 20: L/D versus C_L with cruise and turn C_L indicated for Missions 1 and 3.

Drag Estimates

After the components were selected, the drag was estimated. The vortex drag was estimated using AVL, whereas the viscous drag was estimated using the method of equivalent flat plate areas, as described by Hoerner and Page [1][2]. Figure 21 shows the breakdown of various drag components.

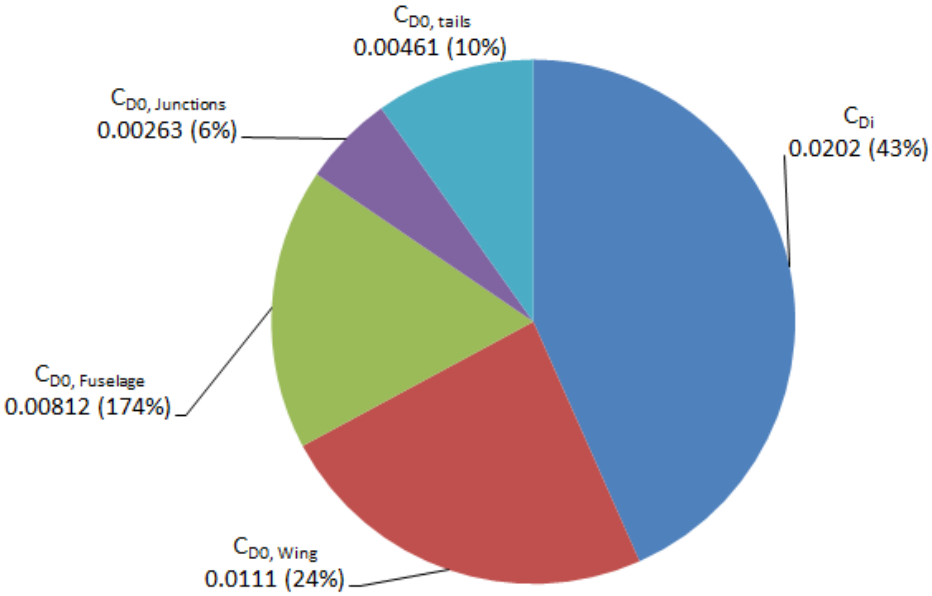

Figure 21: Drag breakdown for Mission 3 turn.

4.4.2 Stability and Control Characteristics

Static Stability

Static stability was iteratively sized in AVL. The static margin goal was set to 15% , and the tail arm and tail size were iterated until the static stability derivatives were valued as desired. The final static margin was 15% , as shown in Section 4.3.3, which located the center of gravity at 25% behind the leading edge of the wing. Additionally, it can be seen from Table 14 that C_{m_α}, C_{m_q}, C_{l_β}, C_{l_p}, and C_{n_r} are negative and C_{n_β} is positive, which is a necessary condition for static stability.

Table 14: Static stability derivatives calculates with AVL.

C_{L_α}	$C_{L_{\delta e}}$	C_{L_q}	C_{m_α}	$C_{m_{\delta e}}$	C_{m_q}	C_{Y_β}
4.83	0.005	8.37	-0.889	-0.020	-14.5	-0.695
C_{l_β}	C_{n_β}	$C_{Y_{\delta a}}$	$C_{l_{\delta a}}$	$C_{n_{\delta a}}$	$C_{Y_{\delta r}}$	$C_{l_{\delta r}}$
-0.068	0.157	0.000	-0.004	-0.001	0.002	0.026
$C_{n_{\delta r}}$	C_{Y_p}	C_{l_p}	C_{n_p}	C_{Y_r}	C_{l_r}	C_{n_r}
-0.489	-0.021	0.552	-0.021	0.552	0.179	-0.244

Dynamic Stability

The plane's five modes of motion were analyzed in AVL to determine the plane's dynamic stability characteristics. Figure 22 shows a root locus plot of the short period, dutch roll, roll, spiral and phugoid modes, plotting damped frequency (ω_d) versus the negative product of damping coefficient and natural frequency ($-\zeta\omega$). Using the stability derivatives in Table 14 and the aircraft's mass moments of inertia, the five modes were calculated using AVL and derivations from Yechout [3]. It can be seen that all modes were stable except for spiral.

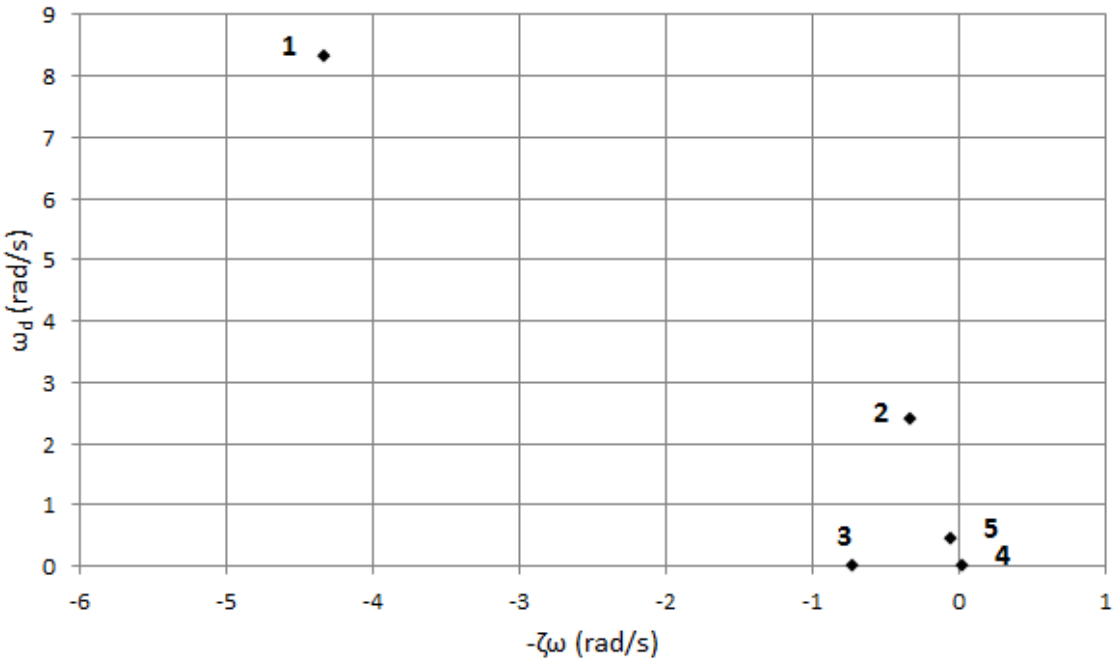

Figure 22: Root locus plot for the five modes of motion: (1) short period, (2) dutch roll, (3) roll, (4) spiral and (5) phugoid.

The damping coefficient (ζ), natural frequency (ω), $\zeta\omega$, and time constant (τ) for the modes are shown in Table 15.

Table 15: Dynamic stability parameters.

Mode Number	Mode	ζ	ω_n (rad/s)	ζω (rad/s)	τ (s)
1	Short Period	0.46	9.4	4.3	0.23
2	Dutch Roll	0.13	2.4	0.32	3.1
3	Roll	-	-	-	1.4
4	Spiral	-	-	-	-30
5	Phugoid	0.12	0.44	0.054	19

4.4.2 RotationRates

Based on comparisons between Table 15 and acceptable stability characteristics from MIL-F-8785C, the plane was found to have the desired characteristics [10].

A dynamic analysis was then carried out based on dimensionless turn rates for the maximum rates expected in any turn maneuver, as determined from the AVL documentation. The rotation rates used are given in Table 16.

Table 16: Rotation rates used in AVL analysis.

Rotation	Roll	Pitch	Yaw
Rate	±0.10	±0.03	±0.25

AVL was used to determine the maximum deflections for any permutation of the above rotation rates, which resulted in conservative sizing as these rotation rates were much more aggressive than those expected in flight [4]. The maximum aileron, elevator, and rudder deflections were found to be 8°, 22°, and 24°, respectively, which were lower than the construction limits of 25° for all surfaces. This shows that the aircraft had acceptable control authority.

4.5 Predicted Aircraft Mission Performance

After an optimum design was found, predictions for the aircraft's mission performance were generated using PlaneTools for each mission and are shown in Table 17, while the total predicted score is shown in Table 18.

Table 17: Preliminary aircraft predicted performance.

Performance Parameter	Mission 1	Mission 2	Mission 3
$C_{L_{max}}$	1.04	1.04	1.04
$C_{L_{cruise}}$	0.13	0.31	0.25
e	0.21	0.64	0.52
C_{D_0}	0.026	0.026	0.026
L/D_{max}	14.1	14.1	14.1
L/D_{cruise}	2.7	5.9	5.0
$TOFL$	3.5 ft (1.1 m)	40.0 ft (12.2 m)	20.0 ft (6.2 m)
Rate of Climb, R/C	37.2 ft/s (11.3 m/s)	17.8 ft/s (5.4 m/s)	22.1 ft/s (6.7 m/s)
W/S	0.85 lb/ft^2 (9.15 lb/m^2)	2.05 lb/ft^2 (22.1 lb/m^2)	1.60 lb/ft^2 (17.8 lb/m^2)
Cruise Speed	77.1 ft/s (23.5 m/s)	76.0 ft/s (23.2 m/s)	76.0 ft/s (23.2 m/s)
Stall Speed	26.8 ft/s (8.2 m/s)	41.6 ft/s (12.7 m/s)	37.0 ft/s (11.3 m/s)
Gross Weight	2.13 lb (0.65 kg)	5.13 lb (2.33 kg)	4.13 lb (1.87 kg)
N_{laps}	6	4.5 PredictedScore -	-
N_{cargo}	-	3	-
t_{USC}	-	-	132 s
Mission Score	1.50	3.00	3.62

Table 18: Preliminary aircraft predicted total score.

Scoring	
$Total\ Flight\ Score$	8.12
EW	2.13 lb (0.97 kg)
RAC	2.13
$\frac{Total\ Flight\ Score}{RAC}$	3.8

The preliminary design was expected to meet the takeoff field length requirement for all flight missions. Fuselage design, payload restraints, and build techniques were assumed to be optimized for a low RAC and a high overall score.

5 Detail Design

Detail design combines theoretical sizing with physical, real-world considerations. Each subteam examined the structural capabilities, subsystem design, weight and balance, and flight and mission performance in order to define the characteristics of the final aircraft.

5.1 Dimensional Parameters Table

Table 19 lists the characteristic parameters for the team's entry, *Mischief*, into this year's DBF competition.

Table 19: *Mischief* characteristic parameters.

Wing	
Airfoil	CC48-513
Span	4.2 ft (1.3 m)
MAC	0.5 ft (0.15 m)
Wing Area (S)	2.1 ft^2 (0.2 m^2)
Aspect Ratio	8.4
Incidence Angle	-2°
Static Margin	16%

Tail Surfaces		
	Horizontal	Vertical
Airfoil	NACA 0012	
Span	1.38 ft (0.42 m)	0.7 ft (0.21 m)
MAC	0.38 ft (0.12 m)	0.38 ft (0.12 m)
Wing Area(S)	0.27 ft^2 (0.025 m^2)	0.52 ft^2 (0.048 m^2)
Incidence Angle	-3°	0°
Tail Arm	1.91 ft (0.58 m)	1.91 ft (0.58 m)

Fuselage	
Length	3.08 ft (0.94 m)
Width	0.58 ft (0.18 m)
Height	0.58 ft (0.18 m)

Controls	
ESC	Thunderbird 18A
Receiver	Futaba R617FS
Servos x 6	D47
Fuse	Impulse 15A

Propeller	
M1	15 x 16
M2	18 x 6
M3	15 x 16

Motor	
Model	NEU 11056D
Gearbox	6.7:1
KV_{eff}	355
Power Rating	200 W constant / 400 W surge
I_0	0.45 A
Resistance	0.055 Ω
Total Weight	0.3 lb (130 g)

Battery	
Model	Elite 1500
Capacity	1500 mAh
Resistance	0.015 Ohm
Cell Voltage	1.2V
Cell Count	11
Pack Voltage	13.2 V
Pack Weight	0.6 lb (266 g)

5.2 Structural Characteristics and Capabilities

The aircraft structure was driven by maximum load cases. The wing was designed and sized to withstand a 4 *g* load case with an empty weight of 5.0 lb (2.3 kg), allowing for a 75° bank angle with a safety factor of 1.5. The wings were designed and sized to pass the wingtip structural test during the competition technical inspection. The monocoque Kevlar fuselage was designed to handle in-flight and landing loads, in addition to accommodating fuselage hatches and hardware mounting.

5.2.1 Wing Design

A balsa built-up wing was sized and analyzed as explained in Section 4.3.5. Figure 23 shows the overall wing design. The main spar is an I-beam with a 0.06 in. (0.2 cm) balsa shear web attached between 0.2 in. (0.5 cm) carbon fiber spar caps, with a height of 0.78 in. (2.0 cm). To handle the moments in the wing roots the center section of the shear web was thickened to 0.19 in. (0.16 cm). Fourteen 0.06 in. (0.2 cm) balsa ribs were evenly spaced to transfer axial and transverse loads into the main spar. Lightening holes were cut out from the ribs in a truss design, reducing rib weight by 57%. The leading edge was covered by one ply of 3 oz/yd^2 (100 g/m^2) ±45° carbon fiber fabric in a D-box to handle torsional loads. The trailing edge contains balsa flaperons with lightening holes.

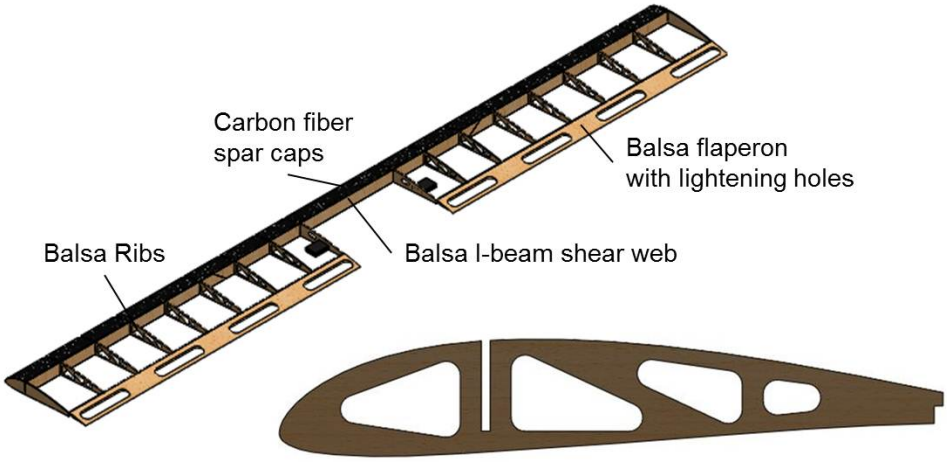

Figure 23: Balsa built-up wing with balsa shear web and carbon spar caps, balsa rib with lightening holes shown in bottom right.

5.2.2 Fuselage Design

The fuselage was designed to support loads in flight and on landing with maximum payload. The monocoque fuselage was designed with a two-layer skin of 1 oz/yd^2 (34 g/m^2) Kevlar: one ply of $\pm 45^\circ$ fabric and one ply of $0/90^\circ$ fabric. The two layers enclosed a foam and carbon tow structure, shown in Figure 24. The foam and carbon tow structure was a truss design based on load-path analysis to support propulsion components, wing load and integration, tail load and integration, and payloads.

5.2.2 FoamStructure

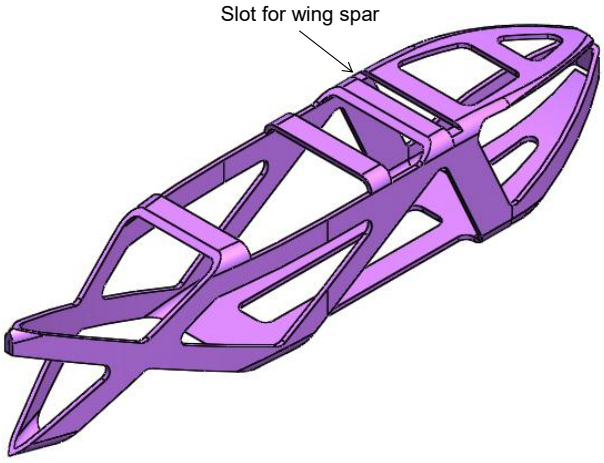

Figure 24: Supportive foam structure of the monocoque fuselage, shown without the Kevlar skin or carbon fiber.

Kevlar skin was chosen based on its high tensile strength-to-weight ratio. One ply of 1 oz/yd^2 (68 g/m^2) carbon fiber was added to the nose of the fuselage to reduce deformation in flight and therefore reduce pressure drag. The foam and carbon tow structure was chosen for its light weight and for its ease of manufacture.

5.3 Sub-System Design

To finalize the aircraft design, the following subsystems were analyzed with greater detail: propulsion, motors, flight batteries, propellers, controls, landing gear, and payloads.

5.3.1 Propulsion and Controls

Based on the conceptual and preliminary design, the propulsion team identified the lightest package with the highest efficiency. A complete package for each mission was optimized in PlaneTools and then validated via lab testing. Table 20 shows the chosen propulsion and controls systems for the final design.

5.3.1 Propulsion components

Table 20: Propulsion and controls components for the final design.

Propulsion Components	Mission 1		Mission 2		Mission 3	
	Description	Weight [g]	Description	Weight [g]	Description	Weight [g]
Motor	1105/6D					65.2
Gearbox	P32					65.2
Rx Pack	Varta 55608					20.0
Fuse	Impulse 15A					10.0
ESC	Thunderbird 36A					20.0
Servos	Dymond D47 (x6)					28.2
Rx	Futaba 617FS					7.0
Connections	Servo wire, electrical connections, solder					20.0
Propeller	CAM 16x13	59.0	CAM 17x9	66.9	CAM 16x13	59.0
Main Battery	Elite 1500 (12s)	276.0	KAN 700 (19s)	264.1	KAN 700 (19s)	264.1
Total (% EW)		**570.6 (63%)**		**566.6 (63%)**		**558.7 (62%)**

5.3.2 Landing Gear

A conventional tail dragger design with differential braking, vertical skids and a rear dragger skid was selected for the landing gear configuration. The main gear was chosen to be bow-shaped, with inwardly mounted wheels that were 3D printed out of polylactic acid (PLA). The wheels had a hub with a torsional spring attached. One end of the spring was mounted to the carbon fiber bow gear and the other end had fishing line attached, which was pulled by a servo mounted on the upper curve of the bow gear. The vertical skids were 0.75 in. (1.9 cm) high and 5.5 in. (14 cm) long and were constructed out of bidirectional carbon fiber. The vertical skid was attached to the main bow gear made of unidirectional carbon fiber and balsa stringers with a height of 4.75 in. (12 cm) and a length of 10.25 in. (26 cm). This main gear was mounted 3.5 in. (8.9 cm) forward of the CG using two 1/4-20 x 0.7in. nylon bolts. The rear of the aircraft was fitted with a 0.5 in. (1.3 cm) high and 4.5 in. (11.4 cm) long skid that was attached to the fuselage with epoxy and filler, which was used to help minimize vibration during the Taxi Mission. The gear was sized using GearSizer, an Excel-based computer program developed by a team advisor that helped determine the shape and material for the main bow gear. The landing gear final design is depicted in Figure 25.

Figure 25: Landing gear design with differential braking and vertical skid.

5.3.3 Payloads

The internal cargo restraints were designed to secure the three Mission 2 payloads and the Mission 3 medical passengers while minimizing weight. The Kevlar fuselage was designed such that the taper of the nose and tail restricts the Mission 2 payloads from sliding along the line of flight and from side-to-side. The fishing line straps were attached to the fuselage bottom and hooked together over the top of the blocks, constraining motion in the vertical direction. Figure 26 shows a closeup of the fuselage with the Mission 2 payload restraint system.

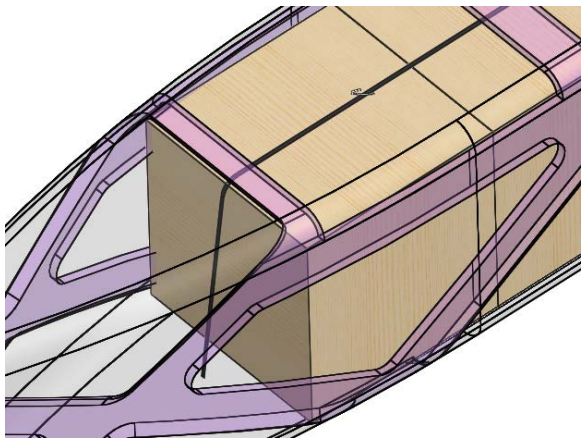

Figure 26: Mission 2 payload restraint system consisting of fishing line strap and hook.

The Mission 3 and Taxi Mission patients were restrained with the same fishing line from Mission 2. The attendants were secured with another fishing line whose ends attached to the fuselage's foam structure. This fishing line was attached to balsa corner pieces that were fitted onto selected corners of the attendants, preventing motion in the vertical direction and from side-to-side. The Mission 3/Taxi Mission restraint system is shown in Figure 27. The total weight of the payload mounting system is 0.01 lb (5.0 g).

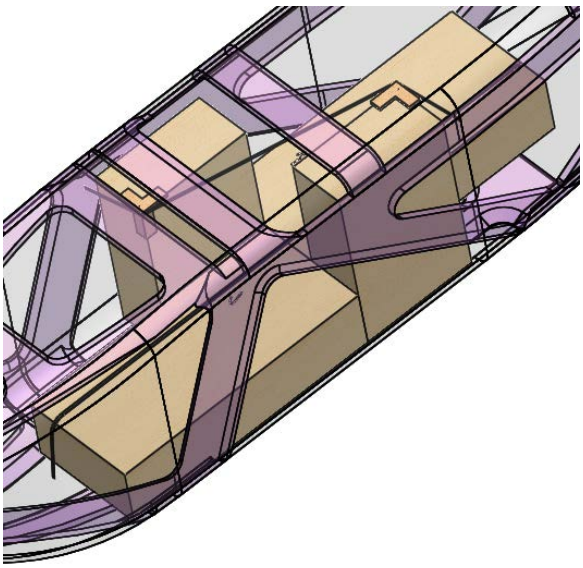

Figure 27: Mission 3 and Taxi Mission payload restraint system consisting of fishing line straps, hooks, and balsa corner pieces.

5.4 Weight and Balance

The designed aircraft weighed 1.75 lb (0.79 kg). The center of gravity (CG) was kept inside the static margin for all four missions to ensure stable taxiing and flight. In order to accommodate any CG shifts from the empty aircraft to the various payloads between Missions 2 and 3, the flight batteries were shifted forward or aft as needed. All CG locations are measured from the nose of the aircraft. The aircraft and component weights and CG locations are shown in Table 21.

Table 21: Weight and balance table for all missions.

Aircraft Component	Weight		CG Location					
			X		Y		Z	
	[lb]	[kg]	[in]	[cm]	[in]	[cm]	[in]	[cm]
Mission 1 - Empty Aircraft Total	1.75	0.79	2.40	6.10	0.36	0.91	-10.08	-25.60
Wing	0.12	0.06	2.28	5.79	4.32	10.97	-4.56	-11.58
Conventional Tail	0.03	0.02	2.28	5.79	6.00	15.24	16.56	42.06
Fuselage	0.33	0.15	2.28	5.79	1.08	2.74	-2.04	-5.18
Motor	0.28	0.13	2.28	5.79	2.04	5.18	-17.16	-43.59
Propellor	0.12	0.06	2.28	5.79	2.04	5.18	-18.96	-48.16
Flight Batteries	0.57	0.26	1.56	3.96	4.20	10.67	-0.72	-1.83
Reciever	0.00	0.00	2.28	5.79	3.84	9.75	-11.88	-30.18
Reciever Batteries	0.03	0.02	1.08	2.74	3.72	9.45	-12.00	-30.48
Speed Controller	0.03	0.02	2.28	5.79	4.20	10.67	-12.00	-30.48
Landing Gear Assembly	0.20	0.09	2.40	6.10	-4.80	-12.19	-10.08	-25.60
Mission 2 - Max. Payloads Total	4.75	2.15	2.40	6.10	0.36	0.91	-10.08	-25.60
Forward Payload	1.00	0.454	2.28	5.79	0.84	2.13	-9.36	-23.77
Middle Payload	1.00	0.454	2.28	5.79	0.84	2.13	-3.36	-8.53
Rear Payload	1.00	0.454	2.28	5.79	0.84	2.13	2.64	6.71
Flight Batteries	0.57	0.26	2.04	5.18	2.76	7.01	-15.36	-39.01
Mission 3 / Taxi Mission - Total	3.75	1.70	2.40	6.10	0.36	0.91	-10.08	-25.60
Forward Attendant-Patient	1.00	0.454	2.76	7.01	-0.12	-0.30	-6.24	-15.85
Rear Attendant-Patient	1.00	0.454	1.80	4.57	-0.12	-0.30	0.24	0.61
Flight Batteries	0.57	0.26	2.04	5.18	3.24	8.23	-13.20	-33.53

5.5 ExpectedFlightPerformance

5.5 Flight Performance Parameters

Table 22 details the expected flight performance for all three missions obtained from the team's MDO software, PlaneTools. These parameters were compared with results from various flight tests to verify their accuracy.

Table 22: Expected flight performance parameters of the aircraft obtained from PlaneTools.

Performance Parameter	Mission 1		Mission 2		Mission 3	
$C_{L_{max}}$	1.1		1.1		1.1	
$C_{L_{cruise}}$	0.20		0.51		0.31	
e	0.8		0.8		0.8	
C_{D_0}	0.077		0.051		0.078	
L/D_{max}	8.26		10.2		8.22	
L/D_{cruise}	2.47		8.00		3.79	
Rate of Climb, R/C	22.5 ft/s	(6.86 m/s)	3.8 ft/s	(1.16 m/s)	10.6 ft/s	(3.23 m/s)
W/S	1.04 lb/ft^2	(5.1 kg/m^2)	2.5 lb/ft^2	(12.2 kg/m^2)	1.99 lb/ft^2	(9.8 kg/m^2)
Cruise Speed	68.4 ft/s	(20.8 m/s)	65.8 ft/s	(20.1 m/s)	74.8 ft/s	(22.8 m/s)
Stall Speed	27.8 ft/s	(8.5 m/s)	43.1 ft/s	(13.1 m/s)	38.5 ft/s	(11.7 m/s)

5.6 Mission Performance 5.6 ExpectedMissionPerformance

Table 23 details the mission performance characteristics of the final aircraft as predicted by PlaneTools.

Table 23: Expected mission performance characteristics for the final design.

Performance Parameter	Mission 1		Mission 2		Mission 3	
$TOFL$	3.2 ft	(1.0 m)	36.8 ft	(11.2 m)	24.1 ft	(7.4 m)
Gross Weight	2.18 lb	(0.99 kg)	5.24 lb	(2.38 kg)	4.18 lb	(1.90 kg)
N_{laps}	6		-		-	
N_{cargo}	-		3		-	
t_{USC}	-		-		135 s	
Mission Score	1.50		3.00		3.48	
$Total\ Flight\ Score$	7.98					
EW	2.24 lb (1.02 kg)					
RAC	2.24					
$\frac{Total\ Flight\ Score}{RAC}$	3.56					

The empty weight of the final design was 2.24 lb (1.02 kg), heavier than the 2.13 lb (0.97 kg) from the preliminary design. The overall score was reduced from 3.8 to 3.56 because the preliminary design drew too much current, more than the fuse could withstand. As a result, the number of cells was reduced from 13 to 11; however, the empty weight estimation did not decrease, but increased due to an underestimation in weight for the preliminary design. The wingspan was also increased from 3.6 ft (1.1 m) to 4.2 ft (1.3 m) in order to compensate for the reduction in number of cells to satisfy the TOFL requirement.

5.7 Drawing Package

The following drawing package includes a dimensioned 3-view, structural arrangement, aircraft systems layout, and mission configuration drawings. All drawings were made using SolidWorks[12].

CG location fixed for all missions

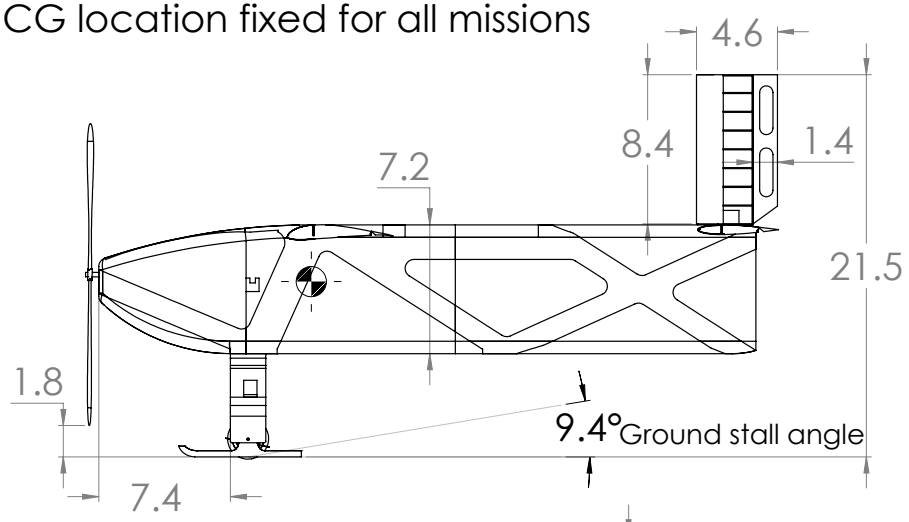

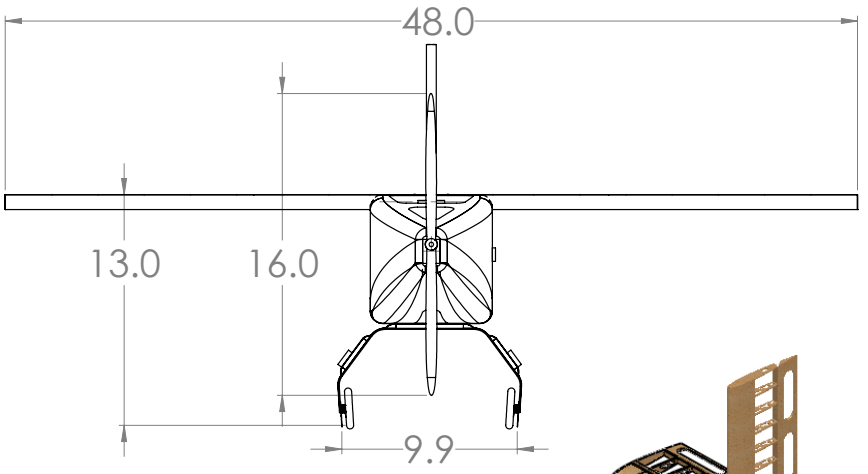

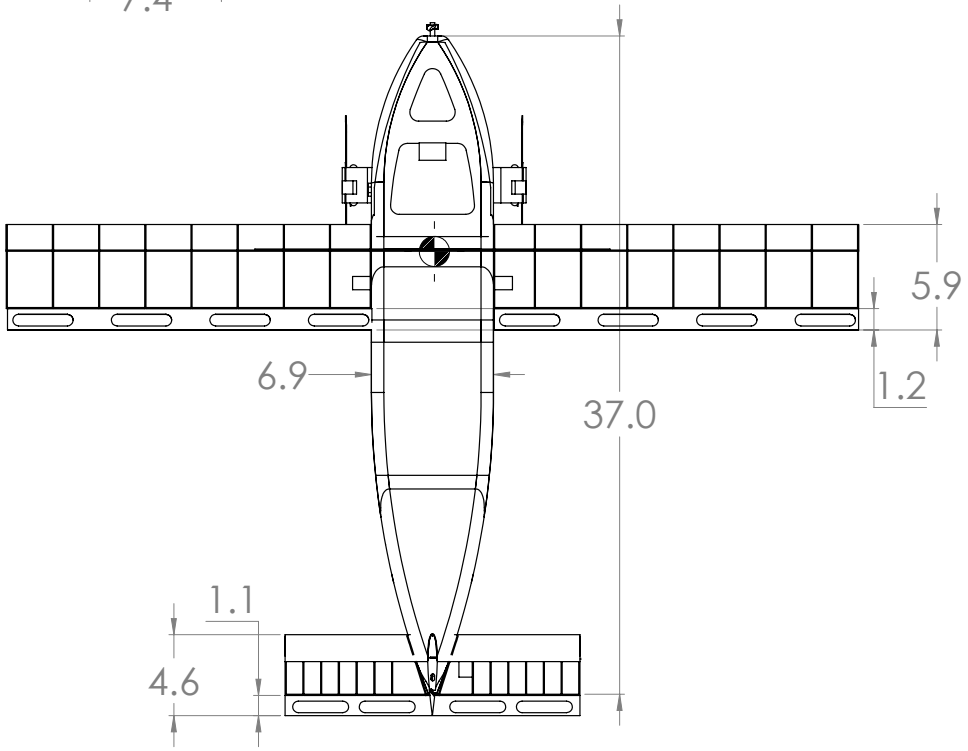

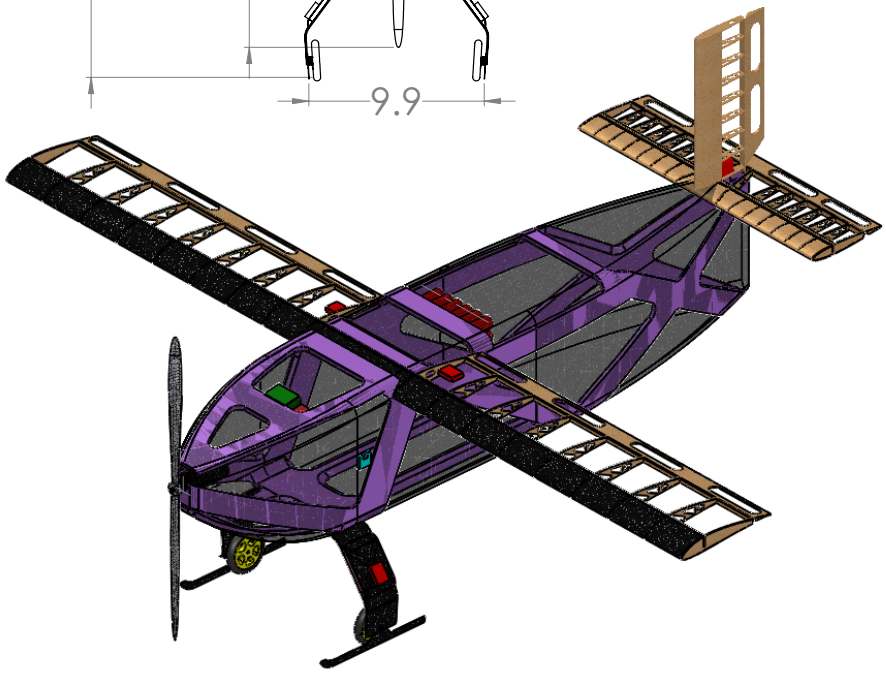

Comments:
Dimenisions are in Inches.

Drawn By:
Jonathan Guerrero

University of Southern California
Cessna - Raytheon - AIAADesign/Build/Fly 2014

MiSChief

SIZE		REV
B	Aircraft 3-View	C

SCALE: 1:7	Drawing Package	2/22/2014	SHEET 1 OF 4

ITEM NO.	COMPONENT	DETAIL	QTY.
1	Wing	Balsa built up, carbon D-Box, So-Lite covering	1
2	Fuselage	Kevlar and Carbon fiber molded	1
3	Propulsion System	NEU 1105 3Y, RFM 15x16"	1
4	Horizonal Tail	Balsa built-up	1
5	Vertical Tail	Balsa built-up	1
6	Fuselage Structures	Extruded polystyrene	1
7	Landing Gear	Carbon fiber bow gear with balsa stringers and polystyrene spacing	1

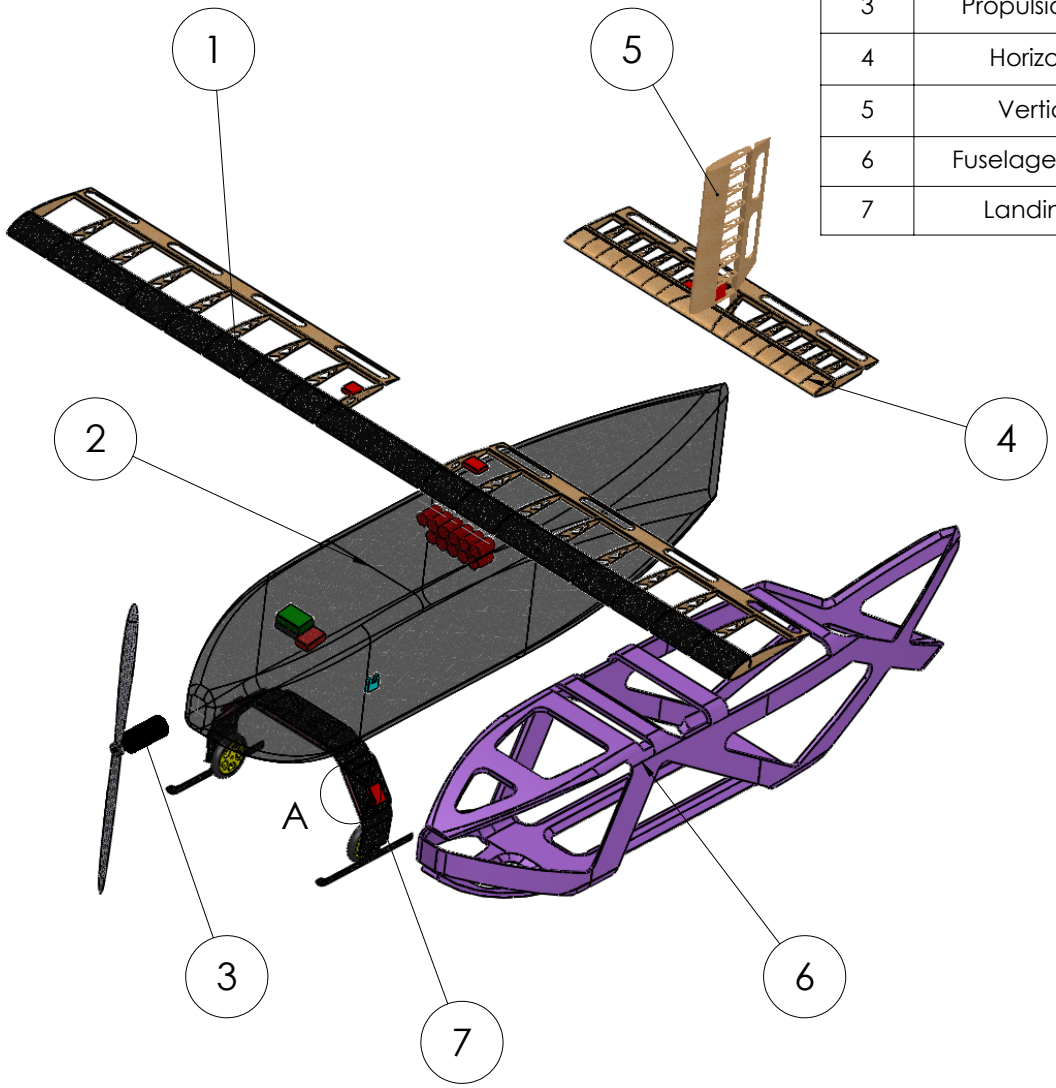

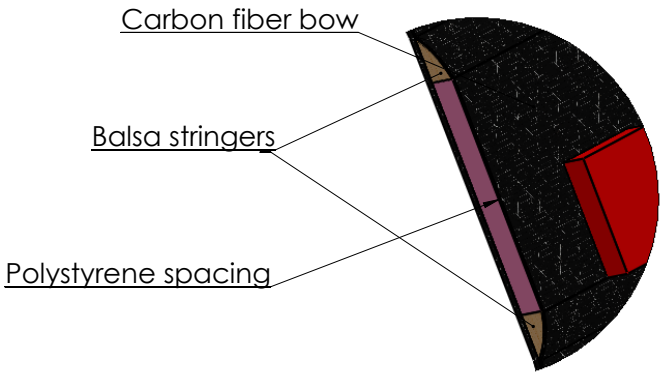

DETAIL A
SCALE 1 : 1

Comments:
Dimenisions are in Inches.

Drawn By:
Jonathan Guerrero

University of Southern California
Cessna - Raytheon - AIAADesign/Build/Fly 2014

MiSChief

SIZE B | Subassembly breakout view | REV C

SCALE: 1:6 | Drawing Package | 2/22/2014 | SHEET 2 OF 4

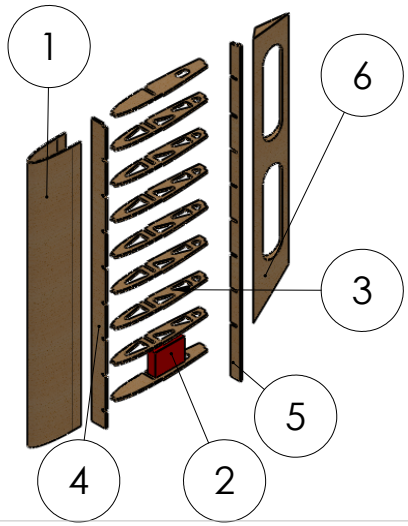

ITEM NO.	COMPONENT	MATERIAL	QTY.
1	D-Box Sheeting	1/32" balsa	1
2	Rudder servo	Dymond D47	1
3	Tail ribs	1/16" balsa	9
4	Shear web	1/16" balsa	1
5	Aft shear web	1/16" balsa	1
6	Rudder	3/8" to 1/16" tapered balsa	1

Vertical Tail

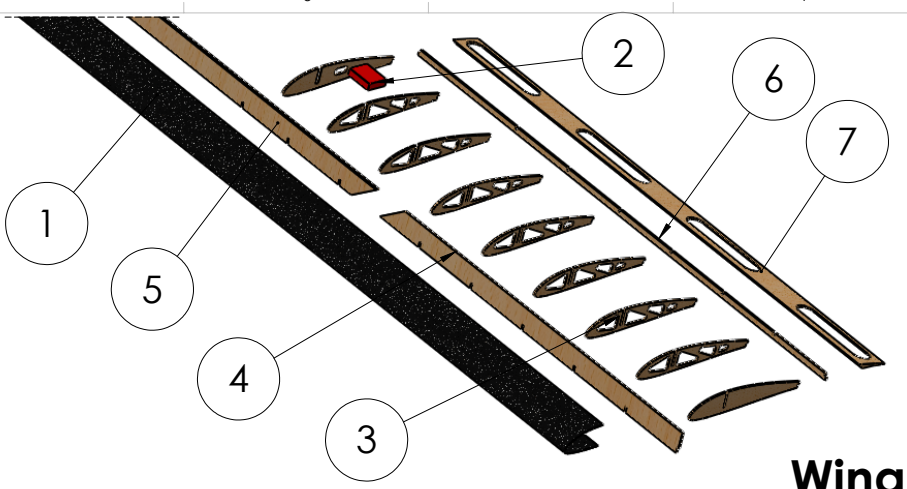

Wing

ITEM NO.	COMPONENT	MATERIAL	QTY.
1	D-Box Sheeting	Carbon fiber	1
2	Aileron servo	Dymond D47	1
3	Wing ribs	1/16" balsa	18
4	Wing Sshear web	1/4" balsa	2
5	Fuselage shear web	1/4" balsa	1
6	Aft shear web	1/16" balsa	2
7	Aileron	3/8" to 1/16" tapered balsa	2

ITEM NO.	COMPONENT	MATERIAL	QTY.
1	D-Box Sheeting	1/32" balsa	1
2	Rudder servo	Dymond D47	1
3	Tail ribs	1/16" balsa	16
4	Shear web	1/16" balsa	1
5	Aft shear web	1/16" balsa	1
6	Rudder	3/8" to 1/16" tapered balsa	1

Horizontal Tail

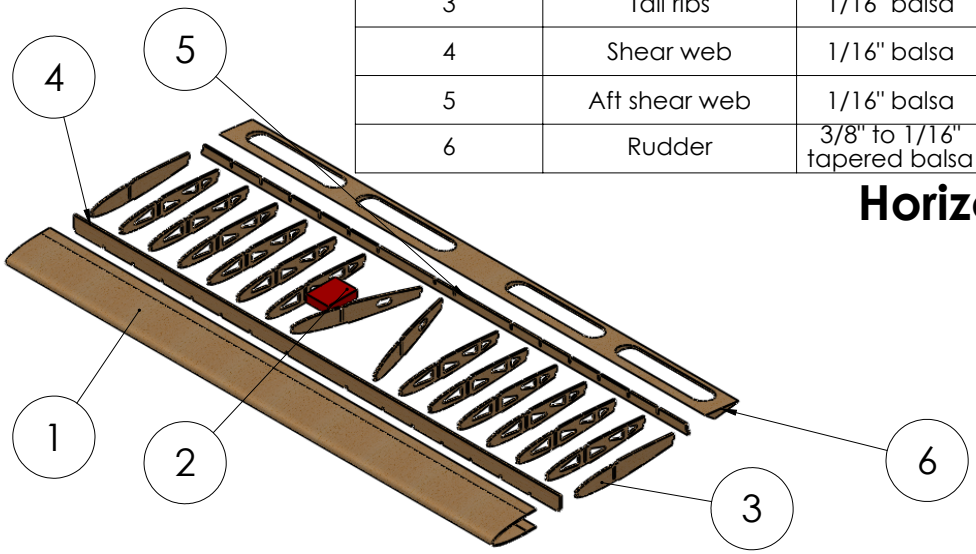

Comments:
Dimenisions are in Inches.

Drawn By:
Jonathan Guerrero

University of Southern California
Cessna - Raytheon - AIAADesign/Build/Fly 2014

MiSChief

SIZE		REV
B	Subassembly structures detail	C

SCALE: 1:3	Drawing Package	2/22/2014	SHEET 3 OF 4

ITEM NO.	COMPONENT	MATERIAL	QTY.
1	Bow gear Skid	Carbon fiber	2
2	Bow gear spacing	Extruded polystyrene	12
3	Bow gear stringer	1/4" balsa	3
4	Braking servo	Dymond D47 connected to fireline wire	2
5	Wheel axel	Carbon fiber	2
6	Hub spring	Steel	2
7	Wheel hub	Poly lactic acid	2
8	Tire	Foam	2

Landing Gear

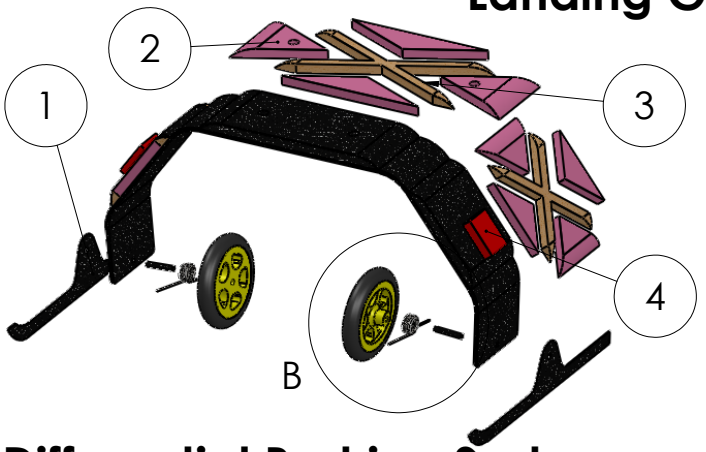

Differential Braking System

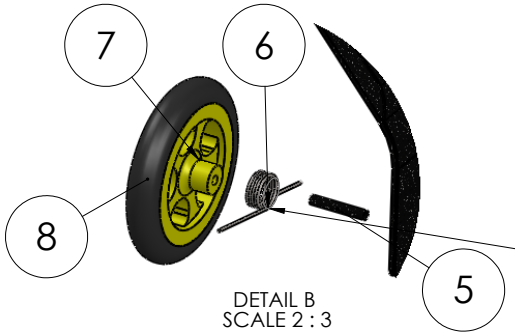

DETAIL B
SCALE 2 : 3

The steel spring wraps around the wheel hub protrusion. With one end of the spring fixed and the other attached to the servo via fireline, the spring acts as a torisonal brake.

Mission 2 Payloads

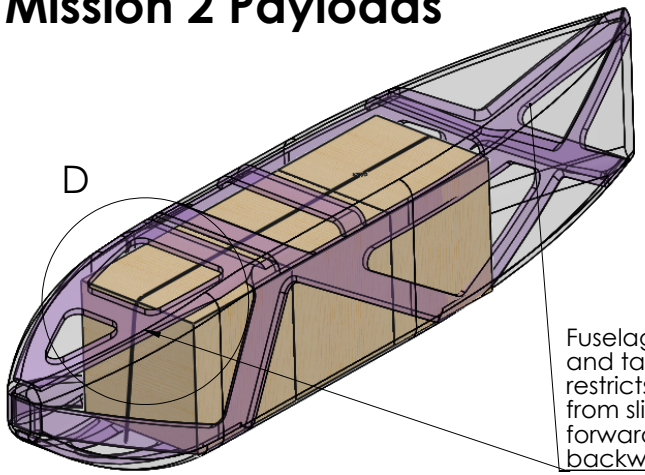

Fuselage nose and tail taper restricts payloads from sliding forwards and backwards.

Fishing line attached to fusealge bottom, restricts up and down movement of payloads

DETAIL D
SCALE 1 : 3

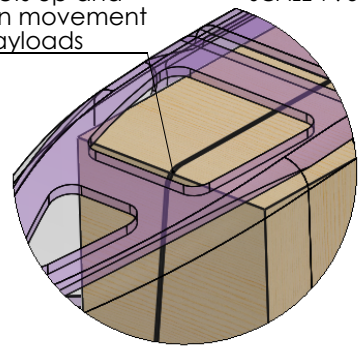

Mission 3 Payloads

The same fishing line used in M3 is used for the same purpose with the patients.

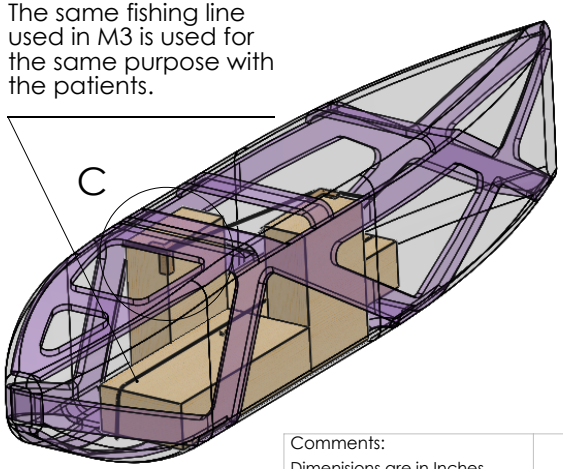

Fishing line attached to polysytrene structure attaches to balsa corner piece to restirct attendant up and down as well as side to side movement.

DETAIL C
SCALE 1 : 2

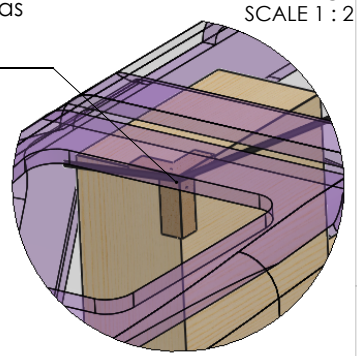

Comments:
Dimenisions are in Inches.

Drawn By:
Jonathan Guerrero

University of Southern California
Cessna - Raytheon - AIAADesign/Build/Fly 2014

MiSChief

SIZE		REV
B	Subassemblies systems detail	C

SCALE: 1:5	Drawing Package	2/22/2014	SHEET 4 OF 4

6 Manufacturing Plan and Processes

The team explored several different methods and processes for each major component of the aircraft (wing, spar, empennage, fuselage and landing gear). Each of these components underwent downselects to determine the best-suited fabrication technique.

6.1 Component Manufacturing and Selection

Careful considerations regarding manufacturing techniques and materials were implemented to minimize weight while ensuring performance and structural integrity. The three main, weight-critical aircraft components were the wings and tail surfaces, fuselage, and landing gear. The wings and tails were manufactured via the balsa built-up method with balsa ribs attached to a carbon-capped balsa spar for minimal weight and high strength. The flaperons comprised laser-cut balsa pieces in order to retain torsional stiffness and light weight. The fuselage was a monocoque Kevlar, carbon and foam structure that was both lightweight and acted as an aerodynamic fairing for the entire aircraft. The landing gear was composed of carbon fiber, foam and PLA wheels and was designed to withstand a 5g landing load.

6.1.1 Control Surfaces

After the wings were sized, the control surfaces were sized by the Aerodynamics captain to ensure that the TOFL would be met and that there would be acceptable control authority as shown in Section 4.4.2. Manufacturing of the wing and tail surfaces consisted of tapered balsa with lightening holes (Figure 28).

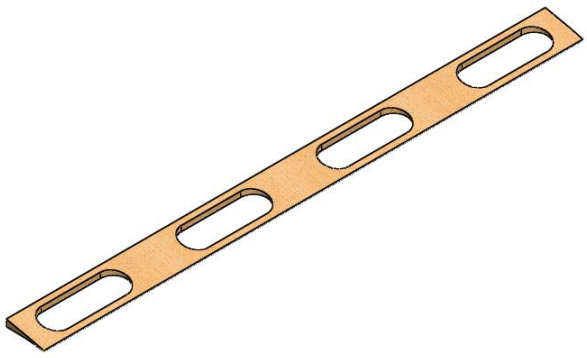

Figure 28: Flaperon with lightening holes.

6.1.2 Structural Component Integration

Fuselage manufacturing was a two-step process. The team first prepared the foam structure and then laid up the Kevlar fiber around the foam. The foam was prepared by first cutting Wing Mold 2 Integration Weight sheets 0.25 in. (0.006 m) thick. The team then proceeded to use prepared molds and heat guns to shape the sheets of foam. After cutting the effective structure from the foam, the team began the layup process with the Kevlar cloth using slow-cure epoxy.

The motor was integrated using a carbon plate at the nose with four M2.5 screws. The landing gear was integrated through the foam structure with two 1/4-20 x 0.75 in. nylon bolts. The main wing was integrated through three contact surfaces, namely the two innermost ribs and the main spar that is placed into the slot in the foam in Figure 24. The two ribs and spar were mounted with 5-minute epoxy. The tail of the plane was integrated in a similar fashion: the two innermost ribs of the horizontal stabilizer as well as the innermost rib of the vertical stabilizer were mounted onto the fuselage skin while the spars were fitted into foam slots as seen in Figure 24. Integration weights (consisting of epoxy and/or fasteners) are shown in Table 24.

Table 24: Structural component integration.

Component	Integration Weight
Motor	0.009 lb (4 g)
Landing Gear	0.002 lb (8 g)
Main Wing	0.033 lb (15 g)
Tail	0.015 lb (7g)

The motor mount of the plane was placed so that the prop has enough ground clearance. The landing gear was placed so that the wing has sufficient clearance over Taxi Mission obstacles.

6.1.3 Landing Gear

Landing gear material selection required downselect processes to determine the optimal material for both the main gear and the tail dragger to fully support the aircraft during a rough landing and Taxi Mission. For the bow gear, the landing gear team investigated the following materials:

- **Carbon fiber –** Unidirectional carbon fiber was laid up using the wet-layup method and vacuumed onto a foam mold at an orientation of 0° (8 layers of 4 oz/yd^2 [136 g/m^2] thick plies) with respect to the long axis of the gear for strength in landing loads.
- **Carbon fiber with balsa and foam –** Unidirectional carbon fiber was laid up using the wet-layup method and vacuumed onto a foam mold at an orientation of 0° (4 layers of 4 oz/yd^2 [136 g/m^2] thick plies) with respect to the long axis of the gear for strength in landing loads. In the middle of the laminate, diagonal balsa stringers (0.375 x 0.25 in. [0.95 x 0.64 cm]) were used along with polystyrene foam spacers to increase the height from the neutral axis in order to increase torsional rigidity with minimum weight penalty.
- **Carbon fiber with foam –** Unidirectional carbon fiber was laid up using the wet-layup method and vacuumed onto a foam mold at an orientation of 0° (4 layers of 4 oz/yd^2 [136 g/m^2] thick plies) with respect to the long axis of the gear for strength in landing loads. In the middle of the laminate, pink foam (0.25 in. [0.64 cm]) was added to increase the height from the neutral axis in order to increase torsional rigidity.

The bow gear underwent a downselect process to compare the three material combinations on a merit-based criteria of weight, strength and durability. As detailed in Table 25, carbon fiber with balsa and foam was selected due to its

comparatively low weight and its high predicted strength.

Table 25: Bow gear material downselect.

Figure of Merit	FoM Value	Carbon Fiber	Carbon Fiber with Balsa and Foam	Carbon Fiber with Foam
Weight	**0.4**	-1.0	1.0	1.0
Strength	**0.3**	0.0	1.0	1.0
Durability	**0.3**	1.0	1.0	-1.0
Total	**1.0**	-0.1	1.0	0.4

Several construction methods were considered for the tail dragger structure and it was determined that the fuselage itself would serve as the dragger structure. To complete the Taxi Mission with minimal vibration, a thin skid of length 5 in. (12.7 cm) made out of 4 layers of 3.3 oz/yd^2 (112 g/m^2) carbon fiber was mounted to the rear of the aircraft to let the dragger slide across the top of the roofing panels. This carbon fiber was laid up using the traditional wet-layup method and vacuumed to a flat metal table.

6.1.4 Payloads

The internal payload restraint was designed to secure three 6 in. wide, 1 lb boxes as well as both pairs of attendants and patients. Because the skin was too light to handle the forces required to restrain the payloads during flight, the integration of this restraint was using the structure from the landing gear and the foam truss. The foam truss provided the necessary structure to maintain the rigidity of the plane around the hatch areas. It also provided attachment points for the fishing line straps within the fuselage. The landing gear provided the straps with another attachment point.

Once the system was completed, shake tests were performed to determine whether the system worked properly. These shake tests were performed by picking up the fuselage and shaking it in multiple directions. The selected system of fishing line straps, hooks, and balsa corner pieces passed the shake test and was verified at a flight test.

6.2 Manufacturing Schedule

Figure 26 shows the manufacturing schedule for the five prototypes and the competition aircraft for the 2013-2014 year. Simultaneous laboratory testing was done on aircraft components before integration.

Table 26: Build schedule for 2013-2014 airplanes. Stars indicate completion dates.

USC DBF 2013-2014 Build	August		September		October		November		December		January		February		March		April	
Babe																		
Fuselage																		
Wing																		
Empennage																		
Systems Installation																		
Pink Panther																		
Fuselage																		
Wing																		
Empennage																		
Systems Installation																		
Mach Schnell																		
Fuselage																		
Wing																		
Empennage																		
Systems Installation																		
SCanta Yaws																		
Fuselage																		
Wing																		
Empennage																		
Systems Installation																		
MiSChief - Iteration 1																		
Fuselage																		
Wing																		
Empennage																		
Systems Installation																		
Competition Aircraft - Mischief																		
Fuselage																		
Wing																		
Empennage																		
Systems Installation																		

7 Testing Plan

Tests were conducted throughout the year to collect experimental data and to verify theoretical aerodynamic, structural and MDO predictions. Test programs included both routine laboratory testing as well as five flight test campaigns.

7.1 Test Objectives and Results

Overview

Rigorous testing was undertaken to verify design tools, methods, and assumptions used to size major aircraft components. Testing was conducted on all propulsion components to minimize weight and ensure that they were adequately sized for the aircraft, while the primary structures were tested to estimated flight loads.

Propulsion

All components of the propulsion and control systems were tested to verify compliance to the rules and mission requirements:

- A receiver was selected with adequate channels for the required programming, as well as to provide a sufficient voltage to the servos.
- A receiver pack was sized to provide necessary voltage and capacity to the receiver for the duration of the missions, including preparation time before the flight. The selected receiver battery was tested on the ground in a test rig simulating flight loads and deflection requirements.

- Servos were sized for the maximum hinge moments expected inflight according to deflections, airspeed, and control surface size. They were tested on the ground to validate selection in the same test rig used for receiver battery testing.
- Several 15A fuses, as specified by the competition rules, were tested to ensure that they would not break during the duration of the flight. To simulate the load on the fuse in flight, the fuse was attached to a test rig consisting of the competition batteries, motor, propeller, and speed controller to ensure competition conditions were replicated as accurately as possible. In addition, the fuses were tested with a power supply that provided a steady current to test the fuse's ability to handle higher currents than the advertised 15A.
- Motor and propeller combinations selected for the competition plane were tested both in flight and on a thrust stand. Current and Voltage data were collected via both Castle Creations ICE as well as through an ammeter and multimeter, allowing the Propulsion and Performance subteams to calibrate and verify PlaneTools.
- NiMH batteries were tested to verify the internal resistance of different batteries provided by the manufacturer, and the results were inputted into PlaneTools. In addition, the competition battery packs were tested in flight to verify that they had sufficient cooling and they performed as expected.

Performance

The Performance subteam conducted several flight tests to verify the assumptions that were used in PlaneTools. The MATLAB program used these assumptions to calculate the propulsion performance as well as cruise velocity and takeoff field length.

Aerodynamics

The Aerodynamics, Stability & Control subteam oversaw several flight tests to verify the static and dynamic stability characteristics that the aircraft was designed to meet. Feedback from the pilot was used to cut down the tail size and find stability characteristics that were suitable for his piloting ability, but that were below the required standards for manned flight.

Structures

The Structures and Payloads subteams tested individual structural members as well as the entire prototype aircraft in order to validate the team's structural design tool, SparSizer, as well as the assumptions made in the structural design process. The wing was tested using a whiffle tree to validate the carbon D-Box structure under expected in-flight loads. This also validated the spar design, as well as the fuselage joint. The payloads team validate the payloads mounts and integration into the aircraft structure by simulating maximum gust conditions as well as the 3-axis restraints using team internal, high stress motion testing.

Landing Gear

The landing gear design was validated on the team's landing gear mule, pictured in Figure 30, to test the conceptual design of using skids to traverse the corrugated sheeting. In addition, the team created a replica taxi mission field and validated the landing gear's capability on previous prototype aircraft.

7.2 Flight Test Schedule and Flight Plan

A schedule of flights for the 2013-2014 DBF competition year is provided in Table 27, below. As specified in the table, each test flight had specific test objectives and parameters which varied from basic walk-throughs to complete mission simulations.

Table 27: Test flight schedule.

Date	Location	Objectives
15 September 2013	Sepulveda Basin, Van Nuys, CA	Introduce new members to the team and to building. Validate Aero, S&C and PlaneTools predictions.
6 October 2013	Sepulveda Basin, Van Nuys, CA	Build a lighter-weight aircraft capable of a 40ft takeoff. Validate PlaneTools and Propulsion predictions.
10 November 2013	El Mirage Dry Lake Bed, El Mirage, CA	Build and fly an airplane with a V-tail. Simulate flight missions.
14 December 2013	Sepulveda Basin, Van Nuys, CA	Fly previous aircraft and cut down V-tail iteratively to find stability limits. Fly new airplane capable of 40 ft takeoff and simulate flight missions.
8 February 2014	Sepulveda Basin, Van Nuys, CA	Competition simulation with all three flight missions, capable of 40 ft takeoffs. Implement new Crew Chief procedures for flight test efficiency.

Each flight test's objectives were analyzed to form a flight test plan. The following table is an example of a test flight plan used at the team's third flight test on 10 November 2013.

Table 28: Sample test flight plan.

Flight No.	Flight Description	Payload	Objectives	Acceptance Criteria
14 December, 2013 – Santa Yaws				
1	Trim Flight	None	- Trim airplane - Acquire power data	○ Airplane trimmed ○ Data acquired
2	M1 Simulation	None	- Fly maximum number of laps in 4 minutes	○ Complete at least 1 lap, aim for 7
3	M3 Simulation	2 lb internal weights	- Fly 3 laps as quickly as possible with internal loads	○ Complete 3 laps
4	TOFL simulation	None	- Take off within 40 ft	○ 40 ft TOFL requirement met

7.3 On-Site Checklists

This year, the team created an additional student leadership position to optimize mission efficiency and success. The Crew Chief was responsible for the aircraft and the safety of others around the aircraft during test flights and at competition. The Crew Chief oversaw aircraft inspections and pre-fligh procedures for every flight and was the central hub for all maintenance performed on the aircraft both inside the lab and on-site. One of the Crew Chief's contributions during the 2013-2014 academic year was the creation of an aircraft inspection procedure, shown in Figure 29. This procedure was designed for use on the day prior to flight tests, at flight tests, upon arrival to the DBF contest, and immediately after each flight. This procedure included every subteam to inspect the aircraft, note discrepancies, perform and verify maintenance, and carry out the pre-flight checklist.

Table 29: Aircraft inspection checklist, a new addition to the USC AeroDesign Team.

Component	Items to Inspect	Discrepancies
Motor	☐ Motor mount bolts ☐ Fuselage around motor mount is free of cracks or fractures ☐ Motor is free of damage to casing and debris ☐ Propeller shaft is straight ☐ Propeller is fastened to shaft properly ☐ Propeller is free of damage	
Fuselage (internal)	☐ Battery is secure to fuselage and connected ☐ Speed-controller is secure and connected ☐ Receiver is secure and has all servos connected properly ☐ Servo wires are all secure ☐ Fuselage is free of debris ☐ Fuse connectors secure (internal and external) ☐ Payload restraints are secured and ready for loading (if applicable)	
Wings	☐ Wings are free of tears, cracks, and fractures ☐ Servo has minimal play ☐ Servo arms are secure ☐ Control surfaces are secure and free of obstructions ☐ Fuselage around wing mount is free of cracks and fractures ☐ Wing is securely mounted to fuselage	
Landing Gear	☐ Wheels spin freely and are secure ☐ Torsional stiffness of gear ☐ Landing gear mount is secure ☐ Fuselage is free of cracks and fractures around mount ☐ Differential brakes are working properly	
Tail	☐ Tail landing gear is functioning properly ☐ Free of tears, cracks, and fractures ☐ Servo has minimal play ☐ Servo arms are secure ☐ Control surfaces are secure and free of obstructions ☐ Fuselage around tail mount is free of cracks and fractures ☐ Tail is securely mounted to fuselage	
Control Surface Check	☐ Check all control surfaces using transmitter ☐ Control surfaces move freely without obstructions ☐ Check all servos are operating properly	

.

7.4 Pre-Flight Checklists

A pre-flight checklist was used before each flight test in order to ensure efficiency, proper data acquisition, and team safety.

Table 30: Pre-flight checklist.

Component	Task
Fuselage (internal)	☐ Secure and connect the fully charged battery ☐ Receiver has all connections plugged in and secured ☐ Load payloads (if applicable) ☐ CG aircraft
Fuselage (external)	☐ Close and secure all external hatches
Turn aircraft over to pilot	☐ Fuse connected ☐ Control checks ☐ Aircraft turn-up/ Flight

.

8 Aircraft Performance Results

Subsystem testing allowed the team to compare all collected data with predictions from the detail design phase. The key subsystems were verified in the laboratory before flight testing to ensure that each individual component was reliable and optimized before integration into the test flight aircraft. Each test either matched or exceeded theoretical predictions from PlaneTools.

8.1 Demonstrated Performance of Key Subsystems

Each key subsystem was tested and optimized according to the design goals of weight and performance, then compared with theoretical predictions. Important subsystems included propulsion, structures and payloads.

8.1.1 Propulsion

To ensure that the propulsion components chosen as a result of the PlaneTools trade studies were appropriate for flight, all components were tested beyond their expected flight requirements.

Motor

The motor was tested using a thrust stand that was designed and fabricated by the team. Each propulsion package was tested to ensure consistency with the PlaneTools predictions. Any discrepancies with the actual measured data versus PlaneTools assumptions were attributed to uncertainty in the internal resistance of the battery cells.

Fuse

In order to verify the plane's capability of flying at certain throttle values while limited by a 15 A slow-blow fuse, extensive fuse testing was performed. Through the testing process it was determined that a current draw higher than the 15 A rating could be sustained for a limited amount of time. The takeoff current, through testing, was shown to be 24 A. This current could be withstood for approximately 10 seconds, which is greater than the time to takeoff of 3 seconds

(confirmed through test flights). This allowed the team to maximize takeoff performance while ensuring the plane could sustain the load of a full flight mission. The fuse testing results are shown in Figure 29. An S-fuse mounted vertically against the side of the fuselage was chosen because it was found to take the longest to blow at high currents.

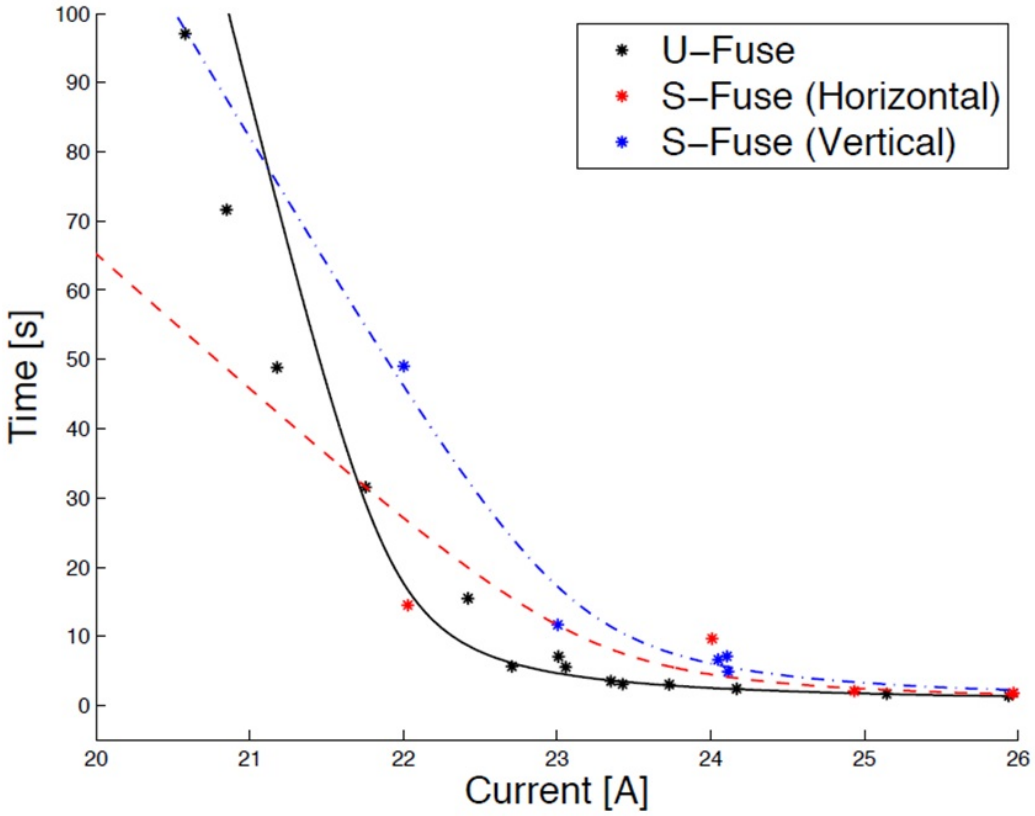

Figure 29: Time for fuse to blow as a function of current for 2 fuse types and mounting orientation.

8.1.2 Landing Gear

Once landing gear fabrication was complete, it was strapped to a test fuselage to confirm that the gear could support the aircraft under a hard landing (3g). Additionally, a full Taxi Mission field was laid out to test and confirm that the aircraft could successfully traverse the roofing panels (Figure 30). The landing gear passed both the hard landing simulation and the Taxi Mission simulation.

Figure 30: An airplane with prototype landing gear maneuvering around obstacles in the Taxi Mission simulation.

8.1.3 Structures

The structural integrity of the wing was tested with a whiffle tree. In order to simulate in-flight loads, the wing was mounted upside down to a carbon fiber nose. The whiffle tree distributed loads in an elliptical profile on the wing (shown in Figure 31). Hot-wired foam blocks were used to distribute the loads over certain sections of the wing. The wing spars failed at the load predicted by SparSizer.

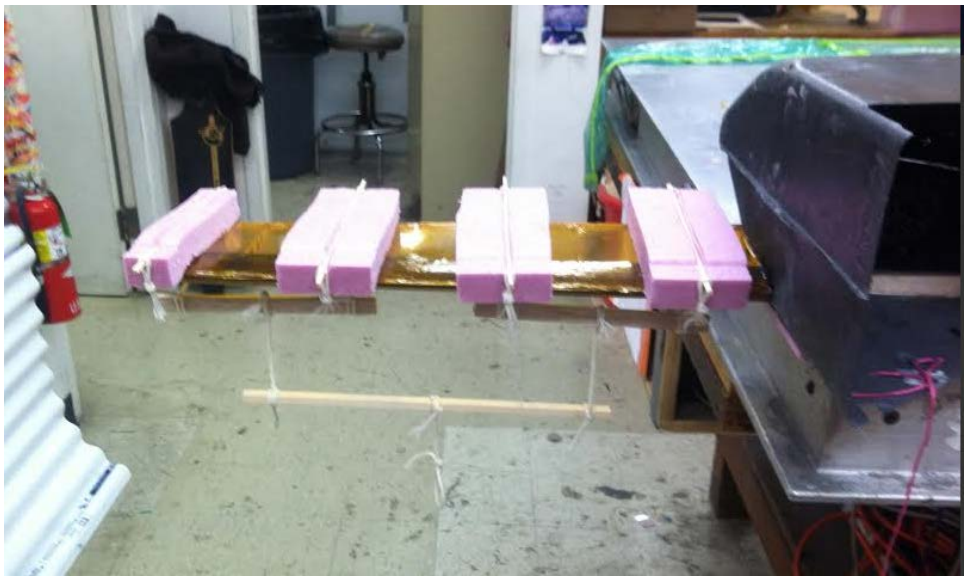

Figure 31: Static load testing of wing in whiffle tree tool, mounted upside-down to carbon nose.

8.2 Demonstrated Performance of Complete Aircraft

Several test flights were carried out to evaluate aircraft performance. Table 31 summarizes these flights, with a brief description of the challenges that were encountered and the solutions that were developed.

Table 31: Aircraft performance evaluation from test flights.

Flight	Description	Solutions
1	• Batteries exploded in flight • Motor overheated	• Re-evaluated propulsion predictions in PlaneTools
2	• Nosed over on landing • Propeller hit the ground on takeoff	• Moved CG forward by shifting the battery pack • Moved the landing gear forward
3	• Nosed over on landing • Wing was too stiff • Motor mount broke	• Reinforced motor mount • Improved manufacturing technique • Moved the landing gear forward
4	• Aircraft overweight • Simulated all missions • Lost control of the ailerons and crashed	• Improved manufacturing technique to minimize empty weight

8.2 Comparisons Predictions Flight Tests

Table 32 compares the predictions of plane performance and mission scores from PlaneTools with measured flight test results.

Table 32: Comparison of predictions and flight test results for all missions.

Mission	Parameter	PlaneTools Prediction	Flight Test Result	Percentage Difference
1	$TOFL$	10 ft (3.05 m)	30 ft (9.14 m)	+200%
	Cruise Speed	68.3 ft/s (20.8 m/s)	65 ft/s (19.8 m/s)	-4.8%
	Lap Time	39 s	42 s	+7.7%
	N_{laps}	6	6	0%
	Weight	2.18 lb (0.99 kg)	2.3 lb (1.04 kg)	+5.5%
	Mission Score	1.5	1.5	0%
2	$TOFL$	68.4 ft (20.9 m)	36 ft (11 m)	-47.4%
	Cruise Speed	65.8 ft/s (20 m/s)	N/A	-
	Lap Time	45 s	N/A	-
	N_{laps}	3	3	0%
	Weight	5.24 lb (2.38 kg)	5.4 lb (2.45 kg)	+3%
	Mission Score	3	3	0%
3	$TOFL$	50 ft (15.2 m)	30 ft (9.14 m)	-40%
	Cruise Speed	74.8 ft/s (22.8 m/s)	66 ft/s (20.1 m/s)	-11.8%
	Lap Time	43.7 s	48 s	+9.8%
	N_{laps}	131 s	145 s	+9.7%
	Weight	4.18 lb (1.9 kg)	4.3 lb (1.95 kg)	+2.9%
	Mission Score	3.66	3.31	-9.6%

There are several differences between the expected and actual performances shown in Table 32. The design aircraft had a TOFL of more than 40 ft (12.2 m) as predicted by PlaneTools because the plane was designed to takeoff within 40 ft (12.2 m) with a headwind of 15 ft/s (4.6 m/s). The predictions were obtained by matching the headwind assumption with the actual headwind during test flights in order to validate the predictions of PlaneTools.

There was a significant difference between the plane's predicted and actual performance on Mission 1 because flaps were not deployed during takeoff. There was also a slight difference in speed because the actual plane was heavier than predicted. For Missions 2 and 3, the plane met the 40 ft (12.2 m) TOFL requirement even though PlaneTools predicted that it would not. It was concluded that PlaneTools overestimated the required TOFL, but since it gave the plane some factor of safety in takeoff, the prediction was not calibrated to match the test flight results.

Based on the lessons learned in test flights, the team improved its understanding of the relationship between predictions and measured performance. Using that knowledge, the team can now move forward in optimizing the competition aircraft by refining the manufacturing techniques in order to further reduce weight and increase total score.

Figure 32: A successful flight test at Sepulveda Basin, Van Nuys, CA

REFERENCES

[1] S. Hoerner, *Fluid Dynamic Drag*, Bakersfield, CA: Hoerner, 1965.

[2] M. Page, *Model Airplane Cook-book*, 2008.

[3] T. Yechout, *Introduction to Aircraft Flight Mechanics*. Reston, VA: American Institute of Aeronautics and Astronautics, Inc., 2003.

[4] M. Drela. (2001, November 30). *XFOIL 6.9 User Primer*. [Online]. Available: http://web.mit.edu/drela/Public/web/xfoil/xfoil_doc.txt

[5] "Wunderground," 2013. [Online] Available: http://www.wunderground.com

[6] "APC Propellers," 2013. [Online] Available: http://www.apcprop.com

[7] J. Melvin H. Snyder, *Effects of a Wingtip-Mounted Propeller on Wing Lift, Induced Drag and Shed Vortex Pattern*, Ann Arbor, MI: University Microfilms, Inc., 1967.

[8] J. Yeargan and E. Smetak, "Aircraft Design Report 2007 AIAA Cessna/Raytheon Design/Build/Fly Competition", University of Southern California, 2007.

[9] J. D. Anderson, Introduction to Flight, New York: McGraw-Hill, 1989.

[10] *MIL-F-8785C, Flying Qualities of Piloted Planes, Military Specification*, 1980.

[11] "Aircraft Design Report 2013 AIAA Cessna/Raytheon Design/Build/Fly Competition", University of Southern California, 2013.

[12] *SolidWorks*. [Computer Software]. Available: http://www.solidworks.com/. [Accessed 01 Jan 2014].

University of California Irvine

Cessna/Raytheon AIAA Design/Build/Fly Competition 2013 - 2014

Table of Contents

1.0 Executive Summary

This report documents the design, manufacturing processes, and testing conducted by the University of California, Irvine (UCI) Design/Build/Fly team for their aircraft entry in the 2013-2014 AIAA/Cessna/Raytheon Design/Build/Fly competition. The objective of the competition is to produce an electric remote controlled aircraft that will receive the highest total score: a combination of the written report score, total flight score, and rated aircraft cost (RAC).

The theme for this year's competition is the backcountry rough field bush plane [1]. The goal of the aircraft is to be as light as possible while carrying internal payloads made of wooden blocks. The aircraft must be capable of completing one ground taxi mission and three flight missions. The ground taxi mission requires that the aircraft taxi and maneuver across 40-ft. of Palruf panels. The objectives of the flight missions are as follows: first, is to fly a maximum number of laps in a four minute period without payload; second, is to fly three laps with a maximum number of payloads stored inside the aircraft; and third, is to fly a three lap course in the shortest time with a given payload. A major challenge is taking off within a 40-ft. runway during the payload missions given the propulsion limitations imposed by a 15 amp fuse and 1.5-lb. maximum battery weight.

Through score analysis, the team determined that the winning aircraft would be one built to complete all four missions with the lightest possible empty weight. Focusing completely on one mission or empty weight alone could not win the competition. The need for effective ground handling on rough terrain adds another level of complexity to the design. To address the challenges posed by each mission, the team designed an aircraft that could balance the mission requirements: primarily ground maneuverability for the taxi mission, high speed for flight mission 1, high number of payload for flight mission 2, and high thrust for flight mission 3. After considering several aircraft configurations, a conventional aircraft design consisting of a high wing with a conventional tail, a taildragger landing gear with skids, and a single tractor motor was selected.

The aircraft optimization revealed that three cargo blocks should be carried during mission 2 in order to maximize score. This sets the maximum payload weight to 3-lb. In addition, as this mission is flown at the aircraft's speed for best range, the aircraft needs to be built with the lightest combination of structure and propulsion weight. The battery pack was sized to provide enough energy for all missions while minimizing weight.

The team chose a low kV motor and opted to increase the voltage and propeller diameter in order to gain enough thrust for takeoff during the payload missions while adhering to the 15A fuse and 40-ft. takeoff requirements. As the second flight mission objective was to carry the heaviest payload, the aircraft's wing was sized specifically for the takeoff portion of that mission. This meant that the wing was overbuilt to fly flight mission 1, which allowed it to pull high G turns to reduce the turn radius and lap time.

Constraints on how to position the payload drove the fuselage design. The cross section of the fuselage was minimized to fit the payloads for missions 2 and 3 longitudinally and enclosed a central

carbon rod that ran from the motor to the tail. The fuselage length adequately accommodated the required payloads, and the landing gear was attached to the fuselage floor, allowing loads to transmit from the landing gear to the central carbon rod through the fuselage structural members. To minimize structural weight, the fuselage section was constructed mainly of balsa sticks and carbon rods with Microlite™ covering as skin.

The team's optimization program ran thousands of plane designs through a mission model and converged on an aircraft with the highest competition score. Table 1.1 summarizes the predicted scoring results. The aircraft is being tested to its performance limits while the design of the aircraft and its components are being improved and optimized.

Taxi Mission		**Mission 1**		**Mission 2**		**Mission 3**	
Score	1	Laps flown	6	Blocks carried	3	Team time (s)	118
		Estimated max	9	Estimated max.	5	Estimated best (s)	100
		Empty Weight (lb)	3.15	Empty Weight (lb)	3.16	Empty Weight (lb)	3.20
		RAC	**3.2**	**Flight Score Total**	**2.11**		

Table 1.1: Predicted Mission Scores

2.0 Management Summary

The UCI team implemented an organizational structure and design timeline that focused on maximizing efficiency and team collaboration. With over 50 dedicated members, the team benefits from a wide range of interests and capabilities.

2.1 Team Organization

The team follows a hierarchical structure similar to those in industry, which places responsibility on members to perform their required tasks. Figure 2.1 shows the team's organizational chart.

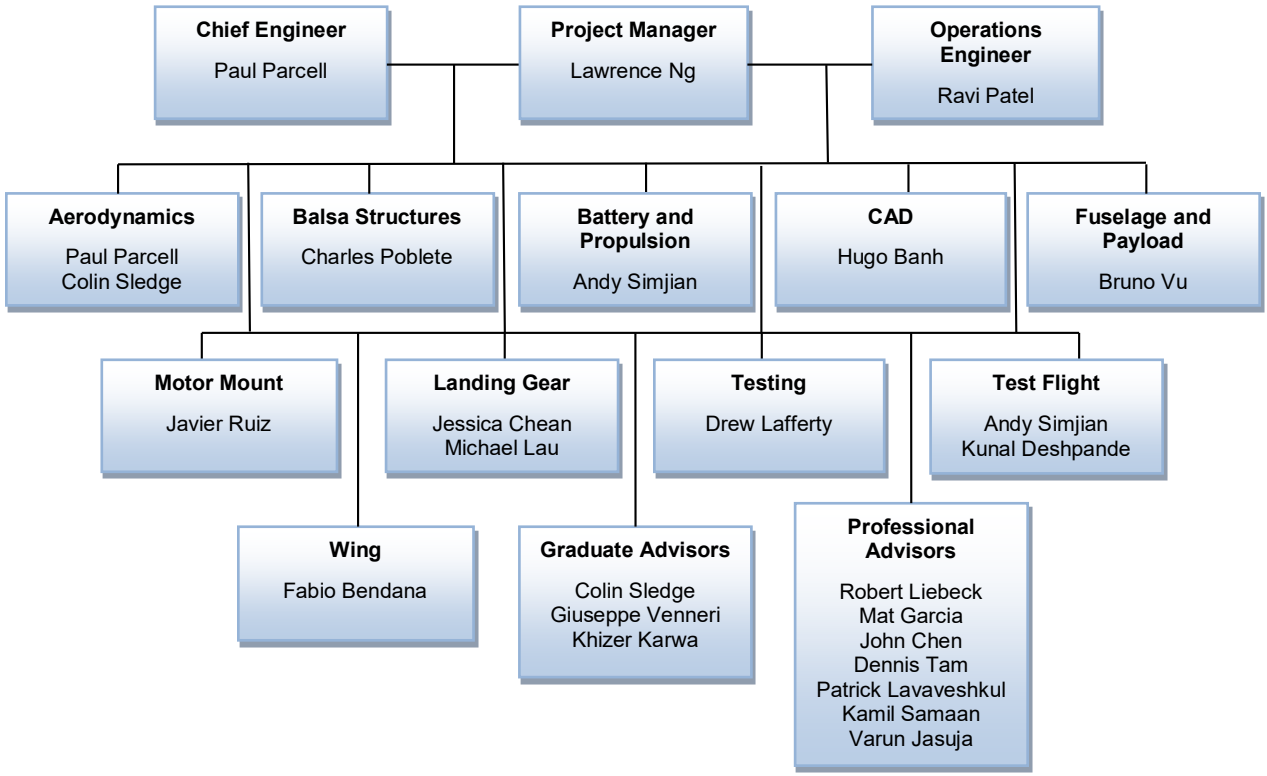

Figure 2.1: Team Organization Chart

The Project Manager is responsible for facilitating productivity in all areas of the project by acquiring material, scheduling, and leading team meetings. The Chief Engineer steers the design effort and facilitates the communication between design groups. The Operations Engineer aids the Project Manager and Chief Engineer in the finance and business aspect of the project by managing logistics and keeping a budget portfolio. All three individuals lead the project, which is further supported by the following teams:

- **Aerodynamics** computes the flight characteristics and necessary wing dimensions. This team also ensures that the aircraft meets certain control and stability standards, and uses numerical modeling to predict flight performance.
- **Balsa Structures** experiments with new manufacturing methods for the wings and fuselage in order to decrease overall weight while maintaining structural integrity.

- **Battery and Propulsion** analyzes and tests the propulsion system to find the best motor, propeller, and battery combination for the aircraft.
- **CAD** creates detailed drawings of every component of the aircraft system and aids in the rapid visualization of possible aircraft solutions.
- **Fuselage and Payload** designs and builds fuselage, fairings, and payload restraint mechanisms.
- **Motor Mount** focuses on fabricating motor mounts that attach to the fuselage boom.
- **Landing Gear** designs and fabricates landing gears integrated with the fuselage floor.
- **Testing** fabricates test apparatuses and conduct load testing for manufactured parts while collecting data for documentation purposes.
- **Test Flight** organizes and conducts test flights, performs preflight/post-flight inspection and collects flight data.
- **Wing** manufactures the wing, tails, and control surfaces using proven methods.
- **Graduate and Professional Advisors** guide and provide insightful suggestions with constructive criticism. Graduate Advisors look over aerodynamics performance aspects of the design and are more accessible than professional advisors. Professional Advisors offer manufacturing tips from previous and current industry experience.

The team held a large scale recruitment event at the beginning of the year to attract new members in order to satisfy the 1/3 underclassmen rule. New team members were placed under the supervision of various team leaders and tasked with learning manufacturing processes as well as their respective team's duties and objectives.

2.2 Project Milestone Chart

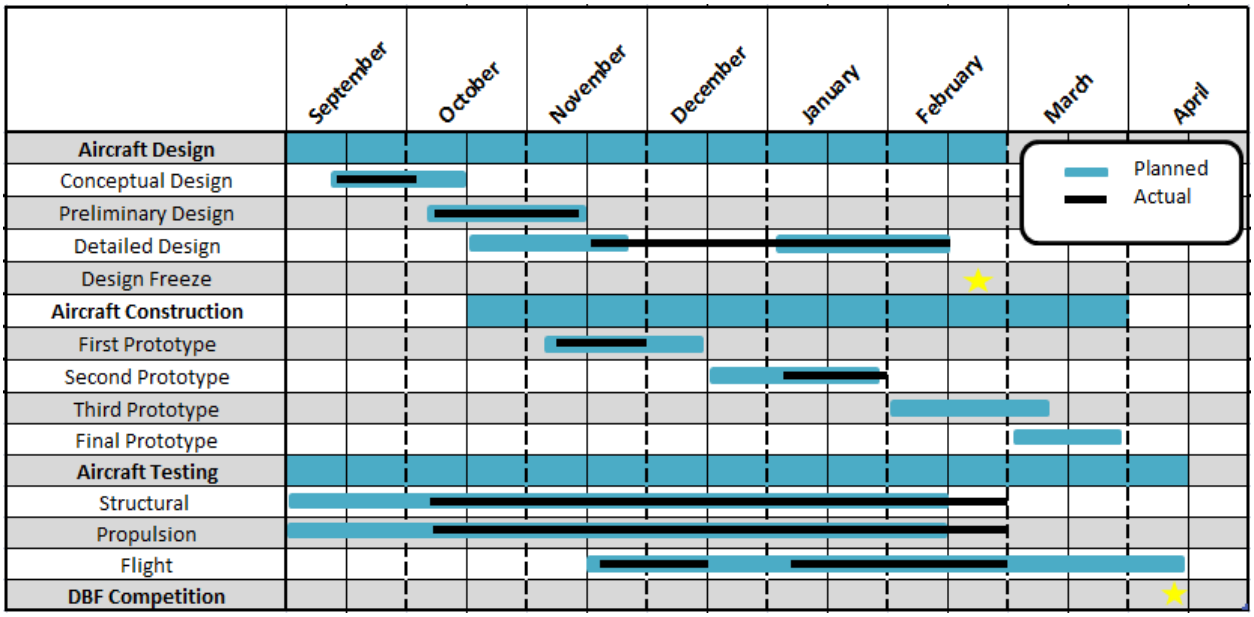

Figure 2.2: Project Milestone

The demand for a competitive aircraft requires an aggressive schedule. The Project Manager maintains a master schedule that tracks the various phases of the design, testing, and important milestones. The planned and actual schedules are shown in Figure 2.2.

3.0 Conceptual Design

The objective of the conceptual design process is to extract a set of figures of merit (FOM) from the analysis of mission goals, requirements, and the design constraints listed in the contest rules. During this process, different design concepts are chosen using the FOM. The end result of this was a high-performance design that maximizes the overall flight score.

3.1 Design Constraints

The team analyzed the contest rules to determine the important design limitations set by the contest. The main requirements for the Design/Build/Fly competition for this year are as follows:

- The weight of the propulsion battery must not exceed 1.5-lb.
- Maximum drawn current supplied by the battery pack(s) or received by the motor(s) is limited to 15A by means of a 15A blade fuse.
- All payloads must be secured sufficiently to ensure safe flight without possible variation of aircraft's center of gravity (CG) during flight.
- The aircraft must have a wing clearance of 3.25-in.
- All payloads must be carried fully internal.
- The aircraft must be designed to fly all three missions.

The ground rolling takeoff for every mission must take place within a 40-ft. runway distance.

3.2 Scoring Formula

The AIAA Design/Build/Fly Competition for 2014 consists of three missions and the design report. The total score is contingent on a combination of the mission scores received along with the rated aircraft cost (RAC). The formula to determine a team's total score is:

$$Total\ Score = \frac{Written\ Report\ Score \times Total\ Flight\ Score}{Rated\ Aircraft\ Cost} \qquad \text{(Equation 3.1)}$$

$$Total\ Flight\ Score = TS \times (M_1 + M_2 + M_3) \qquad \text{(Equation 3.2)}$$

Where TS is the taxi mission score and M_n is the flight score for that mission.

$$Rated\ Aircraft\ Cost\ (RAC) = EW_n \qquad \text{(Equation 3.3)}$$

$$EW_n = Max(EW_1, EW_2, EW_3)$$

Where EW_n is the empty weight, including batteries, measured after the flight with the payload removed.

3.3 Mission Sequence

The team is given 5 minutes to install payload and perform a pre-flight check. Upon completing all three flight missions, the team is allowed a single re-flight of each flight mission with the larger flight score counting towards the total flight score. The assembly and flight line crew is limited to only the pilot, observer, and one ground crew member. The course consists of a 1000-ft. course with two 180° turns and one 360° turn [1]. To receive a score for a mission, the plane must land on the runway without significant damage (as determined by the judges).

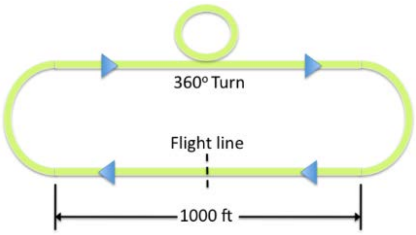

Figure 3.1: Course Layout shown to scale

3.3.1 Ground Taxi Mission

For the taxi mission, the aircraft must taxi across a 40-ft. x 8-ft. course of corrugated roofing panels aligned normal to the long axis of the course. The course will also feature two obstacles reaching from the edge to the centerline at the 1/3 and 2/3 points along the course. The aircraft will carry the 2-lb. payload from mission 3 and cannot go off the course or become airborne. It must complete the course in 5 minutes. Missions 2 and 3 cannot be attempted prior to the taxi mission. Completion of the taxi mission grants a multiplier of 1, whereas failure to complete is given a multiplier of 0.2.

3.3.2 Mission 1 – Ferry Flight

The goal of mission 1 is to complete as many laps as possible in 4 minutes without any payload. The score for mission 1 is given by the equation:

$$M_1 = 2 \times \frac{N_{laps\ flown}}{N_{max\ laps\ flown}} \qquad \text{(Equation 3.4)}$$

Where $N_{laps\ flown}$ is the number of complete laps flown by the team for a successful mission 1 flight. $N_{max\ laps\ flown}$ is the maximum number of laps flown by any team for that mission. The flight time begins when the throttle is advanced for the first takeoff or attempt. Only complete laps are counted in the score.

3.3.3 Mission 2 – Maximum Load Mission

Mission 2 is a three-lap payload flight with no time limit. The goal of this mission is to maximize the number of internal cargo. The cargo is simulated by 6-ft. x 6-ft. x 6-ft. wooden blocks ballasted at 1-lb. each. The flight score for this mission is given by the equation:

$$M_2 = 4 \times \frac{N_{cargo\ flown}}{N_{max\ cargo\ flown}} \qquad \text{(Equation 3.5)}$$

The team that successfully carries the most payloads for this mission normalizes the mission score.

3.3.4 Mission 3 – Emergency Medical Mission

Mission 3 is a three-lap passenger flight consisting of two patients and two attendants. Each patient/attendant is ballasted to 0.5-lb. each with dimensions shown in Figure 3.2. The arrangement of the patient/attendant must meet the following criteria:

- The attendant shall be oriented vertically and the patient shall be horizontal and flat (figure 3.2).
- The attendant must be immediately adjacent to the side of the patient
- The patients must be separated by a minimum of 2-in. side to side or above/below
- At least 2-in. space above the patient shall be "air space" with no structure or systems present.
- The attendants must be separated by at least 2-in. from each other

The objective of mission 3 is to complete the three laps as fast as possible. The flight score for this mission is given by the equation:

$$M_3 = 6 \times \frac{T_{fastest\ flown}}{T_{team\ flown}} \qquad \text{(Equation 3.6)}$$

Where $T_{team\ flown}$ is the time from advancing throttle and $T_{fastest\ flown}$ is the best time recorded by any team getting a successful score for mission 3.

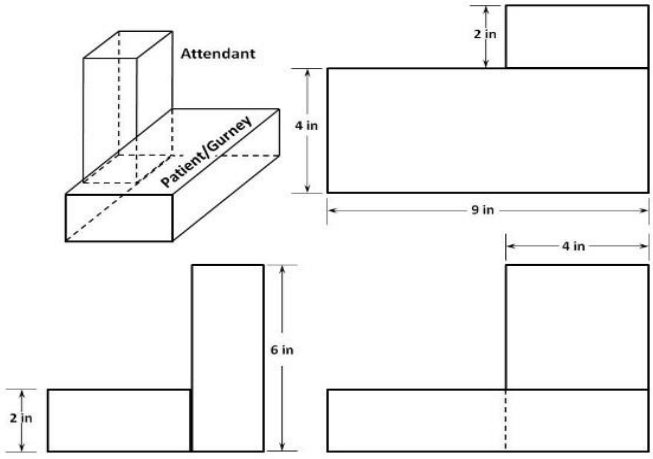

Figure 3.2: Mission 3 Payloads

3.4 Sensitivity Analysis

The score equations were used to perform an analysis and determine the level of impact each score parameter had on the total score. In the first stage of this analysis the team considered the extreme cases to determine if the score equations could have unusual behavior in these conditions. Following this step, an analysis was done using MATLAB to determine the sensitivity of the score parameters. To perform this analysis, the scores were estimated using past years' competition data. The estimated values for an average team were 3.5-lb. empty weight, 6 laps, and 130-seconds mission 3 time. Estimated maximum mission scores were 9 laps for mission 1, 5 payloads for mission 2, and 100-seconds mission 3 time. These estimates were made using data from previous years adjusted for the constraints imposed this year.

3.4.1 Extreme Cases

Several extreme aircraft were analyzed to see if any variable had an extreme effect on the score as a whole. Each case made use of estimates for performance and total weight. The normalized scores for each mission along with the total score are shown in Figure 3.3:

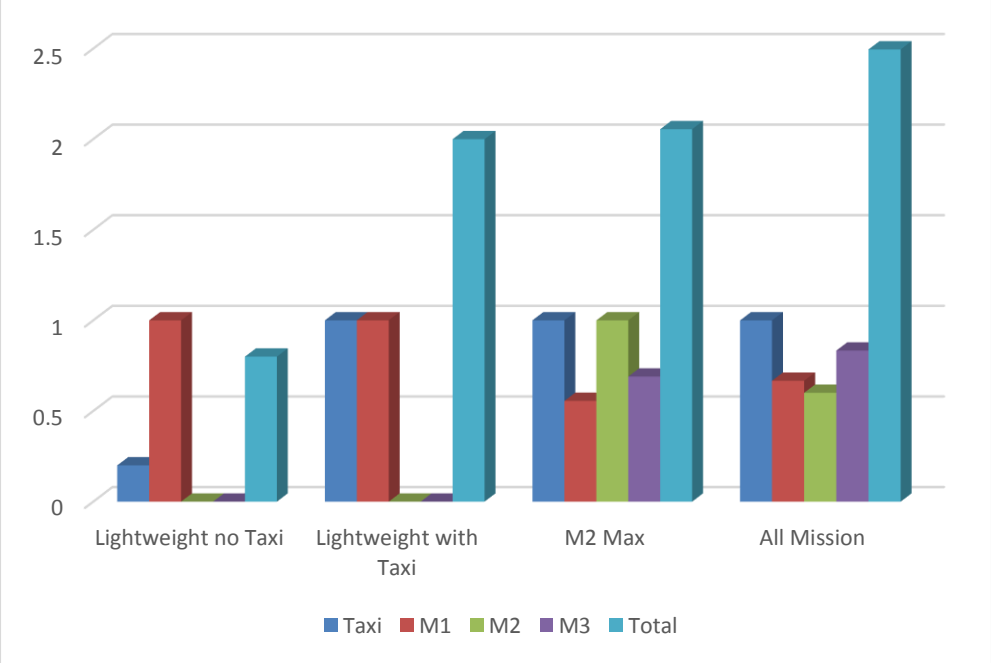

Figure 3.3: Extreme Cases Scores

Two extremely minimal aircraft were considered. The absolute lightest planes capable of flying mission with and without being able to complete the taxi mission are on the left. These planes had a weight of under 1-lb. Due to their light weight, they could reach the maximum mission 1 score, but they could not complete the other flight missions. The aircraft with the maximum score for mission 2 is shown next. Its weight is greater than the average plane because the propulsion system and wing are larger to achieve takeoff in 40-ft. Finally, an aircraft which carries 3 payloads for mission 2 is shown. This represents a compromise of all performance values. The weight and flight time estimates for each case were calculated using UCI DBF data from the past two years. The analysis shows that a maximum score is achieved when a compromise of aircraft parameters and mission scores is reached.

3.4.2 Sensitivity Analysis

A sensitivity analysis was conducted to determine the effects of each score parameter on the total score. This study uses the same average design as the last score study. The impact of each score parameter on the total score was determined by varying one parameter at a time while holding the others constant.

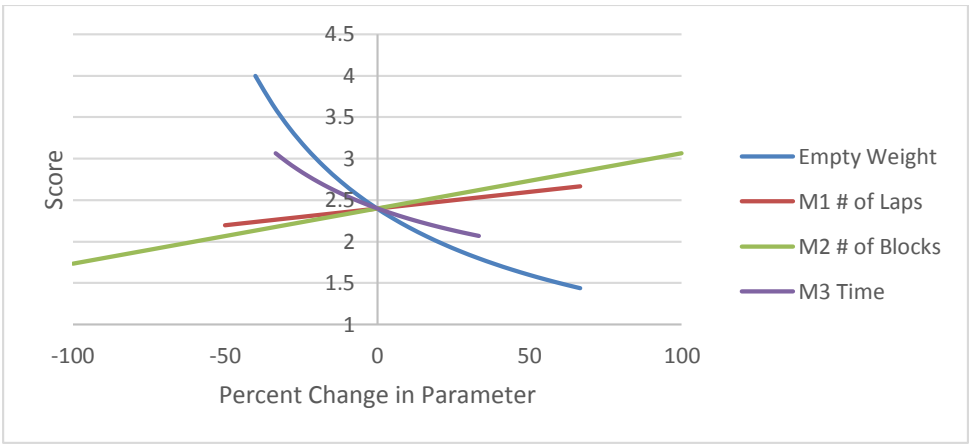

Figure 3.4: Impact of Change in Parameters on the Total Score

Figure 3.4 shows the effects of the change in each score parameter to the total score. Parameters that affect the score most have the greatest magnitude of slope. The empty weight was most important, with mission 3 time being next most important.

3.5 Configuration Selection

3.5.1 Configuration Figures of Merit (FOM)

During the configuration selection process, each part was scored independently using a set of scoring parameters to find the best configuration for this year's competition. Based on the scoring analysis, more weight was given to specific areas. The scoring parameters were:

- **System Weight (45%):** The first and most important characteristic evaluated was system weight. This consisted of the empty aircraft weight without motor, servos, or payload. Because a lighter aircraft will score higher, this area was given the most weight in determining the aircraft configuration.
- **Low Speed/Ground Handling (30%):** The extreme cases analysis showed that completing the taxi mission is critical to a high score. Also, achieving 40-ft takeoff relies on adequate control for rotation.
- **L/D (Lift to drag ratio) (15%):** The lift-to-drag ratio was given the third highest weight. The L/D ratio is a basic function of all aircraft and as such can be used to evaluate the flight performance. Choosing a configuration that maximizes L/D ensures that the aircraft can travel longer distances for a given battery pack by accelerating and flying more efficiently.
- **Manufacturability and Reparability (10%):** The ease with which the aircraft can be manufactured and repaired was a consideration in the design process. The ability to design and build a specific configuration is determined by the experience of the members, with more difficult configurations requiring more time to build. Meanwhile, the aircraft also needs to be simplistic in design in order for repairs to be made in a timely fashion without much difficulty.

3.5.2 Configuration Selection

A few basic aircraft configurations were evaluated as possible options for this year's design. They were evaluated according to how well they could accomplish the tasks of the missions as dictated by the sensitivity analysis, with the conventional configuration acting as the baseline for comparison. Configurations considered were:

- **Conventional:** The benefits of a conventional aircraft are that it is proven and is relatively easy to design and build. However, most components only serve a single purpose, so it would not be the most efficient design when weight and materials are considered. The major drawback to this design is the fuselage, which significantly increases drag.
- **Flying Wing:** This type of aircraft offers a greater L/D than the conventional design. However, the major drawback of this configuration is its inability to carry the mission 2 payload without requiring a substantial increase in size. Its ground handling also suffers because it lacks a fuselage to mount steerable landing gear on.
- **Biplane:** The biplane configuration offers greater wing area per span, allowing for a smaller planform; however, it also requires additional structure to connect the wings together, which adds weight and drag. The interaction between the wings also generally reduces the efficiency of each wing.

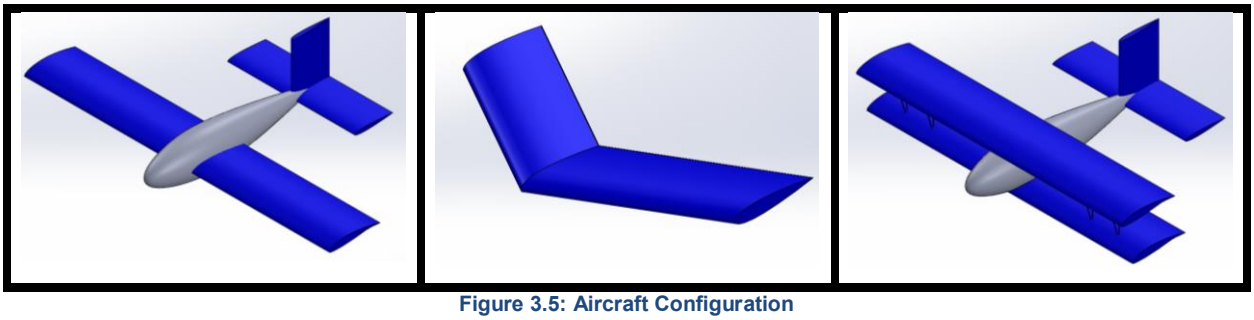

Figure 3.5: Aircraft Configuration

FOM	Weight	Conventional Aircraft	Flying Wing	Biplane
Aircraft Weight	45	0	0	*-1*
Ground Handling	30	0	-1	*0*
L/D	15	0	1	*-1*
Manufacturability	10	0	0	*-1*
Total	*100*	***0***	*-15*	*-70*

Table 3.1: Aircraft Configuration Figures of Merit

A conventional configuration would offer the best compromise of efficiency and ground handling.

3.6 Sub-systems Selection

After a conventional configuration was selected, the major sub-system components were analyzed using a figure of merit analysis to determine the best options. The main sub-systems were motor, tail, and landing gear.

3.6.1 Motor Configuration

The team investigated the placement and number of motors, which affects the aircraft's efficiency and ability to carry payload. A figures of merit chart was used to gauge the different propulsion methods, using the single tractor configuration as the baseline for comparison. The ideal system components were selected later on in the detailed component selection.

3.6.1.1 Motor Figures of Merit

Score weighting for the motor configuration choice was split into four categories: system weight (40%), additional structural weight (30%), system efficiency (15%), and aircraft efficiency (15%). System weight and structural weight were weighted most because the RAC significantly affects the total score. System and aircraft efficiency were both weighted least because differences between systems in these aspects were small.

Motor Configurations

- **Single Tractor:** This configuration is lightweight and is less likely to have propeller strikes on takeoff and landing than a pusher configuration. Forward-mounted propellers have high efficiency because they act on undisturbed air. If high thrust is desired, a geared motor is the required to stay below the 15A limit, which in turn increases system weight.
- **Double Tractor:** Two motors of reduced size can use smaller propellers to attain takeoff speed. The battery voltage may be split between two motors while preserving the current limit, so a gearbox may be avoided. However, this system's weight including electronic speed controllers is greater than that of the single motor system, but only outputs at best the same amount of thrust. The aircraft's wing must also be reinforced to withstand the loads of the motors.
- **Single Pusher:** Mounting a single motor aft of the aircraft would allow better air flow around the airframe, reducing scrub drag. Likewise, it would also suffer from the additional weight of a gearbox needed to obtain high thrust, and the propulsive efficiency is reduced as the propeller operates in the wing and fuselage wake. Finally, a significant disadvantage would be the necessity of more weight or a longer moment arm of the battery in front to balance the aircraft.

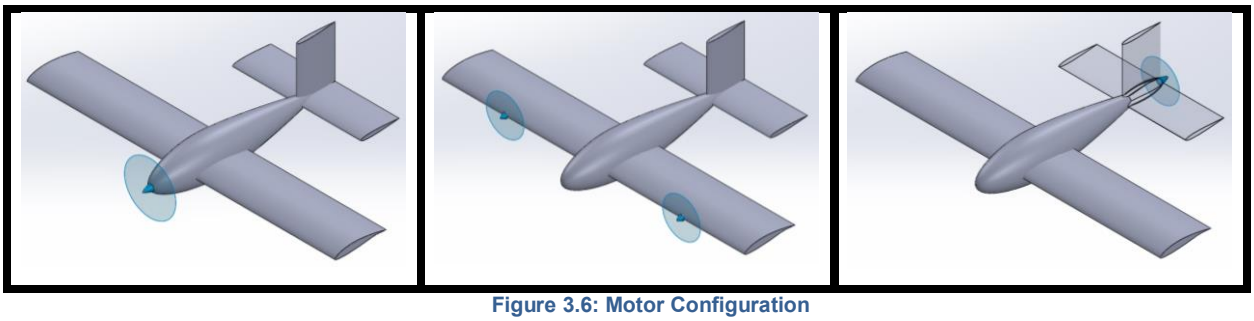

Figure 3.6: Motor Configuration

FOM	Weight	Single Tractor	Double Tractor	Single Pusher
System Weight	40	0	-1	0
Structural Weight	30	0	-1	-1
System Efficiency	15	0	0	-1
Aircraft Efficiency	15	0	0	1
Total	*100*	***0***	*-70*	*-30*

Table 3.2: Motor Configuration Figures of Merit

The single tractor configuration was selected from the FOM chart, because it resulted in a lighter aircraft and simplified balancing by allowing the placement of heavier components near the CG.

3.6.2 Landing Gear Configuration

Takeoff and landing are very critical for the successful completion of the missions. Excellent ground handling for the taxi mission is also necessary. The challenge at takeoff is to maintain sufficient control during the ground roll until the aircraft attains sufficient speed. For this year's competition, the takeoff roll will be very short, so precise control and quick rotation are crucial. Naturally, during the landing portion, the landing gear must withstand the load from the ground impact. A scoring sheet was used to gauge the different landing gear designs, using tricycle as the baseline for comparison. As always, weight was a critical parameter. Handling (40%) and weight (30%) were heavily weighted, while drag (15%) and durability (15%) were also factored into the comparison.

- **Tricycle:** This configuration has main wheels under the wing and a nose wheel for steering. The nose wheel is exposed to the propeller wake, causing a significant drag penalty. However, the nose wheel allows for excellent ground handling on flat terrain.
- **Bicycle:** This configuration has two centerline wheels and two wing tip wheels. The landing gear structure can be significantly reduced as the main loads are transferred through the center wheel, but the configuration adds more components, which add drag.
- **Tail Dragger:** This configuration has two main wheels under the wing and one smaller wheel under the tail of the aircraft. This configuration does not have good ground handling in the presence of a crosswind, but it does have less drag than a tricycle configuration. Its ground footprint is also larger,

effectively reducing the takeoff field length. During preliminary tests, it provided the best handling during the taxi mission because the aerodynamic forces from the tail were used to steer rather than the friction of the wheels.

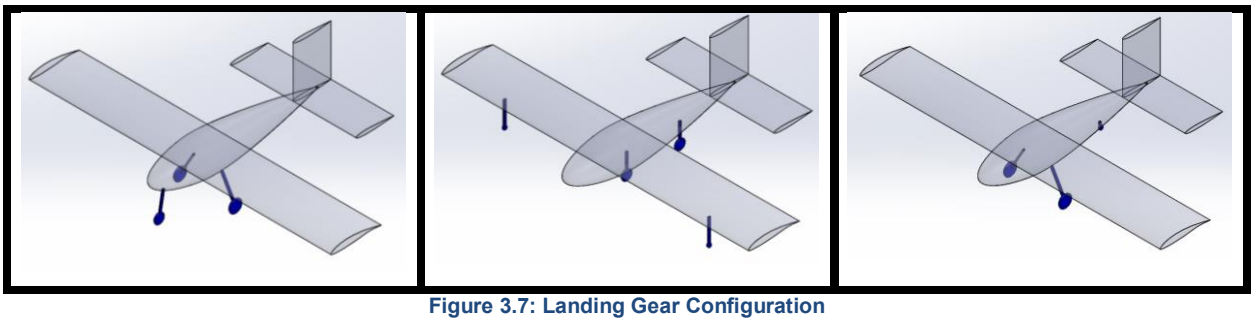

Figure 3.7: Landing Gear Configuration

FOM	Weight	Tricycle	Bicycle	Tail Dragger
Handling	40	0	-1	0
Aircraft Weight	30	0	1	1
Drag	15	0	-1	1
Durability	15	0	-1	0
Total	*100*	***0***	*-40*	*45*

Table 3.3: Landing Gear Configuration Figures of Merit

The taildragger configuration was selected due to its lower drag and weight along with its advantage in handling during the taxi mission.

3.6.3 Tail Configuration

The tail provides stability and allows the aircraft to make high performance turns. Three configurations were considered with a conventional configuration used as the baseline. Weight (40%) was deemed most important because it affects the overall score significantly. Stability and control (40%) was equally weighted because the taxi mission uses the tail for steering, and greater in-flight control yields better flight times. Drag (20%) was not as important because all designs have similar drag.

- **Conventional:** This configuration is simple to install and provides sufficient stability and control.
- **T-Tail:** It is effective at high angles of attack, but placing the horizontal stabilizer on top of the vertical stabilizer will increase its structural weight.
- **V-Tail:** Two surfaces form a “V” with the tail boom and provide both elevator and rudder control. Control authority is reduced in both yaw and pitch, but weight can be reduced.

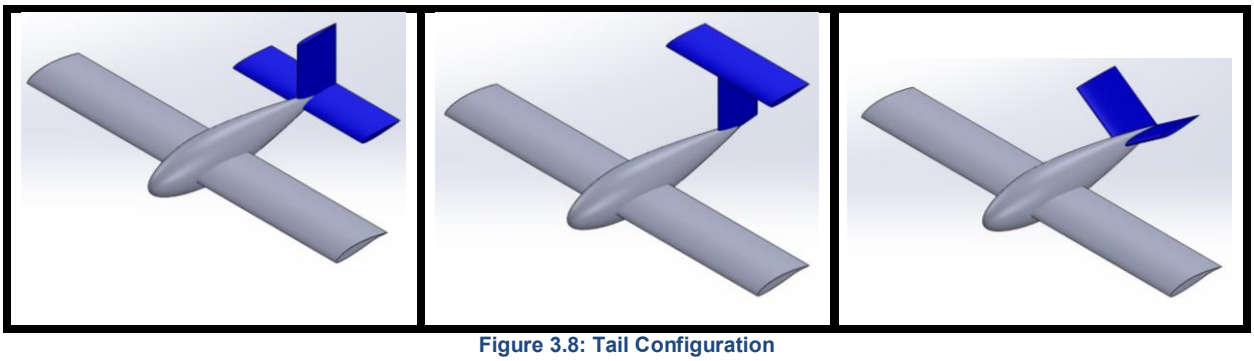

Figure 3.8: Tail Configuration

FOM	Weight	Conventional	T-Tail	V Tail
System Weight	40	0	-1	0
Stability & Control	40	0	0	-1
Drag	20	0	0	1
Total	*100*	***0***	*-40*	*-20*

Table 3.4: Tail Configuration Figures of Merit

The conventional tail was selected because it provided the best control on the ground and in the air along with having low weight compared to the T-tail.

3.7 Conceptual Design Summary

The finalized conceptual design is a conventional aircraft, powered by a single tractor propeller, and features a taildragger landing gear and conventional tail which provides adequate ground control. This final concept reflects the qualities that the team deemed important in order to obtain a high score at the competition.

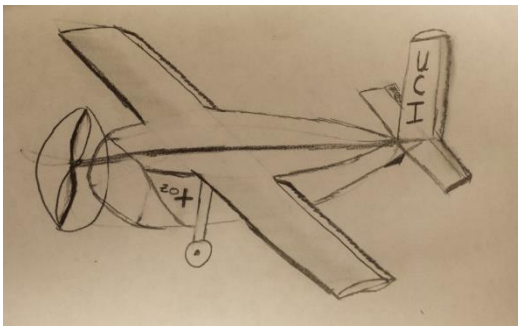

Figure 3.9: Conceptual Sketch

4.0 Preliminary Design

Preliminary design took the configuration proposed during the conceptual design phase and applied it to a mission model that would output several aircraft. This section shows how the sizing and optimization of each subsystem was done to converge on an aircraft that would score the highest at the competition.

4.1 Design and Analysis Methodology

Using the configuration decisions made during the conceptual design phase, a sizing program was written in MATLAB which models the aircraft size and performance parameters to generate a total score. The program can then be used to iteratively vary each size and component parameter, yielding the optimal design with the maximum flight score. All aircraft simulated were assumed to be capable of completing the taxi mission since the conceptual design phase showed this was necessary for a competitive score.

The program has 4 distinct parts: weight buildup, drag buildup, propulsion model, and mission model. The weight buildup summed up weight estimates of each component. This relied on documentation of previous building methods along with material densities and weights. As the aircraft design and construction methods were refined, the weight estimation methods were updated. Initial weight estimations were conservative to ensure the performance goals could be met. The drag buildup makes use of wind tunnel data along with parasite drag estimation equations developed for small-scale aircraft. Aerodynamic characteristics of the entire aircraft are calculated in this section of the program using the airfoil properties and wing dimensions in conjunction with the parasite drag estimations.

Propulsion and mission models use more complex methods to estimate outcomes. The propulsion code find propeller thrust and pitch speeds using empirical data curves with battery voltage and airspeed as inputs. The mission model relies on the aircraft characteristics defined by the weight buildup, drag buildup, and propulsion model to compute flight times, energy consumption, and takeoff distances. Its key features and limitations are described in Section 4.2.

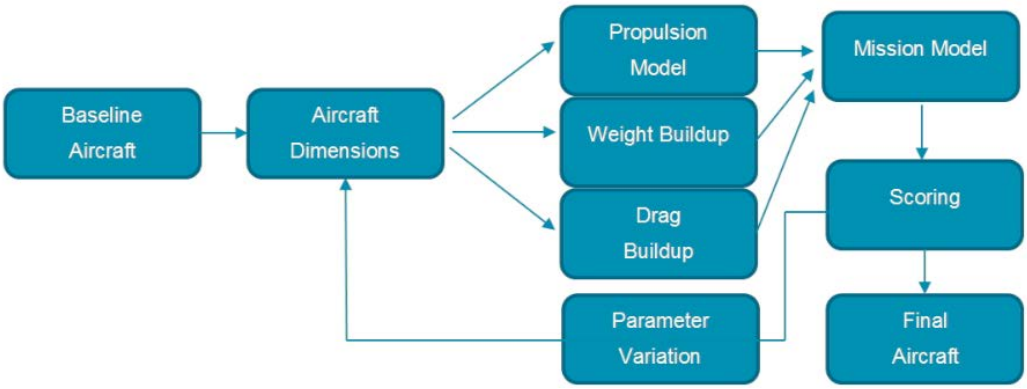

Figure 4.1: Optimization Program Flow Chart

4.2 Mission Model

Due to the interdependence of the key aircraft components and size parameters, the mission model was used extensively to analyze design and sizing trades. The mission model is divided into segments with flight conditions as shown in Figure 4.2 and Table 4.1. The aircraft is modeled as flying at full throttle to achieve minimum flight time along with ensuring the battery energy capacity will not be

exceeded in real life. No headwind or crosswind is assumed. Any aircraft which was unable to complete all three missions either due to insufficient energy or not accomplishing takeoff in 40-ft. was disregarded.

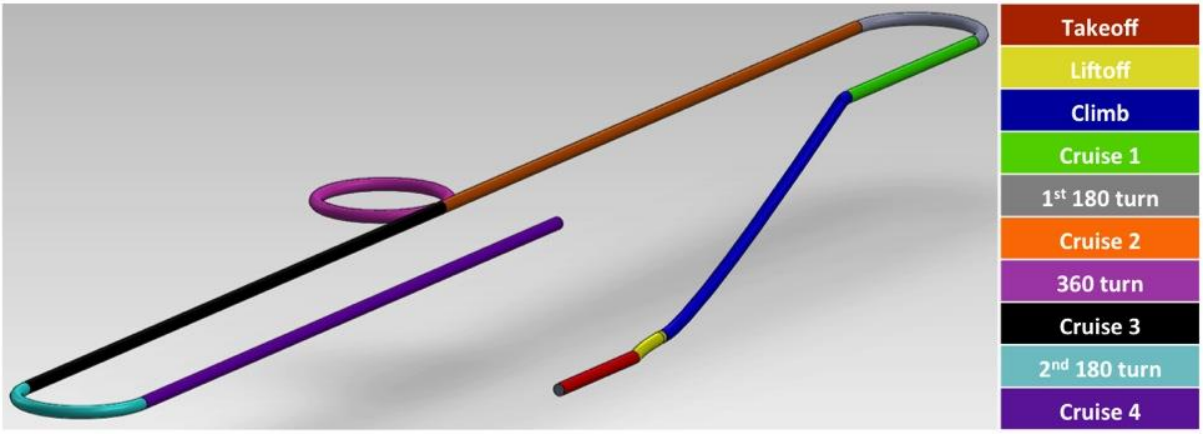

Figure 4.2: Mission Model Segments

Flight Segment	Constraints	Description
Takeoff	Constant angle of attack Rotation when V = 1.2•V_{stall}	Aircraft accelerates on the ground until rotation.
Liftoff	Constant altitude	Aircraft accelerates to ideal climb speed.
Climb	Constant load factor	Aircraft climbs to cruise altitude of 70-ft
Cruise	Constant altitude	Aircraft maintains altitude.
Turn	Constant load factor	Aircraft turns without overloading wings.

Table 4.1: Mission Model Constraints and Segment Descriptions

The load factor represents a 3G loading for the heaviest mission. This means that mission 1 turns are tighter because the aircraft weight is lower.

4.3 Design and Sizing Trades

To see the effect of individual parameters on score as a whole, other parameters were kept constant while running the sizing and performance code.

4.3.1 Aerodynamic Trade-offs

Airfoil

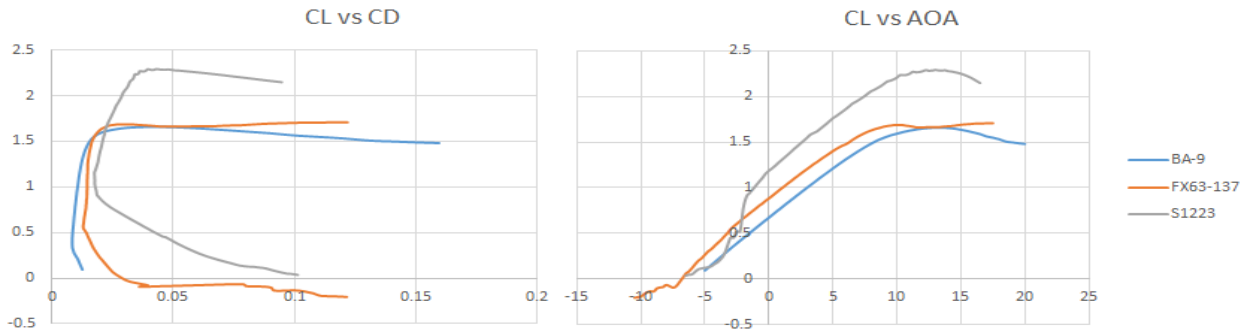

Figure 4.3: Airfoil Polars

Several airfoils were studied and modeled to determine the ideal choice. Wing span was varied during the analysis, allowing high maximum lift coefficient airfoils to take advantage of less wing area required for takeoff. To narrow down the selection process, three airfoils were chosen which have desired characteristics at low Reynolds number. These came from suggestions by Michael Selig in *Summary of Low-Speed Airfoil Data* [2]. Desired characteristics include a high maximum lift coefficient for takeoff and a low drag coefficient at low angles of attack for maximum cruise speed. The airfoils are shown in Figure 4.4 and their polars are shown in Figure 4.3.

BA-9

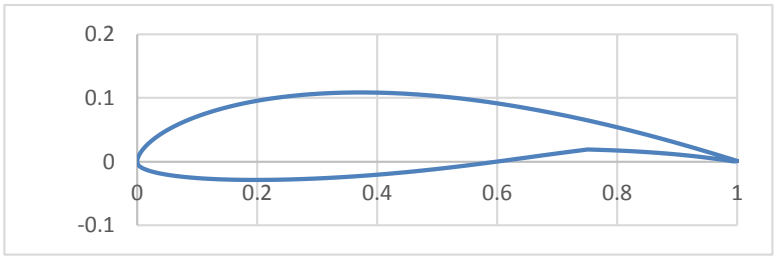

FX 63167

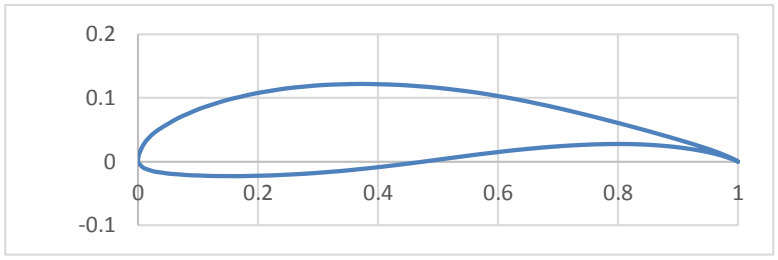

S1223

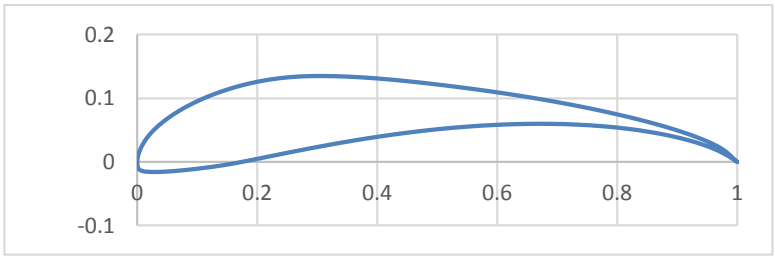

	BA-9	S1223	FX-63137
C_L_max	1.66	2.29	1.69
max t/c	13.3%	12.1%	13.7%
C_d @ C_l = .4	.00845	.05	.01577

Figure 4.4: Airfoil Profiles and Characteristics

Overall, the FX-63137 had the highest score as can be seen in Figure 4.5, but the BA-9 scored within 1% of that score. The FX-63137's performance can be attributed to the high maximum C_L (coefficient of lift) indicated by the X-foil data shown. However, achieving this performance in real life would be very difficult considering surface imperfections and the high probability of hysteresis loops suggested by Martin Simmons [3]. The BA-9 was chosen because its overall scored performance was nearly identical to the FX-63137 and its greater average thickness allowed for lighter internal structure. The BA-9's large drag bucket allows for more versatile performance.

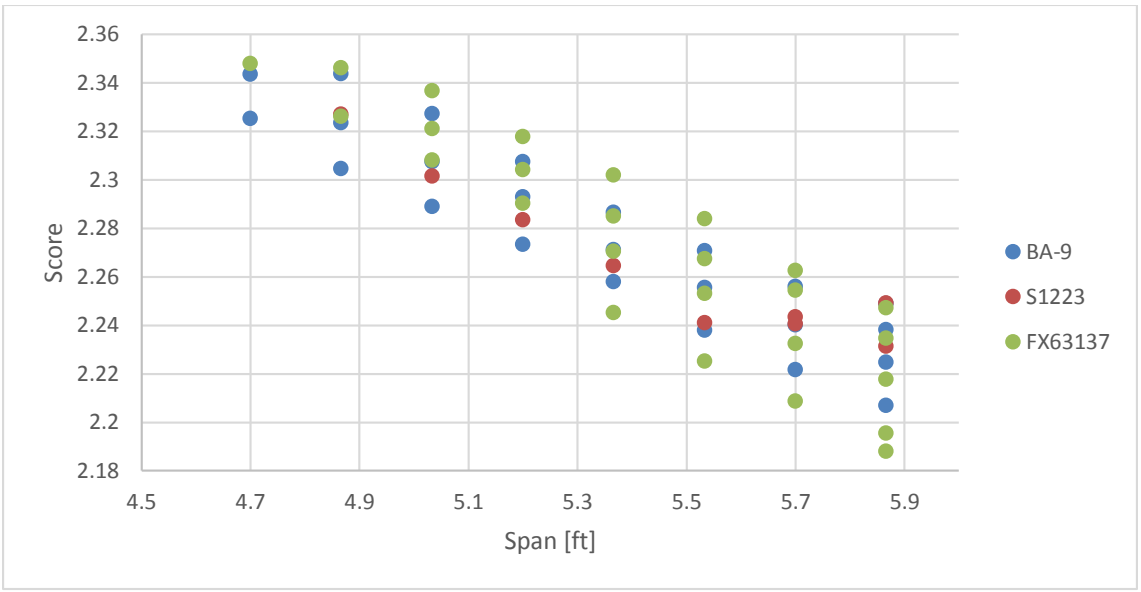

Figure 4.5: Score vs Span

Chord

To minimize induced drag and thereby maximize flight speed and efficiency, wing span should be maximized according to the induced drag equation, were *b* is the wing span:

$$D_i = \frac{\left(\frac{L}{b}\right)^2}{\pi q e} \qquad \text{(Equation 3.7)}$$

For a given lift and wing area, this means chord should be minimized. However, wing chord was limited by both Reynolds number and structural constraints. Wing drag increases dramatically when Reynolds number is below 200,000. To maintain this Reynolds number at takeoff where flight speed is approximately 40-ft/s, the chord must be at least 9-in. Below this chord, the wing construction methods must also be modified to accommodate the decreased wing thickness.

Sweep & Taper

Due to low flight speed and adequate tail sizing required for the taxi mission, no wing sweep was implemented. Wing taper was not used because the gain in efficiency by tapering is outweighed by the complexity of building the wing along with the increased probability of tip stalls.

4.3.2 Propulsion System Trade-offs

Motor

Motor	kV (RPM/V)	Weight with gearbox	Maximum Voltage (V)	Maximum Power (W)	Specific Maximum Power (W/oz)
Neu 1110-6D	1400	5.8	38	1000	172
Neu 1110-3Y	1512		36		
Neu 1110-2.5Y	1814		30		
Neu 1107-6D	1900	5	28.5	600	120
Neu 1107-3Y	2050		27		
Hacker A40-14L	355	9.6	25.2	1500	156
Hacker A40-14S	530	7.3		1000	137

Table 4.2: Propulsion Configuration

Several motor and gearbox combinations were compared to find the best propulsion system. Initially, Hacker and Neu motors with at least 500W and maximum voltage of at least 24V were considered. However, as Table 4.2 shows, the total weight of the Hacker motors which were capable of withstanding the voltage used was much higher than comparable Neu motors. The ability to deliver greater power must be compromised with system weight, so a selection of Neu motors with different kVs was chosen. The gearboxes considered were the Maxon 4.4:1 and the P29 6.7:1 which both weigh 1.8-oz. Many aircraft parameters were varied in this analysis because the motor choice cannot be isolated from other design choices. The parameters varied during the motor simulation include the gearbox, number of battery cells, and propeller for each mission, wing span, and number of payloads for mission 2.

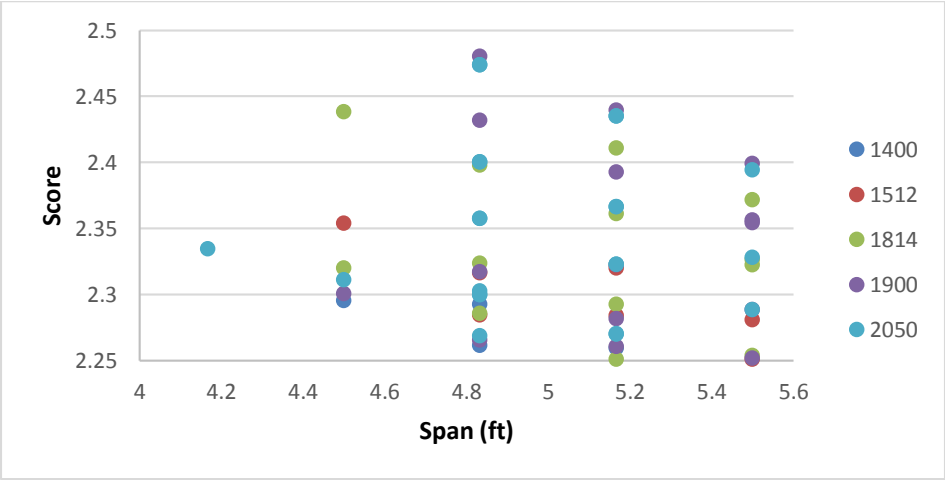

Figure 4.6: Motor Score vs Gearbox Ratio

Ultimately, as shown in Figure 4.6, the 1900 kV Neu 1107-6D with a 4.4 gearbox scored highest with a wingspan just under 5-ft. Motors with lower kV were more efficient by using larger propellers, but they could not generate the pitch speed necessary to complete fast lap times.

Battery Selection

A selection of battery cells outlined in Table 4.3 was analyzed to determine which could provide the power necessary for takeoff during the heaviest mission and provide enough energy to complete the maximum number of laps during mission 1. Larger capacity cells can provide more energy for longer flights and their lower internal resistance means power output is more consistent. Smaller capacity cells have an advantage in weight, but they experience a very significant drop in power during high load at takeoff. A single consistent battery pack was chosen for all missions because the weight advantage of smaller batteries is nullified if a larger pack is used in another mission. Each battery pack was simulated for all missions and energy and current limits were checked.

Battery	Capacity (mAh)	Resistance (ohms)	Weight (oz.)	Energy density
Elite 1500	1500	0.009	0.81	1852
Elite 2000	2000	0.009	1.16	1724
KR1400	1400	0.013	1.2	1167
KR500N	500	0.019	0.6	833
KAN650	650	0.014	0.49	1327

Table 4.3: Battery Selection

The Elite 1500 was chosen because the smaller capacity KR and KAN cells ran out of energy before completing mission 1. The larger Elite 2000 cells were not chosen because they had excess energy and weighed more than the Elite 1500 cells.

During the motor selection, the battery cell count was also varied. A peak score occurred with 20 cells. An aircraft with less cells than this had a weight advantage, but the drag from a larger wing required for takeoff diminished flight speed. Aircraft with more cells could fly faster due to smaller wings, but the additional weight represented by the propulsion battery outweighed the faster flight times in the score.

This analysis also included a variation of mission 2 payloads. Mission 3 requires a total of 2-lb. to be carried, so a tradeoff between carrying more than 2 payloads in mission 2 and the accompanying increase in total aircraft weight resulting from increased battery cell count had to be analyzed. Initially, the payload number was varied up to 5, however the most competitive aircraft carried either 2 or 3. The simulation represented in Figure 4.7 showed that the ideal payload number for mission 2 was three payloads. Aircraft capable of carrying 3 payloads generally had more power than was necessary for takeoff during mission 3, which allowed for faster flight times. Correspondingly, an additional lap could be flown in the 4-minute time period for mission 1.

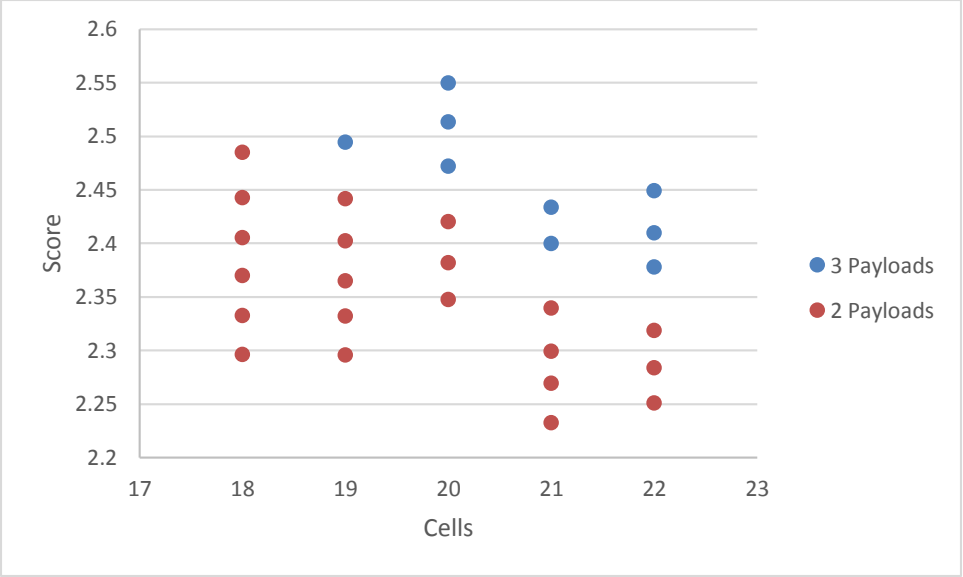

Figure 4.7: Battery Score vs Cells

4.3.3 Final Optimized Aircraft

Airfoil	Motor & Gearbox	Battery	Mission 2 Payloads
BA-9	Neu 1107 6D 4.4:1	20 Cell Elite 1500	3

Table 4.4: Optimized Aircraft Selections

The final aircraft configuration, as shown in Table 4.4, represents a combination of features which maximize the total flight score. A high lift, low drag airfoil and a propulsion system which balances weight with performance represent the optimal aircraft. The propeller choices below maximize mission performance by accommodating the different loading scenarios. A span of 61-in. was chosen to ensure takeoff occurred within the 40-ft. distance with the optimized propulsion system.

Propeller choices are shown in Table 4.5. Mission 1 and 3 use high pitch props to generate a pitch speed that allows the aircraft to reach maximum airspeed. Mission 2 maximizes thrust to accomplish takeoff with 3 payloads.

	Mission 1	**Mission 2**	**Mission 3**
Propeller	11x10	13x6.5	12x8

Table 4.5: Propeller Choice for Each Mission

4.4 Lift, Drag, and Stability Characteristics

The drag polar and L/D for the entire airplane are shown with the in-flight C_L for each mission in Figures 4.8 to 4.10. Mission 2 is the heaviest mission, so its C_L and drag are highest. Mission 1 and 3 fly at maximum speed, so the C_L and C_D (Coefficient of drag) are low. At this high speed, L/D is lower than mission 2 when the aircraft flies slower, and therefore at a higher C_L.

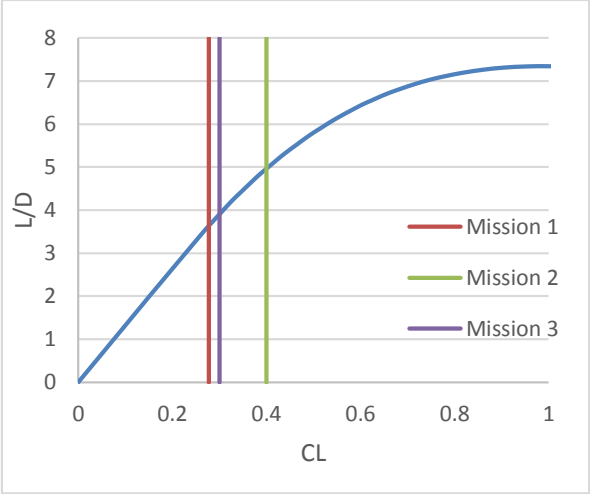

Figure 4.8: Airplane L/D vs C_L

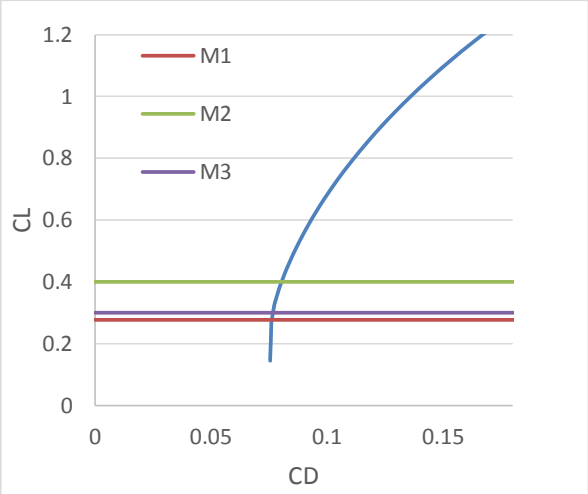

Figure 4.9: Airplane Drag Polar

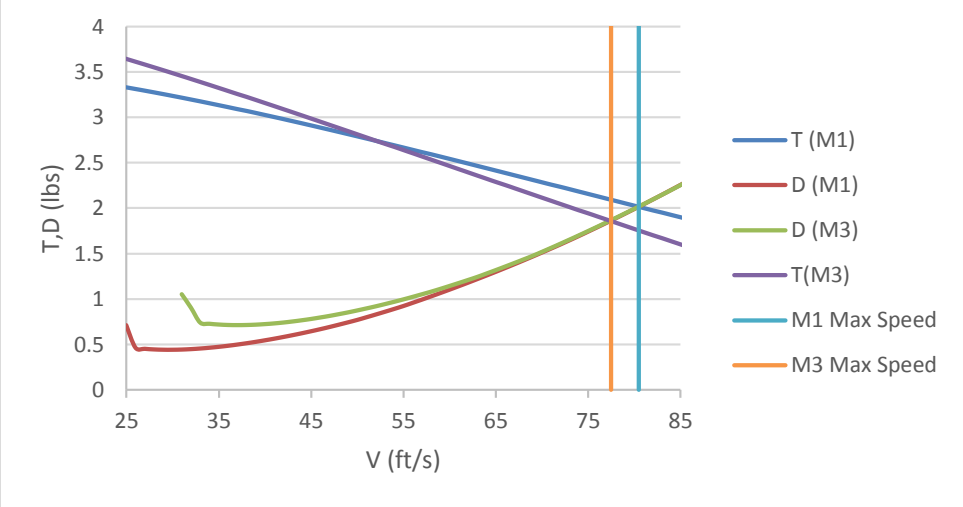

Figure 4.80: Airplane Thrust and Drag vs Velocity

The maximum flight speeds for mission 1 and 3 are shown. Mission 2 only requires completion, so maximum speed is not analyzed. The maximum speed is limited by the drag and thrust produced. Mission 3 flies slightly slower because the additional weight from the attendants and patients increases the induced drag.

The drag buildup for each mission is shown in Figure 4.11. Fuselage drag clearly dominates, with the wing being the next biggest contributor. Induced drag for mission 2 is higher than the other missions because a higher C_L is required.

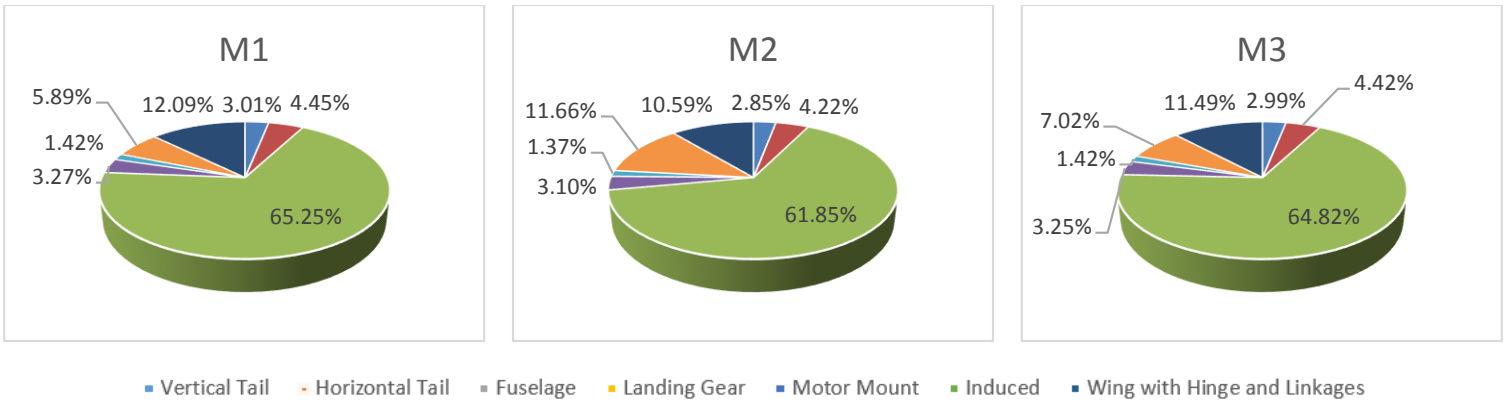

Figure 4.11: Drag Buildup

4.4.1 Stability and Control

The aircraft's C_L is highest for mission 2. A Trefftz plot, shown in Figure 4.13, was created with the geometry input in Figure 4.14, with the Athena Vortex Lattice (AVL) program, which was developed by Mark Drela and Harold Youngern at MIT [4]. This plot verified that peak C_L occurred within 50% of the semi-span and that section C_L's did not exceed $C_{L\,max}$ at any point.

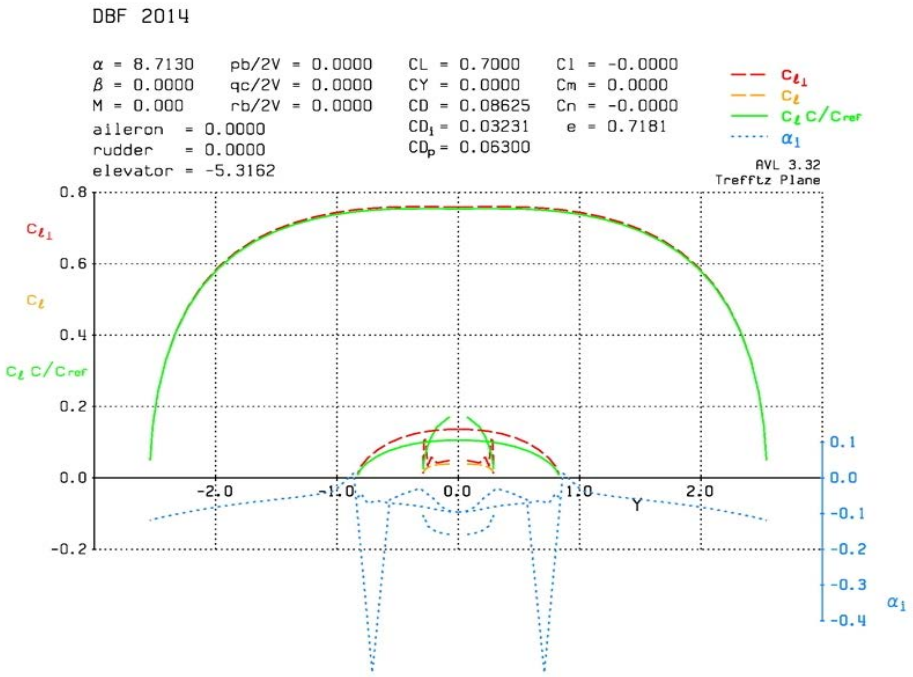

Figure 4.9: Trefftz Plot

In order to evaluate the effects of increased loads and slower speed for mission 2, its flight conditions were simulated in the AVL program. The geometry input model is shown in Figure 4.14. The preliminary weights and drag build-up were used to run the simulation, providing an estimate for C_{Dp}, the mass properties, and inertia for the aircraft.

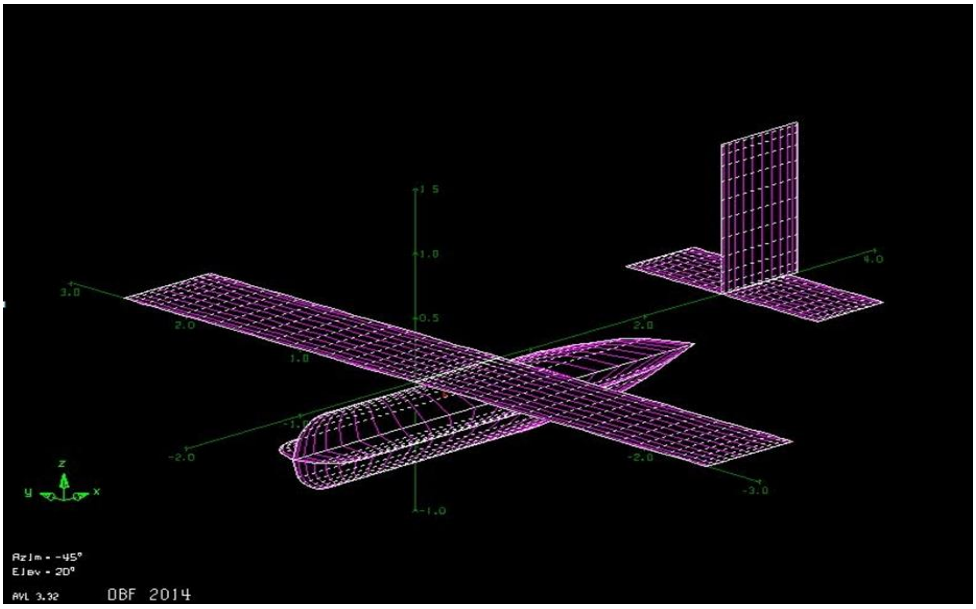

Figure 4.10: AVL Geometry Input

AVL takes the input geometry and uses an extended vortex lattice method to calculate the aerodynamic performance has well as the stability and control derivatives for the unaugmented aircraft. Figure 4.15 shows the resulting pole-zero map of the eigenvalues calculated by the program.

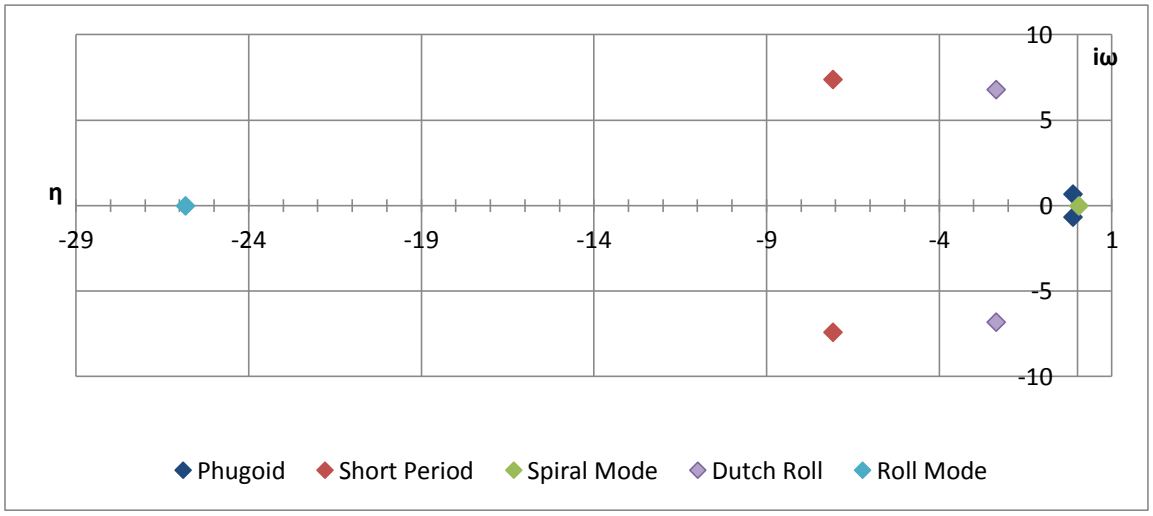

Figure 4.11: Pole-Zero Diagram

All modes achieve level 1 criteria for a class I plane per MIL-SPEC 8785C [5] with two exceptions. The only unstable mode was a slight spiral divergence. But with a time-to-double of 14.3 seconds, it satisfies level one handling qualities. In addition, the Control Anticipation Parameter satisfies level two handling qualities criteria, having an n/α of 8.25 g's/rad with a a short period natural frequency of 7.4 rad/sec. As discussed by Cook [6], level two handling qualities are stated as, 'Flying qualities adequate to accomplish the mission flight phase, but with an increase in pilot workload,' thus not requiring augmentation for mission performance. Upon conducting further research, it was found that the

recommendations in MIL-SPEC 8785C are applicable to small-scale UAVs as discussed by Tyler Foster of Brigham Young University [XII].

4.5 Predicted Mission Performance

An output from the mission model was the time and energy consumption for each mission. As seen from the predicted mission performances in Tables 4.6 to 4.8, the aircraft uses at most 70% of the available energy leaving 30% of the energy as a factor of safety.

	M1	Time (s)	Energy (KJ)
1st Lap	Takeoff	.9	.46
	Liftoff	1.3	.66
	Climb	5.7	2.76
	Cruise 1	8.8	4.15
	1st 180 turn	11.7	5.35
	Cruise 2	17.8	7.81
	360 turn	23.6	10.0
	Cruise 3	30.1	12.5
	2nd 180 turn	32.8	13.5
	Cruise 4	39.3	15.9
2nd through 7th Lap	…		
	1st 180 turn (Lap 7)	239.7	79.7
Landing	End of mission	251.7	83.4

Table 4.6: Mission 1 Predictions

	M2	Time track (s)	Energy (KJ)
1st Lap	Takeoff	2.0	.98
	Liftoff	2.9	1.41
	Climb	6.9	3.14
	Cruise 1	10.4	4.54
	1st 180 turn	13.2	5.53
	Cruise 2	19.5	7.71
	360 turn	25.	9.54
	Cruise 3	31.7	11.7
	2nd 180 turn	34.4	12.6
	Cruise 4	41.9	14.3
2nd and 3rd Lap	…		
	Cruise 4 (lap 3)	118.8	34.9
Landing	End of mission	140.2	38.8

Table 4.7: Mission 2 Predictions

	M3	Time track (s)	Energy (KJ)
1st Lap	Takeoff	2.0	.98
	Liftoff	2.8	1.36
	Climb	6.9	3.14
	Cruise 1	10.3	4.51
	1st 180 turn	13.1	5.49
	Cruise 2	19.4	7.71
	360 turn	25.0	9.51
	Cruise 3	31.7	11.7
	2nd 180 turn	34.4	12.5
	Cruise 4	41.2	14.7
2nd and 3rd Lap	…		
	Cruise 4 (lap 3)	118	36.7
Landing	End of Mission	139.2	40.1

Table 4.8: Mission 3 Predictions

5.0 Detail Design

Following the optimization process and mission profile predictions, the aircraft dimensions were finalized. The prototype of the final design was then built and tested to confirm the mission profile predictions.

5.1 Dimensional Parameters

Table 5.1 details the dimensions, propulsion system and electronics of the final design.

Wing	
Span	61"
Chord	9"
Aspect Ratio	6.78
Wing Area	549 in^2
Airfoil	BA9
Static Margin	31.3%
Aileron	
Span	27"
Chord	2.25"
Deflection	±15°
Fuselage	
Length	34”
Width	7”

Horizontal Stabilizer	
Airfoil	SD8020
Span	21.5”
Chord	7”
Area	150.5 in^2
Incidence	0
Elevator	
Span	21.5”
Chord	2.1”
Deflection	±15°

Motor	
Type	Neu 1107-6D
Kv	1900 rpm/v

Vertical Stabilizer	
Airfoil	SD8020
Span	14”
Chord	8“

Rudder	
Span	14”
Chord	4.4”
Deflection	±20°

Batteries	
Type	Elite1500
Capacity	1500 mAh

Height	9”

Electrical System	
Speed Controller	Castle Creations HV 30
Radio Receiver	Futaba R617FS
Number of Servos	4
Servo Type	HS-65 MG

Gear Box	Maxon 4.4:1
RPM_{max}	60,000
Io	0.45 A
R_m	0.058 Ω
P_m	300 watt
Propellers	11x10, 12x8, 13x6.5

R	0.014 Ω
V	1.2 V
Imax	30 A
Number of Cells	20
Pack Energy	129.6 KJ
R_{pack}	.28 Ω
V_{pack}	24 V

Table 5.1: Dimensional Parameters

5.2 Structural Characteristics and Capabilities

As the sensitivity analysis revealed, weight was the most important parameter, so making the aircraft as light as possible was the biggest focus of the overall design. Before a formal detailed design could be finalized, an analysis of the aircraft loads along the wing and fuselage was made in both flight and landing scenarios. Figure 5.1 shows the shear and moment diagram for the maximum aircraft weight.

The fuselage structure consists of a central boom surrounded by a nonstructural fuselage fairing. All loads during takeoff and landing would be transmitted from the landing gear through the fuselage to the boom. This particular setup creates a lightweight landing gear with built-in suspension. Coupled with the lightweight wing and tails, all the major components combined to make the design a true lightweight aircraft that could effectively compete for the highest score.

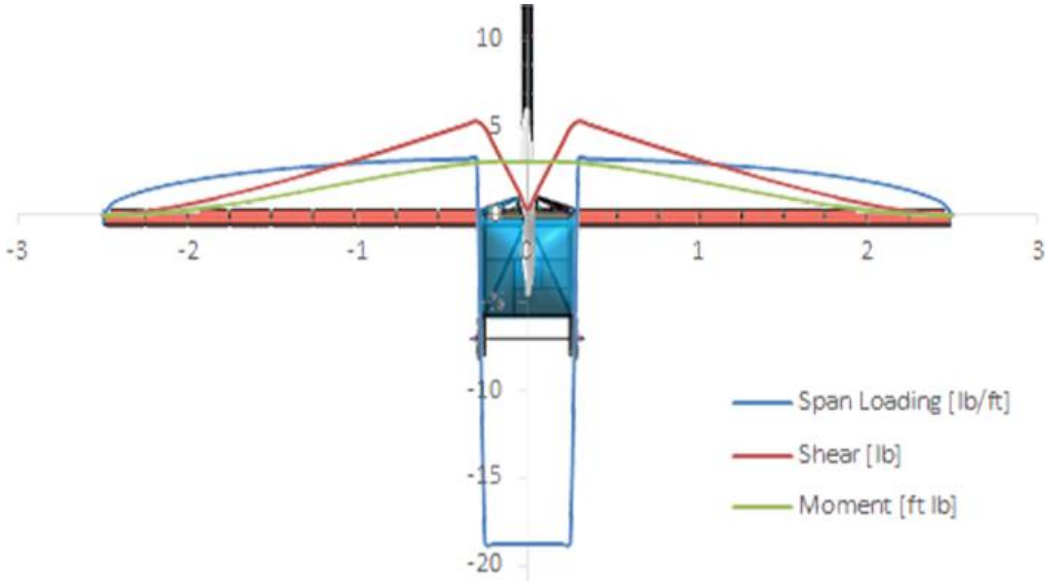

Figure 5.1: Shear Moment Diagram

5.3 System Design and Component Selection/Integration

The following subsystem components were analyzed with more detail to finalize the aircraft design.

5.3.1 Wing

The wing was designed to minimize weight while being able to take all the aerodynamic loads. A balsa built-up wing, consisting of balsa ribs, sheeting, and spar with an iron-on covering, was used due to the weight savings this wing configuration provides.

The wings are attached through a solid balsa block and the airfoil shape is maintained by ribs and sheeting. Lightening holes are cut out of the ribs and wooden caps that join the ribs are reinforced with unidirectional carbon fiber at certain locations. The caps of the balsa wing are of various thicknesses in order to withstand the loads during flight. Balsa sheeting covers the leading edge to maintain the airfoil shape and provide torsional strength.

The tails were built similar to the main wings. The tail is also designed and manufactured with laser cut balsa ribs but differs from the wing in that it is supported by 2 carbon rods that act as spars. In order to save the most weight while maintaining the airfoil shape, balsa stringers were embedded around the balsa ribs and sanded to shape. So-Lite is then used to cover the tail structure.

5.3.2 Motor Mount

A carbon fiber-reinforced epoxy mount was created with several layers of carbon fiber. The motor mount, as shown in Figure 5.2, was attached to the boom through a carbon fiber reinforced opening in the motor mount. The motor is screwed onto the front of the motor mount and uses a back support that absorbs vibration.

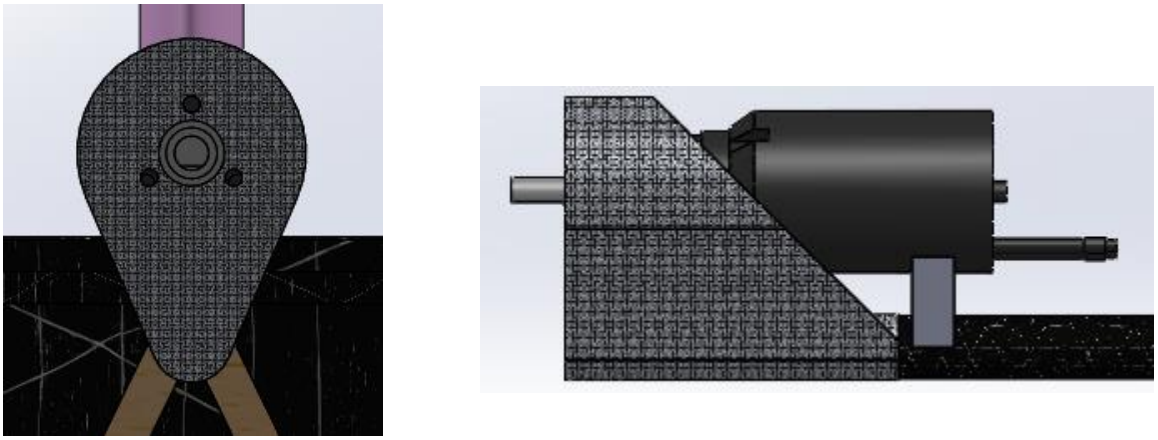

Figure 5.2 Motor Mount

5.3.3 Structural Boom

The central carbon boom acts as the main structural member connecting the entire aircraft together. The motor, battery, wings, fuselage, and tails are all connected to this boom. The team has

previous experience utilizing this type of structural member, and the weight advantages over a load bearing fuselage skin justify the use of the boom.

5.3.4 Control Surfaces

The control surfaces, which include the ailerons, elevators, and rudders, were sized according to the need for adequate ground and air maneuverability. For the taxi mission, without the use of a steerable gear, the rudder had to provide adequate directional control while on the ground, and the elevator had to keep the aircraft from nosing over while taxiing over rough terrain. The full span ailerons provided the necessary safety margin for operating the aircraft under heavy crosswind situation both in the air and on the ground.

5.3.5 Payload

The payload arrangements were chosen to minimize the frontal area and to satisfy the rules. The payload arrangement for mission 2 and 3 is shown in Figure 5.3.

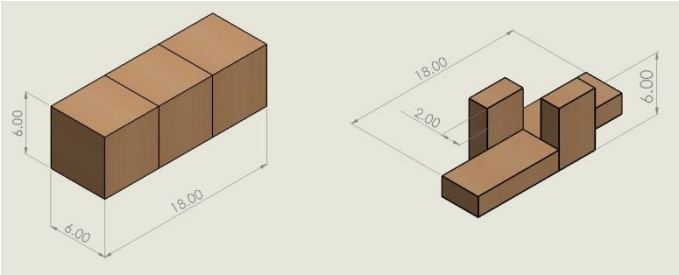

Figure 5.3: Payload Configurations
Mission 2 (left) Mission 3 (Right)

Using these arrangements, the payload structure is roughly 18-in. in length, 6-in. in height and 6-in. in width. The fuselage, shown in Figure 5.4, is composed of a floor and two triangular structures that attach the floor to the boom. The floor is made of a rectangular structure with members going across the rectangle, forming a bed on which the payload can be secured on. The cross members are spaced so that a payload is supported by least two members for stability.

Figure 5.4: Fuselage Design

The rectangular floor and the triangles restrain the motion of the payload horizontally and longitudinally respectively. Spacers placed between the blocks the attendant will prevent them from moving vertically and the patient is held down with ties.

The dimensions of the floor, taking into account the maximum material condition of the payloads, are 18.375” in length and 6.25” in width. The distance between the floor and the spar is 6.5” The extra clearance at the top is necessary for the spacers and it also facilitates the payload loading and unloading. During flights, the load is transferred from the floor to the boom via the triangular structure. Accelerations up to 5G are expected during turns. The shear force/bending moment diagram is shown in Figure 5.5 for mission 2, during which the load will be the highest.

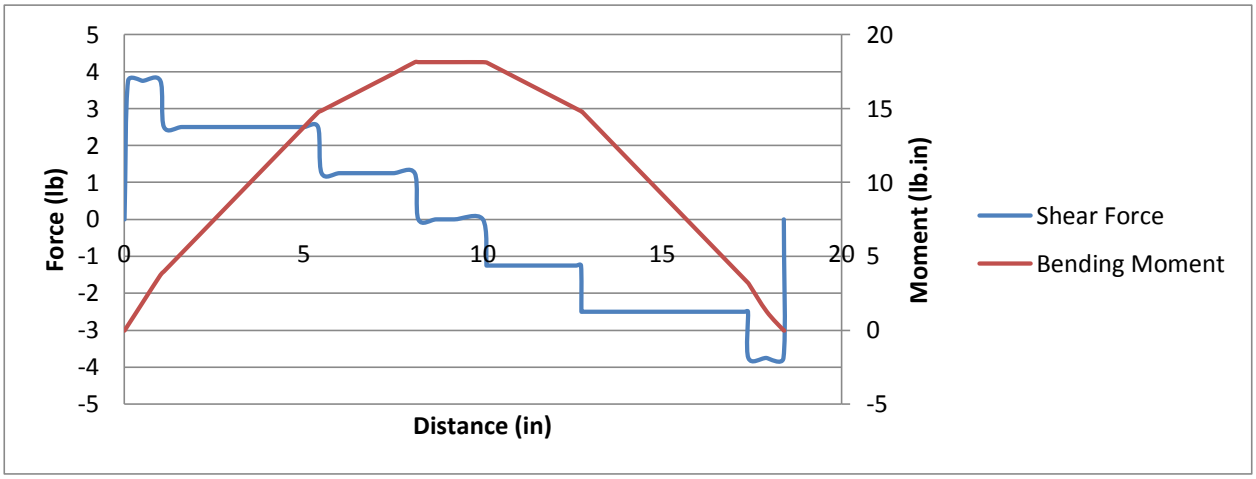

Figure 5.5: Fuselage Shear Moment Diagram

5.3.6 Landing Gear

Two different designs of the main gear were considered: a rigid U-shaped landing gear, and a shock-absorbing integrated landing gear. The U-shaped landing gear suffered from heavier weight and poor landing performance due to its rigidity. On the other hand, the second design resulted in a lighter weight because it was integrated to the fuselage. Moreover, this landing gear is able to elastically deform, absorbing some of the landing loads. A continuous axle prevents the landing gear from detaching due to possible cross wind landing impact. To aid with ground taxi on rough terrain, skids, shown in Figure 5.6, were placed behind the wheels of the landing gear extending back toward the rear of the fuselage. These skids allow the aircraft to glide over the corrugated roof spacing during the taxi mission.

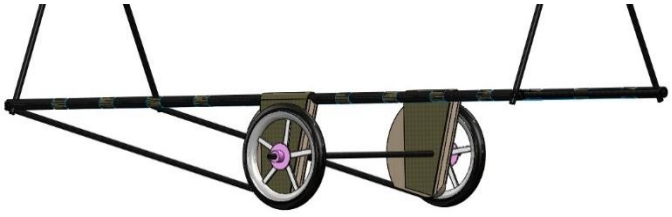

Figure 5.6: Skid Attachment

5.3.7 Fuselage Fairing

The fuselage fairing was made non-structural to minimize weight. The cross section and shape constraint for the payload-carrying section of the fuselage was set by the intended cargo to be carried. The front and rear of the fuselage were gradually tapered for aerodynamic reasons. The top of the fuselage, which encloses the battery, is open at the front and rear for cooling and contains access doors to the inside of the fuselage.

5.3.8 Tail Boom

A tail-sizing model varied the tail boom length and sized the tails using a prescribed tail volume. The variation between boom length and component weight is shown in Figure 5.7. A minimum weight occurred with a tail arm of just under 3-ft.

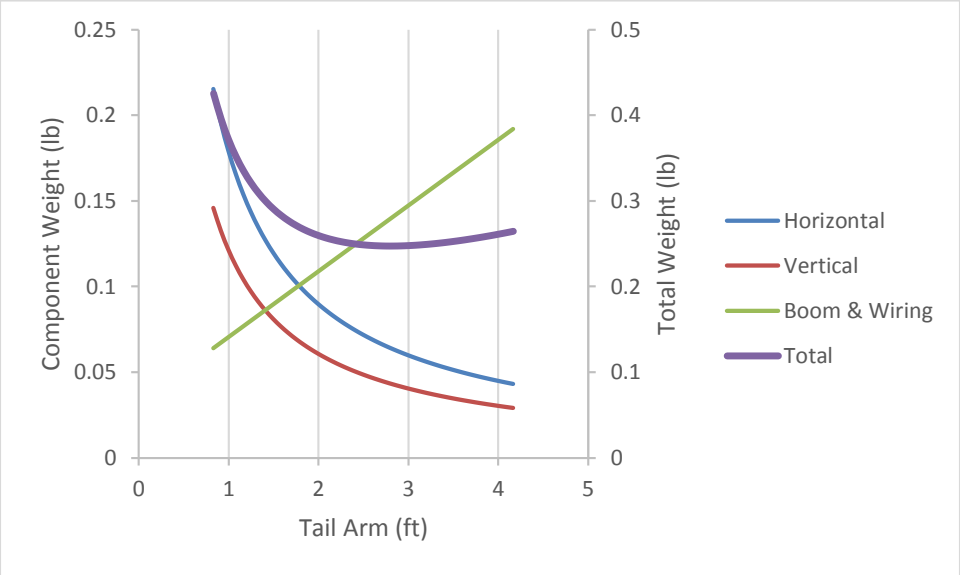

Figure 5.7: Component Weights for Tail

5.3.9 Electronics

Servo Selection

The most important factor when selecting a servo is sufficient torque during flight. They were selected by analyzing hinge-moments for each control surface using AVL and then finding servos that had sufficient control power to handle the calculated moments, with the lightest weight possible. Five Hitec servos were considered: HS-225BB, HS-311, HS-85 MG (Metal Gear), HS-65 MG and HS-81 MG. These were compared according to their stall torque, weight and dimensions, all shown in Table 5.2.

Servo	Stall Torque 4.8v (in-oz)	Stall Torque 6v (in-oz)	Weight (oz)	Dimensions (in)
HS-225BB	54.15	66.65	0.95	1.27" x 0.66"x 1.22"
HS-311	42	48.6	1.51	1.57" x 0.78" x 1.43"
HS-85 MG	41.66	48.6	0.77	1.14" x 0.51" x 1.18"
HS-81 MG	36.1	41.66	0.62	1.17" x 0.47" x 1.16"
HS-65 MG	24.99	30.55	0.42	0.92" x 0.45" x 0.94"

Table 5.2: List of Servo Considered

All of the servos considered had sufficient torque to move the parts; however, since weight and size were important factors to servo selection, the HS-311 and HS-85 MG were deemed too heavy. While the HS-81 provided more than ample torque, the HS-65 was chosen because it provided the required torque in the smallest volume and lightest assembly.

Speed Controller Selection

The competition regulations limit the motor current with a 15A slow blow fuse. Utilizing an amperage factor of safety of 2, the minimum amperage of the speed controller (ESC) must be 30A. In addition, the high pack voltage (24V) necessitated that an ESC rated for high voltage be used.

ESC	Max (amps)	Max (volts)	Dimensions (in)	Weight (oz)
Phoenix HV 30	30	50	1.08 x 0.91 x 0.16	1.5
Phoenix Ice HV 40	40	50	1.8 x 1.7 x 0.8	2.2
Phoenix Ice Lite 50	50	25	1.6 x 1.00 x 0.67	1.7
Phoenix Ice 50	50	34	1.8 x 1.7 x 0.8	2.3

Table 5.3: List of Speed Controllers Considered

The speed controller chosen from the selection in Table 5.3 was the Castle Creations Phoenix HV30. This was the lightest ESC capable of withstanding the high voltage battery being used.

Electronics Integration

All electronics except for the wing and tail servos were attached on the back of the spar or on the structural boom within the fuselage. A 400mAh receiver battery is used. An external switch was used to easily turn on/off the receiver to conserve energy while waiting in the flight line without opening up the aircraft. The fuse was mounted on the exposed boom in between the motor and the main battery pack.

5.4 Weight and Balance

Aircraft weight without payload was estimated to be 3.15-lb. The maximum empty weight was 3.2-lb due to the inclusion of payload restraints for mission 3. All measurements were made from the nose of the aircraft. Components were placed so the CG would fall between 25 and 28%, ensuring stability. Tables 5.4 to 5.6 tabulate the aircraft weight at each mission.

Component		Arm (in.)	Weight (oz)	Moment (oz-in)
Structure	Boom	26.0	2.22	57.72
	Vertical Stabilizer	52.0	1.5	78
	Motor Mount	2.25	0.5	1.125
	Horizontal Stabilizer	52.0	2	104
	Fuselage	23.0	5.1	117.3
	Wing	21.0	6.25	131.25
Propulsion	Speed Controller	7.0	1.04	7.28
	Battery	18.0	16.49	296.82
	Motor/Gearbox /Metal Propeller Spinner	3.5	5.74	20.09
	Propeller	0.5	1.12	0.56
	Fuse/Holder	10.0	0.65	6.5
Avionics	Receiver Battery	10.0	3.16	31.6
	Receiver	22.0	0.34	7.48
	Receiver Switch	25.0	0.1	2.5
	Rudder Servo	52.0	0.7	36.4
	Elevator Servos	52.0	0.7	36.4
	Ailerons Servo	23.0	1.4	32.2
Landing Gear	Skids	21.0	0.22	4.62
	Main Gear	19.0	1.2	22.8
Total	Aircraft	--	50.43	994.645
	Center of Gravity (in)		**19.72**	
	Center of Gravity (% chord)		**24.67**	

Table 5.4: Mission 1 Weight and Balance

	Component	Arm (in.)	Weight (oz)	Moment (oz-in)
Aircraft	Aircraft Without Battery	20.56	33.94	697.825
	Battery	19.5	16.49	321.56
Payload	3 Cargo Blocks	19.5	48.0	936.0
	Payload Restraints	19.5	0.2	3.9
Total	Aircraft	--	98.63	2019.34
	Center of Gravity (in.)		**19.87**	
	Center of Gravity (% chord)		**26.33**	

Table 5.5: Mission 2 Weight and Balance

	Component	Arm (in.)	Weight (oz)	Moment (oz-in)
Aircraft	Aircraft Without Battery	20.56	33.94	697.825
	Battery	19.5	16.49	321.56
Payload	Attendants and Patients	19.5	32.0	624
	Payload Restraints	19.5	0.9	17.55
Total	Aircraft	--	83.33	1660.935
	Center of Gravity (in.)	**19.93**		
	Center of Gravity (% chord)	**27.0**		

Table 5.6: Mission 3 Weight and Balance

5.5 Flight Performance Parameters

Table 5.7 details the flight performance parameters for the three flight missions that were predicted by the mission model. These predictions were later compared to actual parameters obtained at the test flights.

$C_{L,max}$	e	L/D max	Available Energy (kJ)	Empty Weight (lbs)
1.36	0.89	7.6	130	3.15

	M1	M2	M3
Cl_{cruise}	0.28	0.3	0.4
C_{D_o}	0.0719	0.0712	0.0715
L/D_cruise	3.63	3.9	4.98
W/S (oz/ft^2)	13.2	25.9	21.8
V_cruise (ft/s)	80	72	74
V_stall (ft/s)	23.2	32.4	29.8
TO dist. (ft)	14	38	32
T/W (static)	1.13	.76	.82
Flight time (s)	251.7	140.2	139.2
Max G loading	5.87	3	3.55
V_max (ft/s)	80.5	95.5	77.5
Turn rate (deg/s)	64.3	68.3	66.7
Energy required (kJ)	83.4	38.8	40.1
TOGW (lbs)	3.15	6.16	5.20
Cruise Current (amps)	15.0	11.8	13.3

Table 5.7: Flight Performance Parameter

5.6 Predicted Mission Performance

Aircraft parameters and mission outcomes from the mission model were used to predict the final competition score.

Taxi Mission		Mission 1		Mission 2		Mission 3	
Score	1	Laps flown	6	Blocks carried	3	Team time (s)	118
		Estimated max	9	Estimated max.	5	Estimated best (s)	100
		Empty Weight (lb)	3.15	Empty Weight (lb)	3.16	Empty Weight (lb)	3.20
		RAC	**3.2**	**Flight Score Total**	**2.11**		

Table 5.8: Predicted Mission Performance

Ground Taxi Mission – Rough Field Taxi

The ground handling ability of the aircraft will be tested, and the skids are expected to enable the aircraft to "skip" over the bumps of the roofing panels, leading to completion of the mission within the maximum allotted time of 5 minutes.

Flight Mission 1 – Ferry Flight

The main focus of this mission is to perform as many laps as possible within four minutes after taking off from a 40-ft. runway. The entire mission is flown at maximum speed. The aircraft is expected to complete 6 laps with a 30% safety margin on battery energy. The code will be further adjusted to reflect flight test data concerning propulsion system performance and components.

Flight Mission 2 – Maximum Load Mission

Three cargo blocks will be carried for a 3-lap flight. The flight is made at the aircraft's speed for maximum range to conserve energy as the mission is not time critical. At the same time, the number of cargo blocks carried results in a takeoff weight of 6.16-lb. Having enough energy for the takeoff and the duration of the mission is critical.

Flight Mission 3 – Emergency Medical Mission

Energy consumption in this mission is high as the mission is time critical, but the expected duration is much less than that of Flight Mission 1. The flight is predicted to take 117.8 seconds.

5.7 CAD Package

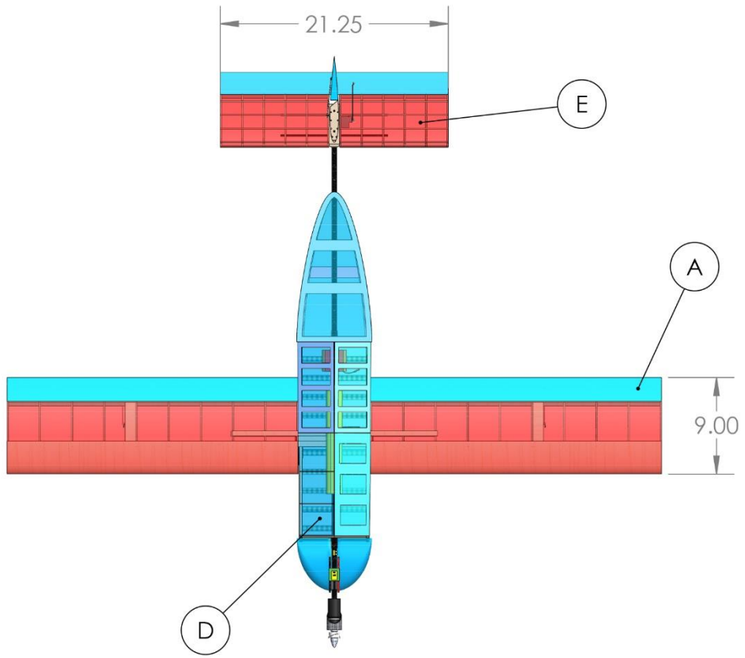

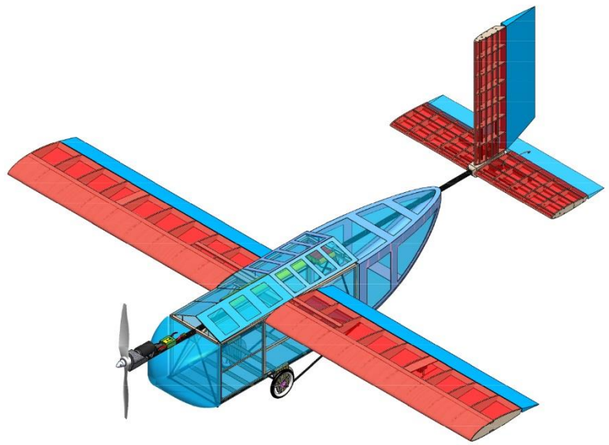

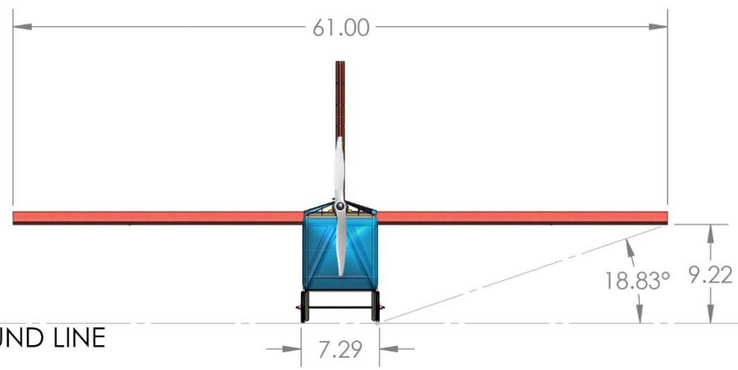

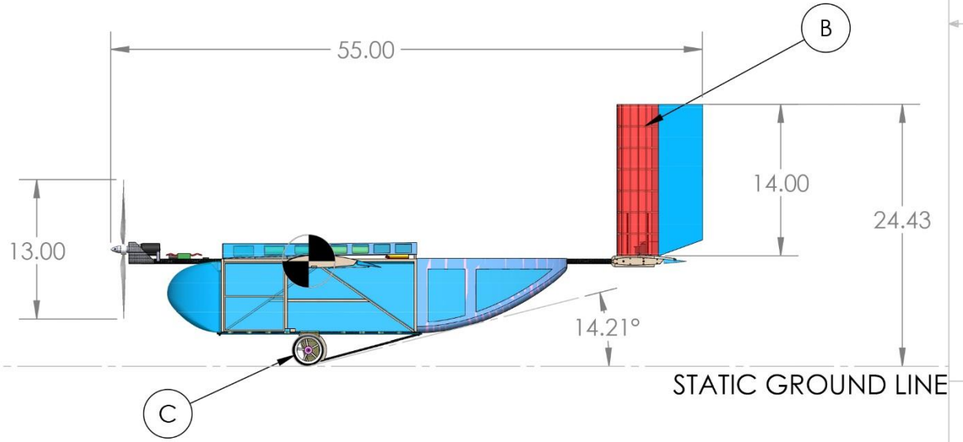

PRIMARY COMPONENTS	
A	WING ASSEMBLY
B	VERTICAL STABILIZER
C	LANDING GEAR
D	FUSELAGE
E	HORIZONTAL STABILIZER

NOTE:
DIMENSIONS ARE IN INCHES
TOLERANCES:
ANGULAR: ± .5°
ONE PLACE DECIMAL ± .100
TWO PLACE DECIMAL ± .030
THREE PLACE DECIMAL ± .005

	NAME	DATE
DRAWN BY:	A. SNYDER	2014-02-20
CHECKED BY:	H. BANH	2014-02-21
CHIEF ENGINEER:	P. PARCELL	2014-02-21

UNIVERSITY OF CALIFORNIA, IRVINE

CESSNA - RAYTHEON - DESIGN BUILD FLY 2013-2014

DOCUMENT TITLE: 3 VIEW

SIZE	APPROVAL DATE:	REPORT TITLE:	REV
B	2014-02-21	DRAWING PACKAGE	NC

SCALE: 1: 13 PAGE 1 OF 5

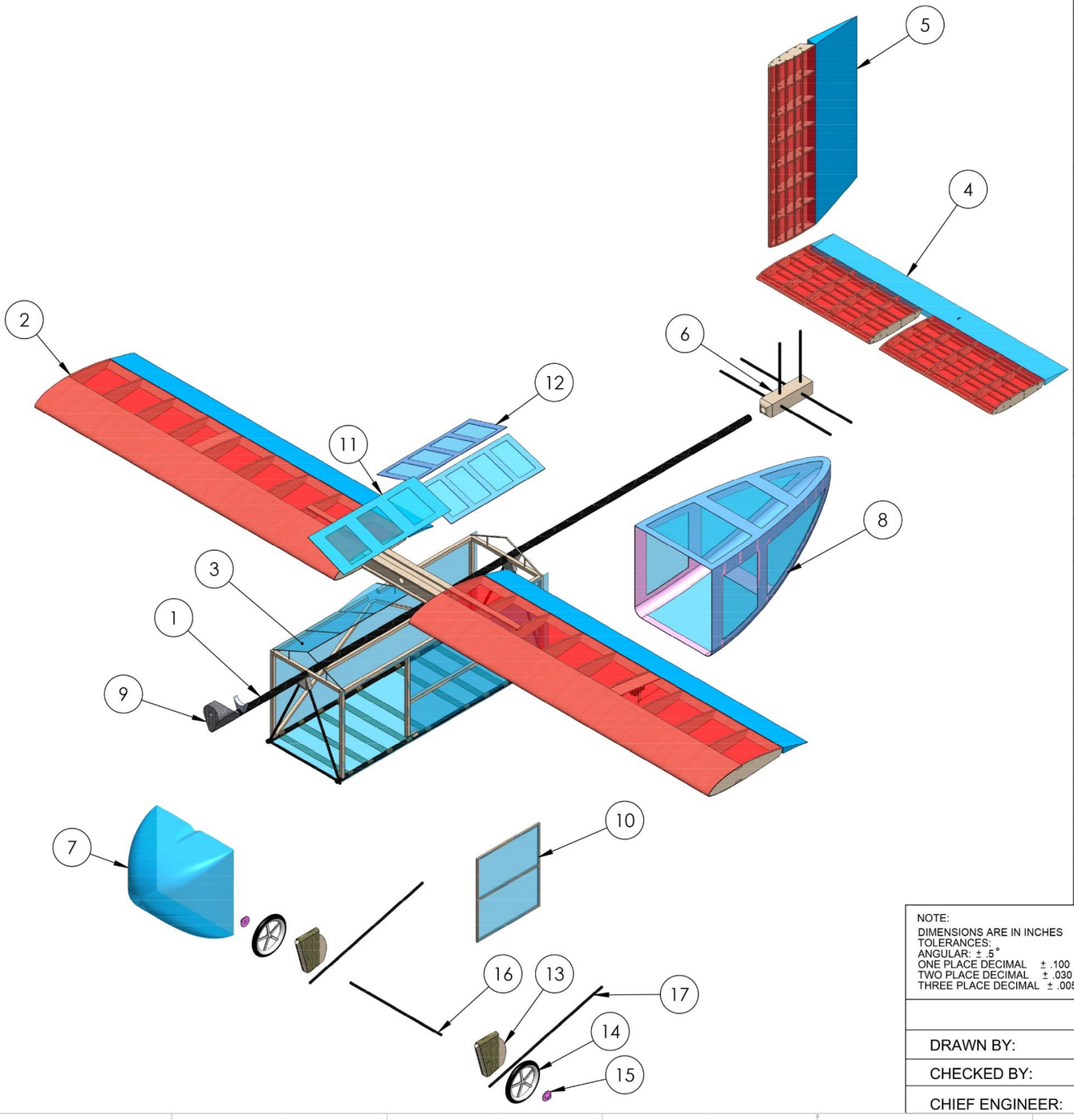

ITEM	NAME	MATERIAL	QTY.
1	BOOM	CARBON FIBER	1
2	MAIN WING ASSEMBLY	BALSA - MONOKOTE - FOAM	1
3	FUSELAGE	BALSA - CARBON FIBER - KEVLAR - MICROLITE	1
4	HORIZONTAL TAIL	BALSA - MONOKOTE - FOAM	1
5	VERTICAL TAIL	BALSA - MONOKOTE - FOAM	1
6	TAIL SUPPORT	BALSA - CARBON FIBER	1
7	FRONG FAIRING	FIBERGLASS	1
8	BACK FAIRING	FOAM - MICROLITE	1
9	MOTOR MOUNT	CARBON FIBER - ABS PLASTIC	1
10	SIDE DOOR	BALSA - MICROLITE	1
11	FRONT DOOR	FOAM - MICROLITE	1
12	BACK DOORS	FOAM - MICROLITE	2
13	LANDING GEAR STRUT	BALSA - KEVLAR	2
14	LANDING GEAR WHEEL	PLASTIC - RUBBER	2
15	LANDING GEAR WHEEL WASHER	PLASTIC	2
16	LANDING GEAR AXLE	CARBON FIBER	1
17	LANDING GEAR SKIDS	CARBON FIBER	2

NOTE:
DIMENSIONS ARE IN INCHES
TOLERANCES:
ANGULAR: ± .5°
ONE PLACE DECIMAL ± .100
TWO PLACE DECIMAL ± .030
THREE PLACE DECIMAL ± .005

UNIVERSITY OF CALIFORNIA, IRVINE

CESSNA - RAYTHEON - DESIGN BUILD FLY 2013-2014

DOCUMENT TITLE:
STRUCTURAL ARRANGEMENT

	NAME	DATE
DRAWN BY:	H. BANH	2014-02-20
CHECKED BY:	B. VU	2014-02-21
CHIEF ENGINEER:	P. PARCELL	2014-02-21

SIZE B | APPROVAL DATE: 2014-02-21 | REPORT TITLE: DRAWING PACKAGE | REV NC

SCALE: 1: 7 | PAGE 2 OF 5

NOTE: WING SPAR, TOP DOOR, AND BOTTOM DOORS OMITTED FOR CLARITY

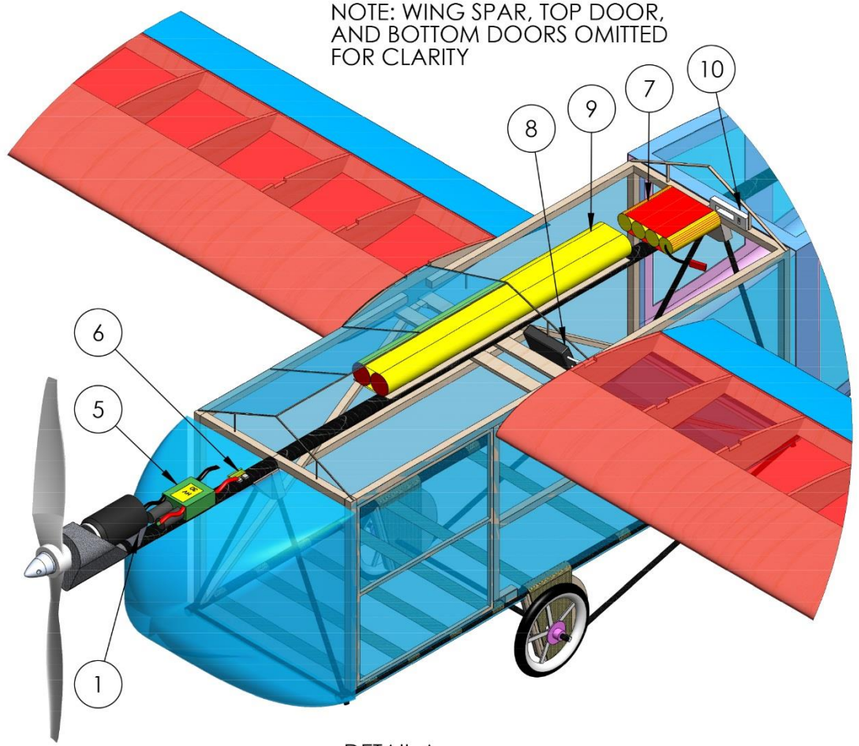

DETAIL A
SCALE 1 : 4

NOTE: WING SKIN OMITTED FOR CLARITY

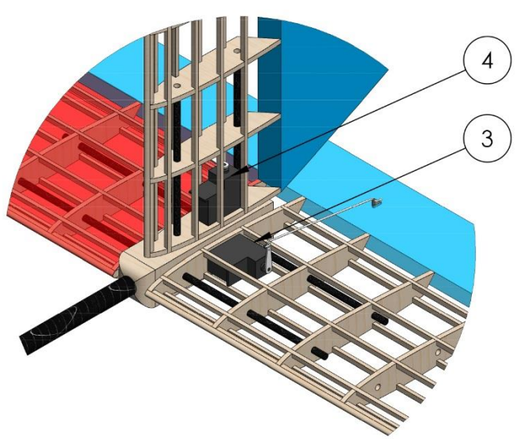

DETAIL B
SCALE 1 : 3

NOTE: WING SKIN OMITTED FOR CLARITY

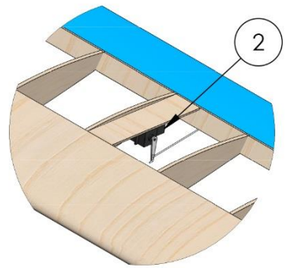

DETAIL C
SCALE 1 : 4

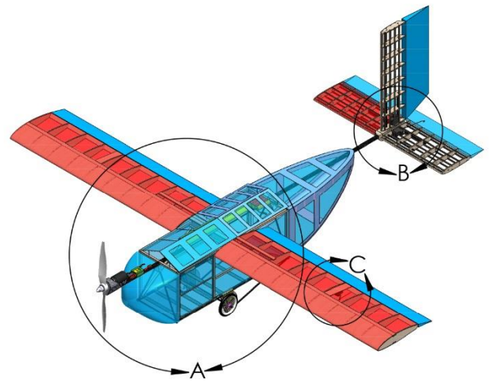

ITEM	NAME	MANUFACTURER	MODEL
1	MOTOR	NEUTRONICS	1107-6D
2	AILERON SERVO	HITEC	HS-65MG
3	ELEVATOR SERVO	HITEC	HS-65MG
4	RUDDER SERVO	HITEC	HS-65MG
5	SPEED CONTROLLER	CASTLE CREATIONS	PHOENIX HV-30
6	FUSE	ALTRONIX	BF15
7	RECEIVER BATTERY	FUTABA	NR4J
8	RECEIVER	FUTABA	R617FS
9	BATTERY	ELITE POWER PRODUCTS	ELITE 1500
10	SWITCH	AIRTRONICS	96334

NOTE:
DIMENSIONS ARE IN INCHES
TOLERANCES:
ANGULAR: ± .5°
ONE PLACE DECIMAL ± .100
TWO PLACE DECIMAL ± .030
THREE PLACE DECIMAL ± .005

UNIVERSITY OF CALIFORNIA, IRVINE

CESSNA - RAYTHEON - DESIGN BUILD FLY 2013-2014

DOCUMENT TITLE: SYSTEMS LAYOUT/LOCATION

	NAME	DATE
DRAWN BY:	A. MAGTOTO	2014-02-20
CHECKED BY:	H. BANH	2014-02-21
CHIEF ENGINEER:	P. PARCELL	2014-02-21

SIZE B | APPROVAL DATE: 2014-02-21 | REPORT TITLE: DRAWING PACKAGE | REV NC

SCALE: 1: 16 | PAGE 3 OF 5

NOTE: FUSELAGE STRUCTURE AND
SIDE DOOR OMITTED FOR CLARITY

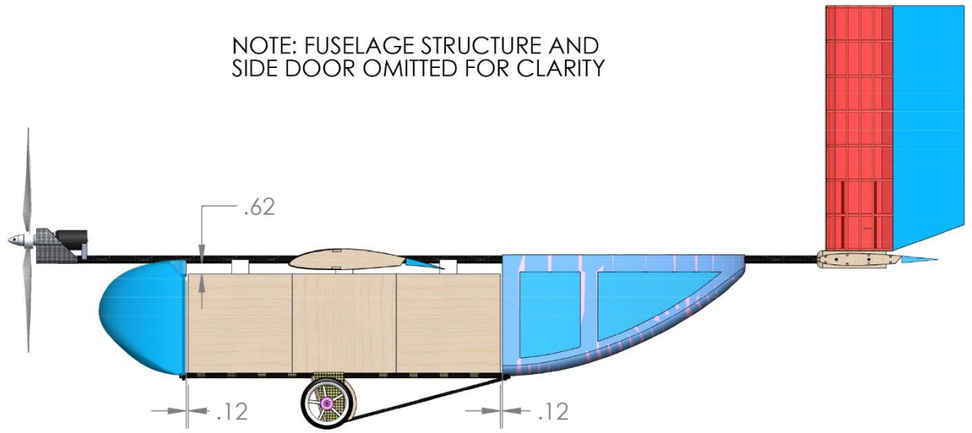

SCALE: 1:8

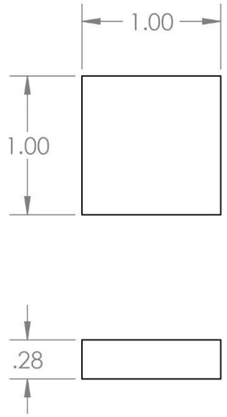

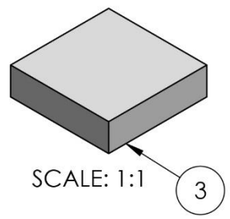

SCALE: 1:1

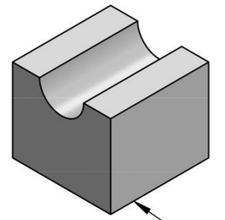

SCALE: 1:1

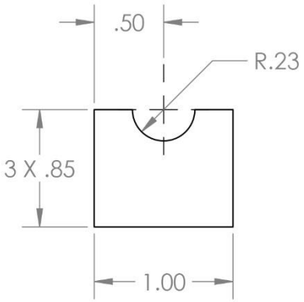

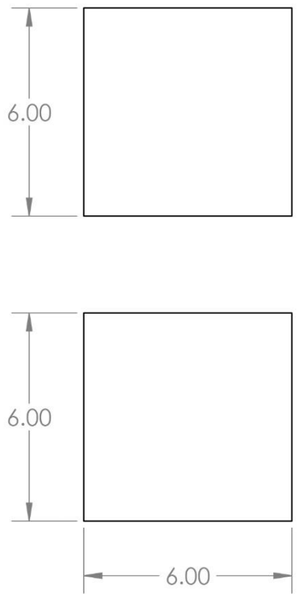

NOTE: PAYLOAD AND FUSELAGE BOTTOM
ISOLATED FOR CLARITY

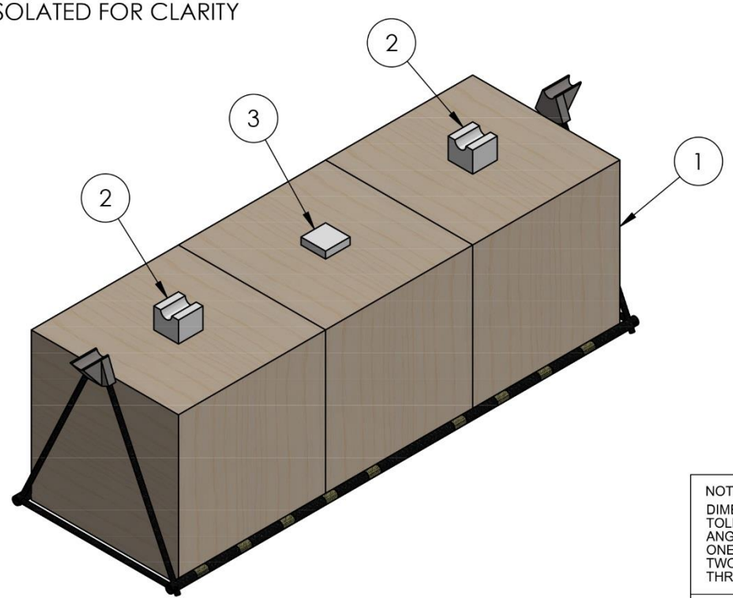

ITEM NO.	NAME	QTY.
1	CARGO	3
2	OUTER CARGO RESTRAINT MECHANISM	2
3	CENTER CARGO RESTRAINT MECHANISM	1

NOTE:
DIMENSIONS ARE IN INCHES
TOLERANCES:
ANGULAR: ± .5°
ONE PLACE DECIMAL ± .100
TWO PLACE DECIMAL ± .030
THREE PLACE DECIMAL ± .005

UNIVERSITY OF CALIFORNIA, IRVINE

CESSNA - RAYTHEON - DESIGN BUILD FLY 2013-2014

DOCUMENT TITLE:
MISSION 2 PAYLOAD ACCOMODATION

	NAME	DATE
DRAWN BY:	H. BANH	2014-02-21
CHECKED BY:	L. NG	2014-02-22
CHIEF ENGINEER:	P. PARCELL	2014-02-22

SIZE B | APPROVAL DATE: 2014-02-22 | REPORT TITLE: DRAWING PACKAGE | REV NC

SCALE: 1: 4 | PAGE 4 OF 5

NOTE: FUSELAGE STRUCTURE AND
SIDE DOOR OMITTED FOR CLARITY

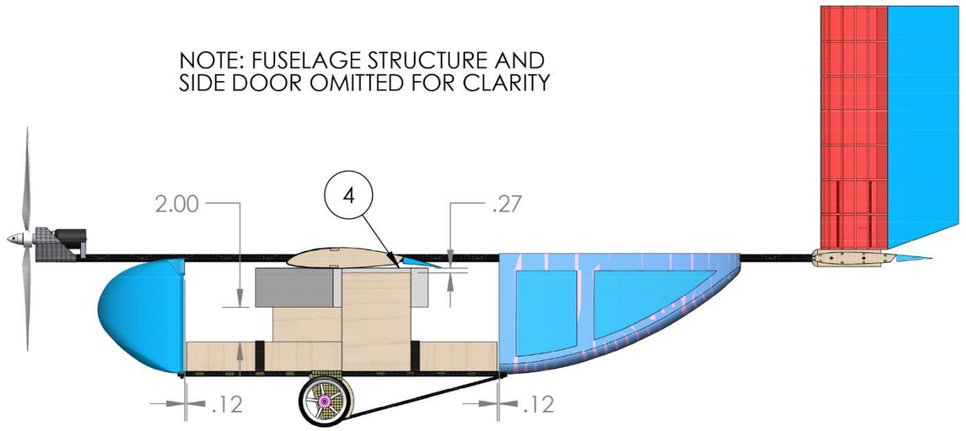

SCALE: 1:8

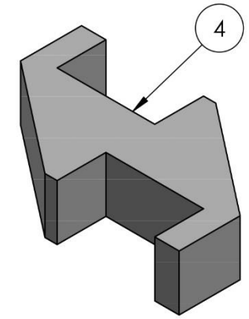

NOTE: PAYLOAD AND FUSELAGE BOTTOM
ISOLATED FOR CLARITY

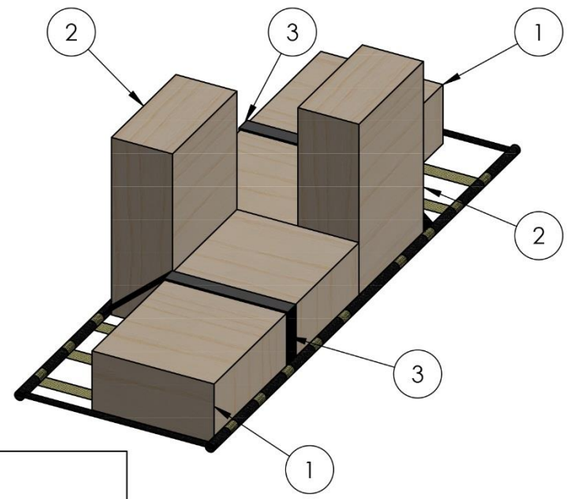

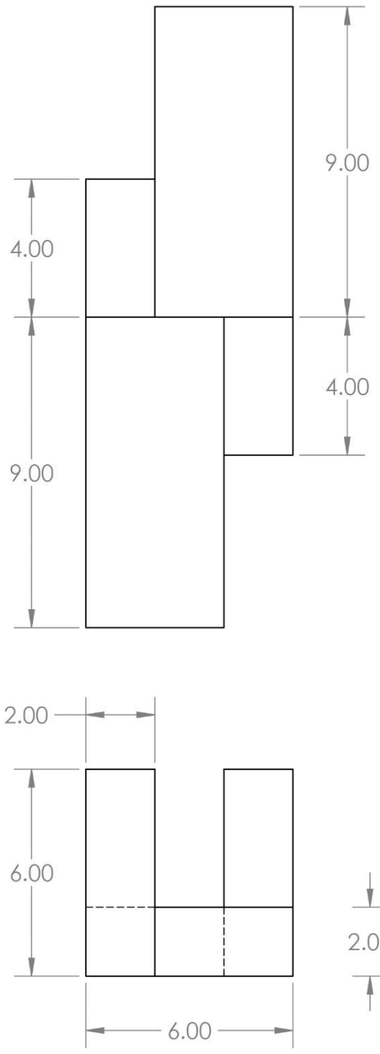

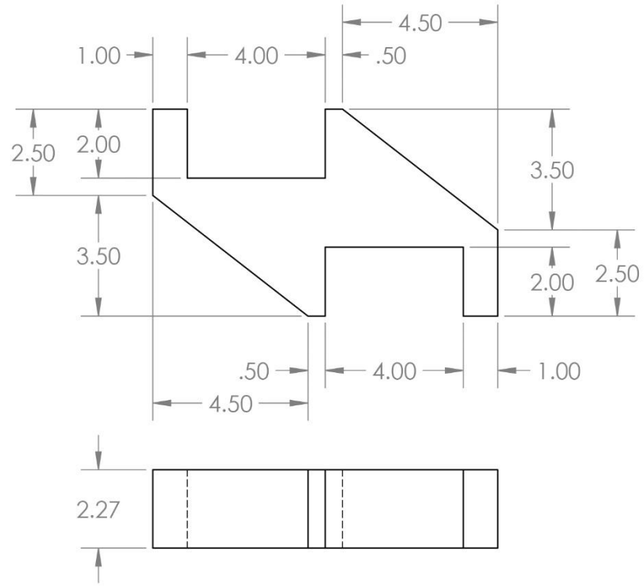

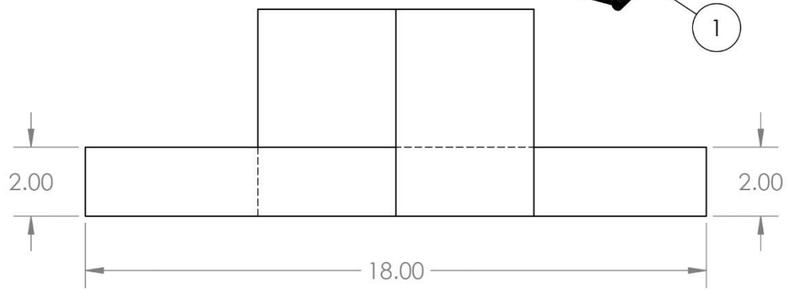

ITEM NO.	NAME	QTY.
1	PATIENT	2
2	ATTENDANT	2
3	PATIENT RESTRAINT MECHANISM	2
4	ATTENDANT RESTRAINT MECHANISM	1

NOTE:
DIMENSIONS ARE IN INCHES
TOLERANCES:
ANGULAR: ± .5°
ONE PLACE DECIMAL ± .100
TWO PLACE DECIMAL ± .030
THREE PLACE DECIMAL ± .005

UNIVERSITY OF CALIFORNIA, IRVINE

CESSNA - RAYTHEON - DESIGN BUILD FLY 2013-2014

DOCUMENT TITLE:
MISSION 3 PAYLOAD ACCOMODATION

	NAME	DATE
DRAWN BY:	H. BANH	2014-02-21
CHECKED BY:	C. SLEDGE	2014-02-22
CHIEF ENGINEER:	P. PARCELL	2014-02-22

SIZE B | APPROVAL DATE: 2014-02-22 | REPORT TITLE: DRAWING PACKAGE | REV NC

SCALE: 1: 4 | PAGE 5 OF 5

6.0 Manufacturing Plan and Processes

Although the aircraft was sized to be as light as possible, multiple manufacturing methods were experimented with to conserve weight. Our manufacturing plan focused on the production of five main components: wings and tails, fuselage fairings, payload accommodation, landing gear, and motor mount.

6.1 Wings and Tails

The wings and tails are large volume components where manufacturing methods have a strong impact on weight reduction. The following methods were considered:

- **Hollowed foam wing:** A hotwire CNC is used to cut out a foam core. The core is vacuum bagged with a composite fabric and hollowed out.
- **Balsa built-up:** Laser cut balsa ribs are assembled using a jig to ensure proper alignment. Sheeting is added on the leading edge to preserve the airfoil shape. The wing skin consist of an iron-on covering. Spar caps are laminated in tapered carbon fiber and connected with a vertical shear web.

The Balsa built up, shown in Figure 6.1, method was chosen due to its lightweight nature. This method can produce structures that are half the weight of that of a hollowed foam wing.

Figure 6.1: Balsa Built up Assembly

6.2 Fairings

The following methods were considered for the manufacturing of the fairings.

- **Female molding** – A foam male plug was hand sanded to a desired shape and then layered with composite material. Tooling gel coat is applied to the plug and becomes the foundation for the female mold. The mold then allows quick manufacturing of identical parts using different lay-up methods. The mold is presenting in Figure 6.2.
- **Foam Sheeting** – Foam sheets of varying thicknesses were cut out using the hotwire CNC machine. These sheets were then cut into the profile shapes of the sides of the fuselage

fairings and assembled together to create a shell representing the fuselage fairing. Weight savings can be made by cutting lightening holes and covering the holes with Microlite™.

Both methods were implemented on the aircraft. The front fairing was made using the female molding methods due to complex geometry, and the rear fairing was made using foam sheeting for weight savings.

Figure 6.2: Front Fairing Female Mold

6.3 Payload

In the original design, the fuselage is integrated to a U-shaped landing gear, which serves as an attachment structure and load transferring member along with the triangles. A newer design uses the triangles as the only load transferring members and attachment structures, which resulted in a 1.38-oz. weight savings.

The length wise member of the payload floor are made with .25-in. carbon tubes. Two holes are drilled at each end, through which 0.15-in. carbon rods are inserted in order to complete the rectangle and to create the triangular structure. In order to obtain consistent angles for the triangular structure, a 3D printed jig was created with guiding holes. The triangular structure, Figure 6.3 (left), is completed at the top with a 3D printed joint that is also used to attach the payload cage to the boom. All joints were reinforced using Kevlar and/or carbon tow. Tensile loads during flights were supported by the carbon/Kevlar tow while compressive landing loads were transferred to the boom by the triangle.

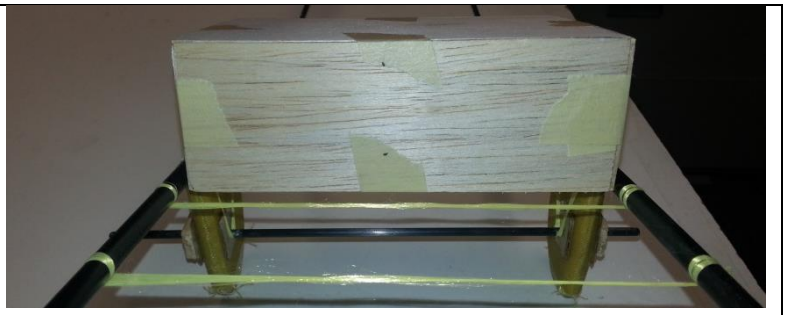

Figure 6.3: Fuselage Compression Structure (left), Payload Bed (right)

Kevlar tow is used for the payload bed because it is lighter than carbon tow and balsa. The tow is wrapped so that it passes underneath the tube, creating a restraint for the payload, (Figure 6.3).

The spacers used for restraining the vertical motion of the blocks and the attendant were made out of EPP foam, which was chosen for its compressibility and load absorption capability during landing. For securing the patient, Velcro ties were chosen over zip ties because of their reusability.

6.4 Landing Gear

- **U Shaped Landing gear** – A balsa core was bent on a mold using ammonia and was reinforced using bidirectional and unidirectional carbon fiber. The initial process and end result is displayed in Figure 6.4.

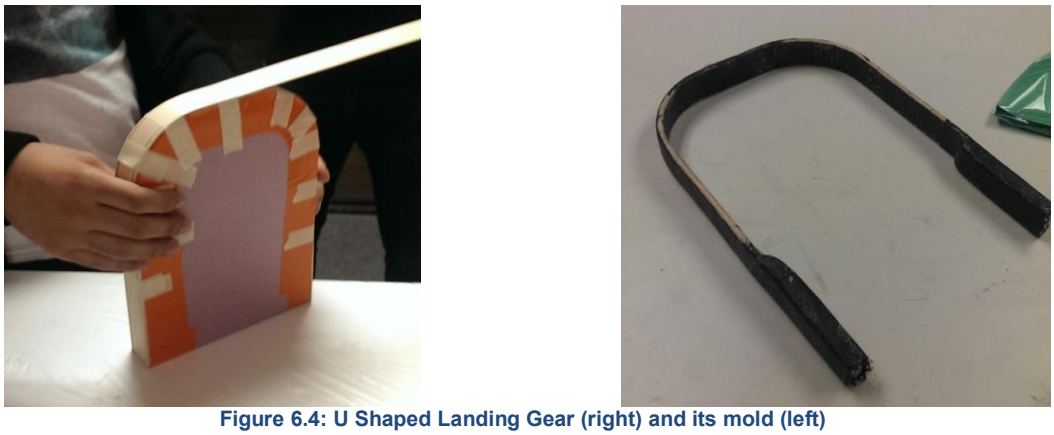

Figure 6.4: U Shaped Landing Gear (right) and its mold (left)

Because the landing gear is integrated in the payload system, different manufacturing methods were used.

- **Landing Gear Struts** –A sheet of balsa was sanded to the desired shape using a template. Slots were sanded into the balsa landing gears to allow integration onto the .25-in. carbon tubes of the payload and landing skids. The landing gear was reinforced by wrapping 45° bidirectional Kevlar around the carbon tubes. The Kevlar was bagged using peel-ply to soak up any excess epoxy.
- **Skids** – Two .15-in. diameter carbon tubes, Figure 6.5, were attached to the bottom of the landing gear struts and secured in place using carbon tow.

Figure 6.5: Landing Gear Skids

6.5 Motor Mount

Three methods of manufacturing a lightweight and durable motor mount, as displayed in Figure 6.6, were considered:

- **Foam male-molding** – A CNC cutout foam was hand sanded to include the tube for the boom. After the foam was wrapped with tape and three layers of wax were placed, three layers of carbon fiber would be soaked in epoxy resin and wrapped around the foam. The motor mount was placed in a vacuum bag and left to harden for 24 hours. This method was the most familiar method of manufacturing motor mounts.
- **3D Printing** – A motor mount is designed on SolidWorks to handle all loads accordingly and 3D printed using ABS plastic.
- **3D Printed female-molding** – A two-piece female mold was 3D printed. After the print, the pieces were sanded to make the inside of the mold smooth. Layers of epoxy-soaked carbon fiber strips were inserted into the mold, as well as a piece of the boom for the opening. The mold was then vacuum-bagged for a day to harden. The pieces are separated after the epoxy sets, revealing the motor mount.

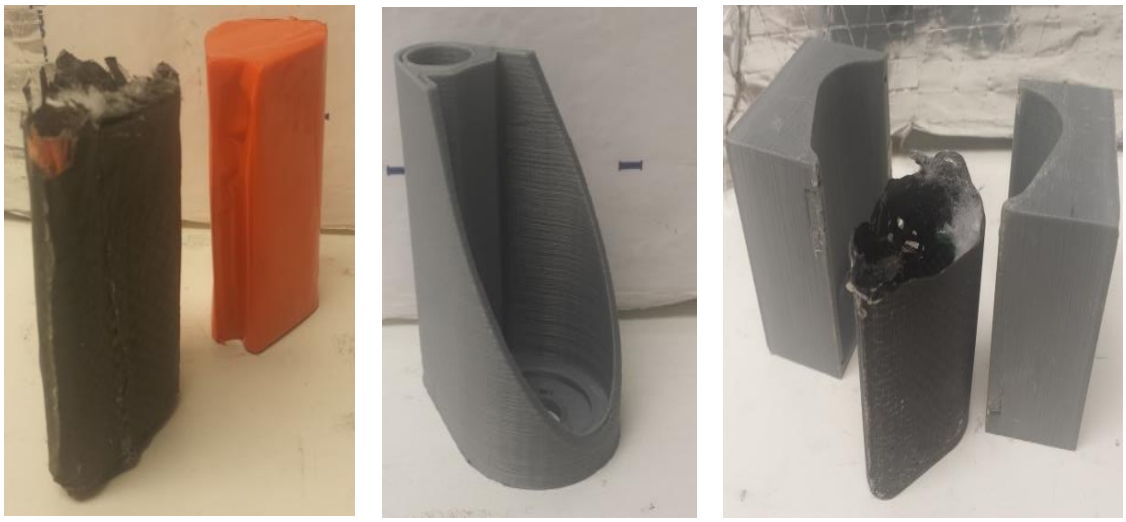

Figure 6.6: Male-molding (left), 3D Printing (center), Female-molding (right)

Although 3D printing simplified manufacturing, the high frequency vibrations from the motor caused delamination, leading to failure from crack propagation. The 3D printed motor mounts also weighed a third more than a male-molded motor mount. Female-molding was attempted, but the manufacturing process was too complex to achieve consistent results. A useable and durable motor mount was consistently manufactured using male-molding techniques.

6.4 **Manufacturing Milestone Chart**

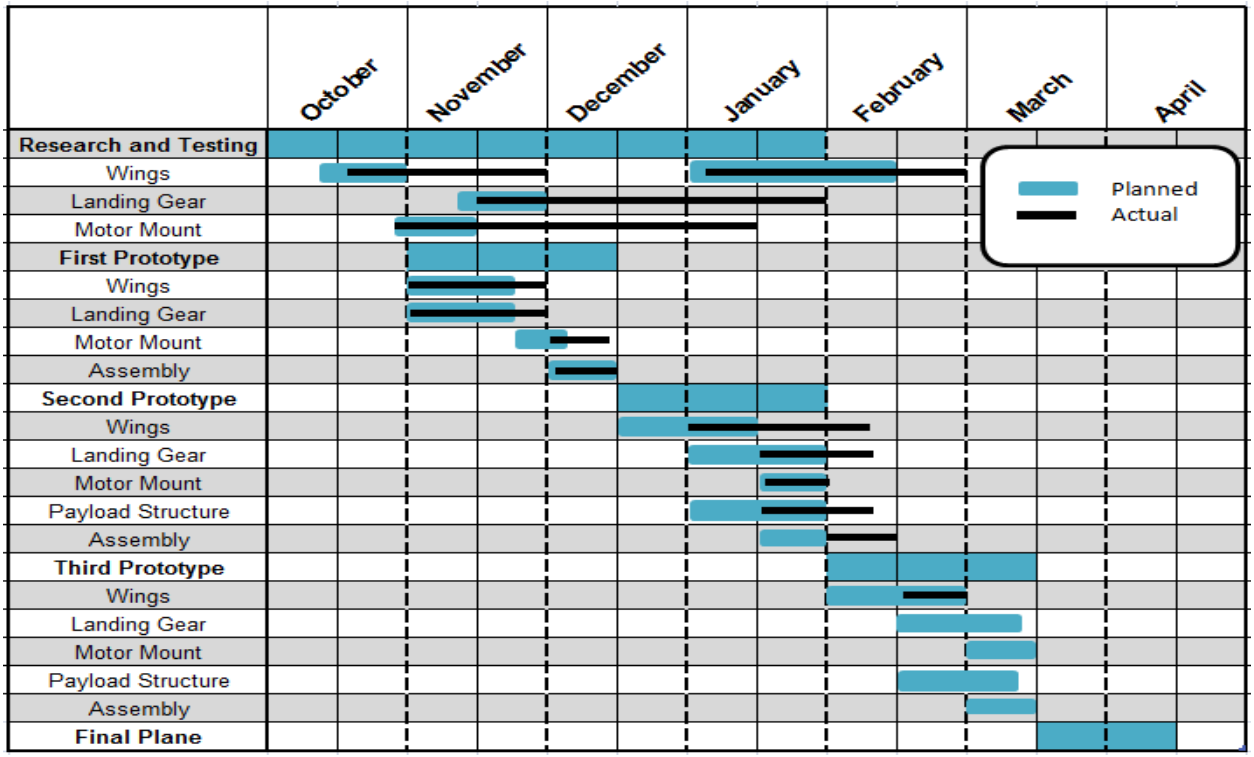

Figure 6.7: Manufacturing Milestone Chart

7.0 Testing Plan

Testing of components and systems allows analysis in the performance of the designs and highlight areas for improvement. Test results indicate where performance needs to be improved or reduced, to trade off for other advantages such as reduced weight. Structural, electrical and propulsion systems, as well as in flight performance of the overall aircraft were tested.

7.1 Objectives

Test objectives were outlined prior to the manufacture of components. Objectives defined the wants and needs of each component in order to meet specific aircraft requirements. Components assembled using current manufacturing methods were compared against past standards and manufacturing principles. Retaining a light weight aircraft was a major concern while an emphasis was placed on consistent strength and reliability.

7.1.1 Components

Fuselage

As the maximum load carried is 3-lb. during mission two, the payload structure was gradually loaded to 15-lb. to simulate a 5G acceleration. A battery of test was done to ensure that the payload for each mission remained properly secured.

Landing Gear

The landing gear, along with the fuselage section to which it is attached to, was tested with a drop test. The assembly was loaded to maximum weight and dropped at a height to simulate landing at a 15° angle at the stall speed. Crosswind landing was simulated by dropping the assembly on a slope.

Wing and Spar

The wing and spar system are tested for structural strength. The design metric is for the system to sustain a 5G turn while fully loaded. A static load test was performed with an elliptical load distribution that simulates the load distribution in flight. Both halves of the wing are divided into five sections, and an average load is calculated for each section. As shown in Figure 7.1, sandbags are used to apply the required loads.

Figure 7.1: Balsa Wing Test

The load factor started at 1 and increased in increments of 0.5 until the wing broke. This test demonstrated the maximum load that the wing can support, and the failure point was recorded.

7.1.2 Propulsion

Propulsion testing was performed to validate the manufacturers' rated performance of the motors, batteries, and propellers. Static thrust tests were performed by holding two components of a system constant while the third component was varied for comparison against other systems.

Thrust Rig

Propulsion test rigs provide information regarding the thrust capability of a motor and propeller configuration. The thrust produced by the propulsion system is transferred by the L-bracket and measured with the scale as depicted by Figure 7.2.

Figure 7.2: Propeller Thrust Rig

7.1.3 Flight Tests

Flight tests were performed and data was recorded using an Eagle Tree™ telemetry system. A pre-flight checklist helped determine faults in the electrical setup and any mishandled components on the aircraft. Flight test plan and objective lists were outlined to assess the performance of scheduled flights. A master test schedule, such as the one in Table 7.1, was used to plan every test that needed to be done.

7.2 Master Test Schedule

Test	Objective	Start Date	End Date
U-Shaped Landing Gear	Verify gear meets bending stress and impact requirements to simulate landings	10/11	10/25
Integrated Landing Gear	Repeat landing gear tests with the revised landing gear system	1/6	2/8
Payload Systems	Ensure no slippage, reliability, and ease of attachment/release	12/17	2/21
Propulsion System	Static thrust performance tests with motor, prop, and battery packs	11/7	2/1
Flight Testing	Compare flight measurements to calculated model	11/14	4/11

Table 7.1: Master Test Schedule

7.3 Preflight Check List

Pre-Flight checklist	
Structural Integrity – Visual inspection for damaged components	
□ Horizontal/Vertical Stabilizers	□ Boom/fairings
□ Control Surfaces / Linkages	□ Landing Gear
□ Payload Mounts	□ Wing
□ Propeller	□ Motor Mount
Avionics – Ensure all wires and electrical components are connected and performing properly	
□ Servo Wiring	□ Receiver Properly Connected
□ Avionic Power Test	□ Receiver Battery Peaked
□ Range Test	□ Main Battery Peaked
□ Servo Test	□ Failsafe
Propulsion – System should perform as desired	
□ Motor Wiring	□ Prop Clearance
□ Battery Connected	□ Motor Test
Final Inspection – Ensure safe, successful flight	
□ Correct Control Surface Movement	□ Ground Crew Clear
□ Mission / Objective Restated	□ Pilot and Spotter Ready

Table 7.2: Pre-Flight Checklist

Table 7.2 is a pre-flight check list followed by the flight test team before each test flight. A standardized checklist ensures all system components are checked efficiently prior to flight.

7.4 Flight Test Plan

Flight Test Plan 02/01/2014 Prototype 2	
□Acquire telemetry for all flights □ Live tracking of battery capacity, speed, current and altitude □ Ramp throttle to 100% before each flight on the ground	
First flight: Trim flight **Battery: 20 cells 1500 mAh, Propeller: 12x8**	**Second flight: Mission 2 simulation** **Battery: 20 cells 1500 mAh, Propeller: 12x8**
□ Trim plane	□ Takeoff weight: 6.25-lb.
□ Understand behavior in straightaways and turns	□ Cruise speed: 60-70 ft/s □ Stall speed: 35 ft/s
□ Switch pilots and repeat	□ Flight duration 3 minutes
	□ Fly the course with spotters
Third flight: Mission 3 simulation **Battery pack: 20 cells 1500 mAh, Propeller:12x8**	**Fourth flight: Mission 1 simulation** **Battery: 20 cells 1500 mAh, Propeller: 11x10**
□ Takeoff weight : 5.25-lb	□ Takeoff weight : 3.25-lb
□ Cruise speed: 60-70 ft/s □ Stall speed: 35 ft/s	□ Cruise speed: 70-80 ft/s □ Stall speed: 30 ft/s
□ Flight duration 2 minute	□ Flight duration 4 minute
□ Fly the course with spotters	□ Fly the course with spotters

Table 7.3: Flight Test Plan

A well-defined flight test plan as shown in Table 7.3 outlines the conditions and objectives that the aircraft is expected to meet during a flight test session.

8.0 Performance Results

Each system was tested to improve designs and validate modeled predictions. The results allow for design corrections and fine tuning of components.

8.1 Performance of Key Subsystems

Wing and Spar

Each wing was mounted upside down on a test stand with a boom to simulate actual loading in flight. Sandbags were placed symmetrically on each side of the wing, starting from the center. The wing was loaded until failure and then analyzed to determine the mode of failure, leading to improvements on next wing. Figure 8.1 shows the balsa wing mounted on the test stand after a failure at a load factor of 5. The results of the wing and spar tests are shown in Table 8.1.

Wing	Load factor withstood	Notes	Weight (oz)
Kevlar skin foam core wing	2		12.47
Peel ply fiberglass skin foam core wing	8	no warning before failure	11.99
Balsa wing 1	4.5	heard cracking before failure	5.5
Balsa wing 2	5	Performed up to expectation	5.99

Table 8.1: Result of Wing Tests

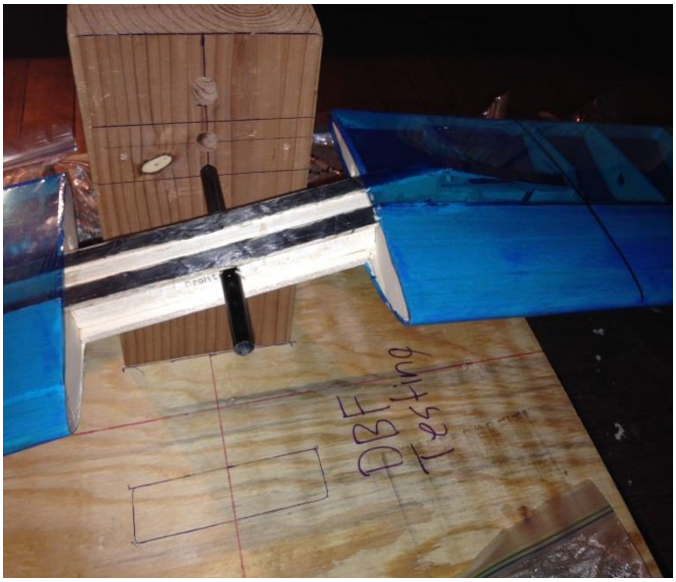

Figure 8.1: Balsa Wing 2 on Test Stand After Failure

Landing Gear Performance

The main landing gear was subjected to a static load test and a dynamic drop test to verify that it was structurally sound and capable of handling rough landings. The static loading test consisted of loading the main gear up to the design load of 5 times the maximum predicted takeoff weight. A dynamic drop test was then conducted that consisted of a series of free fall drops with a 6.5-lb. load, intended to test the integrity of the landing gear under extreme circumstances. These free fall drops increased in height in increments of 1-in. until a maximum height of 12-in. was reached. A side load drop test at a height of 6-in. was also performed to evaluate the performance of the landing gear under a one wheel touchdown condition. Figure 8.2 and Table 8.2 show that the final landing gear design performed as intended.

Taxi missions were performed concluding that the aircraft could successfully complete the taxi mission in 5 minutes. The skids allowed for better control across the Palruf panels.

Figure 8.2: Dynamic Drop Test Resulting in Flexing of the Fuselage Floor

Landing Gear Design	Design Load(lb)	Static Test Results (lb)	Dynamic Test Results
Traditional U-Shaped Rigid Landing Gear	32.5	35	Survived 6 in. drop; failed side loading drop
Revised Flexible Design	32.5	30	Survived 6 in. drop; failed side loading drop
Final Design	32.5	35	Survived 12 in. drop; survived side loading drop

Table 8.2: Dynamic Drop Test Results

Propulsion

Table 8.3 shows the empirical values from tests performed on the static thrust stand using a Neu 1107-6D with a 4.4 ratio gearbox and 20-cell Elite 1500 mAH NiMh battery. Propeller sizes shown were found using the MATLAB calculations optimized for maximum thrust under restricted current and voltage. Actual values recorded are nearly identical to predicted calculations.

Propeller Size	Predicted Thrust (lb)	Actual Thrust (lb)	Predicted Current (A))	Actual Current (A)	Predicted Watts (W)	Predicted Watts (W)
12 x 6	4.32	3.95	18.29	18.25	484.96	488.19
12 x 8	4.04	3.75	15.39	16.75	408	442.2
13 x 6.5	4.76	4.28	19.46	19.75	515.97	519.43

Table 8.3: Comparison of Actual and Predicted Static Propulsion Values

Battery Performance

Figure 8.3 presents the predicted battery consumption compared to the actual battery consumption for a complete trial of mission 1. Predicted consumption assumes a full throttle flight which puts greater strain on the battery and results in greater milliamp-hour total. Actual consumption is under the pilot's discretion, with throttle application. A conservative use of throttle prevents overheating of the motor and battery, and minimizes centrifugal forces acting on the aircraft.

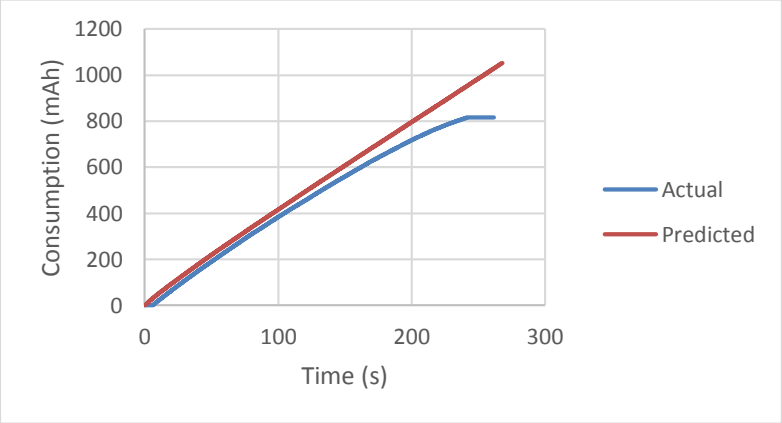

Figure 8.3: Battery Consumption vs. Time

8.2 Complete Aircraft Performance

Flight Test Performance of Wing

Although the wing installed on the prototype passed the static load test, flight testing under windy condition revealed wing twist that hindered aileron control. The torsional stiffness of the wing was examined using an inflight video and found to be inadequate. One method of decreasing the in-flight twisting of the wing can be accomplished through the application of the heavier Monokote© covering instead of the Microlite™ covering. Investigating other methods of preserving the torsional integrity of the wing with the least amount of weight penalty is currently underway along with a test plan for inspecting the torsional strength of the wing.

Figure 8.4: From left to right: Wing at static condition; wing showing washout (evident by creases formed on wing skin near root); wing showing significant twisting

Field test data was gathered using an Eagle Tree™ Telemetry system on board the aircraft. Flight pattern and payload configurations were simulated for each mission for accurate results. The telemetry system monitored the motor rpm, energy consumption, acceleration in the x and y direction, airspeed, aircraft speed relative to the ground, GPS positioning, and motor temperature. Empirical figures helped calibrate MATLAB code for adjustments to propeller sizing, in turn decreasing battery consumption.

Comparisons of values produced during field tests to static thrust values are seen below in Table 8.4. Flight values were slightly reduced from static figures due to heat loss from the motor and battery.

Propeller Size	Predicted Current (A)	Actual Flight Current (A)	Predicted Watts (W)	Actual Flight Watts (W)	Predicted Voltage (V)	Actual Voltage (V)
12 x 6	18.29	21.13	484.96	481	26.51	22.77
12 x 8	15.39	18.20	402.00	384	26.51	21.10
11 x 10	18.37	18.58	487.12	424	26.51	22.83

Table 8.4: Comparison of Field and Static Values

8.2.1 Motor Temperature

Motor temperatures were monitored during each field test using an on-board temperature loop to avoid overheating the gearbox. The temperature of the motor follows a linear increase reaching maximums up to 110˚F, seen in Figure 8.4.

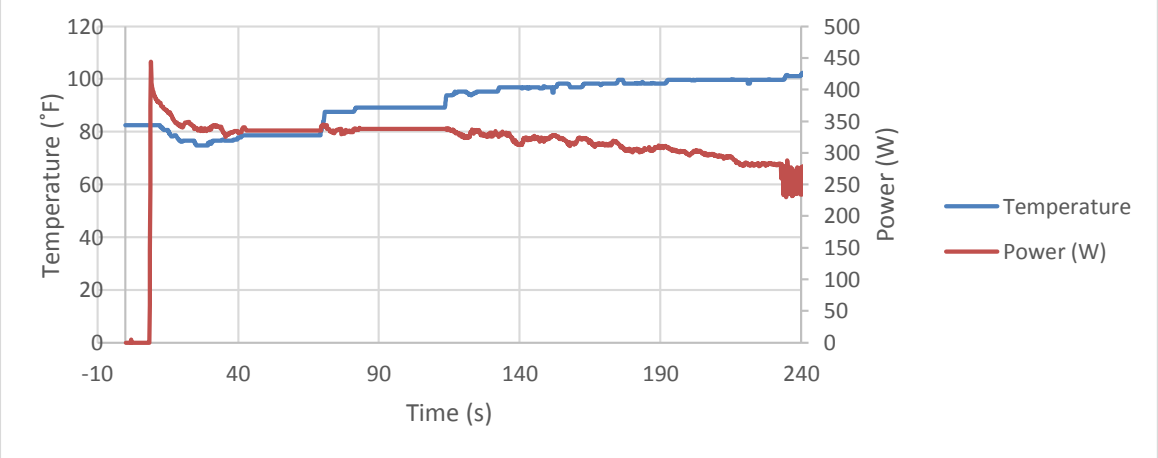

Figure 8.5: Motor Temperature and Power vs. Time

8.2.2 Accelerations

The telemetry G-force Expander was used to monitor the magnitude of accelerations during turns and loops. Magnitudes of up to 4.92G, seen as peaks in Figure 8.5, were experienced during turns, confirming that a 5G loading was a safe estimate since mission 1 is lighter than mission 2 and 3.

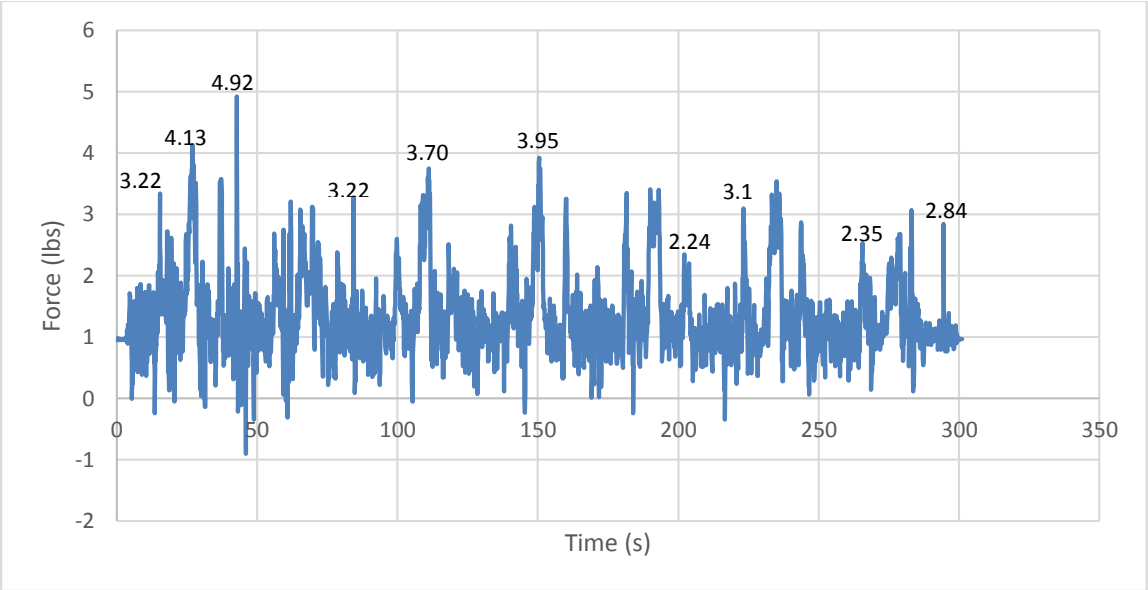

Figure 8.6: Accelerations along Yaw Axis

8.2.3 Power Prediction Comparison

Calculation predictions of power using MATLAB code assume a full throttle flight. Power predictions from code are compared to empirical data recorded in flight in Figure 8.6. Overall, the empirical data and predicted calculations follow each other relatively closely with a noticeable drop toward the end of the mission that can be attributed to increased resistance and lowered current from battery heat.

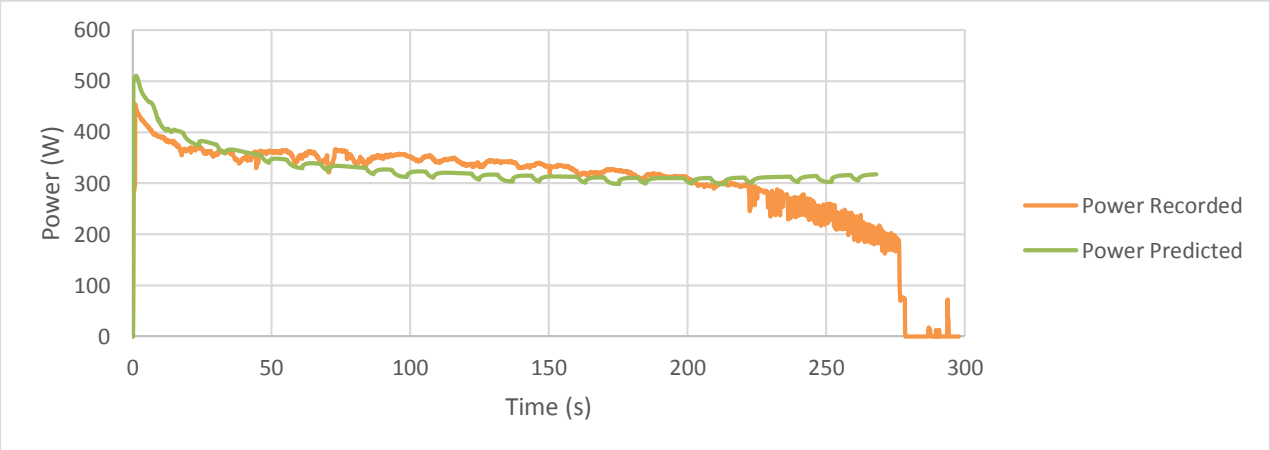

Figure 8.7: Power vs. Time

Pilot Feedback

Aside from data collected by onboard telemetry, immediate feedback of the aircraft's performance could be assessed visually and physically from the pilot's point of view. During the trim flights, the aircraft exhibited steady and controllable flight without stability issues.

The performance of the aircraft in flight mission 1 resulted in lap time in the vicinity of mid-40 seconds and achieved takeoff within 5 feet due to the aircraft's light weight and a headwind. A decrease in lap times toward the end of the mission was predicted by the computer simulation and it was noticeable during the test flight. The aircraft performed tight turns of up to 4.5G and reached a maximum speed of 60-mph.

For flight mission 2, the plane was loaded to 3-lb. and took off in 30-ft. Because the mission had no time constraint, the aircraft was flown at a high altitude with a lower throttle setting in order to complete the required 3 laps.

For flight mission 3 the aircraft was tested to the limits by flying as fast as possible with 2-lb. of payload. This aggressive flying resulted in lap times just a few seconds slower than those in flight mission 1. Table 8.5 summarizes the flight results from numerous test flights with Prototype 2.

For all missions, the computer simulation predicted results slightly more optimistic than what was achieved. This difference could be attributed to the difficulty in predicting the drag accurately. With continuing flight testing over the next few weeks, the team will hope to improve upon the results and achieve consistency in all flight missions.

Mission 1		**Mission 2**		**Mission 3**	
Expected Number of Laps	6	Takeoff within 40-ft	Pass	Expected flight time	118 s
Actual Number of Laps	6	Completion of mission with 3 cargo blocks	Complete	Actual flight time	123 s

Table 8.5: Flight Test Results

8.2.4 Actual Flight Pattern

GPS data logging of the aircraft trajectory is shown in Figure 8.7, and a picture of Prototype 2 in flight is shown in Figure 8.8.

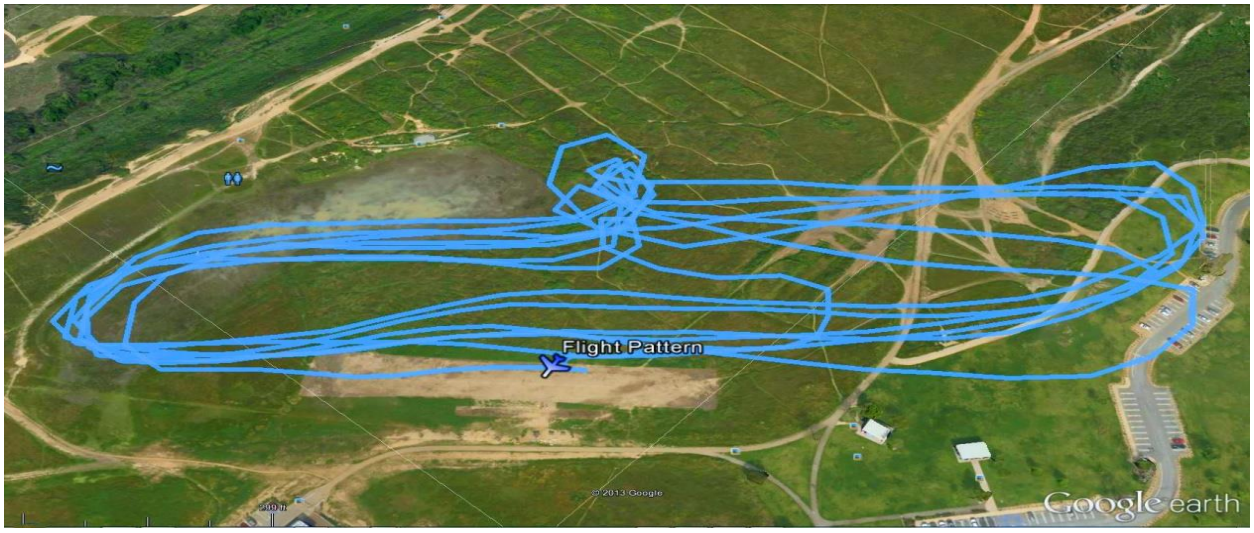

Figure 8.8: Aircraft Flight Path

Figure 8.9: Prototype 2 in Flight

9.0 References

[1] “AIAA Design/Build/Fly Competition - 2013/2014 Rules”, 31 Oct. 2012, <http://www.aiaadbf.org/>.

[2] MichaelS. Selig, J. J. (1995). Summary of Low-Speed Airfoil Data. Virginia Beach: SoarTech Publications.

[3]Simmons, M. (2000). Model Aircraft Aerodynamics. Chris Lloyd Sales & Marketing.

[4] Drela, Mark & Harold Youngren. Athena Vortex Lattice, v. 3.27. Computer Software. MIT, 2008.

[5] MIL-F-8785C. Military Specification: Flying Qualities of Piloted Airplanes, November 1980.

[6] M.V. Cook. Flight Dynamics Principles, Reprinted 2008

[7] Foster, Tyler M. Dynamic Stability and Handling Qualities of Small Unmanned-Aerial-Vehicles, Brigham Young University, April 2005.

AIAA Design, Build, Fly 2013-2014

San José State University

"The Wrong Brothers"

Contents

1. Executive Summary

The following report contains documentation and analysis of San José State University's aircraft design and manufacturing process, final design, and performance results for the 2013/14 AIAA Design Build and Fly competition.

Missions included in this year's competition are primarily intended to simulate a fast response emergency medical aircraft capable of traversing rough terrain to reach its destination and hauling a sizeable payload. The missions include a rough taxi mission, a ferry flight, a maximum payload mission, and a mission to simulate an emergency medical response. The taxi mission tests the on-ground performance of the aircraft, and its ability to traverse a corrugated roofing panel. The ferry flight is a demonstration of the aircraft's speed and handling characteristics. Success on the maximum payload mission is determined on the aircrafts ability to fly with as many one pound, 6"x6"x6" wooden blocks as possible. This puts an emphasis on maximizing volume and weight that the aircraft is capable of hauling. The third and final mission is the emergency medical mission in which two pounds of medical attendants and patients will be escorted through three laps as quickly as possible. This emphasizes both the aircraft's capacity to haul the medical crew as well as demonstrate excellent speed and handling capabilities. Additional limitations include a maximum 40' takeoff distance, and a scoring emphasis on minimizing weight.

Execution and interpretation of a detailed scoring analysis determined the order of importance for each design characteristic, eventually leading to the final design. The most important design points were to maximize speed, minimize weight, and achieve a minimum payload capacity of two pounds. In order to maximize speed while allowing for sufficient loading space, a symmetrical airfoil shape was selected for the fuselage giving a low drag design. Additionally two motors were mounted on the wings to ensure sufficient power for reaching the desired speeds. In order to ensure a minimal weight, a boom was used to extend to the empennage, and a light weight design consisting of mostly balsa wood and carbon fiber reinforcements was selected. To ensure a takeoff distance of 40' is met, the motors are mounted in front of each of the flaperons for increased local velocity over the wing and hence a shortened takeoff distance. Additionally for maximized controllability and lifting characteristics the flaperons span the entire length of the wing. Another major requirement for the aircraft is to complete the rough taxi course. In order to address this need the landing gear has a wide stance and skis to allow for a smoother ride over the corrugations. In order to steer around the obstacles in the taxi course a controller setting allows for individually throttled motors on each wing, and the rear landing gear is allowed to rotate freely on swivel for maximum on-ground maneuverability.

After testing and improving upon the design through the use of prototypes, the current design weighs approximately 2.1 lbs, with a maximum speed of 80 ft/s, and an estimated total flight score of 9. This score coupled with the light weight design will ensure that San José State competes for 1st place in the 2014 DBF competition.

2. Management Summary

2.1 Team Organization

San José State University's recent success in the Design, Build, and Fly contest has helped increase the number of participants. This year's team consists of 11 participants ranging from freshman to graduating seniors. The team structure is shown in Figure 2-1 and was determined to achieve outstanding efficiency and performance.

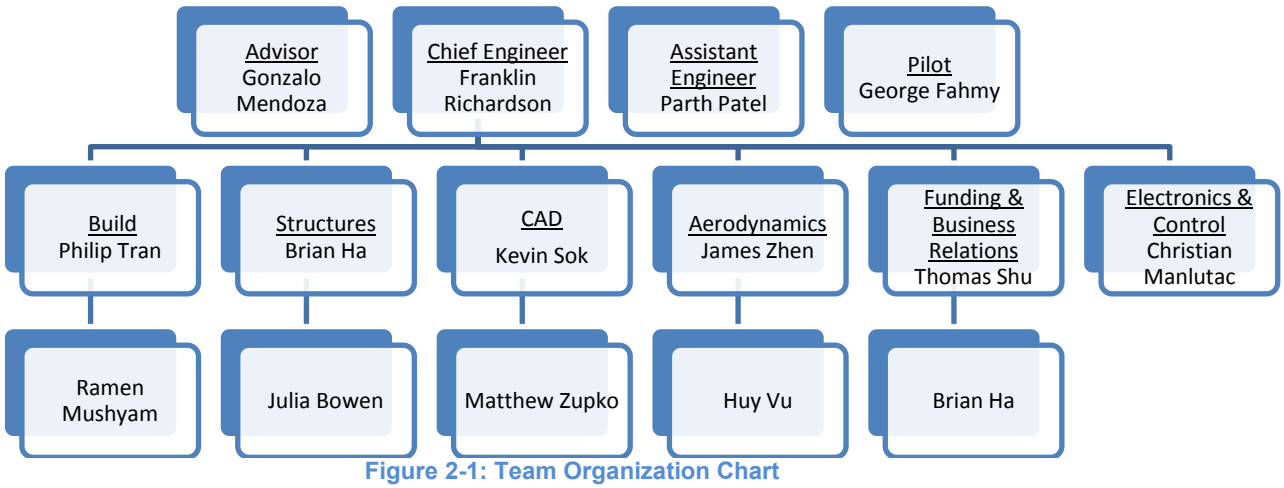

Figure 2-1: Team Organization Chart

The team is divided into sections to ensure superior quality work and is overseen by the Chief Engineer. The sections include: funding and business relations, CAD, aerodynamics, structures, build, and electronics and controls. All team members often overlap sections to help complete tasks in a timely manner. The pilot is George Fahmy - a recent graduate from San José State University and Gonzalo Mendoza is the faculty advisor.

2.2 Milestone Chart

Once the contest rules were released, the team had approximately 6 months to agree on a conceptual design and test it. Multiple prototypes were built and analyzed under taxi and flight conditions. Each consecutive prototype implemented design improvements which led to the final configuration of the competition aircraft. Figure 2-2 shows the project milestones with deadlines required to meet basic requirements for the competition.

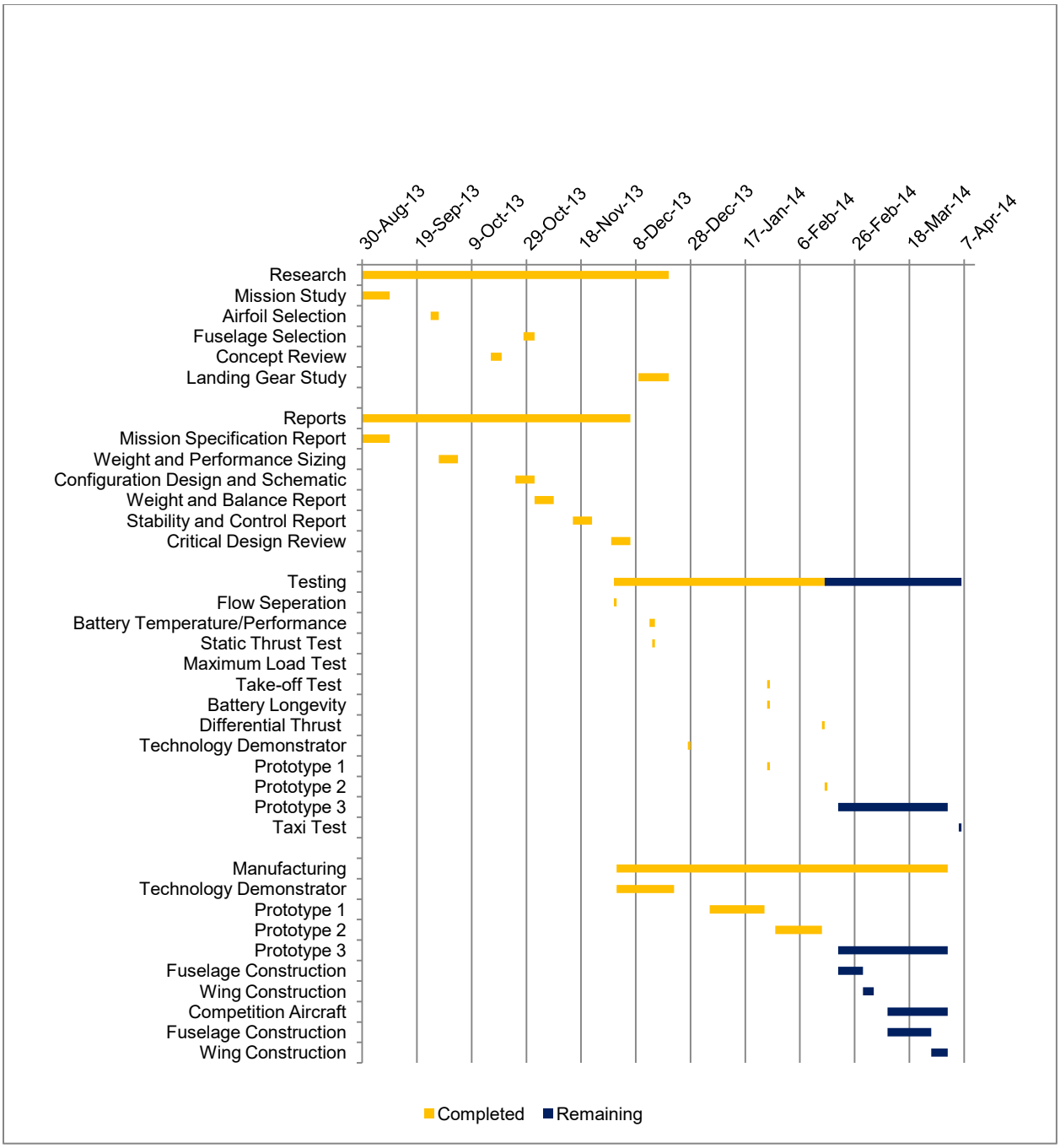

Figure 2-2: Project Schedule

3. Conceptual Design

The mission requirements dictate what design choices are made for the conceptual design in the context of maximizing mission scores. A scoring analysis based on these requirements gives the basis for making these design choices. It is important to note that choices made during the conceptual design stages had a large impact on the final design of the airplane. However, significant modifications to the design have resulted from detailed analysis and testing.

3.1 Mission Requirements

Each of the three flight missions and the on-ground taxi mission are intended to simulate the duties of an aerial emergency response vehicle. The general requirements to complete these tasks include:

- Takeoff must be completed within 40’
- The aircraft must have a high maximum speed (90-105 ft/s)
- The aircraft must be able to carry a minimum of two pounds
- The aircraft must have enough space to store as many one pound 6”x6”x6” cubes as possible
- There must be at least two inches of clearance above each patient on the emergency medical mission
- The aircraft must be stable and controllable on the ground so that it can traverse the rough taxi course. This is not a strict requirement for design; however, it is being treated as one due to the desire to maximize the mission scores. It is noted that the score penalty associated with not completing the taxi mission is unlikely to be offset by advantages in weight and performance that can be had by designing an airplane without the taxi mission in mind.

Additionally there are multiple safety requirements that must be met:

- Current draw from the battery pack must be limited by means of a 15 Amp fuse which must be accessible to the crew without reaching across the propeller plane
- The aircraft must pass a structural wingtip test to ensure that it meets structural integrity requirements
- A maximum of 1.5 lbs of NiMH or NiCad batteries can be used
- A separate battery pack must be used for the receiver to ensure controllability in the event that the propulsion system or main battery pack malfunction.

3.2 Mission Scoring

The total score for the competition is determined using Equation 1:

$$Total\ Score\ = \frac{Written\ Report\ Score * Taxi\ Score * (M1 + M2 + M3)}{RAC} \qquad (1)$$

The written report score is determined by the judges who will give the scores based on the overall quality of the design report. The taxi score is determined by the successful or unsuccessful completion of

the rough taxi mission, and the mission scores (M1, M2, and M3) are determined through flight performance. Lastly, the RAC is determined by the weight of the aircraft in pounds, and is a critical part of the scoring for the competition.

3.2.1 Taxi Mission

Scoring for the taxi mission is determined by the completion of the course shown in Figure 3-1. The solid black lines represent two 2x4 planks which serve as obstacles, and the paneling that must be navigated is corrugated roofing panel which has 3" wide and .625" high corrugations.

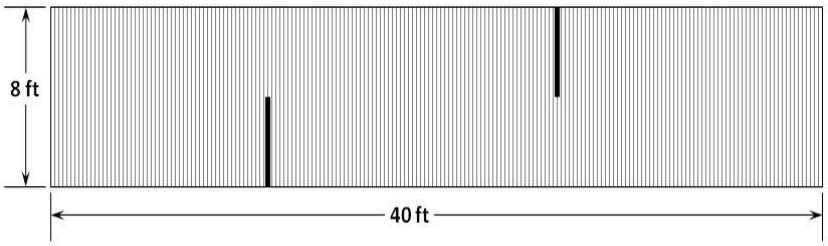

Figure 3-1: Rough Taxi Mission Course

The rough taxi mission is scored as a pass or fail, and failure results in an overall reduction of score by 80%. This makes completion of the course critical in order to remain competitive in the competition. The taxi mission must be completed within a time limit of 5 minutes and the attempt will be disqualified if the airplane:

- Departs the side of the course
- Becomes airborne
- Experiences damage (broken propellers, bolts, rubber bands, etc.)

Taxi score is solely based on the success or failure of the mission. If this mission is completed successfully then the score is equal to 1.0, otherwise the score is 0.2.

3.2.2 Flight Mission 1: Ferry Flight

The Ferry Flight Mission (M1) requires an empty aircraft – no payload – to takeoff within 40 ft. This is a speed mission as there will be 4 minutes to complete as many laps possible. When compared to Mission 2, which includes a significant increase in weight, the Ferry Flight is flown with a much lower wing loading. The light weight of the aircraft significantly lowers the difficulty of takeoff within 40' easily allowing for a smaller wing design. However, balancing the wing size for optimal performance in both the low wing loading Ferry Flight, and the higher wing loading missions poses a challenge. The flight path for each mission is shown in Figure 3-2.

A perfect score results in 2 points, which will only be awarded to the team with the highest number of laps as explained by Equation 2. Time for the mission will start when the throttle is advanced for the first take-off/attempt, and a successful landing must be achieved in order to complete the mission.

$$M1 = 2 * \left(\frac{N\ Laps\ Flown}{Max\ N\ Laps\ Flown}\right) \qquad (2)$$

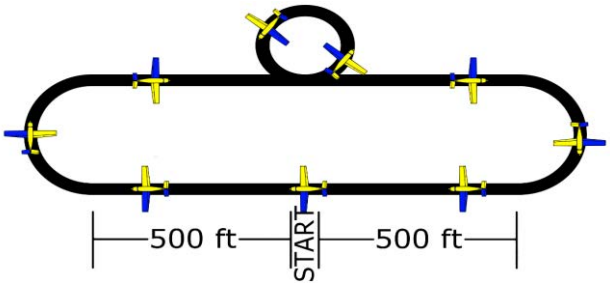

Figure 3-2: Flight Course For Each Mission

3.2.3 *Flight Mission 2: Maximum Load Mission*

The main objective for the Maximum Load Mission (M2) is to complete 3 laps with the maximum payload loaded onto the plane. The cargo must be carried internally and must be properly secured. Maximum achievable score for the Maximum Load Mission is 4 points which will be awarded only to the team that carries most cargo and completes the mission successfully. The scoring for this mission is shown in Equation 3. It is important to note that time is not a factor in this mission, and that takeoff must still be completed within the 40' limit. As a result of the short takeoff requirement and the roughly doubled weight of the aircraft, the Payload Mission requires that a larger wing be considered to overcome these challenges, thus negatively impacting performance on Mission 1.

$$M2 = 4 * \left(\frac{N\ Cargo\ Flown}{Max\ N\ Cargo\ Flown}\right) \qquad (3)$$

3.2.4 *Flight Mission 3: Emergency Medical*

Mission 3 is a timed emergency medical response simulation. The patients and attendants will be simulated by wooden blocks and must be sized and positioned according to specifications including spacing and clearance requirements. Each "patient and attendant" must be ballasted to 0.5 lbs for a total of 2 lbs. The schematic for the patient and attendant are shown in Figure 3-3.

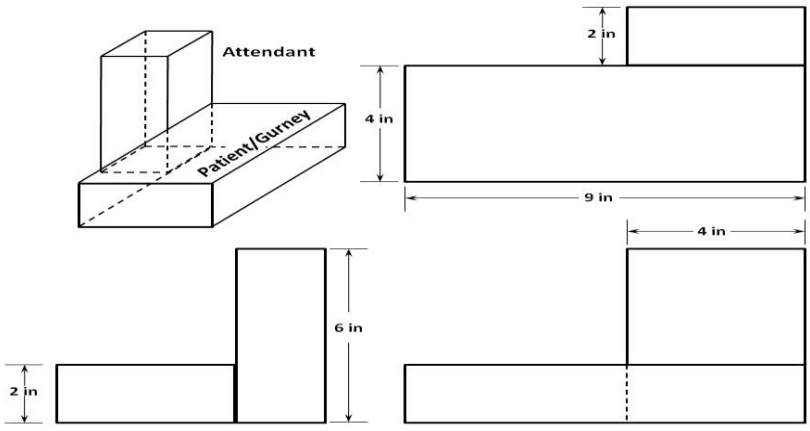

Figure 3-3: Emergency Medical Mission Payload

Scoring in the Emergency Medical Mission is based on the time to fly three laps following the given flight path in Figure 3-2. The team with the fastest time will receive a perfect score of 6 points as

shown in Equation 4. The time for this mission will be stopped when the aircraft crosses the finish line in the air, but a successful landing is required to receive a score.

$$M3 = 6 * \left(\frac{Fastest\ Time\ Flown}{Time\ Flown}\right) \qquad (4)$$

The design for this mission poses multiple opposing design points, more specifically speed and payload capacity. For a fast aircraft a small wing is desired, but for the increased weight in this mission a larger wing may be necessary for takeoff. Essentially, the Emergency Medical Mission is a combination of the requirements for the Ferry Flight and Payload missions. An increase in power would help overcome these obstacles; however this increases the weight (and therefore the RAC) of the aircraft which could be counterproductive. Sizing decisions, including justification for the minimal sizing of the wing as required for loaded takeoff performance, are covered in Section 4.

3.3 Design Requirements

In order to determine what design characteristics must be prioritized, a scoring analysis was completed to shed light on the most important targets. The analysis considered all aspects of scoring with exception to the report itself, which does not impact the actual design of the aircraft. The taxi mission is considered to be critical in order to be competitive in the competition. Therefore on-ground maneuverability is a critical design requirement. Each of the flight missions cannot be completed without reaching the takeoff requirement goal of 40' which is another critical requirement. The real analysis comes into play when considering each of the flight missions and the respective benefits and tradeoffs of designing towards each specific mission. In order to do this, a parametric study was completed which considered the impact of each mission and the RAC.

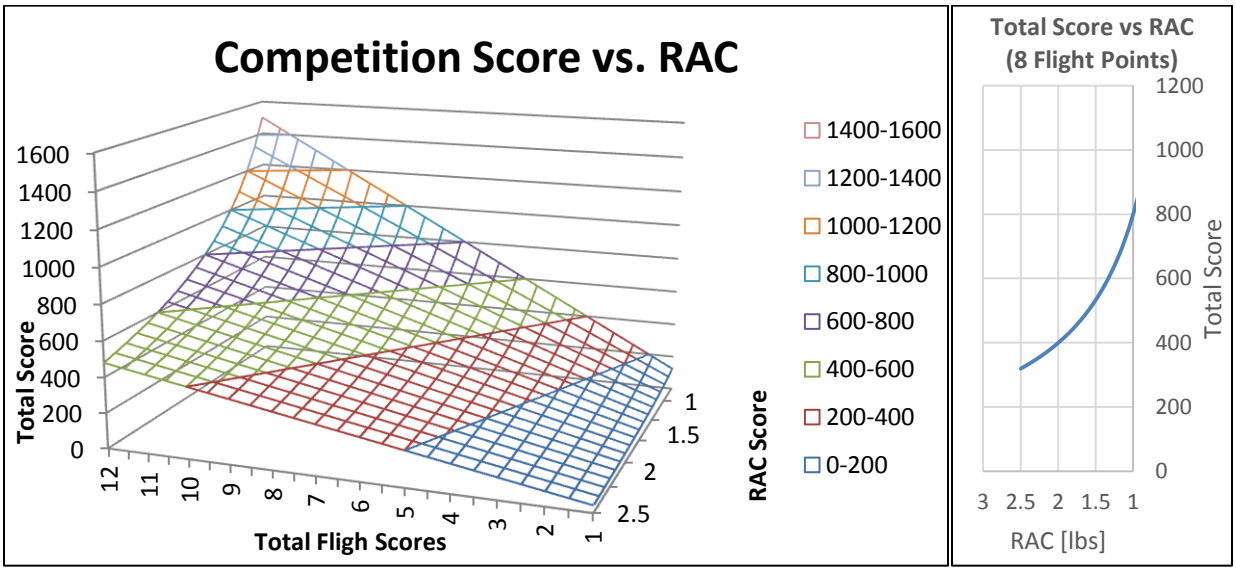

Figure 3-4: Graphical Representation of the RAC vs. Total Competition Score

Figure 3-4 shows the importance of the RAC, which in this case is directly dependent on the weight. One pound difference in weight can be equivalent to much more than 100 points in the overall

scoring, making weight a critical design point. The “Wrong Brothers” do not expect a competitive entry above 4 lbs or a realistic entry below 1.5 lbs. Maximum competitive empty weights were estimated on analysis of the mission score formulae and calculations showing reasonable performance with near 2 lb empty weights. Minimum realistic weights are based on regression of payload versus gross weight trends for past entries, noting that a minimum of 2 lbs must be carried.

When considering each of the three flight missions it became apparent that Missions 1 & 3 are worth a combined 8 points, and Mission 2 is worth 4 points on its own, that is Missions 1 & 3 are twice as important as Mission 2 on its own. However the significance of this comes from the fact that Missions 1 & 3 both benefit from having a light and fast aircraft. Mission 2, however, does not. In fact, an attempt to get a high score at Mission 2, the payload mission, could be counterproductive. The capability to lift more payload weight, and thus more volume, would inevitably increase the drag and weight of the aircraft. This would significantly decrease the scores on Missions 1 & 3, and it would hurt the team’s total score. Additionally, Mission 3 requires two pounds of payload, which is already equivalent to two blocks of payload on the second mission. The internal volume required is also similar between the two missions. The scoring analysis led to conclusion that designing a light weight, fast, and maneuverable aircraft that is capable of completing the ground taxi mission is the best approach to winning the competition. Given the limitations in battery chemistry and electrical current levels, it is difficult to overcome the penalty in RAC associated with increased payload with improved flight performance.

With Missions 1 and 3 both being speed dependent and having a large impact on the total competition score, a speed analysis was created to determine the design target speed of the aircraft. In this analysis, both aircraft speed and wind speed are considered, as the wind speeds in Kansas can be a serious factor in the performance of the aircraft. The time allowable is 4 minutes during the Ferry Flight, so the time per lap depending on the wind and aircraft speed is shown in Table 3-1, and the corresponding number of Ferry Flight laps are shown in Table 3-2 The assumption is that the turn radius is 75 ft, and the turn speed is 80% of the straight and level flight speed.

Table 3-1: Aircraft and Wind Speed Dependent Lap Times

	Wind (kts)				
Speed (fps)	0	5	10	15	20
60	52.97	53.64	55.84	60.20	68.44
70	45.40	45.82	47.17	49.71	54.07
80	39.73	40.01	40.89	42.51	45.15
90	35.31	35.51	36.12	37.22	38.96
100	31.78	31.92	32.37	33.15	34.36
110	28.89	29.00	29.33	29.91	30.78

Table 3-2: Wind and Air Speed Dependent Ferry Flight Lap Count Estimations

	Wind (kts)				
Speed (fps)	0	5	10	15	20
60	4	4	4	3	3
70	5	5	5	4	4
80	6	5	5	5	5
90	6	6	6	6	6
100	7	7	7	7	6
110	8	8	8	8	7

As a result of the speed analysis it became apparent that a minimal speed for the aircraft should be 90 ft/s and the target speed should be at least 100ft/s in order to post a competitive number of laps (6 or more) and to reduce the sensitivity to wind on the mission scores. Speeds above 110 ft/sec are considered unlikely given the limitations in weight, payload capability, and propulsive technology imposed by the rules. In any event, the addition of 1 or 2 laps beyond a target of 6 or 7 would not likely offset the additional weight required to achieve such numbers.

The design requirements determined as a result of the scoring analysis are highlighted in Table 3-3.

Table 3-3: Design Requirements

Mission Requirements	Design Requirements *
High Maximum Velocity	Sufficient thrust, light weight, low drag, high wing loading
Low Weight	Simplification of aircraft structure, and careful component selection
In-Air Maneuverability	High lift, sufficient control authority from control surfaces, effective empennage design
On-Ground Maneuverability/Stability	Thrust control, stable and steerable landing gear
40’ Maximum Takeoff	High lift, high thrust, low wing loading
Storage Capacity	Sufficient fuselage volume, High lift, structural integrity
Low RAC	Maximize power loading, Minimize Size and Material Density

*Red font items show requirements in conflict with other design requirements

3.4 Design Solutions & Selection Process

Each component of the aircraft, as well as the overall aircraft configuration, was carefully selected to meet the needs of the design requirements stated in Table 3-1. The selection process for each component of the aircraft had different or slightly varying techniques; however each component was thoroughly discussed in team meetings to ensure that all of the relevant details were considered before making important decisions.

3.4.1 *Fuselage & Boom*

Table 3-4: Fuselage Selection Overview – Extruded Airfoil Shaped Fuselage

	Positives	Negatives
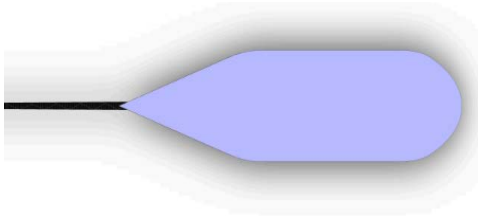	Low drag	Relatively fragile
	Light weight	Flow separation issues over the top and bottom
	Good internal capacity	Lengthy tooling time
	Simple storage of components	

The fuselage was designed with a minimalistic approach. That is, the desire was to minimize weight and drag, while maintaining the capacity to carry two 6”x6”x6” blocks on Mission 2 and the patients and attendants necessary to complete Mission 3. In order to minimize drag for speed purposes, it was decided to use San José State’s traditional airfoil shaped fuselage design. The simplicity of the structure allows for a very light weight fuselage, and a very aerodynamic shape. The goal through this approach is to minimize wetted area and to keep laminar attached flow over the majority of the length of the fuselage. This combination of light weight and low drag made the decision to pursue the airfoil shaped fuselage a unanimous one.

In order to ensure the fuselage would be of minimal weight, a balsa wood and carbon fiber stringer design was devised and fabricated. An additional weight saving measure was to use a boom, allowing for a shorter fuselage and an extension to the empennage so that the vertical and horizontal tails will have sufficient control authority. The decision on the boom placement, however, required iteration. A lower boom design was first proposed; however, after further consideration the boom was raised to the top of the fuselage allowing for cleaner airflow to the empennage, which is now clear above the trailing edge of the fuselage. Additionally, increased structural support is attained by running the boom through the top of the fuselage to a bulkhead that also provides load clearance.

3.4.2 *Empennage*

Table 3-5: Empennage Selection Overview – Conventional Boom-Mounted Stabilator and Fin and Rudder Configuration

	Positives	Negatives
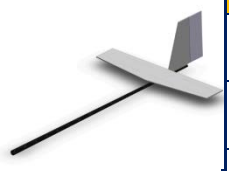	Raised above fuselage for clean flow	Increased need for structural support due to long moment arm
	Long moment arm from the boom for increased control and minimal size	Necessary fabrication of custom mounts due to stabilator design
	Horizontal stabilator for increased pitch control	

After making necessary adjustments, the empennage design was made to be simple, effective, and lightweight. A flat plate approach was used to minimize drag and weight while simplifying the manufacturing process. Using the boom to extend the length of the moment arm from the empennage to the aircraft’s center of gravity increases the effectiveness, and the boom’s position in line with the top of

the fuselage allows for clean flow to the empennage. In the first low boom design a t-tail was chosen to raise the horizontal stabilizer into cleaner flow; however this posed the threat of deep stall and the vertical stabilizer was still subject to the wake of the fuselage. These problems were eliminated by raising the boom and using a traditional empennage design. An H-tail was considered for greater maneuverability, however, since there is a boom this would be difficult to do without adding a second boom for the servos or a significantly more complicated servo system. Placing the empennage in line with the top of the fuselage also allows for the prop wash to pass over the stabilator giving greater control authority, since the aircraft has a high wing design as well. Configurations with increased vertical fin area protruding slightly below the boom have also been tested in an effort to improve directional stability and control authority while minimizing unfavorable roll coupling.

3.4.3 Wing

Table 3-6: Wing Selection Overview – High Wing Installation

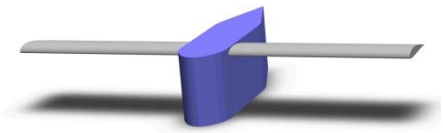

Positives	Negatives
High wing allows for some natural dihedral with the simplicity of a straight spar.	High wing reduces ground effect for takeoff
Good clearance for the taxi mission obstacles	Need to add separate structural reinforcement for the gear, rather than leveraging existing wing structure
Structurally sound design due to intersection with the boom and continuous spar.	
Simplifies the addition of large propellers and flaperon panels	

Initially a mid-wing design was considered for the aircraft, this was looked at as a way to ensure sufficient clearance, and possibly increase the ground effect during takeoff. This was desirable given the short 40’ takeoffs required for each of the flight missions. The clearance is an important issue, not only for the rough taxi mission, but because it is built into the competition rules as well. Ultimately, the reason the mid wing was not selected was the structural difficulties surrounding the clearance of the internal payload for Mission 3. Once it was discovered that at least two inches of clearance had to be above the patients, there was simply no practical way to have anything but a high wing configuration without sacrificing the structural efficiency of the wing and landing gear. Additionally, placing the spar and boom in line with one another allowed for a combination of the two sturdiest structures in the aircraft making it very robust. The wing design is fairly simple, and like the fuselage, it uses a combination of balsa wood and carbon fiber to maintain strength and light weight. The aircraft will be a monoplane as there are no restrictions on span in

this year's competition, and a single wing allows for the lowest drag and simplest, most efficient design. The flaperons will span the entire length of the wing, ensuring sufficient control for maneuvers and high lift for takeoff. A swept wing was not investigated as the configuration of the airplane provides for ample room to position the straight wing for good static margin and there is no aerodynamic benefit from a swept configuration at the speeds of interest.

3.4.4 Propulsion

Table 3-7: Propulsion Selection Overview – Twin Puller Configuration

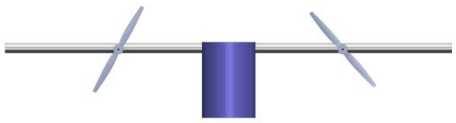

Positives	Negatives
Twin motor allows for differential thrust steering on the taxi mission	Asymmetric thrust can be an issue
Motors on each wing allow for blown flaps to increase lift during takeoff	More structural stress on the wings
Position allows for prop-wash over the empennage increasing control	More components increase costs and risk of failure
	More complicated building process

The placement and configuration of the propulsion system is a crucial part of the design because it has critical effects on the on-ground performance, in-air performance, takeoff distance, center of gravity positioning, speed, and weight of the aircraft. The mission requirements dictated the decision to go with twin puller motors, with one on each wing.

The reasons for this configuration are numerous; however the first reason is due to the requirements of the taxi mission. The twin motor configuration allows for the primary method of steering over the corrugations and around the two obstacles placed on the course. A controller setting will be used that allows for individually throttled motors, and the moment arm between the individual motors and the aircraft's center of gravity will allow for directional control from the motors. This will be the primary method of steering through the course. It is an efficient use of the resources, allowing us to keep the weight of the aircraft down while adding the additional necessary steering tools.

Another requirement that encouraged this decision was the short 40' takeoff requirement. Placing one motor on each wing in a puller configuration has additional benefits especially for takeoff. This is because the local velocity over the wings and flaperons will be increased. The blowing of the flaps results in an increased lift coefficient during takeoff and thus reduces the takeoff distance.

Naturally, a primary use of the propulsion system is to ensure that there is enough power to reach the high speeds necessary for success in both the ferry flight and emergency medical missions. The twin motor design along with proper battery selection ensures that the combination of two motors will give

enough power to reach these speeds. The two motors also allow the speed controllers to stay small since the current will be split between them, allowing for the use of smaller and lighter equipment.

3.4.5 Landing Gear

Table 3-8: Landing Gear Selection Overview – Mixed Wheel /Ski Plate Tail Dragger Configuration

	Positives	Negatives
	Better control during taxi mission	Increased aircraft weight
	Stop and go on taxi mission	Protruding skis increase landing difficulty

Unlike DBF competitions in prior years, much more thought has to be put into the landing gear and landing gear configuration due to the rough taxi mission. An emphasis has to be put on sturdiness and stability, while maintaining a light weight design. For this reason a wide stance ski configuration was selected. The skis keep the possibility of the aircraft tipping forward to a minimum while the wide stance allows for a stable aircraft around the roll axis. The third wheel will be placed at the rear of the fuselage on a swivel to allow for smooth turning on the ground as well. In order to maintain a light weight design the rods for the gears will consist of as much carbon fiber or other low density material as possible.

3.5 Early Stage Design

The final conceptual model shown in Figure 3-5 is a result of multiple iterations and changes made to the conceptual model. It shows the different designs and configurations envisioned in chronological order.

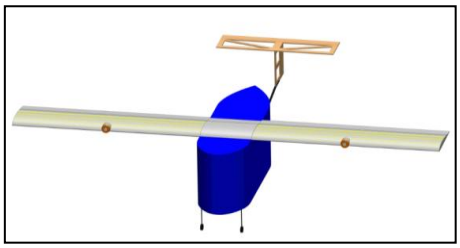

First conceptual model

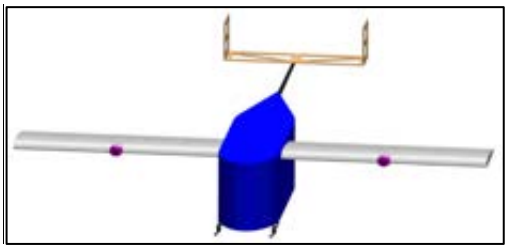

Second conceptual model

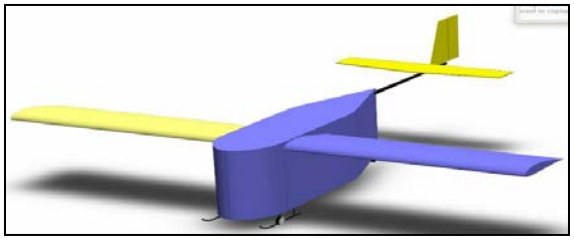

Third conceptual design

Figure 3-5: Conceptual Models

4. Preliminary Design

The conceptual design provides a great start to the project but the preliminary design is necessary to support and quantify the impact of the design choices. Preliminary design provides design guidance and confirmation using models and equations and to ensure progress towards the final design.

4.1 Analysis Methodology

Multiple tools were used to improve upon the conceptual design including a matching graph, speed vs. mission score estimates, static and dynamic stability analysis, and aerodynamic analysis. These tools helped determine the preliminary design of the aircraft.

4.1.2 Fuselage Design

The fuselage is designed to have a streamlined shape for minimal drag and to efficiently enclose the payloads for Missions 2 and 3. Once the configuration for the Emergency medical mission in Figure 5-2 was selected, it became clear that two blocks would fit into nearly the same fuselage volume with almost no adjustments. Keeping with our decision to focus more on light weight and success on the ferry flight and emergency medical mission, the fuselage was designed with a minimalistic approach. The basic design of the fuselage can be viewed in Figure 4-1.

Ttesting was completed to ensure that the flow over the fuselage stays attached by putting tufts on the aft end of the fuselage, and inducing a free stream velocity. The action experienced by the tufts was then observed to determine if the flow remained attached. This is discussed further in Section 7.

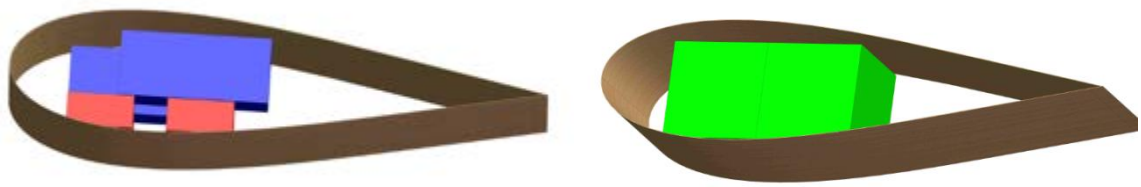

Figure 4-1: Basic Fuselage Shape with Mission 2 and Mission 3 payloads

4.1.3 Wing and Power Loading

A matching graph was constructed to help determine the minimum size of the aircraft. The graph provides the maximum power loading and wing loading required to meet the performance targets of the aircraft. The cruise speed, takeoff distance, and stall speed were all considered to help choose a design point. The necessary equations were derived in terms of wing loading and power loading in order to complete the calculations. Shown in Table 4-1 are some important estimates made.

Table 4-1: Design Assumptions Made in Calculations

Assumptions	
Oswald's Efficiency	0.83
Clmax	1.45
Clmax (flaps)	2
Propeller Efficiency	0.55
C_{do}	0.03
Runway Friction Coefficient	0.04
Wingspan	4ft

The assumptions made in Table 4-1 were educated guesses based on previous aircraft designs, as well as known data about this year's aircraft. The wingspan was adjusted a few times during the process of choosing a design point, and was continually adjusted based on the results shown in the matching graph. Flight testing and the actual final weight of the prototypes determined how much room was left to play with the aircraft's dimensions. The C_{do} was estimated to be 0.030 based on the fact that the fuselage is airfoil shaped and the overall configuration is no less streamlined than airplanes with similar documented drag values. It is known that the SJSU DBF airplane for 2012 had a calculated C_{do} of 0.022, and that the 2013 DBF airplane, a biplane with numerous intersections for the wings and empennage, had an estimated C_{do} of 0.043. Considering the dimensions of those two aircraft the estimated C_{do} of 0.030 appears reasonable. A detailed analysis of C_{do} is shown in Section 4.1.6.3. The $C_{L\text{-}max}$ with flaps value of 2 is likely on the conservative side given the installation of the flaps behind the propeller wake. These assumptions should leave a reasonable safety margin to account for uncertainties in the calculations.

The matching graph shown in Figure 4-2 was used to optimize the aircraft's performance for the third mission, during which the aircraft will be approximately 4.1 lbs and need to go as fast as possible through the 3 required laps. It must also have the capability to take off within 40 ft. The matching graph has the required wing loading and power loading for a cruise speed of 105 ft/s and a takeoff distance of 35 ft. with and without flaps. The graph also shows the requirements for a 40 ft. takeoff for comparison. The design point is marked by the star on the graph. This point is also good for Mission 1, which has similar speed requirements.

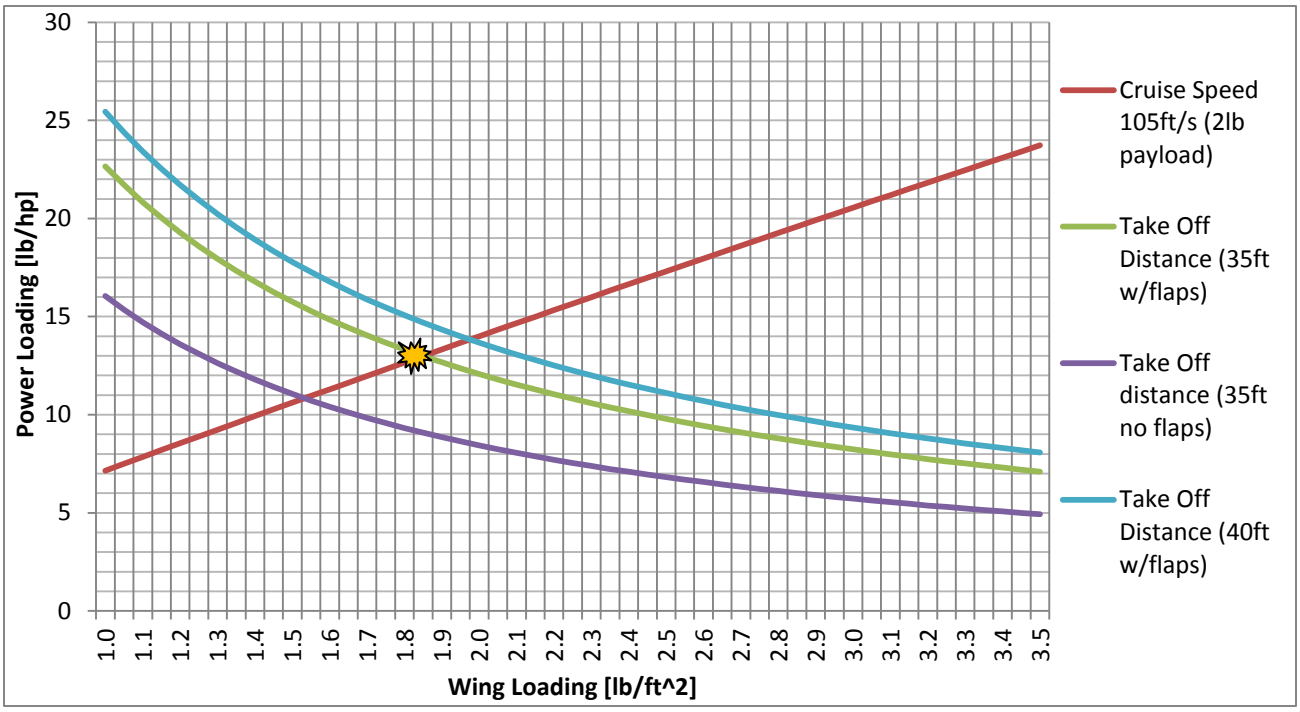

Figure 4-2: Matching Graph

The design point is at the intersection of the takeoff distance and the cruise speed of 105ft/s, marked by a star on the graph. This design point yields a wing loading of 1.85lbs/ft^2 and a power loading of 12.74 lbs/hp. Using the data provided from the matching graph, power loading and wing area, the individual components were selected and used to determine the weight of the aircraft. The aspect ratio and wing area obtained from the results are 7.22 and 2.22 ft^2 respectively. The aspect ratio was later optimized through flight testing to 6.97, and the wing area to 2.90 $ft^{2.}$ The matching graph provides better results for a take-off distance of 40ft, but we had to consider some safety margin to ensure takeoff within the allowable distance. The windy and relatively cool weather conditions in Wichita will likely help the aircraft take-off in a shorter distance but those are factors that shouldn't be counted upon for mission completion.

The weight and sizing estimation and the matching graph obtained provides a great starting point for the specific constrained design.

4.1.4 Empennage Sizing

An X-plot was used to size the horizontal stabilizer to a point that would ensure that the aircraft is longitudinally stable. In order to do this, the tail volume was varied until the aerodynamic center of the aircraft and the center of gravity were an appropriate distance from each other. The static margin at this point was 10.13%. The aerodynamic center is positioned aft of the center of gravity, which concurs with the general rules of static stability. Table 4-2 shows the data acquired and used in Figure 4-3.

Table 4-2: X-plot Data

Tail Volume	Aerodynamic center (%mac)	CG from front [inches]	cg (%mac)	Static Margin [%]
0.56	45	8.6	42	3.1
0.62	47	8.6	42	4.6
0.69	49	8.7	43	6.2
0.74	51	8.7	43	7.7
0.82	53	8.7	44	9.4
0.85	**54**	**8.7**	**44**	**10**
0.88	55	8.7	44	11
0.95	56	8.8	44	12

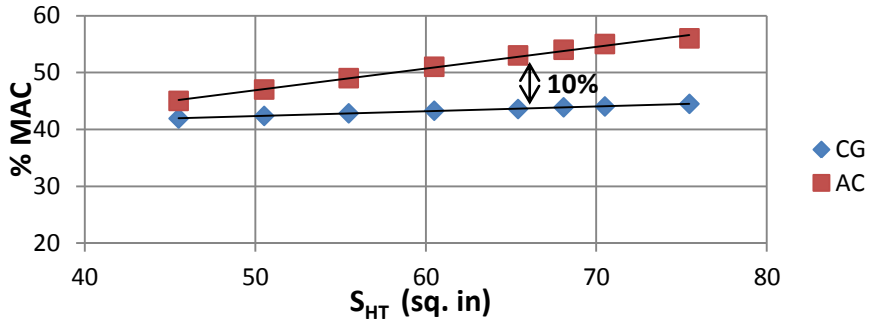

Figure 4-3: X-Plot To Determine The Area Of The Horizontal Tail

4.1.5 Propulsion System

The motor configuration, a twin-puller, was determined in the conceptual design. Selecting the right size motors was critical as over-sizing can lead to a weight and drag penalty. From the matching graph shown in Figure 4-2, it was determined that a realistic amount of power necessary is 240 Watts. After an extensive selection process it was determined that the Hacker A20-26m motors were the perfect fit for our aircraft. Another important factor is the battery sizing. The rule of thumb for 2/3A NiMH batteries is to add one cell for each desired volt. With the current limiting out of the battery at 15 Amps and the power desired being 240 watts two solutions were achieved. Either a single 16 cell battery pack would be used for both motors, with the 15 Amps being split in parallel to each motor and speed controller. This means that each motor could get a maximum of 7.5 amps and with the battery produce 120 Watts. The secondary solution is to split the battery into two 8 cell packs. This allows the motors, speed controllers, and batteries to be connected in series. This way 15 Amps could be run directly to each motor, and with the 8 cell pack 120 Watts would be produced at each motor. There are benefits to both solutions, as using a 16 cell battery pack allows the use of smaller speed controllers since the circuit is in parallel and a lower current goes through each speed controller. This saves weight, however, the physical limitations of the speed controllers are pushed and there is a larger risk of failure. The second solution adds weight to the aircraft, but substantially reduces the risk of motor failure during the missions. Due to the risk of motor failure, the use of two 8-cell battery packs in parallel configuration was selected as a baseline. This

choice was later validated by testing showing the parallel approach providing equal power to both motors more consistently.

4.1.6 Aerodynamic Analysis

The important aspects of a preliminary design are the lift, drag, and stability characteristics of the aircraft.

4.1.6.1 Wing and Airfoil Selection

The airfoil selection process involves the evaluation of several candidate airfoils using a 2D flow simulation for testing and making comparisons of these results, as well as other characteristics. Each of the selected airfoils was compared for a few critical factors including manufacturability, lift at low Reynolds numbers, and low drag at cruise angles of attack. The manufacturability of a selected airfoil means that the dimensions should make the wing possible to build, as well as structurally stable once built. A very thin airfoil makes wings difficult to construct since there will not be enough thickness for the internal structure. Efficiency at low Reynolds numbers is required to meet the take-off requirements. Lastly, a low drag design increases flight speeds and improves Mission 1 & 3 scores.

The Reynolds number has a significant impact on the effectiveness of an airfoil. For Mission 1 the Reynolds number is calculated for cruise speeds only, as it requires the fastest speed. Missions 2 and 3 are evaluated at take-off and climb conditions and have the same payload weight, so the Reynolds number will stay the same.

Table 4-3: Design Reynolds Number for Each Mission

Flight Condition	Reynolds Number
Mission 1 Cruise	315,000
Mission 2-3 Climb	146,000
Mission 2-3 Takeoff	123,000

4.1.6.2 Airfoil Analysis

The software packages used to analyze the airfoils were X-FOIL/XFLRS and JavaFoil. The airfoils selected for analysis are given in Table 4-4.

Table 4-4: Airfoil Parametric Analysis

Airfoils	α at Max C_l(deg.)	C_l Max	Cd	Min Cd	Max L/D
Eppler 193	8	1.15	0.024	0.0097	83.1
Clark-Y	12	1.56	0.019	0.0098	71.2
AG37	8	1.16	0.024	0.0199	48.0
E387	8	1.23	0.019	0.0099	93.8
GEO622	10	1.21	0.024	0.0070	75.6
GEO 623	14	1.64	0.047	0.0118	76.9
HQ258	6	0.88	0.041	0.0065	92.8
MH117	8	1.21	0.013	0.0073	98.2
NACA 2408	12	0.98	0.088	0.0064	57.7
S2048	8	1.10	0.018	0.0107	67.9
S2091	12	1.50	0.034	0.0081	94.5
S3021	8	1.16	0.018	0.0083	84.5
SD7037	10	1.32	0.023	0.0095	82.0

Based on the results from the simulations the S2091 gave the best characteristics for the overall mission specifications. The S2091 has a maximum coefficient of lift of about 1.5 and low coefficients of drag over varying angles of attack, giving a high lift to drag ratio.

Figure 4-4: S2091 Airfoil

The S2091 has the best C_{Lmax} and C_d for the design. Even though the C_{Lmax} didn't match the targeted 2.0 from the matching graph, takeoff requirements will be met successfully through the use of high lift devices and prop wash.

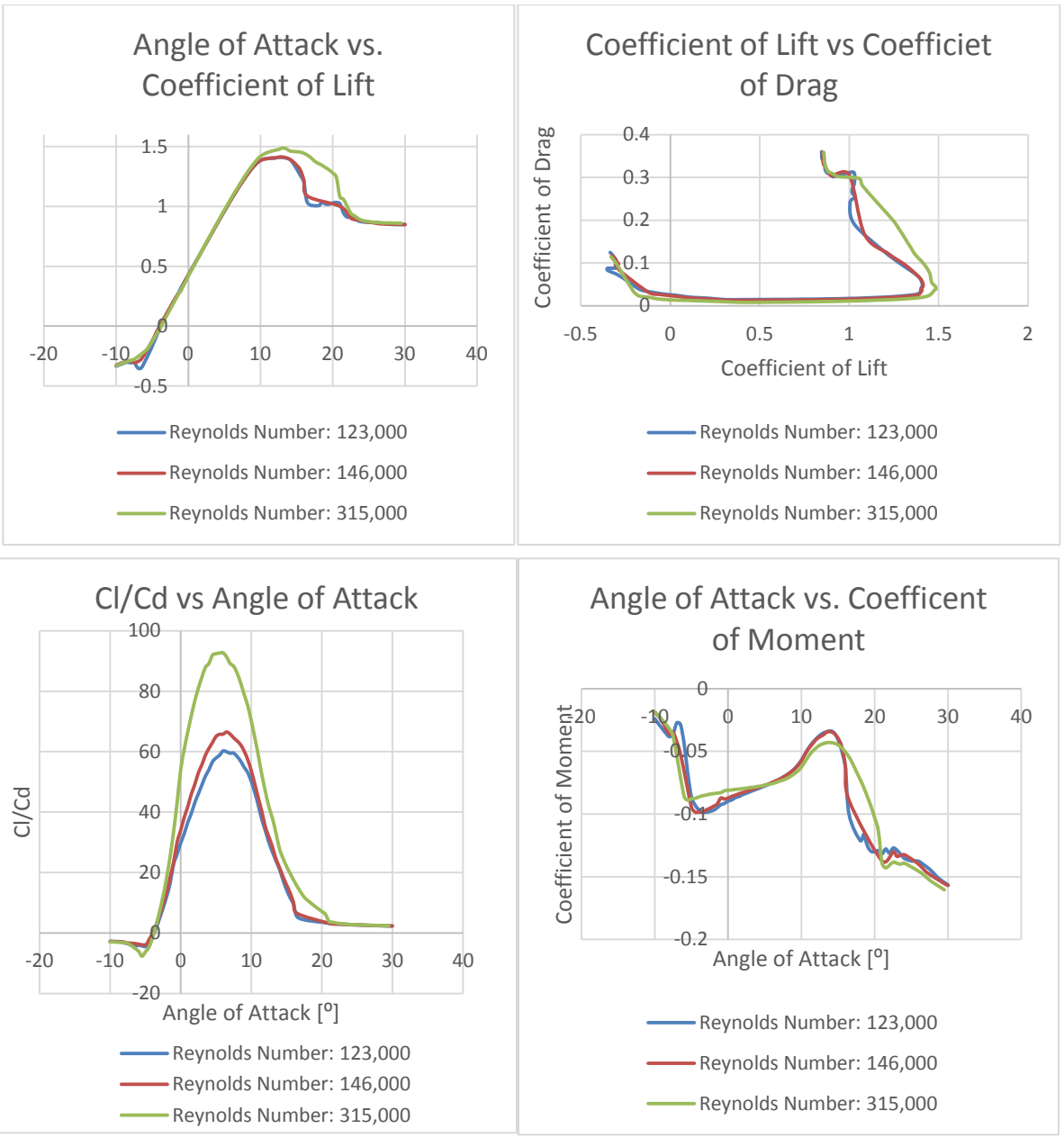

Figure 4-5: Shows The Lift, Drag, and Pitching Moment Curve For The Airfoil At Different Reynolds Numbers

4.1.6.3 Combined Component Drag Analysis

After analyzing the drag of the individual components, an estimation of the total drag can be obtained by summing the drag of all its components and incorporating interference drag. In this case the interference drag was considered to be 15% of the total drag. The values for each component are shown in Table 4-5.

Table 4-5: Zero Lift Drag of Each Component

Component	$C_{d,0}$
Wing	0.012
Fuselage	0.01
H-Stab	0.001
V-Stab	0.0008
Landing Gear	0.0009
Boom	0.0003
Motor 1	0.0001
Motor 2	0.0001
Sum	0.0252
Interference (15%)	0.00378
Total	0.02898

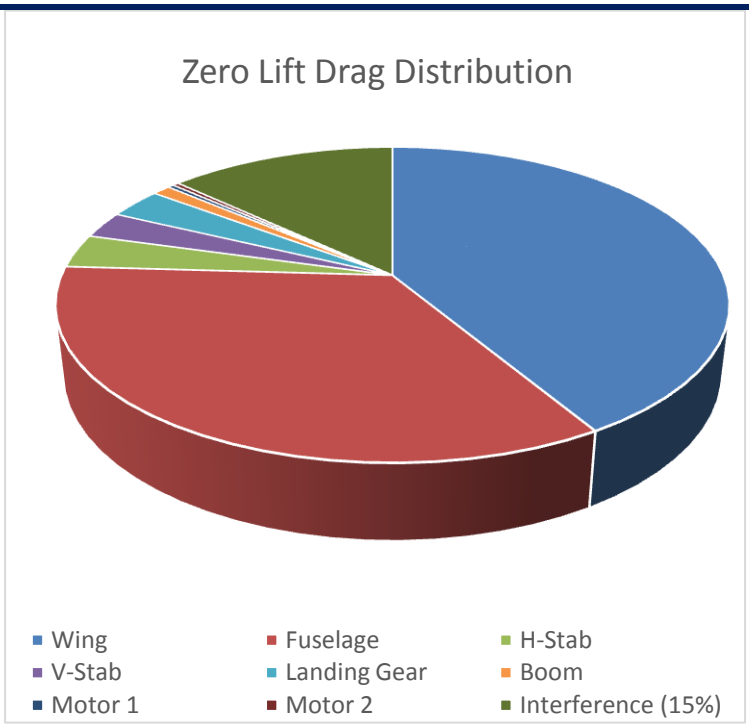

After summing the total drag of the components to get the zero lift drag of the aircraft, the drag polar can be established and analyzed. It is clear that the drag remains low during cruise which is very desirable for both of the speed missions. Figure 4-6 shows the aircraft's drag polar and Figure 4-7 shows the drag polar of the wing at takeoff and cruise conditions.

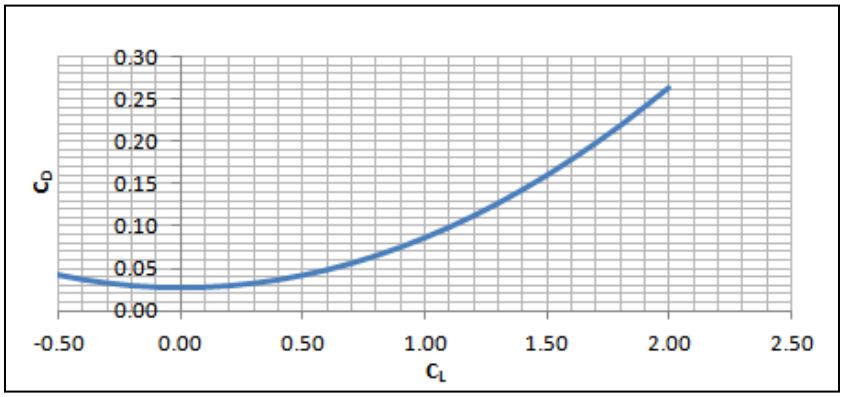

Figure 4-6: Drag Polar For the Entire Aircraft

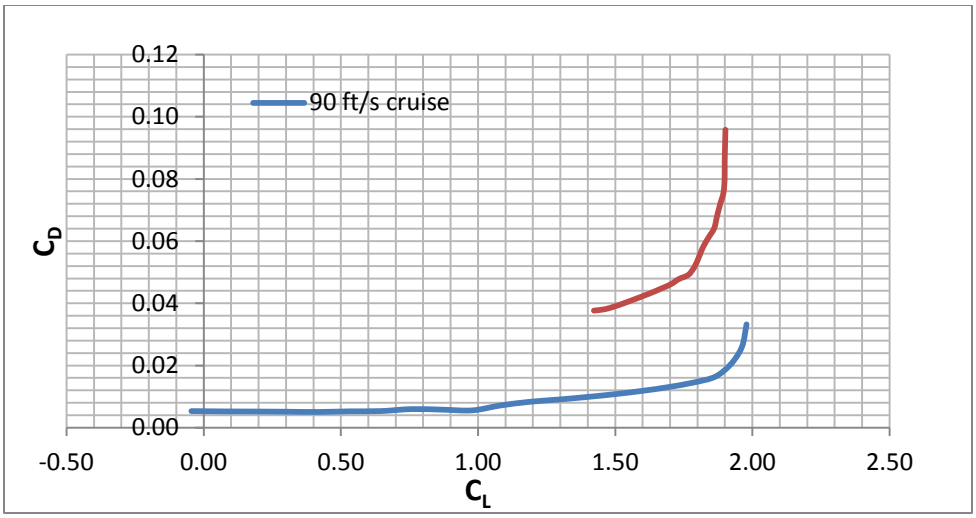

Figure 4-7: Wing Drag Polar At Cruise and Takeoff Conditions

Figure 4-7 also shows that the airplane generates more lift during cruise then at take-off. This is strictly because the use of flaps is offset by the lower Reynolds number at takeoff.

4.1.7 Longitudinal Dynamic Stability Analysis

The dynamic stability and frequency response to control inputs of the aircraft were evaluated using MatLab tools. Table 4-6 includes the aerodynamic data used for analysis.

Table 4-6: Aircraft Data Used to Calculate Airplane's Aerodynamic Coefficients

Designation	Value
$C_{L_{\alpha_w}}$	5.99/rad
$\bar{X}_{ac_w}$	0.25
η_h	0.85
$\frac{d\varepsilon}{d\alpha}$	0.40
$\bar{X}_{ac_h}$	4.70
$\bar{X}_{cg}$	0.40
S_h/S	0.19
$C_{L_{\alpha_h}}$	2.30/rad
e (Oswald's efficiency)	0.83
$C_{L\,cruise}$	0.17
Mach number	0.08
$\bar{V}_h$	0.85
$\frac{l_h}{\bar{c}}$	4.30

Table 4-7: List of Aerodynamic Coefficients

Coefficient	Value	Description
C_L	0.170	Coefficient of Lift at trim
C_D	0.029	Coefficient of Drag at trim
C_M	0	Coefficient of Moment at trim
C_{D_u}	0	Speed damping
C_{D_α}	0.049	-
$C_{T_{xu}}$	0	-
C_{L_u}	0.001	Mach effect on lift coefficient
C_{L_α}	2.650	-
$C_{L_{\dot{\alpha}}}$	1.333	-
C_{L_q}	3.257	-
C_{M_u}	0	No Mach tuck
C_{M_α}	-0.588	-
$C_{M_{\dot{\alpha}}}$	-5.720	-
C_{MT_u}	0	-
C_{MT_α}	0	-
C_{M_q}	-15.406	-
C_{L_η}	0.169	Lift due to stabilator deflection
C_{M_η}	-1.12	Pitching moment due to stabilator deflection
C_{D_η}	0	For trim condition (neglected)

Table 4-8: Dimensional Derivatives for Bode Plot Analysis

Dimensional Derivatives	Value
X_u	-0.059
X_q	0
X_w	0.123
X_{w_dot}	0
M_u	0
M_q	-8.436
M_w	-0.598
M_{w_dot}	-4.214
Z_u	-0.346
Z_q	-1.960
Z_w	-2.682
Z_{w_dot}	-0.979
X_{iH}	0
M_{iH}	-1.916
Z_{iH}	-0.444

The dimensional coefficients were calculated using the coefficient values from Table 4-7 and used to obtain Bode plots for the aircraft to analyze longitudinal dynamic stability of the aircraft. The dynamic stability analysis for the aircraft was done using cruise conditions at a velocity of 90ft/s. From the Transfer Functions given by Equations 5 to 8, the eigenvectors were calculated using MatLab. The values in Table 4-9 clearly show that the aircraft is dynamically stable in the longitudinal axis. That is,

the poles of the characteristic equation are located in the left-hand plane (LHP) of the real-imaginary plot. The first pair of Eigenvalues corresponds to the short-period mode, and the associated damping and natural frequency are listed alongside. The latter pair of complex roots corresponds to the Phugoid mode because they are much closer to the origin, and are also accompanied by their perspective damping and natural frequency values. To reiterate, all of this information says the aircraft is aerodynamically stable longitudinally, its dynamic stability is adequate and minor control changes will be considered if required after additional flight testing.

Transfer Functions - Continuous-time zero/pole/gain model:

$$\frac{u(s)}{\eta(s)} = \frac{-26.8215\ (s - 18.29)(s + 11.6)}{(s^2 + 0.05917s + 0.1822)(s^2 + 7.468s + 14.54)} \quad (5)$$

$$\frac{w(s)}{\eta(s)} = \frac{-92.3612\ (s + 28.97)(s^2 + 0.1277s + 0.2895)}{(s^2 + 0.05917s + 0.1822)(s^2 + 7.468s + 14.54)} \quad (6)$$

$$\frac{q(s)}{\eta(s)} = \frac{29.7171s\ (s + 5.914)(s + 0.1784)}{(s^2 + 0.05917s + 0.1822)(s^2 + 7.468s + 14.54)} \quad (7)$$

$$\frac{\theta(s)}{\eta(s)} = \frac{-29.7171\ (s + 5.914)\ (s + 0.1784)}{(s^2 + 0.05917s + 0.1822)(s^2 + 7.468s + 14.54)} \quad (8)$$

Table 4-9: Longitudinal Mode Eigenvalues and Associated Damping Ratio and Natural Frequency

Eigenvalue	Damping	Frequency (rad/s)
-3.73e+00 + 7.73e-01i	9.79e-01	3.81e+00
-3.73e+00 - 7.73e-01i	9.79e-01	3.81e+00
-2.96e-02 + 4.26e-01i	6.93e-02	4.27e-01
-2.96e-02 - 4.26e-01i	6.93e-02	4.27e-01

More analysis was conducted by investigating the eigenvectors and their amplitudes relative to each mode for longitudinal state dynamics. With the aid of MatLab it was observed that the Phugoid mode is dominant in u-dynamics while short-period mode is dominant for w- and q-dynamics (vertical speed / angle of attack and pitch rate).

From the bode plot in Figure 4-8, it could be seen that at very low frequencies, less than 0.01 rad/s, there is a gain of about 20dB. The 180 phase shift is a result of positive horizontal stabilator deflection which transfers to a nose down moment therefore a negative pitch. The large pitch angle produced for input near the Phugoid mode of the airplane can be neglected as the pilot will not be continuously commanding the aircraft at such low frequencies which take a long time to develop. The

pitch angle response falls back about 90 degrees after the Phugoid frequency which in essence allows the pilot to control the pitch rate of the aircraft and not the pitch angle directly. Controlling the pitch rate is a desired characteristic for real planes and is an adequate characteristic to have for remotely controlled aircraft as well.

As the frequency of inputs are increased to the short-period frequency (3.81 rad/s), the gain slopes down to zero and the phase margin continues to drop. This implies the aircraft will become more responsive and precise to input as input frequency increases up to the short-period mode. However, very high input frequencies (>8 rad/s) will result in limited response as the aircraft acts as an attenuator. The pitch rate response plot, Figure 4-9, also shows the pilots' direct control of the pitch rate of the aircraft for the frequencies of interest. The pitch rate remains in phase with the stabilator command from Phugoid to relatively high frequencies. It is desirable to have an aircraft closely follow pilot input while maintaining a similar order magnitude response for that input. This can be important for pitch rate response to the stabilator as good linear response would help prevent unwanted oscillations. Considering the results of the Bode plot analysis, the aircraft appears responsive enough for a load carrying aircraft.

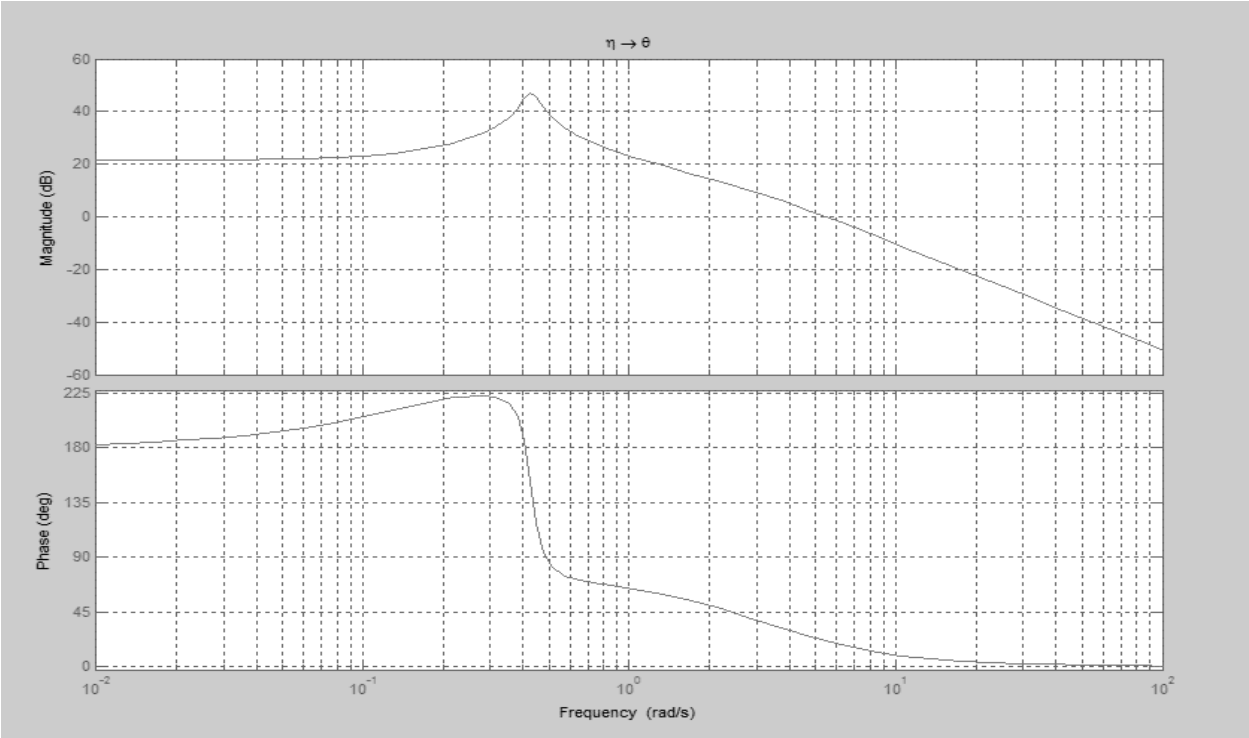

Figure 4-8: Pitch Attitude Response to Stabilator Input in Frequency Domain

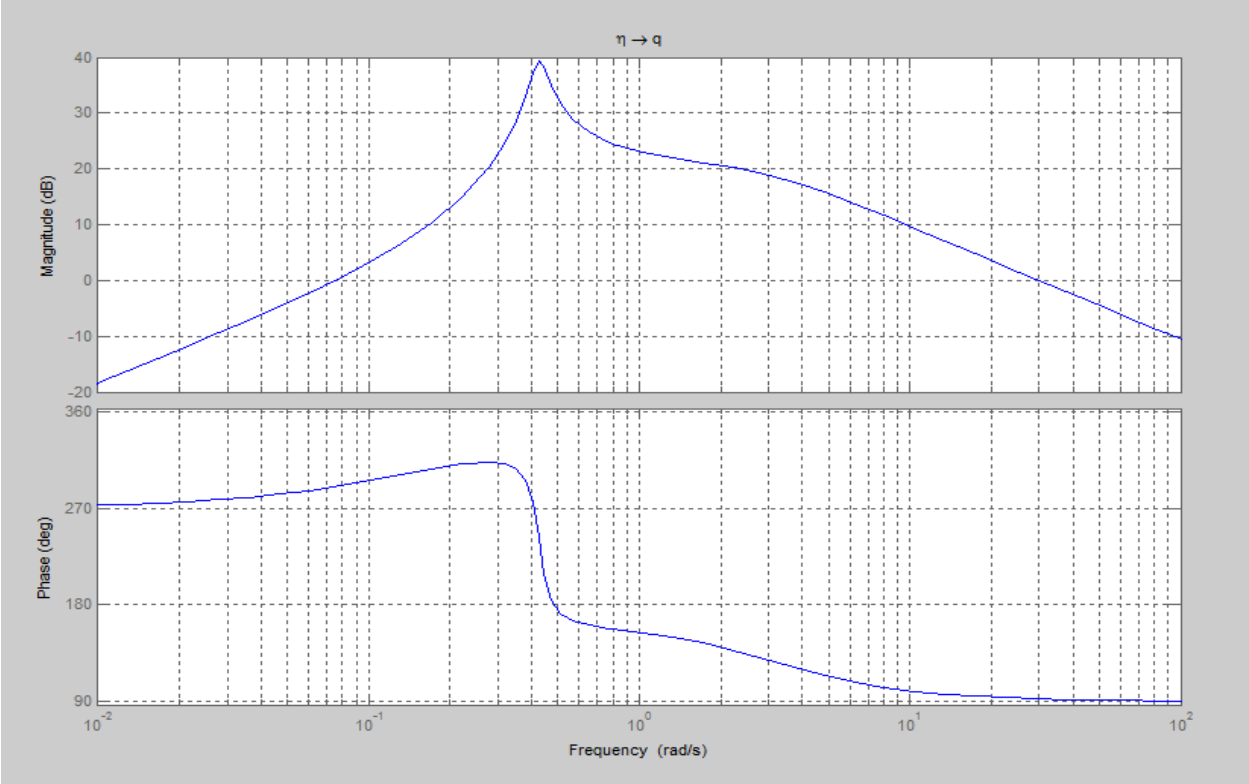

Figure 4-9: Pitch Rate Response to Stabilator Input in Frequency Domain

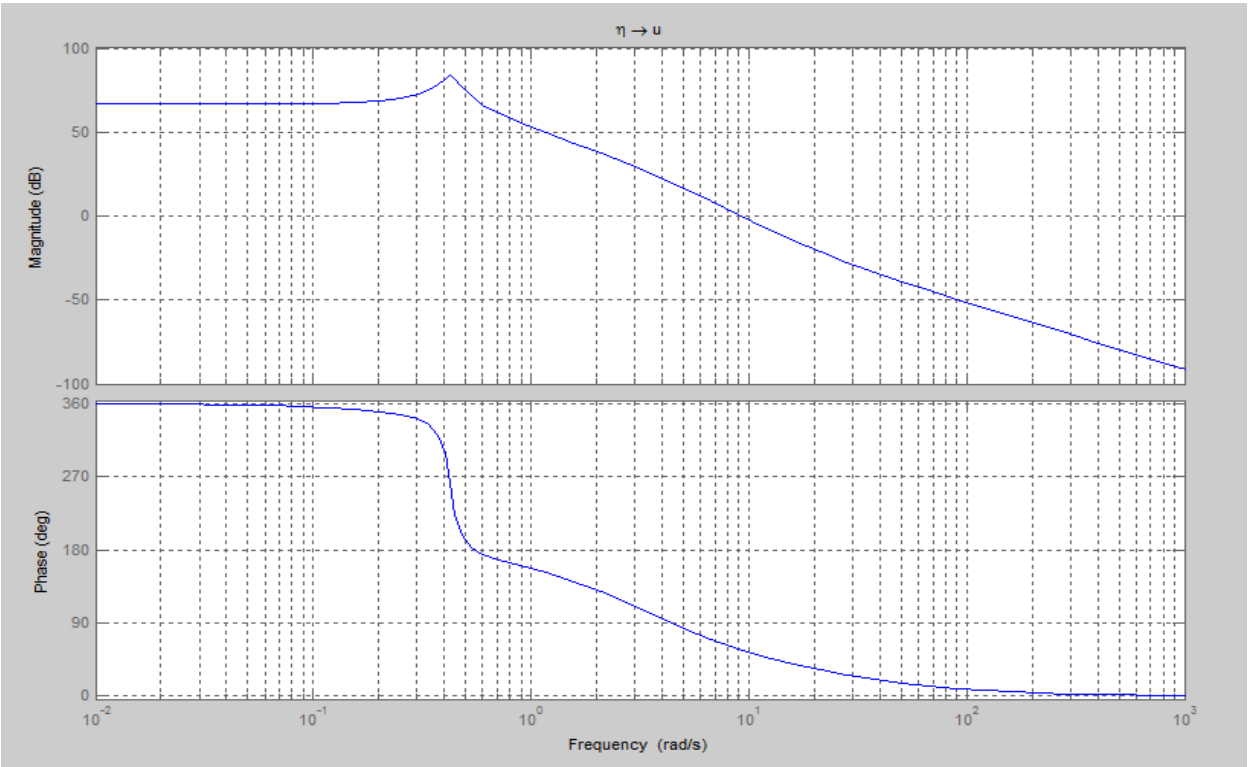

Figure 4-10: X-Component Velocity Response to Stabilator Input in Frequency Domain

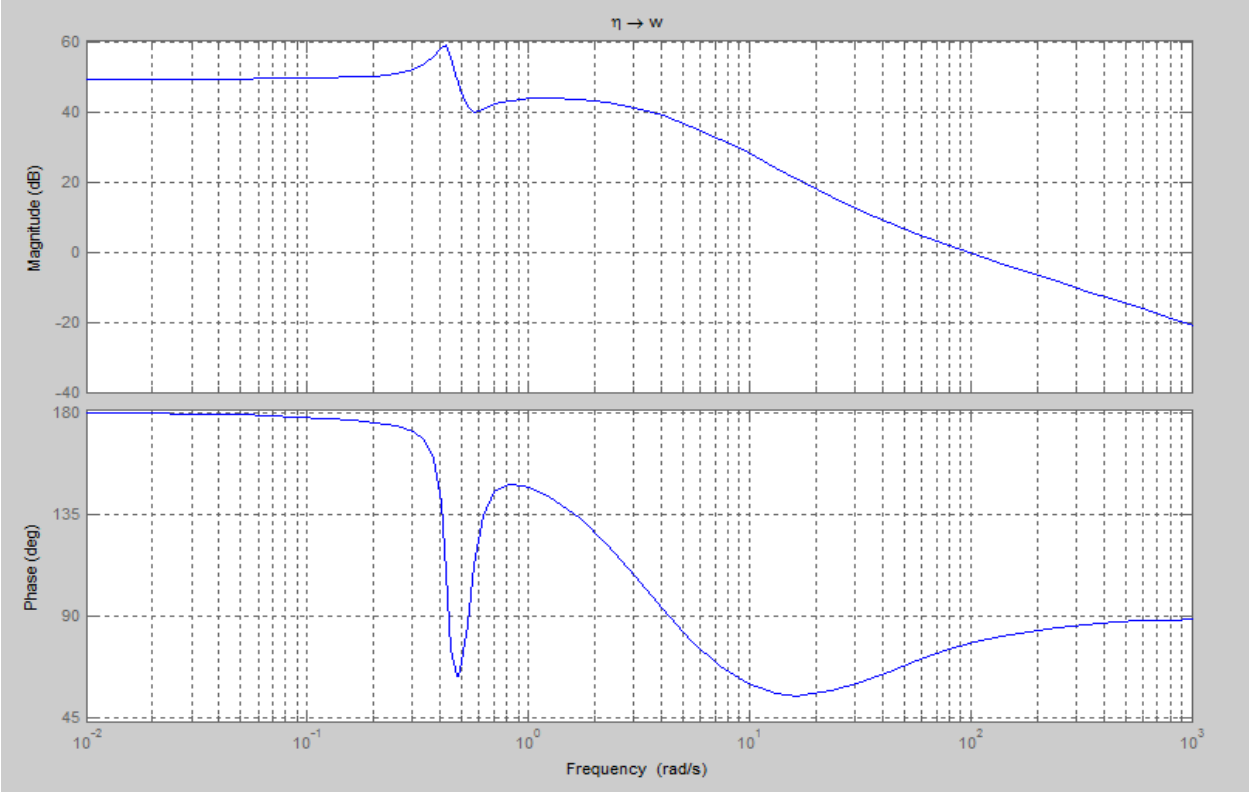

Figure 4-11: Z-Component Response to Stabilator Input in Frequency Domain

The Eigenvalues and the x-plot showed that the aircraft is very stable, the Phugoid mode damping was reasonable at 0.07, given the low frequency of this mode and the short duration of the flights. Additionally, the short period mode damping was 0.979 which is higher than typical, but not a bad start. Flight testing will determine whether fine tuning is required.

4.2 Design Trades

The aircraft's design was geared towards optimizing Missions 1 and 3. In Mission 3, which is worth the most of the three missions, the aircraft must carry a two pound payload. What resulted was an aircraft that can carry two pounds and take off within 35 ft, with a top speed of 105 ft/s. This will allow for very high scores on the first and third missions, but leave the team carrying only two pounds on Mission 2. It is not likely that other teams would carry much more weight on the second mission due to the significant increase in volume that accompanies the increase in payload. While carrying just two blocks on Mission 2 puts the score for that mission at risk, it is a calculated risk and will be compensated for improved performance in Missions 1 and 3, as well as reduced RAC.

Other trades include using a traditional empennage instead of the H-tail configuration, which sacrifices controllability for less weight and lower complexity. After testing it became clear that an H-tail was not a necessary addition. Also, opting for a light weight landing gear leads to a more difficult run at the taxi mission, however as long as the mission is completed this comes without a penalty.

4.3 Estimated Mission Performance

The aircraft was designed to be high scoring in the first and third missions, while completing Mission 2 with ease carrying two internal stores. The aircraft was sized to achieve a top speed of 105 ft/s with payload and the available power of 240 watts allows the aircraft to obtain such velocities for Missions 1 and 3. Table 4-10 shows the estimated scoring for all flight missions.

Table 4-10: Ferry Flight Lap Breakdown

Mission 1		Mission 2		Mission 3	
Empty Weight	2.10 lb	Loaded Weight	4.10 lb	Loaded Weight	4.10 lb
Cruise Velocity	90 ft/s	Cruise Velocity	80 ft/s	Cruise Velocity	80 ft/s
# Of Laps	8	# Of Laps	3	# Of Laps	3
Flight Time	4 mins	Flight Time	1 min 54 sec	Flight Time	1 min 54 sec
Estimated Score	1.75	Estimated Score	2	Estimated Score	5.25
Max. Empty Weight: 2.1 lbs					
Total Flight Score: 9					

The results of past DBF competitions show that 8 laps is a high number of laps for a ferry flight. This leads to the conclusion that our aircraft will be among the leaders in both the Ferry Flight and the Emergency medical mission. The estimated score for Mission 1 is 1.75 out of a possible 2 points, and the estimated score for Mission 3 is 5.25. Mission 2 will not be a high scoring mission for this aircraft, as it is only capable of carrying two blocks. It is difficult to foresee any aircraft carrying more than 4 blocks and not being very large and therefore uncompetitive. As a result, the estimation for Mission 2 is 2 points out of a possible 4. The overall goal for the competition is to get to a total score of 9 points. This, combined with the extremely light weight design of the aircraft should be enough to allow San José State to compete for 1st place.

4.4 Uncertainties

One primary concern that will have an effect on every single mission is the unknown weather conditions in Wichita, Kansas. Historically conditions at DBF competitions in Kansas have been fierce to say the least. The lightweight design puts the aircraft in danger if strong winds occur during the competition. These winds are difficult to replicate in California and therefore the actual performance of the aircraft will remain an uncertainty. In order to better understand the impact of wind on mission performance an estimate of the lap times as a result of different wind speeds was included in section 3.3. Experimental radio controlled aircraft are subject to numerous issues which affect performance. For example, battery preparation can significantly affect the power output, impacting speed and takeoff distance figures. The SJSU 2012 airplane experienced such battery issues, resulting in disappointing speed in the ferry mission. Conservative estimates for power, weight, and performance, as well as extensive testing, are being used to address the unknowns.

5. Detail Design

After concluding preliminary design, a detailed design effort was carried out to kick off the manufacturing process. This section concentrates on the dimensions of aircraft components, systems integration, weight and balance, and flight and mission performance approximations.

5.1 Dimensions

Detailed dimensions and parameters of the aircraft and control surfaces are shown in Table 5-1.

Table 5-1: Aircraft Dimensions

Main Wing		Vertical Stabilizer		Horizontal Stabilizer	
Airfoil	S2091	Airfoil	Flat Plate	Airfoil	Flat Plate
Span	54.0 in	Span	6.25 in	Span	18.4 in
Area	417.96 in^2	Area	19.2 in^2	Area	65.1 in^2
Aspect Ratio	6.97	Aspect Ratio	2.03	Aspect Ratio	5.32
δ_a	±25˚	δ_r	±30˚	δ_e	N/A
Incidence	3˚	Incidence	0˚	Incidence	±15˚
Aircraft Dimensions		**Electrical System**			
Fuselage Length	32.25 in	Power (max)	240 Watts		
Length	50.69 in	Motor	Hacker A20-26M		
Width	7.45 in	Batteries	NiMH Custom Packs		
Height	8.19 in	Cells	16-18		
Gross Weight	2.10 lbs				

5.2 Structural Capabilities

The aircraft is structurally designed to meet the basic wing tip test required by the competition rules. The main structures of the aircraft include a balsa wood wing spar strengthened using carbon fiber, carbon fiber and balsa wood fuselage stringers, and the tail boom. The structure has to be strong enough to carry the payload successfully while maintaining a low empty weight to minimize RAC. The materials used were determined by high strength to weight ratio such as carbon fiber and Kevlar. Weaker joints are reinforced with carbon fiber and Kevlar using epoxy.

The wing spar and boom combination is a critical component of the aircraft as it brings all other components together. The tail boom, which is connected to the fuselage using a bulk head, is completely made of carbon fiber. The boom connection is critical as the airplane will become unstable if the boom rips off in flight. The boom is attached towards the aft of the fuselage to provide clearance for loading payload and is shown in Figure 5-1. The carbon fiber fuselage stringers extend below the fuselage to safely mount the landing gear. The motor mounts are composed of plywood and attached to the wing ribs, as balsa wood lacks the strength to withhold the thrust loads created by each motor.

5.3 Systems and Subsystem Design

5.3.1 Fuselage

The airfoil shaped fuselage allows the aircraft to have low drag and good storing capabilities. The fuselage shape is specially designed using airfoil tools to achieve maximum laminar flow and thickness required to load internal payload. The notional shape of the fuselage is shown in Figure 5-1. This is a more streamlined shape compared to earlier fuselage designs and is being incorporated on the later prototypes.

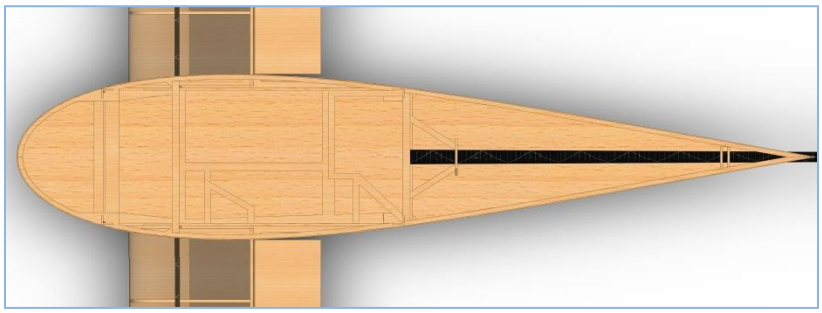

Figure 5-1: Custom Fuselage Design

The fuselage encloses the payload, the center wing spar, the boom and bulkhead attachment, and the electronics system. The wiring for the empennage servos and aileron servos has a designated path to maintain clearance. The payload area is sized to hold two cubes for Mission 2 and the required payload for Mission 3. The payload assembly is loaded from the top and secured using brackets. For Mission 3, the patients and attendants are assembled in a bunk bed configuration, shown in Figure 5-2, while allowing a 2” clearance above them as stated in the competition rules.

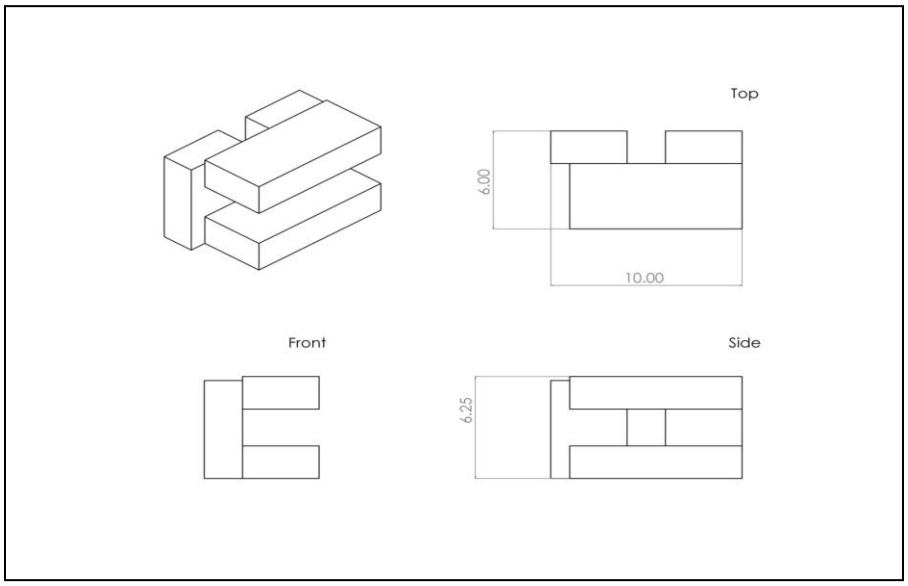

Figure 5-2: Mission 3 Payload Configuration

Additionally, the fuselage has 5 carbon fiber stringers which run vertically to add structural strength as well as holding the landing gear. The rear section of the fuselage holds two servos for the

stabilator and the rudder. They are placed internally to reduce overall drag and are connected using control rods. The battery pack is located at the nose of the aircraft to help shift the cg forward. The speed controllers, the fuses, and the receiver are placed at or near the top of the fuselage to provide easy access.

5.3.2 Main Wing

The main wing is designed to provide the optimal wing loading required to perform all missions. Since there were no restrictions on the wing configuration in the competition rules, the main wing has a wing span of 54 inches, with an aspect ratio of 6.97. The airplane has a high wing configuration to obtain the 2” clearance above the payload for mission 3 and ground clearance for taxi mission.

The main wing is constructed using a balsa wood spar capped with carbon fiber and 1/8” laser cut balsa wood ribs which help provide the airfoil shape. The airfoil used is a S2091 which provides acceptable stall characteristics and a favorable lift to drag ratio. The airfoil also provides a reasonably high maximum lift coefficient. The entire wing is covered with balsa sheets to enhance aerodynamic efficiency while taking a small weight penalty. The main spar is located at the quarter chord and is one of the strongest components of the aircraft to uphold the payload and aircraft weight.

The wing features full span flaperons to meet take-off requirements without incurring the weight of extra servos. The flaperons provide good controllability and enhance the lift characteristics of the wing while resulting in a minimal penalty in roll authority during take-off versus conventional ailerons.
The airplane features a dual motor configuration. The motors are mounted symmetrically into the wings using laser cut plywood mounts and are installed flush into the wing to reduce drag.

5.3.3 Propulsion System

The airplane is powered by 2 motors, both located on the wing leading edges. The motors chosen are Hacker A20-26m brushless motors. These were chosen based on their high power density and their ability to provide the required power to yield the target power loading from the matching graph.

Both motors spin counter clockwise when looking at the aircraft from the front. The benefits of having counter rotating props will be investigated before the competition and remain a pending action item for the propulsion team.

The propellers chosen for the aircraft are 9X7.5 APC-E. These propellers are ideal for the motor selection and they are efficient at providing flow over the wings. Larger APC propellers were tested and have been identified as potential candidates for the taxi and heavy lift missions as described in Section 8. The motor selection requires at least a 16 volt battery. This would require that at least 14 1.2 volt 2/3A NiMH cells be used, but a common rule of thumb is to assume 1 volt per cell, and therefore a 16 cell battery arrangement is being used.

5.3.4 Empennage

The empennage design of the aircraft is of conventional configuration, as shown in Figure 5-3. This design is effective in maintaining stability for the aircraft and provides good controllability.

The conventional tail configuration is easy to setup with the boom. The servo wires and control rods run on the inside of the boom which minimizes drag and uses empty space wisely. The boom is mounted towards the top of the fuselage to avoid the turbulent flow caused from the wake of the fuselage.

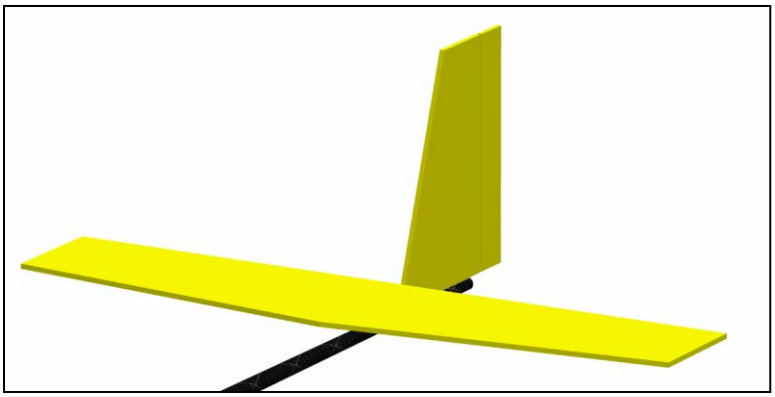

Figure 5-3: Empennage Design

The empennage is manufactured using 1/8" balsa wood. The horizontal stabilizer is used as a flying tail plane also known as a stabilator. This helps provide enhanced controllability and reduces intricacy of the design. Both the rudder and the stabilator are modeled as flat plates to minimize weight and complexity during the construction phase. The symmetrical airfoil in the empennage doesn't provide much improvement when compared to flat plate for small size remote controlled aircraft.

5.3.5 Landing Gear

The landing gear is very relevant for the competition, as failure to complete the rough field taxi mission would make winning the competition an extremely improbable event. Numerous different landing gear configurations were tested before choosing the final landing gear for the aircraft. The different configurations tested include: a conventional gear with a swivel back wheel; a combination of wheels and skis in the front with a swivel wheel in the rear; and a conventional car configuration with four wheels. A conventional tricycle gear had problems restarting on the taxi course once it had come to a stop. The conventional car configuration was too heavy and also experienced the similar problems as the tricycle gear.

Ultimately, the landing gear was constructed using a combination of skis and wheels in a conventional layout (main gear up front, auxiliary gear in the back). Many different variations were tested before the skis were sized and mounted for them to be effective. The ski/wheel combination along with differential thrust from the motors is used to successfully complete the taxi mission.

5.3.6 Control System and Electronics

The main focus while designing the control system and electronics package was low weight. Light weight components that provided the control authority required were chosen to improve the RAC and performance of the aircraft. The aircraft is equipped with a total of four Dymond D47 servos – two for the flaperons, one for the stabilator, and one for the rudder. The flaperons are equipped with individual servos

to eliminate linkages across the span of the wing. Ultimately, the servo package turned out to be relatively inexpensive and lightweight.

The receiver on board is the Spektrum AR 6260. It is a widely used receiver as it is light weight and provides broad range. The receiver is powered with a battery that provides power for up to ten minutes of flight time.

Two Castle Creations Phoenix 10 speed controllers control the motors on the aircraft. These speed controllers provide adequate performance within the power limitations. The Phoenix 25 speed controllers were considered, but were three times as heavy and therefore discarded. Finally, the control system is restricted by two 15 amp fuses because of the limitations provided from the competition rules. The details of each individual component are shown in Table 5-2.

Table 5-2: Control System and Electronics Choices

Component	Part Name
Wing Servos	Dymond D47
Empennage Servos	Dymond D47
Receiver	Spektrum AR6260
Receiver Battery	5-cell NiMH (180mAh)
Speed Controller	2x Phoenix 10
Battery	16-18 cell NiMH

5.3.7 Weight and Balance

Based on the contest rules, it is clear that the empty weight and performance are essential factors in the competition. Component breakdown and weight estimations using Solid Works resulted in an estimated empty weight of 2.10 lbs. Solid Works provided a good estimate of the aircraft structure while component weights were obtained from manufacturer's and used for initial estimations. The component breakdown is shown in Table 5-3 and is broken down into 3 sub-categories: control system, propulsion system, and airframe.

As shown in Table 5-3, the propulsion system accounts for 58.57% of the total empty weight. The airframe and control system are quite light relative to the propulsion system.

Table 5-3: Estimated Component Weights for the Aircraft

Controls	Weight (grams)	Weight (ounces)	Weight (lbs)	% Total
Aileron Servo 1	4.70	0.17	0.01	0.48
Aileron Servo 2	4.70	0.17	0.01	0.48
Elevator Servo	4.70	0.17	0.01	0.48
Rudder Servo	4.70	0.17	0.01	0.48
Receiver	5.50	0.19	0.01	0.48
Receiver Battery	28.00	0.99	0.06	2.86
ESC 1	6.00	0.21	0.01	0.48
ESC 2	6.00	0.21	0.01	0.48
			% Total	6.19
Propulsion				
Motor 1	42.00	1.48	0.09	4.29
Motor 2	42.00	1.48	0.09	4.29
Prop 1	16.00	0.56	0.04	1.90
Prop 2	16.00	0.56	0.04	1.90
Fuse	4.70	0.17	0.01	0.48
Main Battery	388.39	13.70	0.86	40.95
Battery Safety Margin	44.00	1.55	0.1	4.76
			% Total	58.57
Airframe				
Boom	13.60	0.45	0.03	1.43
Wing	140.61	4.96	0.31	14.76
Fuselage	98.40	3.47	0.22	10.48
Landing Gear	45.36	1.60	0.1	4.76
Empennage	36.29	1.28	0.08	3.81
			% Total	35.24
		Total (lbs) =	2.10	

Table 5-4: Inertia Properties for the Aircraft

	No Payload	Max Payload
Weight (lbs)	2.1	4.1
Ixx (lb*in2)	49.4	70.7
Iyy (lb*in2)	70.7	150
Izz (lb*in2)	146	219

Table 5-4 shows the inertia properties used to analyze the stability and controls of the aircraft. The inertia properties were obtained through SolidWorks. The C.G. location for each mission was recorded in Table 5-5 and broken down for individual components. The C.G. location for the aircraft was

limited forwards and aft by stabilator controllability and static margin requirements to achieve desired static stability. All C.G. distances are measured from the nose of the aircraft.

Table 5-5: Weight and Balance Table

	Mission 1			Mission 2			Mission 3		
Component	Weight (lbs)	C.G. Location (in)	Moment (lb-in)	Weight (lbs)	C.G. Location (in)	Moment (lb-in)	Weight (lbs)	C.G. Location (in)	Moment (lb-in)
Aileron Servo 1	0.01	8.05	0.08	0.01	8.05	0.08	0.01	8.05	0.08
Aileron Servo 2	0.01	8.05	0.08	0.01	8.05	0.08	0.01	8.05	0.08
Elevator Servo	0.01	22.40	0.23	0.01	22.40	0.23	0.01	22.40	0.23
Rudder Servo	0.01	22.40	0.23	0.01	22.40	0.23	0.01	22.40	0.23
Receiver	0.01	3.10	0.04	0.01	3.10	0.04	0.01	3.10	0.04
Receiver Battery	0.06	1.95	0.12	0.06	1.95	0.12	0.06	1.95	0.12
ESC 1	0.01	1.96	0.03	0.01	1.96	0.03	0.01	1.96	0.03
ESC 2	0.01	1.96	0.03	0.01	1.96	0.03	0.01	1.96	0.03
Motor 1	0.09	6.20	0.57	0.09	6.20	0.57	0.09	6.20	0.57
Motor 2	0.09	6.20	0.57	0.09	6.20	0.57	0.09	6.20	0.57
Prop 1	0.04	4.98	0.18	0.04	4.98	0.18	0.04	4.98	0.18
Prop 2	0.04	4.98	0.18	0.04	4.98	0.18	0.04	4.98	0.18
Fuse	0.01	5.13	0.05	0.01	5.13	0.05	0.01	5.13	0.05
Main Battery	0.86	8.80	7.54	0.86	0.87	0.75	0.86	0.87	0.75
Boom	0.03	29.95	0.90	0.03	29.95	0.90	0.03	29.95	0.90
Wing	0.31	8.75	2.71	0.31	8.75	2.71	0.31	8.75	2.71
Fuselage	0.22	10.03	2.18	0.22	10.03	2.18	0.22	10.03	2.18
Landing Gear	0.10	6.20	0.62	0.10	6.20	0.62	0.10	6.20	0.62
Empennage	0.08	38.49	3.08	0.08	38.49	3.08	0.08	38.49	3.08
Battery Safety Margin	0.10	-	-	0.10	-	-	0.10	-	-
Payload	-	-	-	2.00	9.34	18.68	2.00	9.03	18.06
Total	2.101	-	19.41	4.10	-	31.31	4.10	-	30.69
Aircraft C.G	8.70"			8.72”			8.59"		

Because of the simplicity in the RAC for 2013-2014 DBF competition, the RAC is estimated to be 2.10. A RAC of 2.10 or less will allow the aircraft to be extremely competitive assuming it attains reasonable mission performance.

5.4 Expected Flight Performance

The performance of the aircraft is analyzed using basic aerodynamic coefficient data and other aircraft data presented in Table 5-6. Aerodynamic coefficients are not affected between missions since the exterior of the aircraft does not change throughout the competition.

Table 5-6: Aircraft Parameters

Performance Parameter	Mission 1	Mission 2	Mission 3
Flight Weight (lbs)	2.1	4.1	4.1
$C_{L,max}$ with flaps	2.0	2.0	2.0
e	0.83	0.83	0.83
$C_{D,0}$	0.027	0.027	0.027
Min. Takeoff Distance (ft)	20	30	30
$(L/D)_{max}$	12.2	12.2	12.2
Max. Speed (ft/s)	105	95	95
Level Cruise Speed (ft/s)	90	80	80

5.4.1 Taxi Mission

A successful taxi mission is required if any team wants to have any shot at winning the competition. As stated above, the landing gear on the aircraft is chosen highly dependent on taxi mission performance. The taxi mission is a pass or fail mission and continuous testing has helped secure a successful taxi mission.

5.4.2 Mission 1 – Ferry Flight

The performance breakdown for ferry flight is recorded in Table 5-7. This helps estimate the number of laps our aircraft will record within the four-minute time limit. The power calculations required for choosing the propulsion system were done using the data estimated in Table 5-6, as the team decided to target 8 laps.

Table 5-7: Detailed Mission 1 Performance

Lap 1		Consequent Laps	
Maneuver	**Time (s)**	**Maneuver**	**Time (s)**
Takeoff	3	500ft dash	5
Climb	4	First 180 Turn	3
First 180 Turn	3	1,000' dash	9
1,000' dash	9	360 turn	4
360 Turn	4	Second 180 turn	3
Second 180 Turn	3	500' dash	5
500' dash	5	-	-
Total	31	**Total**	29
Number of Laps: 8		**Total Time = 3.9 mins**	

5.4.3 *Mission 2 – Maximum Load Mission*

Mission 2 is a max cargo mission and is scored based on the number of 6”x6”x6” cubes stored inside the aircraft. The internal payload consists of 2 blocks ballasted to 1 lb each. Two blocks were chosen to avoid extra weight and drag penalty that would come from carrying additional blocks. This also maintains the 2 lb minimum payload required and allows for similar performance for Missions 2 and 3. Mission 2 was rated as the least important mission in the scoring analysis as designing for Mission 2 specifically will hurt Mission 1 and Mission 3 scoring. The flight weight for Mission 2 is estimated to be 4.1 pounds.

5.4.4 *Mission 3 – Emergency Medical Mission*

Mission 3 is similar to Mission 1 in that it calls for a speedy aircraft. The mission is scored based on the time it takes the aircraft to successfully complete 3 laps with internal payload. The payload required for Mission 3 consists of 2 patients and 2 attendants, each ballasted to 0.5 lbs, totaling 2 lbs. The flight weight is determined to be 4.1 lbs, equivalent to Mission 2. The performance breakdown for this mission is shown in Table 5-8.

Table 5-8: Detailed Mission 3 Performance Breakdown

Lap 1		**Consequent Laps**	
Maneuver	**Time (s)**	**Maneuver**	**Time (s)**
Takeoff	4	500ft dash	7
Climb	5	First 180 Turn	3
First 180 Turn	3	1,000' dash	12
1,000' dash	12	360 turn	6
360 Turn	6	Second 180 turn	3
Second 180 Turn	3	500' dash	7
500' dash	7	-	-
Total	40	**Total**	38
Number of Laps: 3		**Total Time = 1.9 mins**	

5.4.5 *Mission Flight Score Summary*

Assuming that the aircraft lap times are 88% of the fastest aircraft at the competition’s laps and the maximum number of cubes carried is 4 by any team, the expected flight score is 9 and shown in Table 5-9. A total score of 9 points with a low RAC will allow San José State University to compete for first place in the contest.

Table 5-9: Flight Score Breakdown

Mission	**Score**
Mission 1	1.75
Mission 2	2
Mission 3	5.25
Final Flight Score: 9	

5.5 Drawing Package

A comprehensive drawing package for the aircraft is presented in this section. The drawing package is generated using SolidWorks and includes: three view drawing of the aircraft, its structural arrangement, systems layout drawing, and payload accommodation for different missions.

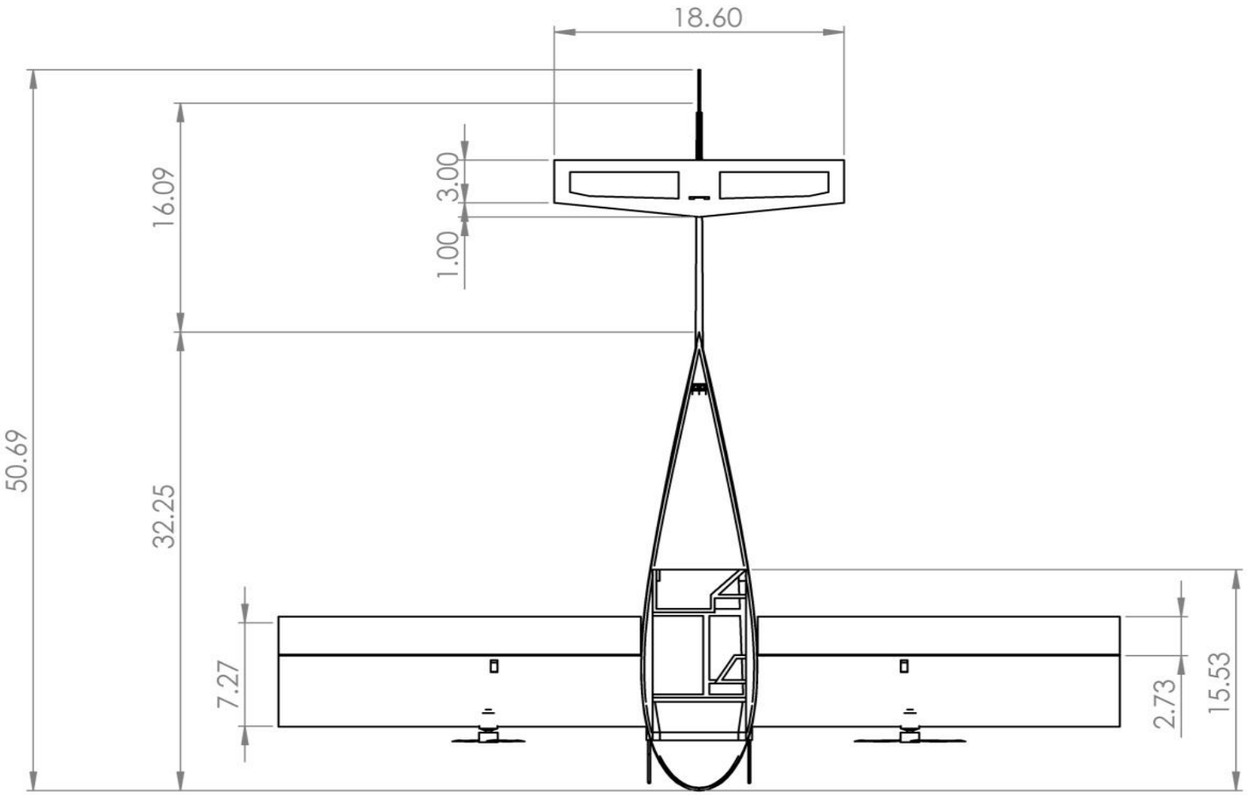

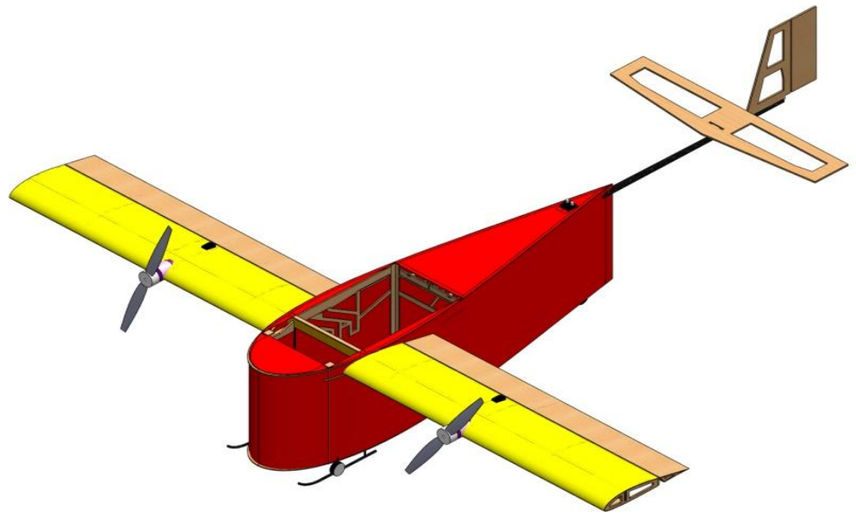

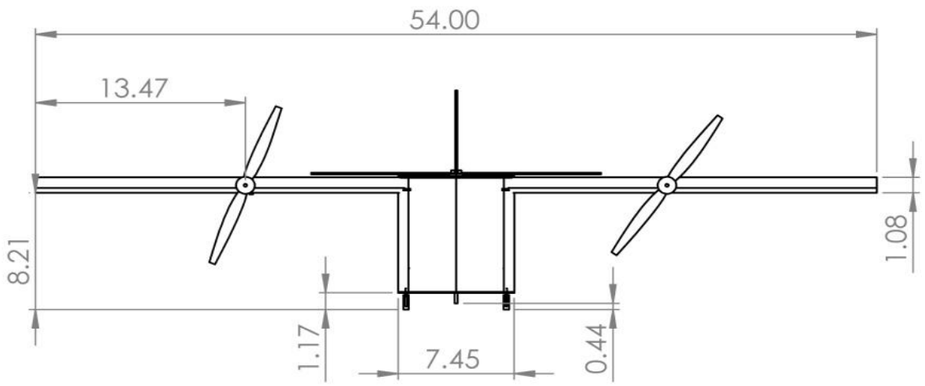

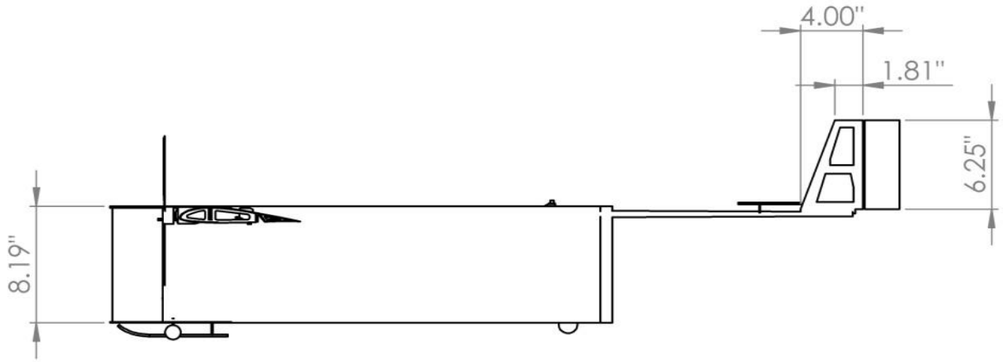

SCHOOL: SAN JOSE STATE UNIVERSITY

UNLESS OTHERWISE SPECIFIED:
DIMENSIONS ARE IN INCHES

Cessna AIAA - Design/Build/Fly 2014

TITLE: 3-VIEW

DWG NO. 1

SCALE 1:10

SHEET 1 OF 5

	PART	DESCRIPTION	QTY
1	MOTOR BATTERY	ELITE 1500 NiMh	16
2	RECEIVER	SPEKTRUM AR6210	1
3	SPEED CONTROLLER	PHOENIX 25	2
4	RECEIVER BATTERY	KAN 400 mAh	1
5	MOTOR	HACKER A20-26M	2
6	PROPELLER	APC 9X9	2
7	AILERON SERVO	DYMOND D47	2
8	ELEVATOR SERVO	DYMOND D47	1
9	RUDDER SERVO	DYMOND D47	1

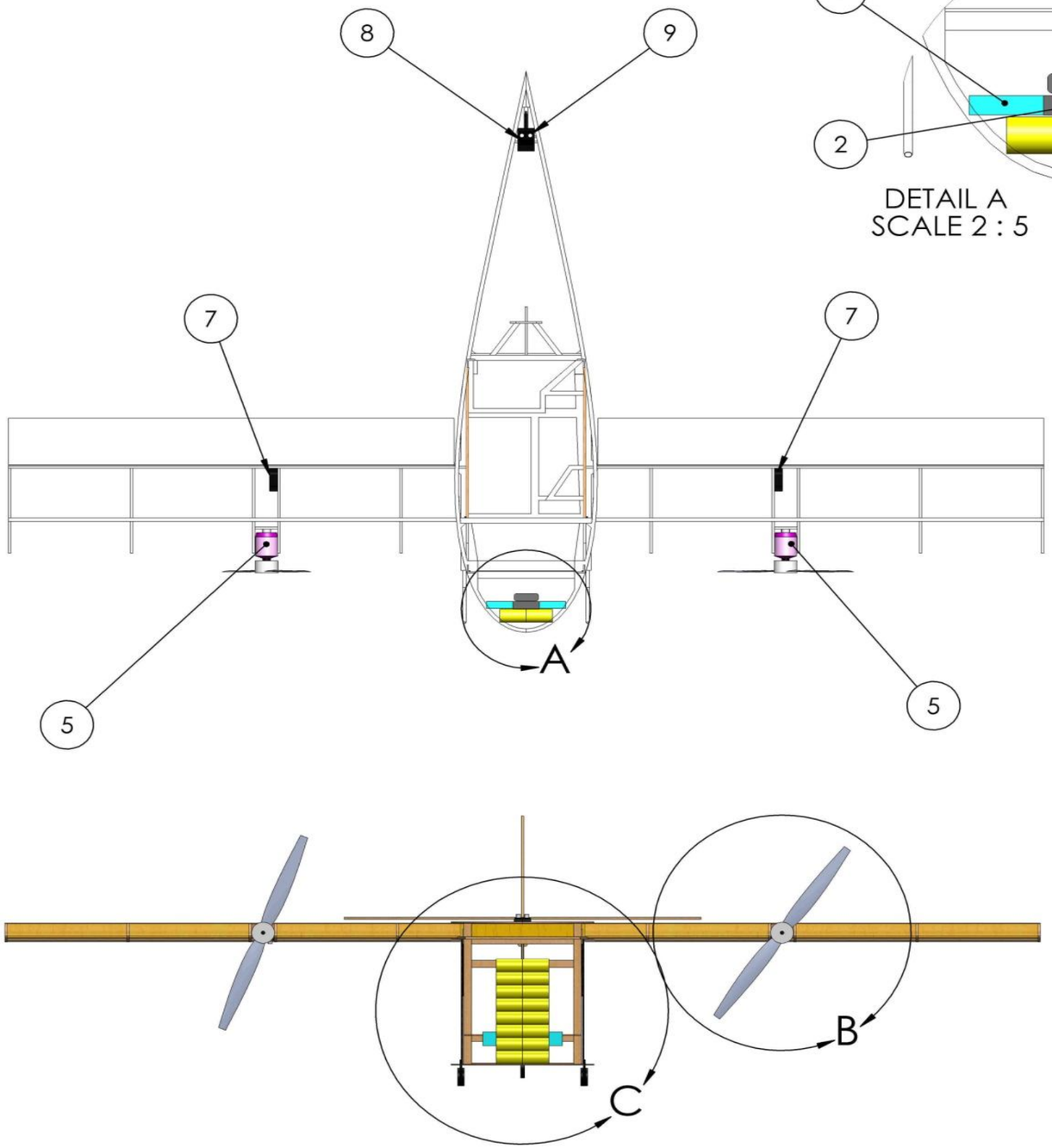

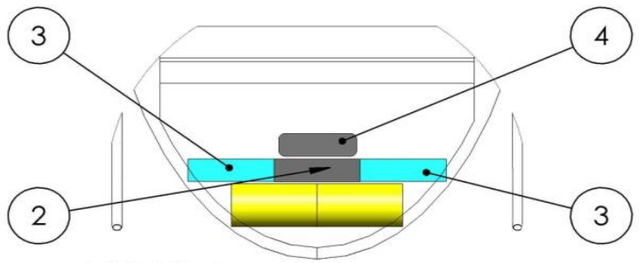

DETAIL A
SCALE 2 : 5

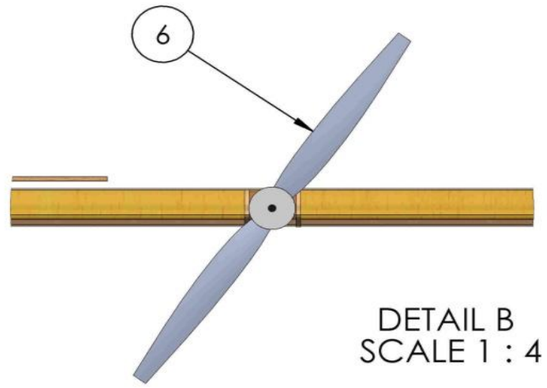

DETAIL B
SCALE 1 : 4

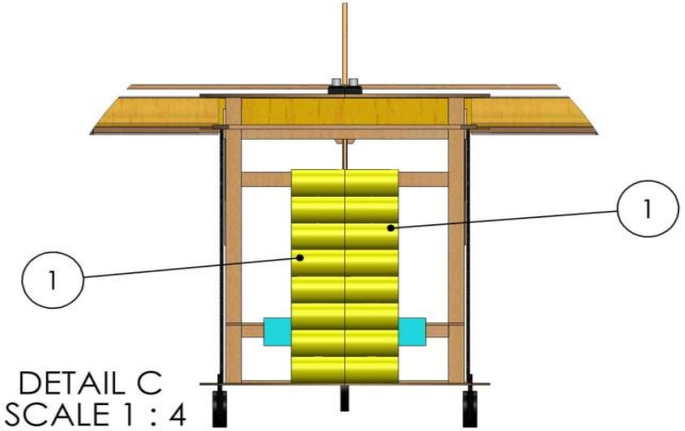

DETAIL C
SCALE 1 : 4

SCHOOL: SAN JOSE STATE UNIVERSITY

UNLESS OTHERWISE SPECIFIED:
DIMENSIONS ARE IN INCHES

Cessna AIAA - Design/Build/Fly 2014

TITLE:
SYSTEMS LAYOUT/LOCATIONS

DWG NO. 2

SCALE 1:20

SHEET 2 OF 5

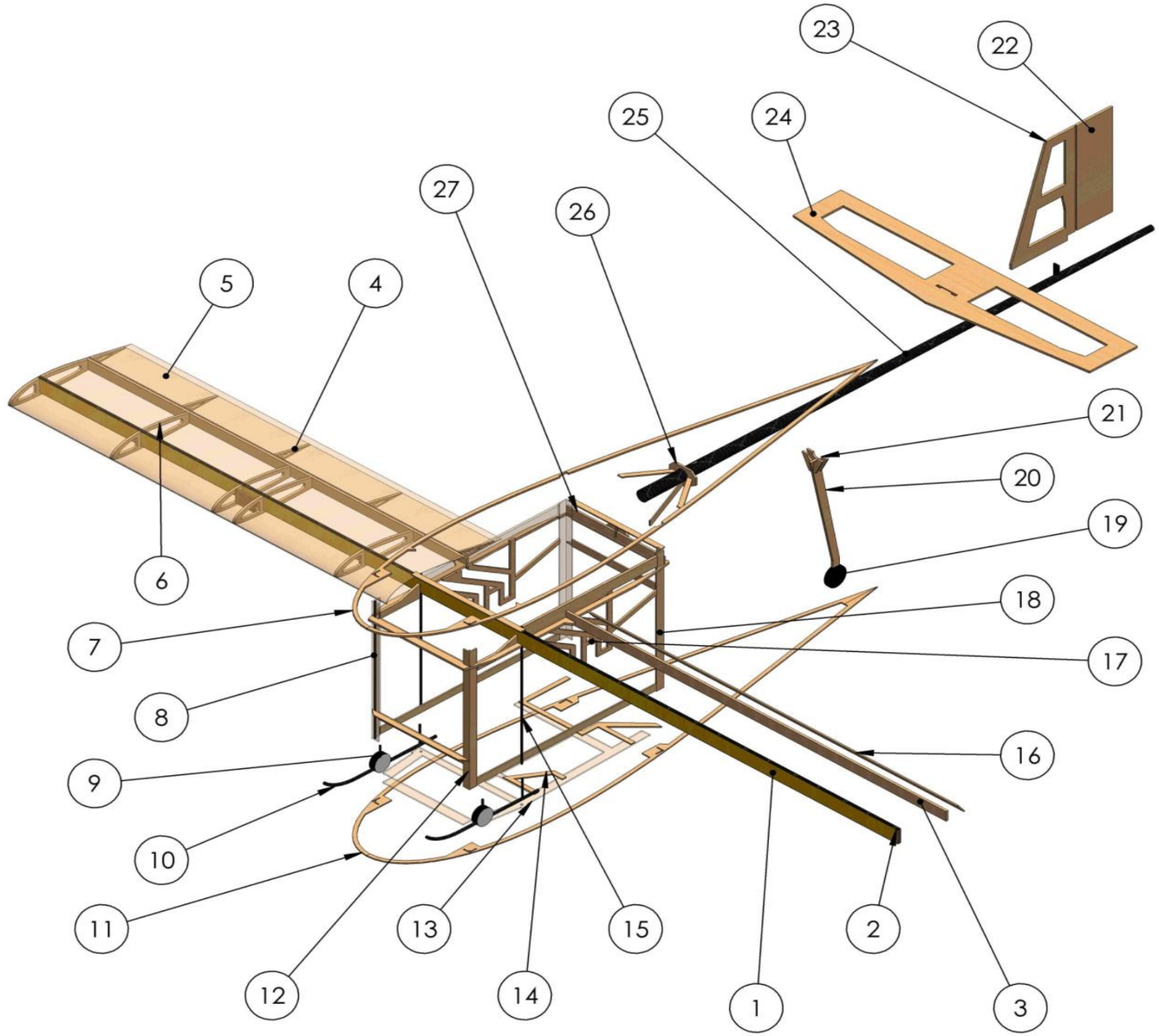

	PART	MATERIAL	QTY.
1	WING MAIN SPAR	BALSA	2
2	SPAR STRIP	CARBON FIBER	2
3	WING REAR SPAR	BALSA	2
4	AILERON RIB	BALSA	8
5	AILERON SKIN	BALSA	2
6	WING RIB	BALSA	8
7	TOP FUSELAGE RIB	BALSA	1
8	FRONT FUSELAGE STRINGER	CARBON FIBER	2
9	FRONT LANDING GEAR	COMPOSITE	2
10	SKI	COMPOSITE	2
11	BOTTOM FUSELAGE RIB	BALSA	1
12	FRONT SUPPORT	BALSA	2
13	PAYLOAD SUPPORT	BALSA	1
14	PAYLOAD GUIDE SUPPORT	BALSA	1
15	REAR FUSELAGE STRINGER	CARBON FIBER	2
16	AILERON SPAR	BALSA	2
17	PAYLOAD RISER SUPPORT	BALSA	2
18	REAR SUPPORT	BALSA	2
19	REAR LANDING GEAR	COMPOSITE	1
20	LANDING GEAR SUPPORT	BALSA	1
21	LANDING GEAR BOOM SUPPORT	BALSA	1
22	RUDDER	BALSA	1
23	VERTICAL STABILIZER	BALSA	1
24	HORIZONTAL STABILIZER	BALSA	1
25	BOOM	CARBON FIBER	1
26	BOOM ATTACHMENT	BALSA	1
27	BOOM SUPPORT	BALSA	1

SCHOOL: SAN JOSE STATE UNIVERSITY

UNLESS OTHERWISE SPECIFIED:
DIMENSIONS ARE IN INCHES

Cessna AIAA - Design/Build/Fly 2014

TITLE:
STRUCTURAL ARRANGEMENT

DWG NO. 3

SCALE 1:20

SHEET 3 OF 5

PAYLOAD CONFIGURATION

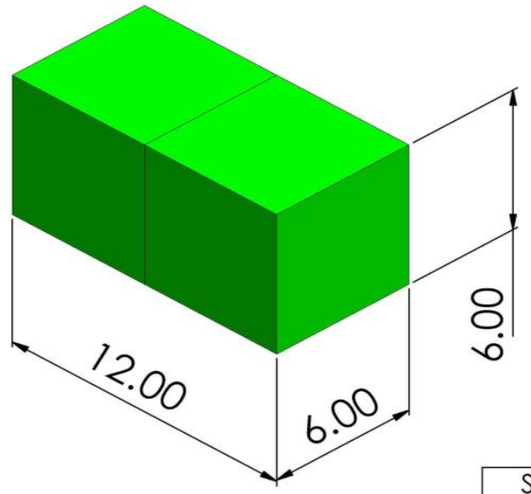

SINGLE BLOCK WEIGHT	1 LBS
TOTAL PAYLOAD WEIGHT	2 LBS

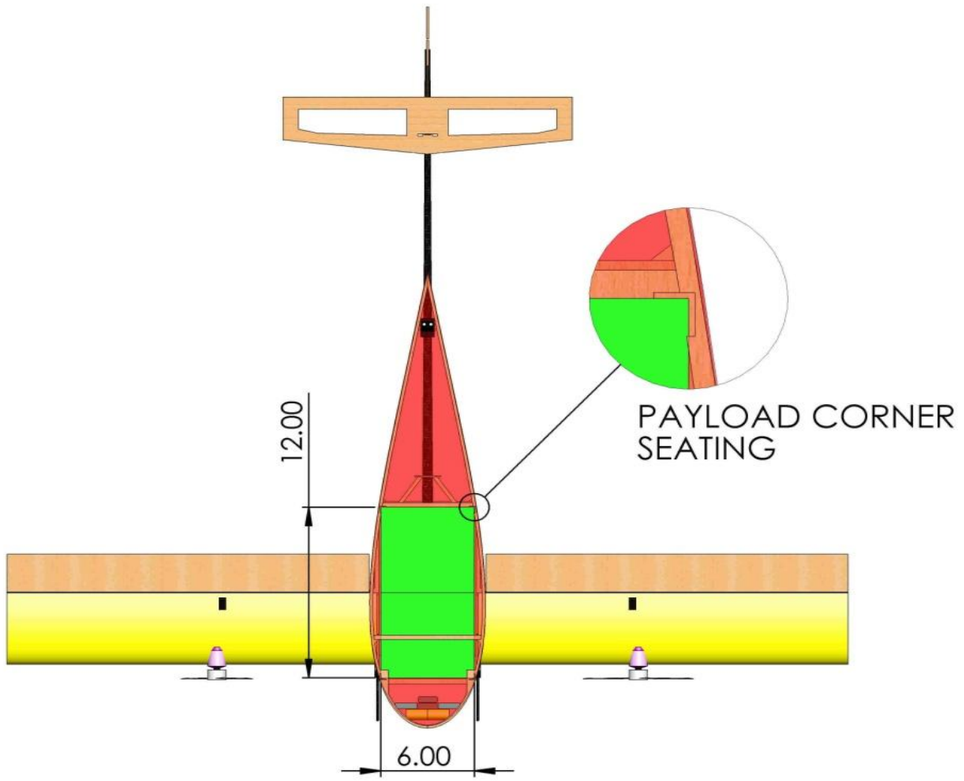

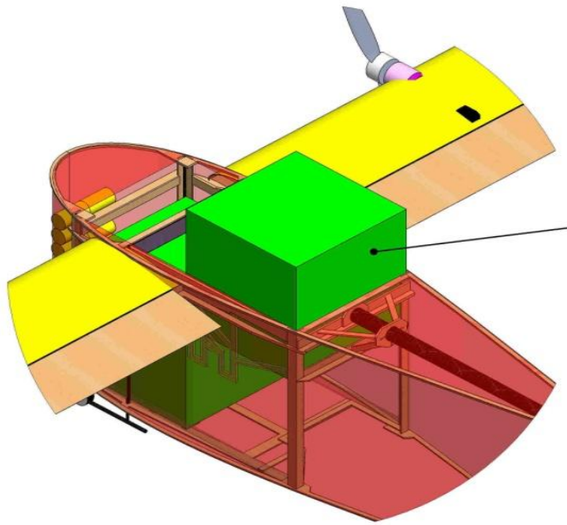

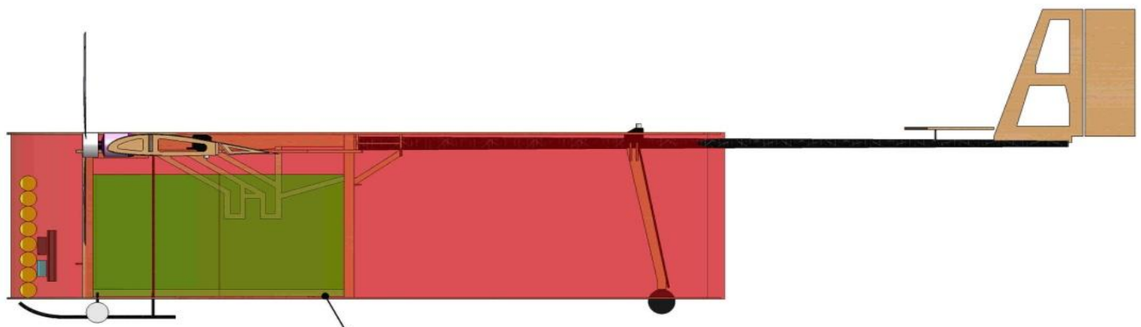

SCHOOL: SAN JOSE STATE UNIVERSITY

UNLESS OTHERWISE SPECIFIED:
DIMENSIONS ARE IN INCHES

Cessna AIAA - Design/Build/Fly 2014

TITLE:
6x6x6 PAYLOAD ACCOMODATION

DWG NO. 4

SCALE 1:20

SHEET 4 OF 5

PAYLOAD CONFIGURATION

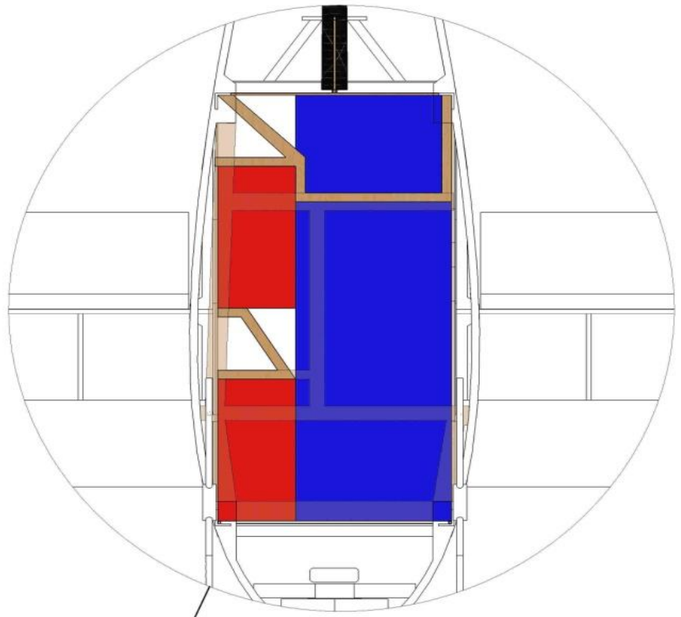

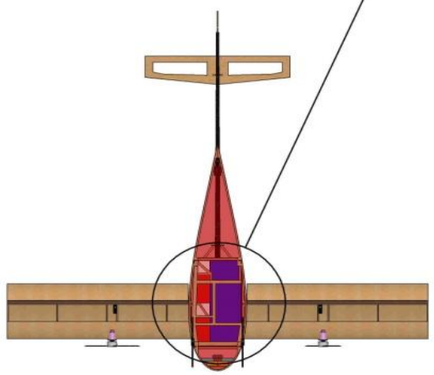

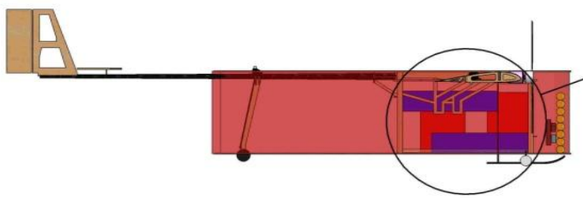

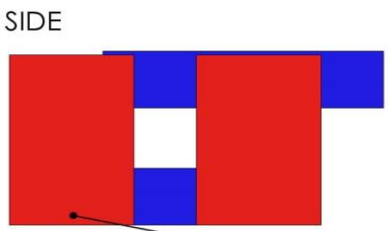

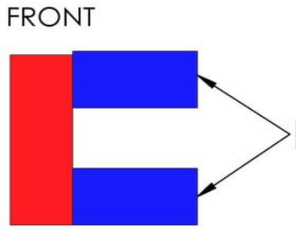

ATTENDANTS

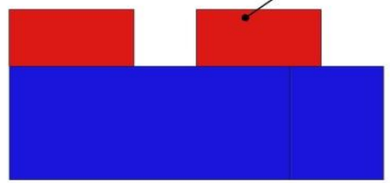

SINGLE BLOCK WEIGHT	1/2 LBS
TOTAL PAYLOAD WEIGHT	2 LBS

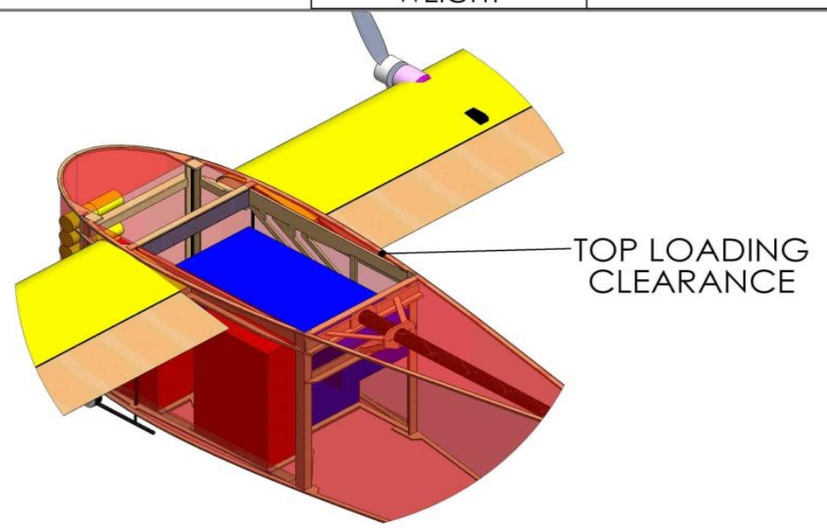

SCHOOL: SAN JOSE STATE UNIVERSITY

UNLESS OTHERWISE SPECIFIED: DIMENSIONS ARE IN INCHES

Cessna AIAA - Design/Build/Fly 2014

TITLE: PATIENT AND ATTENDANT PAYLOAD ACCOMODATION

DWG NO. 5

SCALE 1:20

SHEET 5 OF 5

6. Manufacturing

This section outlines the construction technique and different materials used for the construction of the aircraft. A large number of primary airframe components have been computer designed and laser cut from balsa wood. Laser cutting has provided great precision and assembly speed for past DBF teams from San José State University. The TechShop in San José, CA sponsored the team with free memberships, thus allowing access to this technology.

6.1 Final Materials/Manufacturing

The various components of the aircraft require different construction techniques and types of materials. The wing is constructed using balsa ribs and a carbon capped balsa spar to produce a strong and light weight structure. The empennage is also built from laser cut balsa wood and reinforced with carbon fiber tow for increased strength. The empennage is connected to the fuselage using a carbon fiber boom of the kind often used in sail planes and is secured using epoxy. A list of materials used is summarized in Table 6-1.

Table 6-1: List of Materials Used for Aircraft Manufacturing

Manufacturing Component	Material
Primary Structural Materials	Balsa Wood and Plywood
Strengthening Material 1	Carbon Fiber
Strengthening Material 2	Kevlar
Adhesive	CA and epoxy

6.2 Plan and Processes

The build process began by constructing individual components such as the main spar, wing, and the fuselage. The main spar is constructed using one-eighth inch balsa wood glued back to back to create a quarter inch spar. The spar is then reinforced with carbon fiber caps and wrapped with carbon fiber string to increase its strength and stability. The grain of the wood for the spar is aligned vertically as the wood acts stronger in compression.

The fuselage is built around a mold which ensures consistent quality between prototypes. This construction process is illustrated in Figure 6-1. The mold also ensured the fuselage is as symmetrical as possible, which helped in maintaining the precise airfoil contours to minimize flow separation and therefore drag penalties. The mold is constructed using laser cut layers of cardboard. The layers of cardboard were glued on top of each other until the mold formed a 10” tall “extrusion” of the desired top view. Figure 6-2 shows how the mold was used to construct the fuselage.

After having made the foundation, construction of the fuselage followed with the use of cyanoacrylate adhesive (CA). One-sixteenth inch balsa wood is used to construct the top, bottom and mid-section ribs of the fuselage. The aforementioned symmetry requirement is maintained through the use of side to side carbon reinforced balsa cross members.

Figure 6-1: Fuselage Mold Manufacturing

Figure 6-2: Fuselage Construction with Mold

Connecting all three rib sections are one-eighth inch balsa stringers located at the corners of the rectangular cargo-bay. The stringers are reinforced with carbon fiber strips to obtain structural strength for the fuselage. Once the fuselage construction is finished, the combination of the main spar, rear spar, and wing ribs are attached to the airframe and secured using adhesive. The rear spar, constructed using one-sixteenth inch balsa wood, is not strengthened using carbon fiber to save additional weight. The airframe and wing structure combination is shown in Figure 6-3.

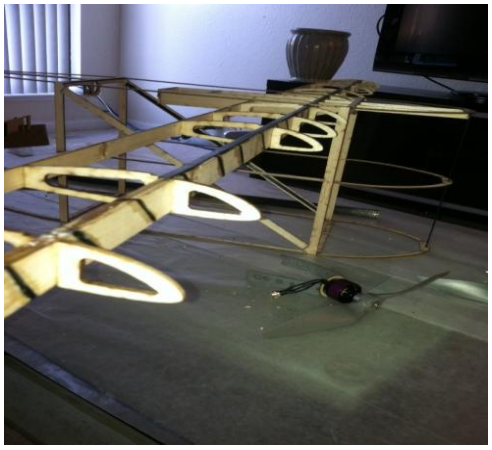

Figure 6-3: Wing Attached to the Airframe

Figure 6-4: Motors Mounted Into the Wing

Installing the boom is the subsequent step and it was decided that the boom would be connected to the fuselage using bulkhead. The boom's anchoring bulkhead is made using quarter inch balsa wood and glued to the fuselage airframe using CA. Once the bulkhead is installed, the boom is slid onto the bulkhead using epoxy.

1/32" balsa wood is then added to the airframe, shown in Figure 6-4, which serves as the fuselage skin. The skin provides additional rigidity and helps maintain attached flow during flight. Next, carbon fiber stringers are inserted, connecting the main spar, fuselage ribs, and skin to create a superstructure. Having this superstructure ensures that forces on any of the lifting surfaces are transferred throughout the airframe while avoiding unfavorable stress concentrations. Construction of the main spar and integration with the fuselage structure marked a significant manufacturing milestone for the airframe.

The wing ribs are laser cut to obtain the desired airfoil shape and are constructed using various thicknesses of balsa wood. The root and tip ribs use one-eighth inch balsa while all additional ribs use one-sixteenth inch balsa wood to reduce weight. With the exception of the two motor-mounting ribs, all wing ribs are spaced evenly from the side of the body to the wingtip. Before the motors can be mounted, quarter inch plywood is screwed into the back end of the motors. The motors with the plywood mounts are then secured to the spar, minimizing drag and providing the necessary strength. The wing and engine mount structures are shown in Figure 6-4.

Upcoming manufacturing steps include installations of electrical components and adding skin to the wing and the nose of the airframe. Space and weight limitations dictate that certain components be installed before skins are secured in place. For example, only the lower wing skins can be installed before the aileron servos are mounted. The top skin is then installed, leaving the flaperon actuation mechanisms covered.

Flaperon construction is relatively simple and follows similar methods as those used to make the wing. The flaperons are attached with scotch tape and a special application process is used to ensure up and down flaperon deflection. After the flaperons are attached to the servo using servo rods, the entirety of the wing is closed off using 1/32” balsa skin, with the grain of the skin is aligned in span wise direction. A custom made horizontal stabilizer pivot mount is attached to the rear end of the carbon fiber boom and the laser cut solid balsa stabilizer installed. The vertical fin is also cut from solid balsa wood and is bonded to a slot on the aft end of the boom. Balsa sheeting is then added to the back of the fuselage and vertical 1/8" wood stringers connecting the fuselage ribs are glued on the inside of the skins. The empennage mounting completes the base structure of the aircraft. Final airframe assembly steps include the installation of the landing gear and covering of the airplane with Monokote material.

The landing gear of the aircraft is attached to the vertical stringers which also secure the main spar. The landing gear uses carbon fiber skis and wheels which are secured using Kevlar tow. Finally, all the electric components are wired. The empennage servos are mounted at the aft of the fuselage and the wires are routed along the side of the fuselage to the nose of the aircraft. The receiver and receiver battery are housed in this forward section. The electronic speed controllers are secured at the nose of the fuselage and are connected to the motors using appropriate gauge wire routed within the wing structure. The ESC’s are then wired with 15A fuses which lead to the battery pack.

6.3 Investigated Processes

Time and resource constraints dictated that construction methodologies do not differ substantially from previous year's designs. The specifics of construction of the various components, however, evolved somewhat from the initial concepts.

6.3.1 Wings

Construction of the finalized main spar was dissimilar relative to earlier prototypes. The early prototypes were first made by adhering two, 1/8 inch, balsa wood members face-to-face for a total of one-quarter

inch thickness. The resulting 6 inch span members were in turn adhered edge-to-edge in order to reach a 54" span. For later prototypes, however, the spar was constructed using end to end connections of different lengths on both sides such that the joints would be offset. The two different configurations are shown in Figure 6-5.

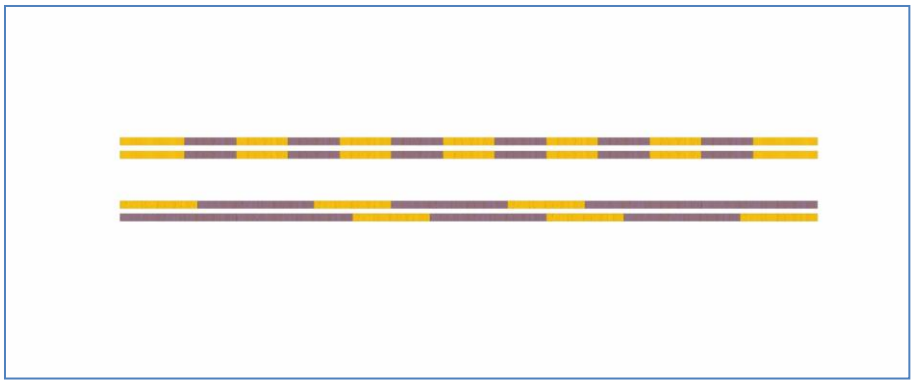

Figure 6-5: Evolution of Main Spar Manufacturing Process

Next, the spar gained carbon fiber caps over the top and bottom. Preceding prototypes also had carbon fiber tow wrapped spars, but this greatly increased the manufacturing time and made it more difficult to attach wing ribs. The carbon fiber wrapping was removed as the carbon fiber caps provided sufficient strength. This allowed the wing ribs to attach on a smooth surface and in their designated spaces.

For early prototypes, the wings were only covered with balsa sheets at the leading edge. The rest of the wing was only covered using monokote. This decreased the efficiency of the wing, as the monokote did not hold the intended shapes as precisely as desired under flight loads. Upon further research, it was determined that the past SJSU DBF teams had covered the entire wing with balsa sheets to gain efficiency. This change was implemented and resulted in a shorter take-off distance.

6.3.2 Fuselage

Construction of the fuselage remained fairly constant throughout the prototypes, with the exception of one noteworthy change. For early prototypes, the fuselage was not sheeted to cut weight. The covering and the stringers provided the symmetrical airfoil shape to the fuselage and the structure was deemed strong enough. This backfired as the flow separated too early during flight causing an increase in drag. Therefore, the fuselage of the later prototypes was sheeted to increase efficiency and reduce drag. Although there was a weight penalty to sheeting, it was a good decision overall as it significantly improved flight performance. Note that final prototypes have a continuous airfoil shape, rather than the compound shape shown in Figures 6-1 through 6-4.

6.3.3 Landing Gear

Many landing gear configurations were evaluated due to the importance of the taxi mission. The early stages of landing gear designs encountered problems such as: inability to get onto the roofing

panel, failure to restart after a stop on the panels, and weakness in the structure causing the landing gear to collapse.

These issues transpired as conventional landing gear was being used and secured using carbon fiber tow. The unique mission requires a unique landing gear. A ski and wheel combination landing gear was developed to successfully complete the taxi mission. The ski's allowed the aircraft to restart after a complete stop on the roofing panel. Additionally, the landing gear was secured using Kevlar tow instead of carbon fiber tow to increase strength.

6.4 Manufacturing Schedule

Figure 6-6 charts the manufacturing schedule up through Prototype 1. Note that there are two prototypes shown; however, the first was made from foam and not balsa wood and thusly designated as a Technology Demonstrator.

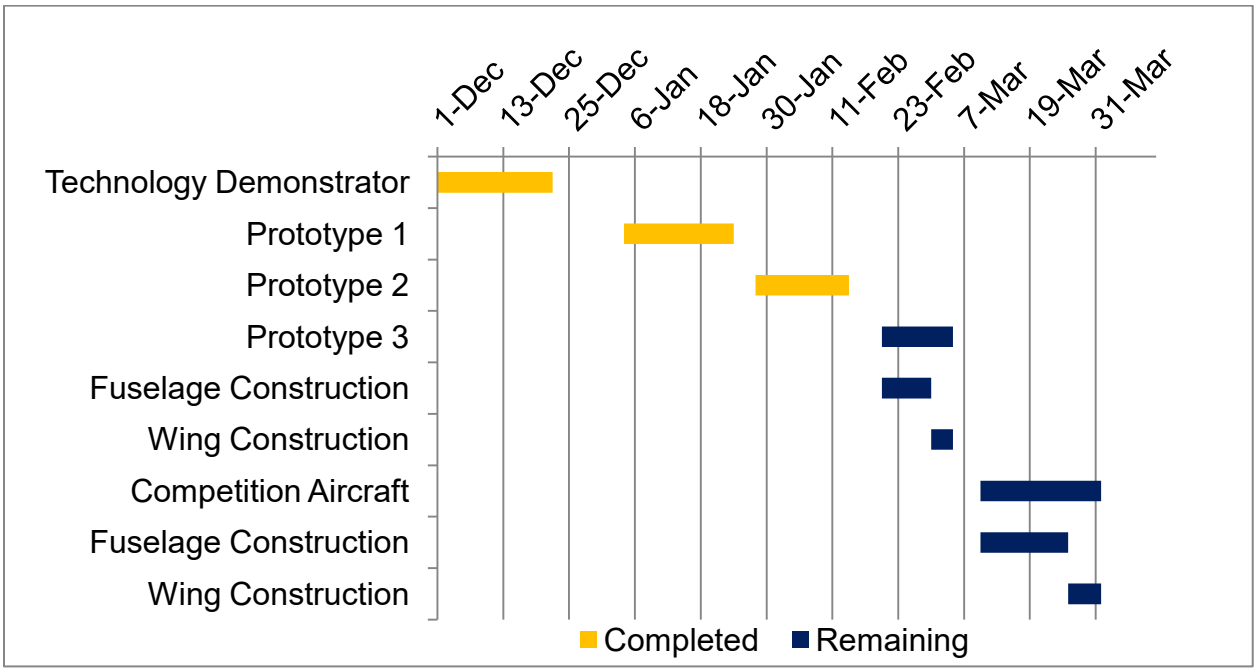

Figure 6-6: Manufacturing Milestone Chart

7. Testing Plan

Testing is a vital part of any system and is done to validate design choices before moving into the final production. There are a few subsystems that were tested; these include batteries, propulsion system, and aircraft structure in order to ensure mission requirements are met with good efficiency. Flight tests were also performed in order to check the overall performance of the aircraft and to assure that the plane will complete the mission requirements.

7.1 Subsystem Tests

The different tests conducted are listed in Table 7-1.

Table 7-2: Different Tests Conducted on Subsystems

Component	Type of Test
Batteries	Endurance
Batteries	Temperature/Performance
Propulsion	Differential Thrust
Propulsion	Static Thrust Test
Main Spar	Maximum Load Test
Fuselage	Flow Separation
Propulsion	Take-off Test
Landing Gear	Taxi Test

7.1.1 Battery Testing

Battery testing was done to ensure the aircraft has sufficient power for each mission. An endurance test was performed to obtain the total amount of time before the aircraft started losing power and hence performance. The endurance test was performed in flight. Each mission was performed with a fully charged battery and continued until the pilot noticed a substantial drop in power.

A temperature test on the batteries was also performed. It has been a trend in competitions for pilots to heat up their batteries to gain a power advantage. The batteries were tested in flight under two different conditions- room temperature batteries and pre-heated batteries up to 100°F. The batteries were kept warm using an electrical blanket until seconds before take-off.

7.1.2 Propulsion System Testing

The propulsion system requires substantial testing in order to optimize the aircraft. A test for differential thrust was conducted just to prove that the aircraft could be maneuvered on the ground using differential thrust. The concept of differential thrust to provide directional control on the taxi mission was one of the drivers for a twin-motor configuration for the aircraft. The aircraft showed good ground maneuvering performance.

Static thrust tests were conducted on various motor and propeller combinations by mounting the assemblies to an L-bracket that transferred load from the propeller to a scale. An electrical power meter

was connected in series with the required 15A fuse and power source. The power meter allowed for observations to be made on power production and current draw. The results varied from propeller to propeller, as expected. Since the rules allow for propellers to be changed between missions, testing was done with several different props. The results are presented in Section 8.

7.1.3 Structure

The main spar underwent tests to find the lightest structure required to pass the mandated wingtip test. Tests were performed on three different spars including balsa spar with carbon caps, balsa spar with carbon caps and carbon tow, and balsa spar with carbon tow.

Each spar was clamped to a table at the tip and a load was applied at mid span. The load was increased until the spar failed and the failure location was recorded for further analysis. Figure 7-1 shows the spar test being performed.

Figure 7-1: Strength Test Performed on the Spar

Due to the unique fuselage shape, tests were performed to see if the flow remained attached towards the aft of the fuselage. The fuselage shape was drawn to accommodate the payload for Mission 2 and Mission 3. The test was conducted by attaching small strings or “tufts” towards the aft of the fuselage and then securing the fuselage a sufficient distance outside a car window. The vehicle was then driven at different speeds and the behavior of the tufts noted. Combinations of flow trips will be tested to improve results if necessary. The preparation for the test is shown in Figure 7-2.

Figure 7-2: Flow Test with Flow Visualization Tufts Attached Aft of the Fuselage

7.1.4 Take-Off Test

A take-off test was conducted to meet the take-off requirement of 40ft. The test was done under different weather conditions, as the winds in Kansas will impact the flight characteristics of the airplane. The 40ft distance was measured on the runway and each flight was recorded to determine take-off distance. Multiple characteristics such as incidence angle and flaperon deflection were changed to successfully meet the take-off requirement goal.

7.1.5 Flight Test

Flight testing was needed to evaluate the overall performance. Extensive testing is being performed, from basic tests (cruise, stall, take-off, etc.) to mock mission tests (lap times, payload flight, and hospital carriage). The data was taken using electronic scales, stop watches, telemetry instruments, and pilot feedback. All flight tests were performed using the checklist shown in Section 7.2.

Flight testing for the prototypes was performed in the following order as required to verify performance and minimize the risk to the airframe:

1. Unloaded testing focused on trim and handling qualities (no limitations on takeoff or landing distances)
2. Unloaded progressive speed expansion to full throttle
3. Same as 1 and 2, with single 1 lb payload block
4. Same as 3, with 2 lb medical evacuation payload
5. Same as 4, with 2 payload blocks
6. Takeoff distance test, empty
7. Takeoff distance test, maximum load
8. Performance testing
    a. Average speed
    b. Mock competition
9. Taxi tests

7.2 Flight Checklist

Date:	
Location:	
Aircraft:	
Pilot:	
Temperature:	
Wind Speed/ Direction:	
Flight #	

Safety Checks:

- ☐ Aircraft Control Surfaces OK
- ☐ Aircraft Control Linkages OK
- ☐ Motor Mounts OK
- ☐ Landing Gear OK
- ☐ Propellers Secure
- ☐ Range Check

Pre-Flight Checklist:

- ☐ Transmitter Voltage OK
- ☐ Flight Pack Charged
- ☐ Receiver Pack Charged
- ☐ Control Surface Direction
  - Aileron Left/Right
  - Elevator Up/Down
  - Rudder Left/Right
- ☐ Throttle Check

Post-Flight Checklist:

- ☐ Main Battery Unplugged
- ☐ Receiver Power Off
- ☐ Transmitter Power Off
- ☐ Inspect Aircraft

Objectives

Flight Notes and Observations

Additional Comments

7.3 Test Schedule

Figure 7-3 shows the testing plan for each subsystem and prototype. The included testing methods are explained above.

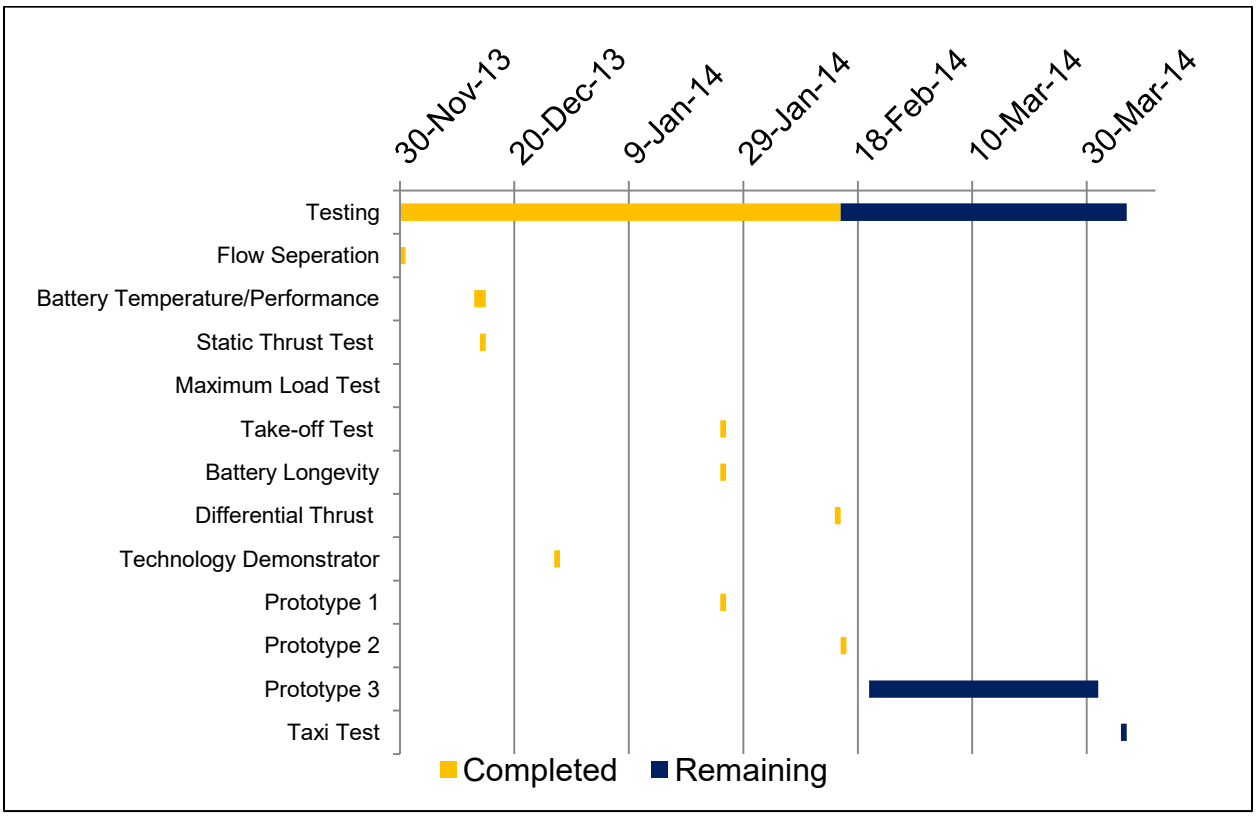

Figure 7-3: Testing Schedule

8.0 Performance Results

Two prototypes and one technology demonstrator have been produced so far. This section specifies the results based on performance of the aircraft and its subsystems.

8.1 Subsystem Tests

8.1.1 Batteries

The batteries provided sufficient power for acceptable flight performance but problems occurred when they were wired in a series configuration. Both motors weren't drawing equal amounts of current forcing the aircraft to yaw in one direction. This added trim drag to the aircraft and therefore the battery configuration transitioned to a parallel configuration where each motor is powered by its own 8 cell battery with a 15A limiting fuse. Average results of the battery endurance test are shown in Table 8-1. A total of 4 flights were conducted with fully charged batteries for each mission until the aircraft suffered substantial power loss.

Table 8-3: Battery Endurance Test Data

Mission	Time before Power Loss
Mission 1	~8.2 mins
Mission 2/Mission 3	~6.5 mins

The battery endurance test provides beneficial results. Since Mission 2 and Mission 3 carry equivalent payload the results are combined. The battery power for the aircraft is sufficient and provides safety margin since all missions are expected to be performed within a 4 minute period.

Battery temperature tests showed that the heated batteries provided a measurable increase in power output the room temperature batteries. Lap times for the empty flight improved by 8 seconds which can help add an entire lap compared to the room temperature batteries.

8.1.2 Propulsion System

Table 8-2 shows data obtained from static thrust testing. Different size APC brand propellers were used to determine optimal propeller for each mission. It is important to note that the results shown in Table 8-2 are for a single engine and not the entirety of propulsion system which is equipped with two motors. The optimal propellers were found to be the 9x9 for Mission 1. For Mission 2, Mission 3 and Taxi Mission, the 10x7 propellers serve best as they provide greater amount of thrust and do not overload the motors.

Table 8-4: Static Thrust Test Data

Propeller	Max Amps	Power per Motor	Thrust	Notes
9x7.5	13.1 A	117 W	1.25 lbs	Does not reach power expectations
9x9	14.8 A	124 W	1.30 lbs	Ideal power output, and the high pitch is ideal for reaching high speeds required for Missions 1. Smaller and lighter than the 10” diameter propellers
10x7	15.2 A	125 W	1.40 lbs	Exceeds fuse limits, but has good power. Surpassing the fuse limits may be sustainable for short durations. The Larger prop with low pitch is ideal for the taxi mission due to increased thrust at low speeds
10x10	15.4 A	138 W	1.55 lbs	High power output, and high thrust. The motors heated up to dangerous temperatures

8.1.3 Wing and Wing Spar

Earlier prototypes validated that the designed wings were adequate for successful take-off within a 40 ft runway. To save weight, four inches of wing span were removed and the modified wing tested on the second prototype. The shorter wing span wasn’t able to provide enough lift for take-off requirements and also had problems climbing with an internal payload of 2lbs. As a result, the latest prototype was altered to the original wingspan.

Table 8-5: Spar Strength Test Data

Manufacturing Process	Weight	Max Load	Fracture Point
Balsa Spar With Carbon Caps	32g	10lbs	1/2 Span
Balsa Spar With Carbon Fiber Tow	30g	5lbs	1/4 Span
Balsa Spar with Carbon Caps and Carbon Tow	35g	15lbs	1/2 Span

Table 8-3 shows the data from spar testing. All spars were manufactured simultaneously to ensure consistency in materials used. All spars are stronger than required so selection was made based on weight, fracture point, and manufacturing time considerations. The balsa spar with carbon caps was easiest to construct, while relatively lightweight. This configuration had the advantage of not requiring changes in rib placement due to its constant cross section, making it an optimal choice.

8.1.4 Fuselage Aerodynamics

The first two prototypes had fuselages that were custom drawn to carry the internal payload with aerodynamic leading and trailing edge closeouts added to the constant section center body. Even after optimization of the motor-propeller combination, poorer than expected takeoff and high speed performance were noted. This performance deficit pointed toward excessive drag on the airframe. Flow visualization using tufts indicates that the flow separation exists over the aft section of the fuselage. The custom fuselage thus produced higher than anticipated drag which in turn slowed the plane down. The fuselage shape was then altered. The new fuselage uses a true symmetrical airfoil modified in terms of

percent thickness and will be tested for flight performance on future prototypes. The two different fuselage shapes are shown in Figure 8-1.

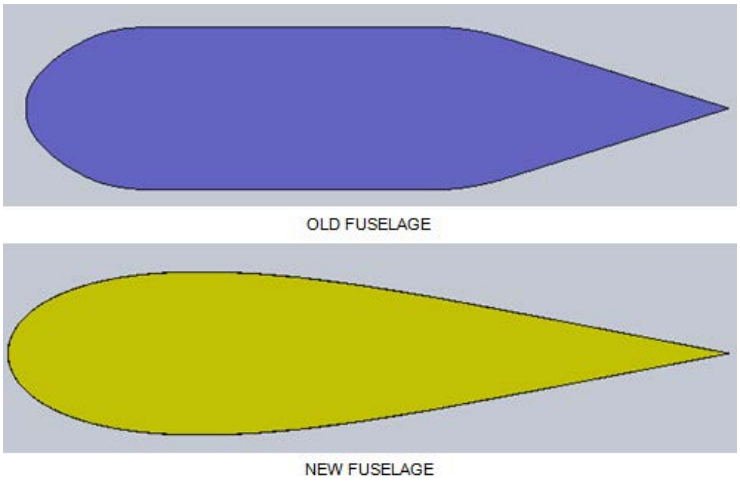

Figure 8-1: Fuselage Airfoil Comparison

8.2 Flight and Mission Performance

Both prototypes and the technology demonstrator have gone through considerable flight testing and their performance is recorded in this section. The performance results are shown in Table 8-4. Mission 2 and Mission 3 are combined since the payload has been established as equal; the center of gravity is virtually the same. The fastest time from Mission 2 and 3 was recorded. Level speed was estimated from the average of multiple level passes in opposite directions. A summary of gathered flight data is compared with expected results is presented in Table

Table 8-6: Expected vs Demonstrated Flight Performance

Mission 1			
	Expected	Demonstrated	Discrepancy
Level Cruise Speed (ft/s)	90	80	-11%
Takeoff Distance (ft)	20	25	+25%
Number of Laps*	8	6	-25%
Gross Weight (lbs)	2.1	2.33	+11%
Mission 2 and Mission 3			
	Expected	Demonstrated	Discrepancy
Level Cruise Speed (ft/s)	80	62	-22%
Takeoff Distance (ft)	35	37	+6%
Time for 3 laps	1 min 54 sec	2 min 48 sec	+47%
Gross Weight (lbs)	4.1	4.33	+6%

*Estimated number of laps in still air

Comparing the expected and demonstrated flight performance shows significant discrepancies in all areas.

The most significant discrepancy is weight. Since the RAC equals weight, the total weight of the aircraft is a major concern and greatly impacts total score. During the manufacturing process of future prototypes, any additions onto the aircraft will be evaluated thoroughly to reduce overall weight. Smaller battery cells are also under consideration, as they will provide same voltage while saving weight. The current receiver battery has enough power to last over 10 minutes. Therefore a smaller and lighter battery pack with a lower safety margin will be used for future prototypes and the competition.

The competition aircraft will be manufactured using competition grade balsa wood which weighs as little as half the weight of ordinary balsa wood. For testing purposes, regular balsa wood is optimal as it is inexpensive and readily accessible. The changes listed above will help cut weight from the aircraft, with the goal being to get the total weight under 2lbs for the competition.

The take-off distances were larger than expected for all missions. This was directly impacted by the higher aircraft weight and higher drag than expected. Mission 2 and Mission 3 show a 6% increase in take-off distance. This increase is nearing the limit of 40 ft and is not acceptable as it can result in a failed flight mission if exceeded.

Discrepancies in cruise speeds are also significant and will lower mission scores for Mission 1 and 3. Section 8.1.4 describes the testing and evolution of the fuselage profile.

Analysis shows that the aircraft will need to reach about 90ft/s for Mission 1 in order to be competitive. The cruise speed is expected to increase once lighter cells are considered, which may allow for additional cells to power the aircraft. The current cells (1500mAh) were optimal for the competition with a 20A limit. With the new 15A limit, smaller cells (~1000mAh) will be effective and help increase the number of cells for the same weight, thus increasing power.

Steps are being taken to reduce weight, increase cruise speeds, and reduce take-off distance to ensure higher mission scores, while maintaining overall dimensions and characteristics of the design.

9. Bibliography

[1] AIAA Student Design|Build|Fly, “2013 DBF Q&A,” 2012-2013. [Online]. Available: http://www.aiaadbf.org/2013_files/2013_QA.htm.

[2] AIAA Student Design|Build|Fly, “DBF Rules,” 31 October 2012. [Online]. Available: http://www.aiaadbf.org/2013_files/2013_rules.htm.

[3] B. W. McCormick, *Aerodynamics, Aeronautics, and Flight Mechanics*. Wiley, 1994.

[4] D. P. Raymer, *Aircraft Design: A Conceptual Approach*. AIAA, 2006.

[5] J. D. Anderson Jr., *Fundamentals of Aerodynamics*. Boston: McGraw Hill, 2007.

[6] J. D. Anderson Jr., *Introduction to Flight, 7*th ed. New York: McGraw Hill, 2007.

[7] M.V. Cook, "Longitudinal dynamics," in *Flight Dynamics Principles, 2nd* ed. Oxford, UK: Elsevier, 2007, pp. 158-167.

[8] San Jose State University, “AIAA Design/Build/Fly 2011-2012 Design Report,” April 2012. [Online]. Available: http://www.aiaadbf.org/2012_files/reports/2012DBF_SanJoseStateUniversity_TeamPhalanX.pdf.